City Research Online

City, University of London Institutional Repository

# A NEW METHOD TO ESTIMATE WHOLE BODY PROTEIN TURNOVER IN MAN

by

Ian Joseph Gowrie

A thesis submitted in partial fulfilment of the
requirements for the degree of

Doctor of Philosophy

City University

2002
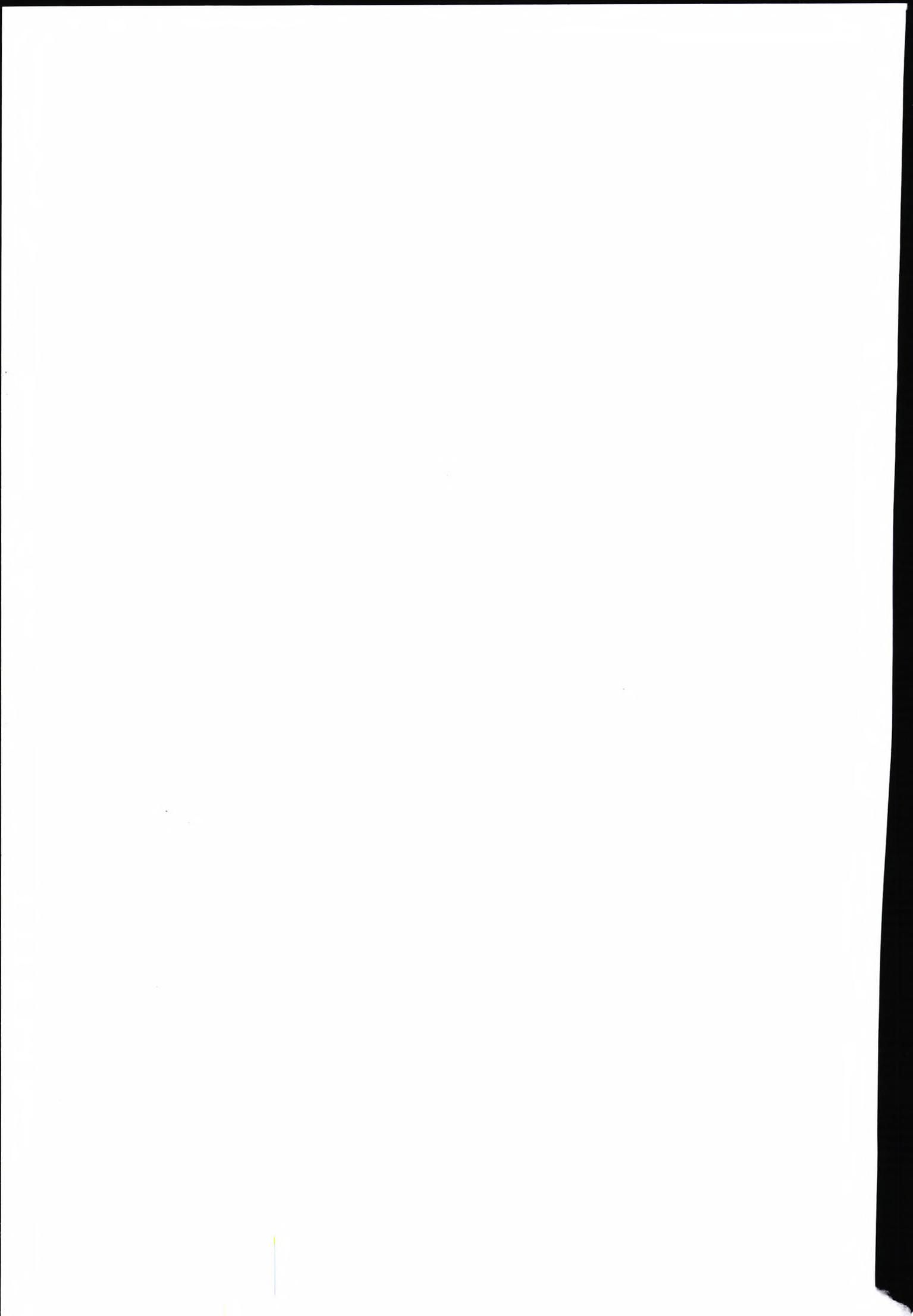
ABSTRACT

The complexity of amino acid and protein metabolism has restricted the development of comprehensive, accurate whole body kinetic models. For leucine, the so-called primary and reciprocal pool models, have been used extensively to measure *in vivo* leucine fluxes. The influence of several variables (age, gender, weight, BMI, plasma leucine concentration and the method used to estimate protein turnover) on whole body protein turnover (WBPT) estimates in normal adult males (N= 29) was investigated. The analysis showed that compared to the reciprocal pool model, the primary pool model will underestimate leucine *Ra* by ~30%. Furthermore, over the range of values in this study, the influence of age, gender, weight, BMI, plasma leucine concentration on WBPT is small. Our data show, that of the variables considered here, the single most important factor in determining WBPT is the method/model used.

The use of $[^{15}N,^{13}C]$-leucine tracer to estimate whole-body fractional rates of a fast-turning-over protein pool in humans is proposed here. The kinetics of $[^{15}N,^{13}C]$-leucine tracer are simplified compared to those of traditional leucine tracers and benefit from irreversible transamination to $[^{13}C]$-α-ketoisocaproaic acid (KIC) resulting in a simplified model structure. We developed a model based on the infusion of $[^{15}N,^{13}C]$-leucine tracer and measuring $[^{15}N,^{13}C]$-leucine in plasma. The resulting three-compartment model is *a priori* uniquely identifiable. The model was evaluated in two phases, a synthetic and an experimental phase. In the synthetic phase, we simulated data (with added measurement error) for six subjects using a reference model (Cobelli et al, 1991). In the experimental phase we performed the experiment on six healthy male subjects. In both the synthetic and experimental phase we were able to quantify the model with good precision. It was possible to estimate the intracellular rate of appearance of leucine derived from protein breakdown (∝ B); the rate of incorporation of leucine into proteins (∝ S) and the rate of leucine de-amination. Furthermore, the model provides estimates of the sizes of various compartments including a plasma/interstitial fluid compartment, an intracellular leucine compartment and a fast turning over protein pool.

In conclusion, the model proposed here is conceptually no more complex than the reciprocal pool model, and in practice it may be simpler to use than other, more comprehensive, compartmental models. The model allows the estimation of several leucine fluxes and masses in man, provides estimates in line with theoretical and empirical expectations and is on firm theoretical ground.

ACKNOWLEDGEMENTS

DECLARATION

I hereby declare that as the author of this document, that all the analyses, derivations, results, etc., described herein were performed by myself. Assistance provided by other persons has been acknowledged, and all previous published work has been identified and acknowledged.

This work is original and has not been submitted for any other degree.

Ian Joseph Gowrie

September 2002

TABLE OF CONTENTS

TABLE OF TABLES

ABBREVIATIONS USED

This list contains details of the most commonly used abbreviations, however, many others have been used but these are defined in the text where appropriate.

B   Leucine flux from protein breakdown (μmol/kg/min)

BMI   Body mass index (kg/m^2)

KIC α–ketoisocaproate

k_{ij} Transfer rate parameter from compartment j to i (min^{-1})

Ox   Leucine oxidation rate (μmol/kg/min)

$\dot{q}_i$ Derivative of q_i (μmol/min)

$\dot{Q}_i$ Derivative of Q_i (μmol/min)

q_i Tracer mass of compartment i (μmol)

Q_i Tracee mass of compartment i (μmol)

S   Leucine incorporation into proteins (μmol/kg/min)

TTR   Tracer to tracee ratio, also z, defined as $q_i \div Q_i$ (unitless)

u Tracer input (μmol/kg/min)

WBPT   Whole body protein turnover

z Tracer to tracee ratio, also TTR, defined as $q_i \div Q_i$ (unitless)

1 OVERVIEW OF THESIS

1.1 Introduction

The accumulation of body proteins is the net result of the synthesis and breakdown of body proteins. The term protein synthesis describes an intracellular process whereby amino acids are converted into proteins; protein breakdown is the converse of synthesis, and describes the process whereby amino acids are released from protein. Protein turnover refers to the combined process of synthesis and breakdown, it is a dynamic process where body proteins are continuously being degraded and re-synthesised. The knowledge of the dynamic nature of protein turnover in man is of relatively recent origin, and its discovery can be traced back to the pioneering work of Schoenheimer and colleagues in the 1930s (Schoenheimer and Rittenberg 1935;Schoenheimer and Rittenberg 1938).

In recent years there has been a considerable increase in the application of quantitative methods to the study of metabolic processes. These increases have certainly been aided by the availability of raw computing power but, in addition, they have been fuelled by comparable advances in measurement techniques and by advances in the methods available for the analysis and interpretation of experimental data. The study of protein metabolism is an ideal candidate to benefit from these advances in technology and methodology.

1.2 Research hypothesis

The most important features of whole-body protein turnover are protein breakdown and protein synthesis, because together these define turnover. Fundamental to the study of whole-body protein turnover is the idea that it is possible to create a (mathematical) model that can measure, predict or explain features such as synthesis and breakdown. In order to investigate protein turnover, it is thus necessary to ask the question: Is it possible to develop a model that can describe protein turnover? Since several models already exist, the answer to this question is yes, and the question becomes: Is it possible to develop a *new* model to describe whole body protein turnover in man? It is implicit that a *new* model would be better than older ones, for instance, a new model might make fewer assumptions than older ones, or a new model would give more accurate estimates than older models, or perhaps a new model would be more comprehensive than previous models,

describing additional features etc. The basic premise or hypothesis of this work is thus: A *new model to estimate whole body protein turnover in man can be developed.*

1.3 Aims and objectives

The primary aim and the specific objectives follow from the hypothesis. The primary aim of this work is thus, to develop a new method to estimate whole body protein turnover in man. This primary goal can be accomplished by achieving a set of lesser objectives. These secondary objectives are:

- To assess the current methods used to estimate whole body protein turnover in man.

- To describe a new model which may be used to estimate whole body protein turnover in man.

- To validate the proposed model in a simulated experiment.

- To validate the proposed model in a clinical experiment.

- To explore the validity of the model, especially in respect to existing methods

- In addition, because the use of stable isotopes is crucial to whole-body protein turnover studies, the tracer to tracee relationship will be investigated, focussing especially on [^{13}C]- and [^{15}N,^{13}C]-leucine tracers.

1.4 Plan of thesis

Chapter Two is devoted to a review of the literature and associated techniques used in the study of protein turnover. The chapter includes some background information on proteins, amino acids and protein metabolism, followed by a review of the main approaches used to estimate protein turnover in man. The chapter ends with an examination of the supplementary tools needed and commonly used in protein turnover studies, including compartmental modelling and the use of isotopic tracers.

Chapter Three provides details of a linear regression analysis on data from 29 healthy subjects. The aim of this study was to determine the effect of several variables (including age, weight, body mass index, plasma leucine concentration, and the model used to determine protein turnover) on key whole body protein turnover indices, namely the rate of appearance of leucine from protein

breakdown, non-oxidative leucine disposal and the rate of leucine oxidation. In addition, we compare the influence of the models (the primary and reciprocal pool models) on WBPT data.

In Chapter Four, a new model to estimate whole body protein turnover in man is proposed. The use of an $[^{15}N,^{13}C]$-leucine tracer and a three compartment model is explored. The model makes use of the unusual kinetics of $[^{15}N,^{13}C]$-leucine, exploiting the fact that leucine transamination, which is reversible for leucine and $[^{13}C]$-leucine, is irreversible for the $[^{15}N,^{13}C]$ tracer. The leucine system is thus reduced to a three-compartment structure. The proposed model is validated using simulated data.

A study involving six healthy subjects was performed; this experiment is fully described in Chapter Five. In addition, the model is compared, both theoretically and empirically, to the primary and reciprocal pool models.

Chapter Six provides a summary and discussion of the work presented in the thesis and outlines possibilities for future work.

There are five appendices. Appendix I contains charts and plots relating to Chapter Three. Appendix II contains tracer data curves, fits and residuals for Chapter Four. Appendix III includes the ethics committee form and patient consent form used for the experiment in Chapter Five. Appendix IV contains details of the tracer to tracee ratio calculations used in Chapter Five. Appendix V contains a publication that was derived from work included in this document.

2 REVIEW OF LITERATURE AND ASSOCIATED TECHNIQUES

2.1 Background

The regulation of protein metabolism is crucial for survival, yet the area of protein metabolism has received less attention in terms of system modelling than say the glucose or lipid system. Bier (1989) argues in his survey that it is the intrinsic complexity of the system that has limited the development of a definitive and accurate whole body kinetic model. Whatever the reasons, the study of protein metabolism has played second fiddle to other areas of similar interest and considering the essential role that protein metabolism plays in the survival of an organism, it is clear that more comprehensive models are needed.

This chapter initially provides some background on protein and protein metabolism, then a comprehensive overview of the methods used to estimate protein turnover, followed by some of the accompanying methodologies underlying these techniques.

2.1.1 Proteins

At the cellular level of organisation, the main chemical processes of all living matter are similar, if not identical. This is true for humans, animals, plants, fungi or bacteria, and although variations may exist, these are but variations on common themes. Thus, all living matter is made up of large molecules called proteins. These molecules provide the structural framework for cells and organs; regulate intracellular and intercellular communication; and as catalysts, enable chemical reactions to take place rapidly and specifically under mild temperature, relatively low concentration and pH neutral conditions.

Proteins make up about 12% of the weight of the human body (water 70%, and fat 15%). In man proteins are assembled from some 20 amino acids, and just as the 26 letters of the alphabet may be assembled in specific ways to form various words with various lengths and different meanings, similarly the constituent amino acids may be combined in chains to forms specific proteins. Additionally, some proteins contain carbohydrates (glycoproteins) and lipids (lipoproteins).

The biological properties of a protein depend on the exact sequence of different amino acids in the chain (primary structure) and their orientation (secondary structure), and the shape of the chain as

a whole (tertiary structure). Small differences in the structure may result in a completely different protein, and the possible permutations are vast. In general, while other components of living matter vary little, it is the arrangement of proteins that distinguish between different species and individuals. In essence what parents pass on to their children is the ability to produce particular proteins; this is the central dogma of molecular biology.

Protein must be present in the diet, and humans ingest proteins of plant and/or animal origin. These ingested proteins are in themselves useless to the body, and they must be broken down into their constituent amino acids and re-assembled in a form that the human body can utilise. Ingested proteins are digested in a number of stages in the body. Firstly, ingested proteins are broken down into large polypeptides in the stomach; then peptides of various chain lengths are liberated along with a few free amino acids in the duodenum (the first part of the intestine). Finally, the breakdown of proteins into free amino acids is completed in the small intestine. The liberated amino acids are absorbed into the intestinal capillaries and via the portal vein to the liver into general circulation. Protein is used mainly in the structure of tissues, although any surplus can be used as fuel. It should be noted that if the diet does not contain enough fuel (carbohydrates, fat), in many cases proteins will be oxidised to provide energy – instead of being used for growth and repairing tissue.

2.1.2   Amino acids

Amino acids are any of a class of organic compounds having a carboxyl group (COOH) and an amino group (NH_2). Some 20 amino acids are found in man and over 100 less common forms are found in nature, chiefly in plants. When the carboxyl carbon atom of one amino acid binds to the nitrogen of another with the release of a water molecule, a linkage called a peptide bond is formed. Small chains of amino acids are called peptides or polypeptides. The distinctions between peptides, polypeptides and proteins are not well defined and in some senses the distinction is arbitrary. Generally however, chains containing 2-10 amino acids residues are called peptides, chains containing more than 10 to 100 amino acid residues are called polypeptides, and chains containing more than 100 amino acids residues are called proteins.

Amino acids are composed of carbon, hydrogen, oxygen, nitrogen and sometimes sulphur. Most proteins contain about eighteen amino acids - although some proteins are built from only a few. Amino acids have the general formula:

$$R.CH(NH_2).COOH$$

5
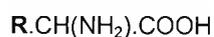
where R is any of a variety of organic groupings. In the case of the amino acid leucine, R is $(CH_3)_2CH.CH_2$, the chemical structures of leucine, glycine and phenylalanine are shown in Figure 2.1.

leucine   glycine   phenylalanine
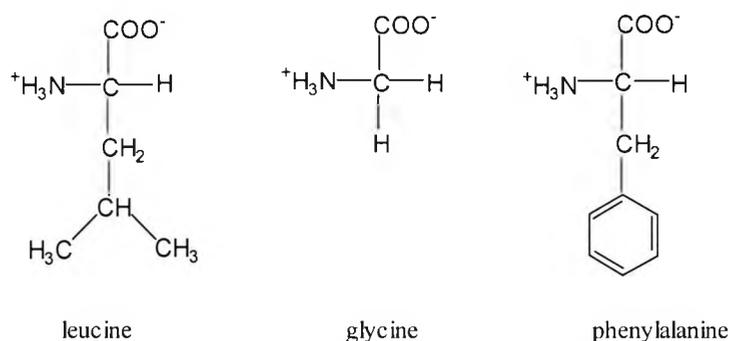
Figure 2.1: Chemical structure of leucine, glycine and phenylalanine

The inability of humans to synthesise all of the amino acids they require has led to the classification of amino acids as either essential or non-essential. Essential amino acids are those, which the body cannot synthesise endogenously, i.e. essential amino acids must be present in the diet if the organism is to maintain a positive nitrogen balance. A list of the amino acids found in man is shown in Table 2.1.

Table 2.1 List of essential and non-essential amino acids in man

Essential amino acids	Non essential amino acids
Isoleucine [ile] (I)	Alanine [ala] (A)
Leucine [leu] (L)	Arginine [arg] (R)
Lysine [lys] (K)	Asparagine [asn] (N)
Methionine [met] (M)	Aspartate [asp] (D)
Phenylalaine [phe] (F)	Cystine [cys] (C)
Threonine [thr] (T)	Glutamate or Glutamic acid [glu] (E)
Tryptophan [trp] (W)	Glutamine [gln] (Q)
Valine [val] (V)	Glycine [gly] (G)
	Histidine [his] (H)
	Proline [pro] (P)
	Serine [ser] (S)
	Tyrosine [tyr] (Y)

Three letter abbreviations shown in square parentheses and single letter abbreviations shown in round parentheses.

2.1.3 Protein metabolism

Living organisms are unique in that they are able to extract energy and materials from their environments and use them to carry out activities such as movement, growth and reproduction. But how do organisms – or more precisely their cells – extract energy from their surroundings, and furthermore how do the cells use this energy to synthesise and construct the components from

which the cells are made? The answers to these questions lie in the study of the enzyme-mediated chemical reactions that take place in living matter – metabolism.

Metabolism describes the chemical reactions that take place within each cell of a living organism and thus provides energy for vital processes and the synthesis of new organic material. The study of metabolism thus aims to describe hundreds of co-ordinated, multi-step reactions, fuelled by energy obtained from nutrients (or solar energy in the case of plants), which convert available materials into the molecules required for growth and maintenance. Metabolism consists of *catabolism* - the breakdown of large, unmanageable molecules into smaller, manageable components (e.g. the breakdown of proteins into amino acids), and *anabolism,* the reconstruction of large molecules.

Protein metabolism is thus the term used to describe the vast number of processes whereby amino acids are incorporated into and released from proteins. Protein metabolism is continuously occurring in the body; there is constant protein catabolism or proteolysis, the breakdown of proteins and the release of amino acids into general circulation; and constant anabolism, the bonding of various amino acids to form protein molecules. This process results in the loss of nitrogen compounds from the body; these compounds must be replaced if health is to be maintained. It is useful to note that no functional distinction can be drawn between amino acids drawn from food and those derived from tissue breakdown. Since the metabolism of each amino acid is different, protein metabolism is a broad term, which encompasses the metabolism of all the constituent amino acids present in man.

2.1.4   Amino acid metabolism

Amino acids derived from protein breakdown enter the 'free amino acid pool', and may be reused for protein synthesis. These amino acids are incorporated into cell structure as required. If a cell takes up as much amino acid as it loses, the cell is said to be in a state of 'dynamic equilibrium'; if the loss of amino acids is greater, then the cell wastes; conversely if the gain of amino acid matter is greater, the cell grows. Inter-conversions between amino acids and the products of carbohydrate and fat catabolism at the level of the common metabolic pool involve the transfer, removal or formation of amino groups. Transamination reactions - conversion of one amino acid to the corresponding keto-acid with simultaneous conversion of another keto-acid to an amino acid - occur in many tissues. The amino acid pool is undergoing constant depletion and constant restoration - amination and de- amination. In adult humans, about 80% of amino acids released by proteolysis are used for protein synthesis (Welle 1999a); this value is a whole-body estimate, and does not necessarily reflect the reutilization of amino acids in all cell types. The amino acids that

are not used for protein synthesis are deaminated, and the carbon skeletons can be oxidised for use in ATP production, or used in glucose or lipid production. The majority of the nitrogen from oxidised amino acids is excreted as urea; the excretion of amino acids in the urine is negligible.
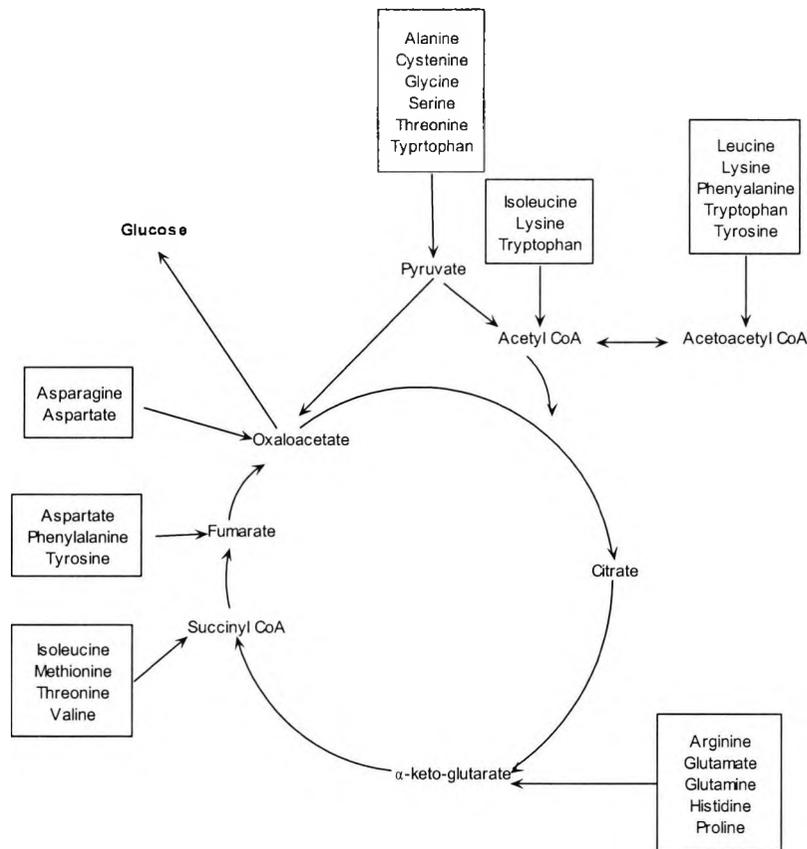
Figure 2.2: Amino acid disposal (Kreb's cycle)

Although the liver is the major site of nitrogen metabolism in the body, all tissues have some ability to synthesise non-essential amino acids, remodel amino acids, and convert non amino acid carbon skeletons into amino acids and other products that contain nitrogen. In times of dietary surplus, the potentially toxic nitrogen of amino acids is eliminated via transamination, deamination, and urea formation; the carbon skeletons are generally conserved as carbohydrate, via gluconeogenesis (i.e. glucose production), or as fatty acid via fatty acid synthesis pathways. Amino acids can thus be grouped into three categories: glycogenic, ketogenic, or glucogenic and ketogenic. Glucogenic amino acids are those that give rise to a net production of pyruvate or the Citric Acid cycle (TCA) intermediates, such as α-ketoglutarate or oxaloacetate, all of which are precursors to glucose production. Lysine and leucine are the only amino acids that can be described as purely ketogenic; all the other amino are at least partly glucogenic. Leucine and lysine only give rise to acetyl-CoA or acetoacetyl-CoA; neither of which facilitates net glucose

production. In addition, the amino acids isoleucine, phenylalanine, threonine, tryptophan, and tyrosine are characterised as being glucogenic and ketogenic because give rise to both glucose and fatty acid precursors.

2.1.5   Branched chain amino acid metabolism

Leucine, valine and isoleucine belong to a group of amino acids known as the branched-chain amino acids (BCAAs). Since humans cannot make the arrangement of carbon atoms found in BCAAs, these amino acids are an essential element in the diet. The catabolism of all three of these amino acids uses the same enzymes in the first two steps. The first step in each case is a transamination using a single BCAA aminotransferase, with α-ketoglutarate as amine acceptor. As a result, three different α-keto acids are produced and are oxidised using a common branched-chain α-keto acid dehydrogenase, yielding the three different CoA derivatives. Subsequently the metabolic pathways diverge, producing many intermediates (see Figure 2.2). The principal product from valine is propionyl-CoA, the glucogenic precursor of succinyl-CoA. Isoleucine catabolism terminates with production of acetyl-CoA and propionyl-CoA; thus isoleucine is both glucogenic and ketogenic. Leucine, which is classified as strictly ketogenic, gives rise to acetyl-CoA and acetoacetyl-CoA.

2.1.6   Protein turnover

While most proteins (e.g. skin) appear to remain virtually unchanged, especially during adult life, the true nature of proteins was suggested in the nineteenth century (Munro 1964) and demonstrated with the use of isotopic tracers in the first part of the twentieth century (Schoenheimer et al. 1939). Proteins are constantly being degraded into their constituent amino acids, and to maintain constant protein mass, new proteins are constantly being constructed. The degradation or breakdown of proteins is termed proteolysis; the construction of new proteins is termed synthesis. The term protein turnover is used to describe this simultaneous and steady breakdown (B) and synthesis (S).

There are roughly 11 kg of protein in a typical 70 kg man; typically 300 g of protein are broken-down and replaced every day, a turnover of about 2.7%. It has been estimated that one fifth of energy expenditure at rest after overnight fasting is dedicated to protein turnover; with much of this energy used in synthesis rather than proteolysis (Welle and Nair 1990). If the body spends that much energy on protein turnover, then clearly it is of great biological importance. Protein turnover

9

is necessary to maintain the quality of body proteins; in addition, the rate of turnover is an important factor in regulating the concentration of a given protein.

2.1.7   Problems in determining protein turnover in man

Whether the quantification of the rates of protein synthesis and breakdown is possible or physiologically meaningful is still received by some with a degree of doubt. This is because (and as discussed below) measuring whole body protein turnover (WBPT) is an intrinsically difficult problem. If one does agree that there is value in knowing protein turnover rates, the process of determining these is not without difficulty, and there are several problems facing investigators. Bier (1989) gives an insightful look at these and we outline the major issues below.

In order to study WBPT, one is faced with, what Bier (1989) calls, the intrinsically difficult problem. The problem is that there are 20 amino acids in man and 20 different amino acid subsystems. Each subsystem is unique and closely related with the other amino acids subsystems. These subsystems are responsible for providing the raw materials for not only proteins, but for the synthesis of other (non-essential) amino acids. In practise, investigators tend to use one or more amino acids (often, but not necessarily an essential amino acid) and generalise their findings for the whole body.

There are practical difficulties as well. For instance, WBPT is usually estimated in humans by measuring the enrichment of an amino acid in the plasma; although, both protein synthesis and breakdown occur intracellularly and there are several stages before a protein is catabolised into its constituent amino acids (see Figure 2.3). Many of the techniques used to estimate WBPT do not consider intermediary products, although the hydrolysis of a single peptide bond is enough to make a protein inactive.

Perhaps the largest problem facing those who investigate protein turnover in man, is the fact that WBPT represents the metabolism of a vast number of different proteins in the body. Thus, WBPT does not therefore refer to a single process, but includes countless processes representing protein synthesis and breakdown and the many intermediary steps occurring at any given time in the body. It is therefore very difficult to say whether an estimate of protein turnover is correct or not. There is no way to independently validate the results. One method of assessing the correctness of a model is to compare WBPT data provided by differing techniques in the same subject (and when possible at the same time). There are several questions regarding the accuracy and authority of the techniques used; and many assumptions are made which are knowingly incorrect, over-simplified or unprovable, but protein turnover is too fundamental a biological process to be ignored. And it

10

is precisely because estimating WBPT is difficult that several techniques have been developed, each with its own assumptions, limitations and drawbacks.

J.C. Waterlow, who has been involved in protein turnover studies for the last 40 years, observes that the concept of 'whole body protein turnover' is not dissimilar to the concept of the 'metabolic rate'; and that exploration of the latter has proved extremely valuable in the study of energy metabolism (Waterlow 1980). So, whatever its shortcomings, the study of WBPT is necessary and useful.
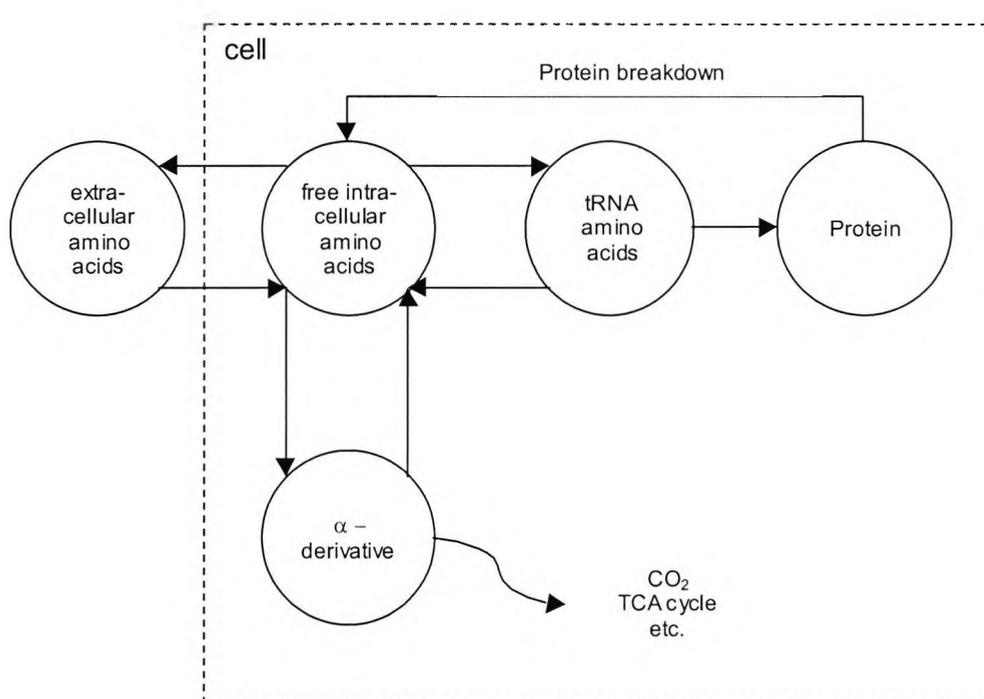
Figure 2.3: Amino acid pathways for protein synthesis and breakdown.

2.2 Review of methods used to measure whole body protein turnover

As noted before, protein turnover in man was first estimated during pioneering studies starting in the 1930s (Schoenheimer et al. 1939;Schoenheimer 1942;Schoenheimer and Rittenberg 1938). During the last two decades there has been increased interest in the area of protein metabolism (especially *in vivo*). This has come about due to availability of a large range of commercially produced stable labelled isotope tracers, along with the development of reliable and relatively cheap mass spectrometers, and the advances in computing and data processing techniques. The

11

use of stable isotopes will be dealt with below (Section 2.4), but first let us review the methods used in the study of protein turnover in man.

The study of protein turnover can be categorised in several ways. For instance, it is has been traditionally appropriate to compare tracee mass balance approaches (essentially the nitrogen balance technique) with tracer kinetic approaches. However, it is also useful to make the distinction between methods that directly or indirectly measure *whole-body* protein turnover (Section 2.2.2), and those that measure tissue protein metabolism *in vivo* (Section 2.2.6). In addition, the methods may also be categorised according to the underlying mathematical assumptions made by the technique, for instance, compartmental (Section 2.2.4.5) vs. stochastic analyses (most other models).

2.2.1   Nitrogen balance technique

The earliest studies of measuring protein metabolism in man involved determination of the nitrogen balance. The nitrogen balance is determined by measuring the amount of nitrogen ingested and subtracting nitrogen losses in urine, faeces and sweat. The technique thus attempts to quantify overall protein synthesis and breakdown by analysing the differences between nitrogen intake (N_i) and nitrogen losses (N_o). Since nearly all nitrogen in the body is contained within proteins, a positive nitrogen balance (i.e., $N_i - N_o > 0$) implies that body proteins have increased; conversely a negative N balance ($N_i - N_o < 0$) implies that body proteins have decreased. During growth, the nitrogen balance is positive, while during starvation or forced immobilisation, nitrogen losses exceed intake, and the nitrogen balance is negative. Most of the information available on the regulation of whole body protein metabolism in man has been obtained using the nitrogen balance technique.

Although the N balance technique requires no unprovable (or incorrect) assumptions, there are many problems associated with nitrogen balance studies that make its continued use questionable. The technique routinely results in nitrogen losses being underestimated because it is extremely difficult to measure nitrogen lost from all body routes. For example, it is difficult to measure nitrogen losses through perspiration during exercise (Calloway et al. 1971;Kopple 1987); and gaseous nitrogen losses (Costa et al. 1968;Kurzer and Calloway 1981). In addition faecal and urine samples may adhere to collection containers, thus underestimating N_o. There is the problem of overestimating dietary nitrogen intake, as food may be left on eating and cooking utensils, thus overestimating N_i. Although these may seem like trivial details, the nitrogen balance technique relies on measuring the small difference between intake and output, and these small errors can produce large differences in the calculated N balance.

The inadequacy of the nitrogen balance method has not gone unnoticed, and several scientists (Hegsted 1963;Hegsted 1976;Young 1986) have questioned the validity of using nitrogen balance techniques and arguing that there is 'systematic inherent error in the way nitrogen balance studies are performed'. Young (1987) points out that *'body N equilibrium does not necessarily reflect an adequate state of organ protein metabolism or of the nutritional status because it does not reveal possible alterations in the intensity, quality and/or distribution of tissue and organ protein metabolism'.*

The main criticism of balance techniques is that they provide insufficient (albeit useful) information. Balance studies only yield information concerning the static condition of the system. For instance if there was a decrease in protein synthesis and a corresponding change in proteolysis a method such as the nitrogen balance method would show no evidence of these changes, i.e., 10 – 9 is 1, 100 – 99 is also 1. The nitrogen balance technique simply measures external processes, it takes a black box approach to protein metabolism, and does not attempt to examine, measure or even distinguish between internal mechanisms. As Schoenheimer and Rittenberg (1938) noted:

> *The weakness of biological balance studies has been aptly illustrated by comparison with the working of a slot machine. A penny brings forth one package of chewing gum; two pennies bring forth two. Interpreted according to the reasoning of balance physiology, the first observation is an indication of the conversion of copper into gum; the second constitutes proof.*

Waterlow (1999) has recently reviewed 'the mysteries of the nitrogen balance', and notes that 'although the achievement and maintenance of N balance is a fact of life that we tend to take for granted, there are many features of it that are still not understood'. We consider several alternative approaches to estimating protein turnover in man in the following section.

2.2.2 Tracer kinetic approaches

To address some of the limitations of the N balance method, Schoenheimer and colleagues used isotopically labelled amino acid *tracers* to determine protein turnover in a series of pioneering studies starting in the 1930s (Schoenheimer et al. 1939;Schoenheimer 1942;Schoenheimer and Rittenberg 1938). Some of the main methods used to determine protein turnover in man will be reviewed, but first it is necessary to dwell on some general issues concerning isotopically labelled tracers.

Isotopically labelled amino acids or tracers are used extensively in the study of protein turnover - the endogenous substance is known as the *tracee*. According to Atkins (1969), the perfect tracer should have the following properties:

1. The tracer is detectable by the observer, i.e. there must be some method by which the amount of tracer in a sample can be quantified.

2. The biological system should not be able to distinguish between the tracer and the tracee. This is sometimes referred to as the Principle of Tracer Indistinguishability. In the case of a ^{13}C and ^{15}N labelled amino acid tracers, this is a reasonable assumption; as the effects of these isotopes are below the threshold of biological importance.

3. The tracer should be able to be added in small amounts, so as not to disturb the steady state existing in the system as a whole.

Although these requirements are usually met, it is useful to note the principles underlying what makes an ideal tracer, as problems associated with these principles can arise. By definition a tracer has its own kinetics. Data collected represent the kinetics of the tracer and not the tracee. The goal of the study is however to infer from tracer kinetics the kinetics of the tracee. If the tracer has met the three criteria above, this may be possible. The relationship between tracer and tracee is described below (Section 2.4.4).

2.2.3 Methods using [^{15}N]-glycine (end product method)

Springson and Rittenberg (1949) were the first to use [^{15}N]-glycine to measure whole-body protein turnover. They administered a single bolus of [^{15}N]-glycine and measured and analysed urinary [^{15}N] data over three days. The schematic of the model used is shown in Figure 2.4.

The tracer is allowed to mix thoroughly in the body active nitrogen pool through various processes; (Figure 2.4) the dilution of tracer represents the net flow of unlabelled amino acid nitrogen (tracee) from dietary sources or from protein breakdown. The original model was incrementally improved by a series of studies. San Pietro and Rittenberg (1953a;1953b) modified the mathematics of the model to account for the slowly turning-over urea pool. Olesen et al (1954) made a distinction between fast and slow turning over protein compartments. Others (Birkhahn et al. 1981;Jeevanandam et al. 1979;Taruvinga et al. 1979;Tschudy et al. 1959;Wu et al. 1959;Wu and Bishop 1959;Wu and Sendroy 2001) have examined the use of several other [^{15}N] labelled amino acids as alternatives to [^{15}N] glycine.
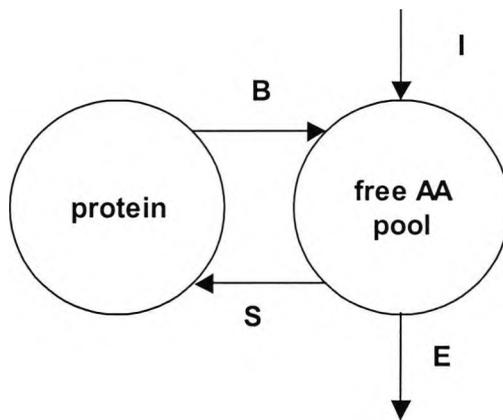
Figure 2.4: General model for estimating whole body nitrogen kinetics – end product method. S = protein synthesis; B = protein breakdown; I = dietary nitrogen intake; and E = nitrogen excretion. A bolus of [^{15}N] glycine is administered, and its dilution by amino acids from diet (D) and by amino acids released from protein breakdown is estimated by sampling [^{15}N] in urine.
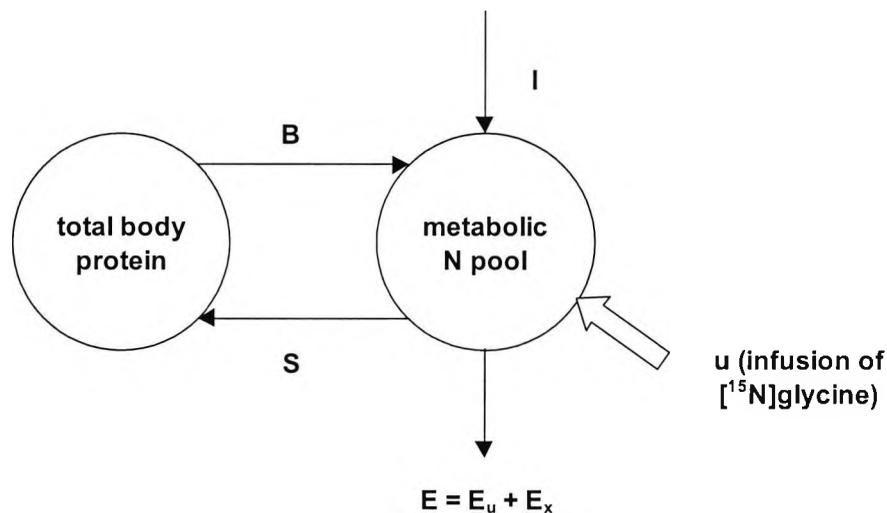
Figure 2.5: Pico and Taylor-Roberts model of [^{15}N]-glycine protein metabolism. I = intake from dietary protein, B = protein breakdown; S = protein synthesis; E excretion from urinary urea (E$_u$) and non-urea end-products (E$_x$).

Picou and Taylor-Roberts (Picou et al. 1969;Picou and Taylor-Roberts 1969) modified the technique by administering a constant infusion, this has the benefit of simplifying the mathematics of the model and it also reduces the number of samples required. The Picou and Taylor-Roberts method (shown in Figure 2.5) involves the administration of [^{15}N]-glycine (intravenously or orally) until a plateau in [^{15}N] enrichment is achieved. This is usually obtained within 20 – 40 hours; the length of infusion can be reduced to as little as 6 hours with a primed constant infusion (Jeevanandam et al. 1985). Urine samples are taken at the plateau, and the enrichment of [^{15}N] urea is then calculated. Once the system is in steady state (i.e. when the rate of amino acids

entering the metabolic pool is equal to the rate at which they leave) the model may be expressed as:

$$I + B = S + E = Q$$

where Q is the amino flux. In the steady state the Q is equal to the rate of infusion (u) divided by the enrichment of tracer (e):

$$Q = \frac{u}{e}$$

Protein synthesis (S) can be estimated by:

$$S = Q - E$$

and protein breakdown (B) by:

$$B = Q - I$$

The [^{15}N]-glycine model is based on the following assumptions (Golden and Jackson 1981): (1) [^{15}N] and [^{14}N] are biologically indistinguishable and the tracer is weightless; (2) the tracer is not recycled (3) the metabolic pool of N remains constant during tracer infusion; (4) there is a single metabolic N pool; (5) the tracer is thoroughly mixed within the N pool; (6) tracer dilution is mainly caused by diet and protein breakdown; (7) synthesis and excretion are the major pathways of glycine N disposal; (8) glycine N is an appropriate tracer for amino acid N.

The most significant practical problem with the [^{15}N]-glycine method occurs when a primed infusion is not used, since up to 40 hours may be required for the system to reach steady state. Under such circumstances it is difficult to be certain that the assumption that the metabolic N pool remains unchanged is held. A possible solution is to give the subject hourly meals throughout the experiment; this however disrupts the physiological (and normal) behaviour of the subject. Even if it were possible not to feed the subject for 40 hours, the method cannot estimate true post absorptive turnover rates, because after 40 hours without food physiological changes will occur.

Ignoring practical problems, many of the assumptions that the model makes are either incorrect or highly questionable (Waterlow 1981), and as early as 1959, Tschudy et al. (1959) noted that there were 'inherent errors' in the assumptions. For instance, the model depends on the assumption that

there is a one, well-mixed and active N pool. Several experiments have shown that this assumption is most likely incorrect. For instance, a) orally and intravenously administered [^{15}N]-glycine tracers provide different turnover rates (Fern et al. 1981;Fern et al. 1985); b) N flux is different depending on the choice of N tracer (Jackson and Golden 1980;Taruvinga et al. 1979); and c) [^{15}N] enrichments from urinary urea and ammonia end products are consistently different (Fern et al. 1981;Fern et al. 1985;Waterlow et al. 1978b). All of these results indicate the existence of more than one N pool. Nevertheless, the model has remained in use despite its theoretical limitations, because it is simple conceptually, and also because the results obtained using the N balance method are in agreement with the expectations of the investigators.

2.2.4   Methods using [^{13}C]-leucine

The branched chain amino acids (BCAAs) leucine, isoleucine and valine play a prominent part in the muscle amino acid metabolism. The BCAAs are all essential amino acids, and they alone make up about 40% of the minimal daily requirement of amino acid in man. The BCAAs are important not only as essential substrates, but also as biochemical regulators or precursors in complex metabolic reactions (Adibi 1976). The BCAAs are principally metabolised in tissues such as muscle; this is fundamentally different from the other essential amino acids, which are oxidised principally in the liver. The unusual metabolism of the BCAAs, coupled with the fact that they are not produced endogenously makes this subset of amino acids well suited to the study of estimating protein turnover in man. Of the 20 or so amino-acids systems in the body, the leucine system has been studied to the greatest degree.

Leucine is an essential amino acid; and is thus not produced *in vivo*. The first metabolite of leucine is α-ketoisocaproate (KIC). Leucine is in constant flux with its keto-acid, KIC, through a reversible transamination reaction (Taylor and Jenkins 1966). During de-amination, the amino (NH$_2$) group is lost to the nitrogen pool; the resulting KIC has two fates, it may be re-aminated to leucine, or it may undergo an irreversible decarboxylation to CO$_2$. Both leucine and KIC have metabolic pools in the plasma and in intracellular space. The transamination process occurs only in intracellular space and is reversible and fast. Leucine enters the system from protein breakdown, and leaves the system through incorporation into proteins or through irreversible oxidation (see Figure 2.6 and Figure 2.7)
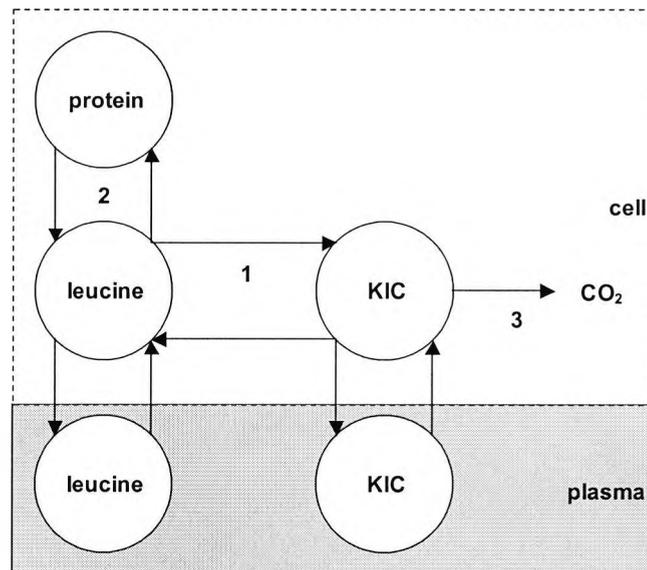
Figure 2.6: Leucine metabolism: major metabolic events of leucine and KIC; 1) The reversible transamination; 2) the incorporation of leucine into proteins and release from leucine from proteins, 3) the irreversible decarboxylation.
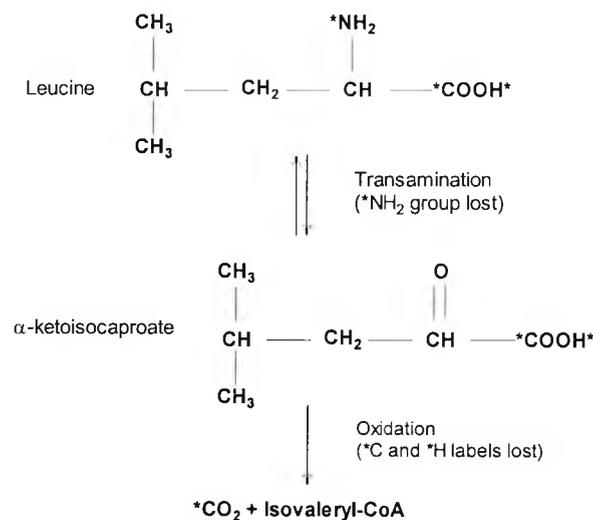
Figure 2.7 Schematic of leucine metabolism, showing the chemical structure of leucine, and associated products. The symbol * indicates where commonly labelled isotopes may lie.

2.2.4.1 Early [^{13}C]-leucine models

Waterlow (1967) originally proposed the model shown in Figure 2.8 to describe the kinetics of an essential amino acid, initially using a lysine tracer. O'Keefe (1974) was the first to use this model for a leucine tracer. The model is oversimplified and it assumes that a) there is a single leucine pool; and b) a single source of protein entering and leaving it. Neither of these assumptions is true,

there are at least two leucine pools (intracellular and plasma), and there are hundreds of different proteins each with their own metabolism. The original investigators were well aware of the shortcomings of the model; nevertheless several decades later, and we will see below, many of the models in use today are still based on similar assumptions, which are either questionable or unprovable.
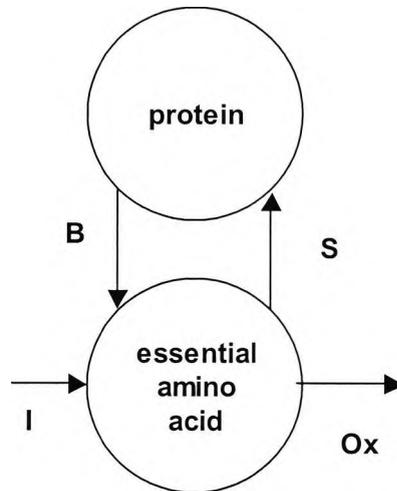
Figure 2.8: Original model for kinetics of an essential amino acid.

The keto-acid of leucine, KIC was first incorporated into a leucine model by Matthews (1981), the model involved the use of a $[^{15}N,^{13}C]$-leucine tracer and allowed the calculation of leucine transamination rates, in addition to B and S. Next, Matthews (1982) and Wolfe (1982) further incorporated KIC into leucine system modelling and allowed a more accurate account of leucine oxidation rates. This model is now known as the primary pool and it is dealt with in more detail below. A few years later Schwenk (1985a) described what is now known as the 'reciprocal' pool model

The primary (Matthews et al. 1982;Wolfe et al. 1982) and reciprocal pool models (Schwenk et al. 1985a) proposed in the 1980s have since dominated the study of leucine kinetics, and they represent the *de facto* tools for estimating leucine turnover in man. Both models are based on infusing labelled tracer over a few hours and then analysing the resulting isotopic plateau. The model implied by both the primary and reciprocal pool models is shown in Figure 2.9. In the steady state

$$Q = S + Ox = B + D$$

under fasting conditions, the dietary intake $D = 0$, where Q = the rate of leucine turnover or leucine flux, S = protein synthesis or non-oxidative leucine disposal, Ox = oxidation of leucine, B

= endogenous leucine appearance from protein breakdown, D = leucine from dietary intake. We will examine the primary pool and reciprocal pool models more closely in the sections below.
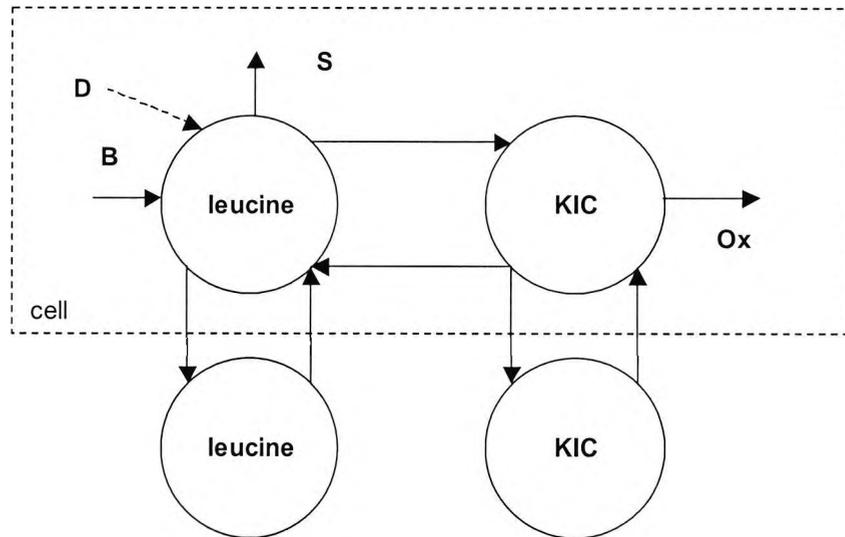
Figure 2.9: The implied open four-pool model used to study leucine and KIC kinetics. where D = dietary intake, B = protein breakdown, S = protein synthesis, Ox = leucine oxidation. Note the model includes intracellular and plasma pools for both leucine and KIC.

2.2.4.2 The primary pool model

The primary pool model requires a constant infusion (which may be accompanied by a priming bolus) using either a single tracer (labelled leucine, u_L), or two tracers (labelled leucine, u_L, and labelled KIC, u_K). After isotopic plateau is reached, tracer concentrations and expired CO_2 are measured. Assuming tracer / tracee indistinguishability, the rate of appearance of leucine (Ra_L) and KIC (Ra_K), can be calculated as follows:

$$Ra_L = \frac{u_L}{z_L}$$

$$Ra_K = \frac{u_K}{z_K}$$

where $z \approx sa$ (specific activity) for radioisotopes; and z is the tracer to tracee ratio (TTR), a detailed explanation of TTRs can be found in Section 2.4.2 below. Leucine from protein breakdown B_P (subscript P denotes primary pool model) may be estimated in two ways, depending on whether one or two tracers are in use. For single tracer experiments

$$B_P = Ra_L$$

and for two tracer experiments

$$B_P = Ra_L + Ra_K$$

The equation for single tracer experiments is conceptually sound, however, one would expect it to underestimate *intracellular* leucine release from protein breakdown, because it measures the appearance of leucine into *plasma*. Cobelli (1991) notes that there is no theoretical basis for the summation in the equation for two tracer experiments, rather the summation is used to correct numerically the underestimation found in the single tracer experiments.

The precursor site for leucine oxidation, i.e. the intracellular KIC pool, is inaccessible to direct measurement. However, information on tracer enrichment of this pool is required in order to calculate leucine oxidation (*Ox*). The primary pool model assumes that measurements made in the plasma leucine pool approximates the enrichment of the intracellular precursor (leucine) pool, and calculates Ox_P by dividing the rate of expired labelled CO_2 (ϕ_{CO_2}) by $z(t)_L$:

$$Ox_P = \frac{\phi_{CO_2}}{z_L . c}$$

where c is some factor, which accounts for bicarbonate kinetics. The value c expresses the imperfect recovery of CO_2, and is always less than 1; usually the value used is 0.8 as reported by James (1976).

Leucine incorporation into proteins is calculated as the difference between protein breakdown and leucine oxidation.

$$S_P = B_P - Ox_P$$

2.2.4.3 The reciprocal pool model

The reciprocal pool model was proposed to estimate protein breakdown B and synthesis S and leucine oxidation Ox in steady state conditions. The reasoning is based on the observation made by Matthews (1982); since KIC is produced only by leucine in intracellular space, it is reasonable to assume that plasma KIC tracer to tracee ratios accurately reflect those of intracellular leucine. Schwenk (1985a) developed this model further and proposed that the same measure of leucine turnover can be obtained regardless of tracer infused. That is, if leucine is infused then plasma

KIC is measured; and if KIC is infused then plasma leucine is measured. Thus, protein breakdown B may be expressed as:

$$B_R = \frac{u_L}{z_K}$$

$$B_R = \frac{u_K}{z_L}$$

where subscript R refers to reciprocal model, subscripts L and K denote measurements of leucine and KIC respectively. Leucine oxidation and leucine incorporation into proteins are calculated as follows:

$$Ox_P = \frac{\phi_{CO_2}}{z_K.c}$$

$$S_R = B_R - Ox_R$$

2.2.4.4 Validity of primary and reciprocal pool models

Although the primary and reciprocal pool models are in widespread use, there are several known issues with these techniques, and the domain of validity of these models has been questioned (Bier 1989;Cobelli and Saccomani 1991;Matthews and Cobelli 1991); the major criticism is that the models are too simple to adequately describe the complex leucine system. The assumptions made by these models are shown in Table 2.2.

The primary pool model routinely underestimates protein breakdown, because it assumes that leucine Ra is equal to protein breakdown. However, Ra_L only estimates the release of *intracellular* leucine into the *plasma* pool and **not** the arrival of leucine into *intracellular* space (which is true protein breakdown). Schwenk (1985a) among others tried to correct for this under valuation of B, simply by adding the rate of plasma appearance of KIC (see Figure 2.10). There is however no theoretical basis for adding these two variables, and physiological interpretation of this sum is vague (Cobelli and Saccomani 1991). Furthermore, it can be shown that primary pool calculations will always provide a value of Ox that is not equal to true rate of leucine oxidation; and the difference, may either over- or underestimate true Ox (Cobelli and Saccomani 1991).

The reciprocal model suggests that since KIC is produced only by leucine in intracellular space (see Figure 2.10), plasma KIC enrichment accurately reflects those of intracellular leucine, so much so that plasma KIC enrichment may be used an index of intracellular leucine enrichment and thus may be used to calculate leucine turnover and oxidation i.e., for a leucine tracer $B_R = u_L / z_K$ and for KIC tracer $B_R = u_K / z_L$ (Matthews et al. 1982;Wolfe et al. 1982). Cobelli and colleagues (Cobelli et al. 1991;Cobelli and Saccomani 1991) have shown, using a compartmental model similar to that implied by the reciprocal model, that the reciprocal model estimates B exactly for a leucine tracer, but for a KIC tracer, it will routinely overestimate protein breakdown. Secondly, the reciprocal model is also in error in assuming that c - the recovery factor of expired CO_2 is fixed (usually $c = 0.8$), as the recovery factor is known to exhibit an inter-subject variation (Hoerr et al. 1989).

For reciprocal pool model

$B_r = u_L / z_K$

or

$B_r = u_K / z_L$

For primary pool model

$B_p = Ra_L = u_L / z_L$

or

$B_p = Ra_L + Ra_K$
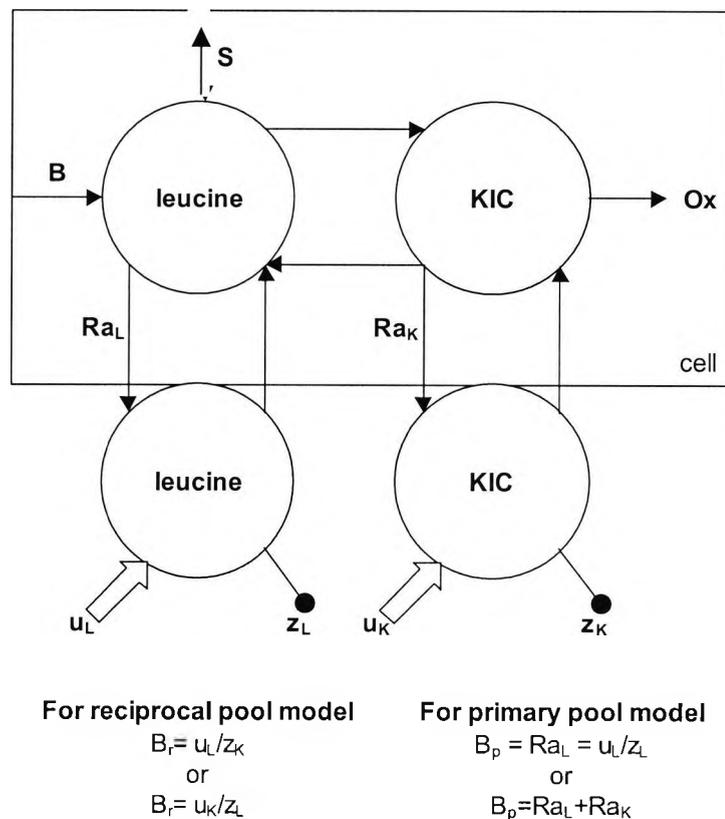
Figure 2.10 Assumptions made by primary and reciprocal pool models

Table 2.2: Assumptions of primary and reciprocal models

Assumptions
For both reciprocal & primary pool models
• There is no difference in the metabolism of [^{13}C]-leucine and endogenous leucine or [^{13}C]-KIC and endogenous KIC
• There is negligible recycling of tracer, i.e. there is negligible release of tracer labelled leucine once it has been incorporated into protein structure.
• The four-compartmental model (Figure 2.9) accurately describes leucine kinetics.
• The bicarbonate system may be quantified by a fixed value between individuals.
Primary pool model assumptions
• Protein breakdown may be quantified by either Ra_L or $Ra_L + Ra_K$
Reciprocal pool model assumptions
• Enrichments of plasma KIC reflects those of intracellular leucine (i.e. leucine transamination is so rapid that intracellular leucine and plasma KIC have roughly the same level of tracer enrichment)

2.2.4.5 Compartmental models of leucine kinetics in man

There are two general approaches to the measurement of whole-body protein turnover using a leucine tracer, compartmental analysis and stochastic analysis. The main difference between the two methods is that in a compartmental approach there is an assumption that the exchanges between compartments occur by first order kinetics, stochastic approaches make no assumptions about how transfers occur, but focuses on the overall process. In practice, compartmental models usually require a larger number of samples than stochastic approaches and require significant computing power to estimate the parameters. It has been noted that there is often large variability between the derived parameters from compartmental analyses. Despite these objections, the compartmental approach is useful because it allows more complex models to be designed and analysed, and furthermore it offers the potential to produce far more information about the studied system than stochastic approaches. We consider two models, which use compartmental analysis. An introduction to compartmental analysis may be found in Section 2.4.1.

Umpleby (1986) presented the first true attempt at modelling leucine metabolism and its oxidation to CO_2 (Figure 2.11). The study involved a bolus injection of ^{14}C leucine; plasma leucine and expired CO_2 samples were measured. However, since no attempt was made to include KIC, Bier (1989) notes that this reduces the overall domain of validity of the model. According to the authors, leucine metabolism must occur in compartment 1 or 2, or the model would be unidentifiable. In addition, the model (see Figure 2.11) shows no site of net leucine inflow, because the model describes only labelled substance. Since the site of net leucine inflow was unknown, rates of leucine production, oxidation and incorporation into protein were calculated for a net inflow into either compartment 1 or 2 or 3. They found that protein synthesis was 14-24% lower when net leucine inflow was considered to enter into compartment 1 compared with compartments 2 or 3. This is consistent with the 'primary' and 'reciprocal' pool approaches

described previously. Another important feature of this model was its ability to predict measured CO_2 values over a wide range of leucine oxidation rates in normal and diabetic subjects.
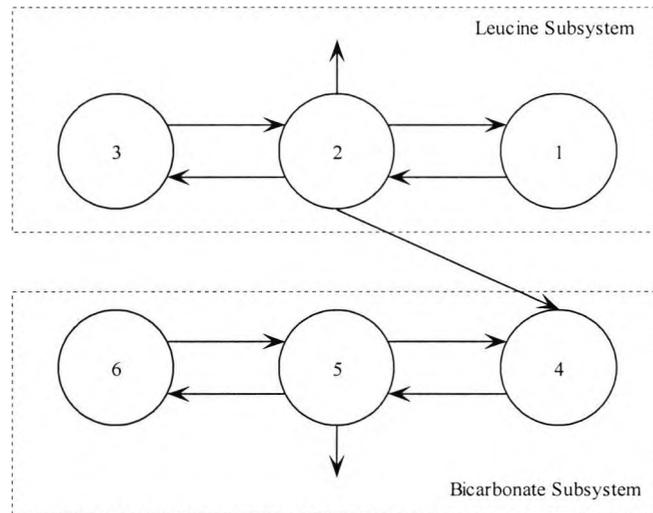
Figure 2.11 Compartmental model of leucine kinetics as proposed by Umpleby (1986). Compartment 1 was fixed as plasma, and tracer was injected into, and samples were taken from it. Compartment 2 was selected as the site of leucine oxidation (k_{42}) and protein synthesis (k_{02}). If Compartment 3 were taken as the site for leucine metabolism, the model would be unidentifiable.

Cobelli et al. (1991) provides the most comprehensive work to date on leucine kinetics. The model of leucine and α-ketoisocaproate (KIC) in humans is shown in Figure 2.12. Their findings are based on the results of a two-part experiment. Part I involved the simultaneous infusion of [^{13}C]-leucine and [^{2}H]-KIC into the plasma. This results in four tracer enrichment curves, namely [^{13}C]-leucine, [^{2}H]-leucine, [^{13}C]-KIC and [^{2}H]-KIC. In Part II, labelled bicarbonate was injected into the plasma, and labelled CO_2 in the expired air was measured. The authors suggest an 11 compartmental model, which includes a four-compartment bicarbonate sub-model concerned with the irreversible oxidation of KIC. The model allows the measurement of several leucine kinetic events, including the incorporation of leucine into proteins, leucine release from proteins, and the irreversible oxidation of KIC. The authors infer that there are three separate compartments where leucine is incorporated into protein, one of which is a 'protein-linked leucine pool' (compartment 6). It is assumed that this pool is composed of fast turning-over proteins.

Although Cobelli et al. (1991) admit that 'it is difficult to assign to the various compartments a specific physiological entity, since they may reflect either specific intracellular sites or different kinetic events occurring in the same location'. Their findings reveal the existence of three free leucine pools (1, a plasma leucine compartment, 3 and 5 primarily intracellular pools). Transamination occurs through compartment 3, and incorporation into proteins occurs through

25

compartment 5. This compartmental structure is consistent with previous in vitro experiments that have shown that there are physically distinct intracellular leucine pools for protein synthesis (Clark and Zak 1981;Everett et al. 1981;Kelley et al. 1984;Martin et al. 1977). Compartment 6, the 'protein linked pool', accounts for perhaps 5% of whole body proteins, and consists of 'fast turning over proteins'; only quickly turning over proteins may be accessed during a 6 hour experiment.
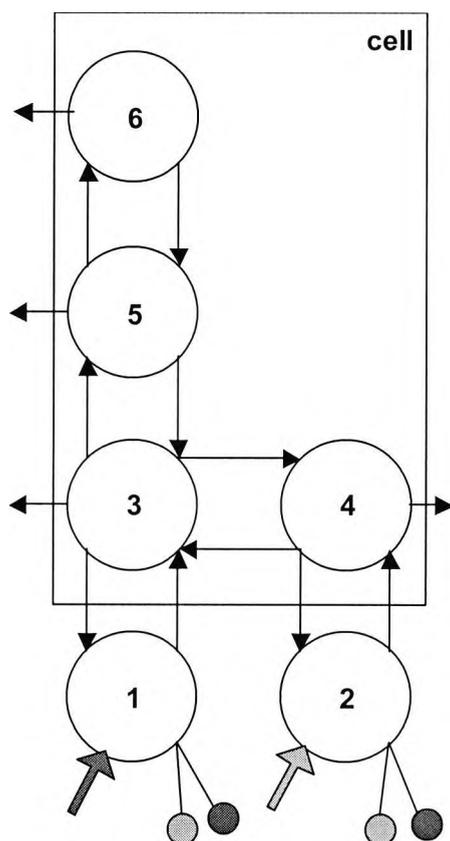
Figure 2.12: The Cobelli (1991) model . The diagram shows the infusion of $[^{13}C]$-leucine (into compartment 1) and $[^2H]$-KIC (into compartment 2); all four species are measured ($[^2H]$-leucine and $[^2H]$-KIC, $[^{13}C]$-leucine and $[^{13}C]$-KIC). All compartments represent tracer masses. Compartment 1 is plasma leucine; compartment 2 plasma KIC; compartment 3 and 5 represent intracellular leucine, compartment 4 represents an intracellular KIC and compartment 6 is thought to be a protein linked leucine pool.

2.2.5   Methods using $[^2H_5]$-phenylalanine

Like leucine, phenylalanine is an ideal tracer for studying whole body protein turnover. Phenylalanine is not synthesised endogenously, and only has two fates. It may be incorporated into proteins (synthesis) or converted to tyrosine. The first step in phenylalanine catabolism is

hydroxylation to tyrosine, this process occurs mainly in the liver. Thompson et al. (Thompson et al. 1989) developed a model using a primed continuous intravenous infusion of [^{2}H$_5$]-phenylalanine tracer along with a [^{2}H$_4$]-tyrosine primer. Following the administration of tracers, plateau plasma enrichment (of both tracers) is reached within 2 - 4 hours. The method allows the calculation of protein breakdown, synthesis and oxidation. Oxidation rate can be calculated from the enrichment of [^{2}H$_4$]-tyrosine at steady state. Whole body kinetics for phenylalanine and tyrosine are calculated using the equations (shown below) initially described by Thompson et al. (1989). Phenylalanine flux is calculated from the dilution of arterial plasma phenylalanine. The rates of flux (Q) of phenylalanine and tyrosine are calculated using knowledge of the infusion rate i, and the enrichments of infusate ($E_{infusate}$) and plasma amino-acid (E_{plasma}):

$$Q = i \cdot \left(\frac{E_{\inf usate}}{E_{plasma}} - 1 \right)$$

The rate of phenylalanine hydroxylation (Q_{pt}) is calculated by a similar expression, thus:

$$Q_{pt} = Q_t \cdot \left(\frac{E_t}{E_p} \right) \cdot \left[\frac{Q_p}{i_p + Q_p} \right]$$

where the Q_t and Q_p represent tyrosine flux and phenylalanine flux respectively; E_t and E_p represent labelled plasma enrichments of [^{2}H$_4$]-tyrosine and [^{2}H$_5$]-phenylalanine respectively; and i_p is the infusion rate of [^{2}H$_5$]-phenylalanine. The term $Q_p / i_p + Q_p$ corrects for the contribution of infused amino acid to hydroxylation. Using the knowledge that the flux of different amino acids into (synthesis) and out of (breakdown) protein must be in a constant ratio, which reflects the amino acid composition of the protein (Munro and Fleck 1969), we may write:

$$Q_t = Q_r \left(\frac{P_t}{P_p} \right) + Q_{pt} \left(\frac{i_p + Q_p}{Q_p} \right)$$

and rearranging the above equations provides a method for determining Q_{pt} which does not require the direct measurement of Q_t:

$$Q_{pt} = \frac{P_t}{P_p} \cdot \frac{Q_p^2}{\left(\frac{E_p}{E_t} - 1 \right) \cdot (i_p + Q_p)}$$

where P_t and P_p relate to the protein contents of tyrosine and phenylalanine, the ratio P_t / P_p is normally taken to be 0.73 from data derived from animal studies (Munro and Fleck 1969). In a modified version of this model an additional [^{2}H$_2$]-tyrosine tracer is administered (Pacy et al. 1991). This allows the measurement of total tyrosine R_a in arterial plasma. The method is similar to the measurement of CO_2 in [^{13}C]-leucine methods. The authors suggest that the [^{2}H$_2$]-tyrosine tracer should be used when the ratio P_t / P_p is not known. More recently, Short et al. (1999) demonstrated that approximating phenylalanine hydroxylation and tyrosine flux is associated with unacceptably high levels of variation and concluded that the full model (i.e. including the [^{2}H$_2$]-tyrosine tracer) should be used whenever possible.

Under fasting conditions and phenylalanine steady state:

$$Q_p = S_p + Q_{pt} = B_{phe}$$

where S_p represents the incorporation of phenylalanine in the free pool into proteins, and B_{phe} represents the entry of phenylalanine into the free pool from protein breakdown.

Since the [^{2}H$_5$]-phenylalanine does not require CO_2 breath samples it is sometimes preferred to [^{13}C]-leucine based methods. While collecting breath samples is not necessarily a practical issue when dealing with healthy subjects, it may be difficult in cases where subjects are, for example, ventilated or anaesthetised. In addition, leucine based methods require three different pieces of specialised equipment namely: a Gas Chromatography – Mass Spectrometer (GC-MS) for measuring leucine/KIC enrichment, an Isotopic Ratio - MS (IR-MS) for $^{13}CO_2$ enrichment and indirect calorimetry for determining CO_2 production. In clinical studies, the phenylalanine tracer has often been chosen since the method requires only a GC-MS.

The innate problems in using [^{2}H$_5$]-phenylalanine as a tracer are similar to those of a leucine tracer. The enrichment in plasma is generally less than in the cells so protein breakdown may be underestimated. Phenylalanine does not have a precursor similar to leucine's KIC that can be used as a marker of intracellular enrichment. The closest analogous metabolite is tyrosine, and as noted before the hydroxylation to tyrosine occurs mainly in the liver and not in many tissues. Nevertheless, using [^{2}H$_5$]-phenylalanine tracer in the manner described above, produces estimates of protein turnover very similar to those obtained using [^{13}C]-leucine (Pacy et al. 1991).

2.2.6 Measurement of tissue protein metabolism *in vivo*

The methods described above estimate whole-body protein turnover; whole-body methods do not provide information on the relative contribution of various tissues or organs to WBPT. For example, in an animal study, Ballmer et al (Ballmer et al. 1995) found that an injection of turpentine is associated with an increase in synthesis in the liver, but a decrease in skeletal muscle. These changes would not be detected by a whole-body technique. To overcome such limitations there has been much activity in developing methods that allow the estimation of protein synthesis rates of individual tissues *in vivo*.
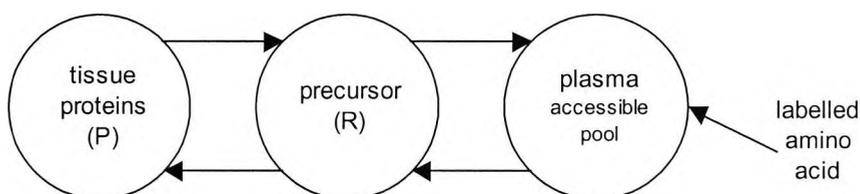
Figure 2.13: Conceptual representation of tracee precursor-product relationship used in the models estimating tissue protein synthesis *in vivo*.

These methods typically involve administering labelled amino acid tracer into the bloodstream, and taking samples of the specific tissue protein. They rely on the observation that the rate of isotopic enrichment of labelled amino acid in protein is equal to the difference between the flows to and from the tissue protein site. The mathematics of these approaches is based on knowledge of relationships between precursor and product (tissue protein). The following equation (from Figure 2.13) describes the general relationship:

$$\frac{dP}{dt} = k_R R - k_P P$$

where k_R is the fractional rate of incorporation of amino acid into protein (or the fractional synthesis rate, FSR), and k_P is the fractional rate of protein breakdown, in the steady state $k_R R = k_P P$; Toffolo et al (1993) describe the mathematics of this method in more detail. From the equation above, it is clear that in order to estimate the fractional synthesis rate it is necessary to measure the enrichment of the precursor pool. Two of the main approaches available include the constant infusion method and the flooding dose method. Both methods allow the fractional synthetic rate (FSR) of a protein (or a group of proteins) to be estimated from the change of incorporation of labelled amino acid into a specific protein (or group of proteins) over time. And

while the two methods are based on similar concepts, they differ in respect to a) how the labelled amino acid is administered; b) the amount of labelled amino acid used; c) how the incorporation of labelled amino acid into tissue is measured; and d) the timing of the measurements.

2.2.6.1 Constant infusion

The constant infusion method was first used by Loftfield (1956) and developed subsequently by Waterlow and Stephen (1966) and Garlick (1969). The approach was developed to avoid the problem of having to measure simultaneously a) the incorporation of labelled amino acid into tissue protein and b) the time course of the enrichment in tissue or plasma free amino acid; as both of these change very rapidly after a single injection (Waterlow et al. 1978a). Loftfield and Harris (1956) noted that when tracer was given as a constant intravenous infusion, the free amino acid enrichment would quickly rise to a steady state (plateau). In the steady state, protein synthesis can be calculated from measurements of i) precursor pool enrichment and ii) enrichment of tracer amino acid in the tissue being studied (Waterlow et al. 1978a;Waterlow and Stephen 1968). In the constant infusion method (with or without a priming dose), tracer is administered to achieve an enrichment of 5-10%, the length of the infusion (typically between 4 –12 hours) depends on the tissue of the protein of interest.

When the enrichment of the free amino acid pool becomes constant, the kinetics of incorporation of label into tissue protein becomes linear. FSR can be calculated by the equation (derived from the equation in Section 2.2.6):

$$FSR = k_R = \frac{(P_{t1} - P_{t0})}{R \cdot (t_1 - t_0)}$$

where P_{t0} and P_{t1} are the enrichments of tracer amino acid in the tissue protein at two different time instances, and R is the average precursor enrichment during the same time period, t_1 and t_0 represent the times at which sampling occurs. Theoretically the measurement of the precursor enrichment R should be made from the pool of aminoacyl tRNA in tissue, but this is impractical because the turnover rate of aminoacyl tRNA is extremely rapid and the pool size is small, thus measuring aminoacyl tRNA enrichment requires large tissue samples. The alternative is to use either the plasma or the tissue (intracellular) free amino acid, and in the case when a [^{13}C]–leucine tracer is used, plasma [^{13}C]–KIC is used as an index of precursor enrichment.

30

2.2.6.2 Flooding dose

Loftfield and Harris (1956) also developed what is now known as the flooding dose method. Loftfield noticed that when a labelled amino acid was administered to rats, the isotopic enrichment in tissues and plasma rose to a plateau; but the values in tissue were substantially lower than the plasma values. The dilemma then, was which of these (if any) should be used as a marker of precursor enrichment. The flooding dose method was devised in order to make the enrichment in intracellular equal to the enrichment in extracellular space, and thus overcome the problem of what should be used as the correct (or true) precursor enrichment in the calculation of protein synthesis *in vivo*. This was accomplished by injecting tracer (labelled amino acid) with a large bolus of tracee (unlabelled amino acid). For instance, Garlick (1989) demonstrated that 4g of $[^{13}C]$-leucine per 80kg body weight is sufficient to achieve almost complete equality between plasma and intracellular pools in muscle in healthy subjects over a two hour period. The FSR is determined using the following formula:

$$FSR = \frac{(P_{t1} - P_{t0})}{\int_0^1 R}$$

where P_{t0} and P_{t1} are the enrichment of tracer amino acid in the tissue protein at different times, and R is the average precursor enrichment during the same time period, t_1 and t_0 represent the times at which sampling occurs. $\int R$ is typically calculated as the area under the curve of the precursor enrichment between time t_1 and t_0. The relative merits and limitations of the constant infusion vs. the flooding dose method have been extensively discussed (Garlick et al. 1994;Rennie et al. 1994), and some key points are shown in Table 2.3.

Table 2.3: Merits and limitations of the 'constant infusion' and 'flooding dose' methods, two commonly used approaches to estimate protein tissue synthesis *in vivo*.

Constant infusion method	Flooding dose method
Advantages	*Advantages*
- Applicable even when studying slowly turning over proteins.	- There is less uncertainty regarding precursor enrichment
- Whole-body protein turnover can be measured simultaneously, thus the relationship between specific tissue proteins turnover and whole body turnover may be identified.	- There is no requirement that steady state conditions are met or maintained
- The method does not (or should not) disturb metabolism	- The procedure is much quicker than constant infusion method (1.5 h vs. 4-6 h for infusion method)
Disadvantages	*Disadvantages*
- The need for metabolic steady state – this may exclude acute metabolic events (e.g., after a meal, acute illness, during surgery).	- The 'flooding dose' may itself affect protein turnover.
- If aminoacyl tRNA measurements are not used there is uncertainty about what should be used as an index of precursor enrichment.	
- If aminoacyl tRNA measurements are used large tissue samples must be taken.	

2.2.6.3 Arterio-venous balance method

The arterio-venous (AV) balance approach was developed to allow the simultaneous measurement of protein synthesis and breakdown in muscle (Cheng et al. 1985). The advantage of the technique is that it does not require tissue biopsies – biopsy procedures themselves may alter protein turnover behaviour. Some researchers thus use arterio-venous difference to define the net balances of amino acids originally across the forearm, but has been also been used in the leg (Cheng et al. 1985;Cheng et al. 1987;Fryburg et al. 1990;Gelfand and Barrett 1987;Tessari et al. 1996b;Thompson et al. 1989). In addition the method has been used across several organs and other sites, for example, kidney (Tessari et al. 1996a), adipose tissue (Coppack et al. 1996), splanchnic tissue (Tessari et al. 1996a), cardiac muscle (Young et al. 1991). It is generally assumed that the arterio-venous difference across a limb is mainly due to muscle metabolism, and that other tissues, e.g., skin, bone and adipose tissue etc., contribute little (Macdonald 1999;van et al. 1999). Cheng (1985) originally infused a $[^{15}N,^{13}C]$-leucine tracer and measured concentrations of leucine, KIC, CO_2, as well isotopic enrichments of $[^{15}N,^{13}C]$-leucine, $[^{13}C]$-leucine, $[^{15}N]$-leucine, $[^{13}C]$-KIC and $^{13}CO_2$ as well as the flow in arterialised and deep venous blood. Barrett and Gelfand (1987) developed a simpler method which used a $[ring-2,6-^3H]$-phenylalanine tracer. One advantage of the phenylalanine method is that it requires much fewer measurements that the leucine model. The advantage of using leucine tracers, however is that information on leucine oxidation and transamination are obtained. Using the example when phenylalanine tracer is used in a limb, the net balance of amino acid tracee and tracer across the limb can be estimated from the equations:

$$Balance_{Tracee} = (C_a - C_v) \cdot F$$

and

$$Balance_{Tracer} = (C_a \cdot E_a - C_v \cdot E_v) \cdot F$$

where C is the concentration and E is the enrichment of tracer, the subscripts a and v denote arterial and venous sampling respectively, and F is the blood flow. Since the net balance in tracer and tracee are measured simultaneously, and phenylalanine is not oxidised or transaminated in the muscle; protein synthesis, can be derived from:

$$Synthesis = R_d = \frac{Balance_{Tracer}}{E_v}$$

Protein breakdown, which is equal to R_a, is calculated from:

$$Breakdown = R_a = R_d - Balance_{Tracee}$$

There are problems with this method. Since the arterial and venous differences are extremely small, these variables must be very precisely measured, even very small errors made in their measurement will propagate through the model, rendering the estimate useless. The model is thus only useful in relatively large animals. In addition, there is no consensus in the literature whether whole blood flow or plasma flow should be used to measure F.

2.2.7 Other methods

Numerous other methods have been used to measure protein turnover in man, and there are some excellent reviews available (Bier 1989;Smith and Rennie 1996;Wagenmakers 1999;Waterlow 1995;Welle 1999b). In particular, the model of lysine kinetics in young women proposed by Irving (1986) is one of the most comprehensive amino acids kinetics models. There are methods based on measuring the rate of release of hydroxyproline from tissues into blood, this allows accurate measurement of the rates of 3-methylhistidine or 3-methyllysine. The method has been used mainly for measuring 3-methylhistidine production (Lundholm et al. 1987;Rennie et al. 1984;Sjolin et al. 1989). The measurement of 3-methylhistidine excreted in urine has also been used to estimate myofibrillar protein breakdown (Cowgill and Freeberg 1957;Long et al. 1975;Rennie and Millward 1983;Tallen et al. 1954;Young and Munro 1978); use of this method

has been discouraged because the method is considered unreliable (Rathmacher 2000;Rennie et al. 1984;Rennie and Millward 1983).

2.3 Whole body protein turnover data in normal man

Infants and children have a positive N balance, for instance, a typical infant gains about 7kg of fat free mass in the two years following birth (Forbes 1987); about 1400g protein (230g nitrogen), the equivalent of a positive N balance of about 0.3 g per day (g/d). This slows to about 0.17 g/d between ages 2 and 10. This is then followed by a period of rapid growth (N balance of 0.3 g/d), the average male gains about 32 kg of fat free mass (females about 16 kg). Growth ends in adulthood. A weight-stable healthy adult has in principle a zero N balance, and typically (s)he only loses an insignificant amount of N over a period of days. In fact, if a weight-stable healthy adult shows an N balance which reflects a change of over 2% in protein mass, the most likely explanation is that the measured N balance is incorrect rather than that protein mass has changed so significantly.

Table 2.4: Normal whole body data in healthy adults for selected amino acids

Amino acid	Isotope (tracers) used	R_a (μmol/ kg/h)	Plasma concentration [1] (μmol/L)	Muscle concentration [1] (mmol/L)	
Glutamine	$[2\text{-}^{15}N]$- or $[5\text{-}^{15}N]$- glutamine	250 - 350	570 ± 88	19.45 ± 1.52	[2]
Alanine	$[^{15}N]$-,$[3,3,3\text{-}^2H_3]$-, $[1\text{-}^{13}C]$-, or $[3\text{-}^{13}C]$-alanine	250 - 350	330 ± 98	2.34 ± 0.45	[3]
Glycine	$[^{15}N]$-glycine	200 - 250	210 ± 54	1.33 ± 0.37	[4]
Leucine (w/ KIC enrichment)	$[1\text{-}^{13}C]$- or $[^{15}N,^{13}C]$-leucine	80 - 140	120 ± 24	0.15 ± 0.08	[5]
Leucine (w/ leucine enrichment)	$[1\text{-}^{13}C]$- or $[^{15}N,^{13}C]$-leucine	60 - 100	120 ± 24	0.15 ± 0.08	[6]
Lysine	$[^{15}N]$-, $[^2H_3]$ or $[^{13}C]$lysine	80 - 100	180 ± 30	1.15 ± 0.28	[7]
Valine	$[^{13}C]$-valine	60 - 85	220 ± 42	0.26 ± 0.10	[8]
Glutamate	$[^{15}N]$-glutamate	60 - 100	60 ± 21	4.38 ± 0.62	[9]
Phenylalanine	$[\text{ring-}^2H_5]$-phenylalanine	30 - 40	50 ± 6	0.07 ± 0.02	[10]
Tyrosine	$[1\text{-}^{13}C]$-tyrosine	35 - 45	50 ± 11	0.10 ± 0.03	[11]

[1] (Bergstrom et al. 1974)

[2] (Cortiella et al. 1988;Darmaun et al. 1986)

[3] (Yang et al. 1984;Yang et al. 1986)

[4] (Nissim et al. 1983;Robert et al. 1982)

[5] (Brillon et al. 1995;Matthews et al. 1990;Matthews et al. 1993;Russell-Jones et al. 1994;Umpleby et al. 1986;Umpleby et al. 1995) & Chapter 5

[6] (Brillon et al. 1995;Matthews et al. 1990;Matthews et al. 1993;Russell-Jones et al. 1994;Umpleby et al. 1986;Umpleby et al. 1995) & Chapter 5

[7] Numerous studies (Welle 1999c)

[8] (Meguid et al. 1986;Staten et al. 1986)

[9] (Darmaun et al. 1986)

[10] (Clarke and Bier 1982;Darmaun et al. 1986;Gelfand and Barrett 1987)

[11] (Clarke and Bier 1982;James et al. 1976)

The fact that weight stable adults have roughly zero N balance suggests that whole-body-protein synthesis is roughly equal to protein breakdown. In healthy young adults, using the [^{15}N]-glycine method over at least 48 hours, the average rate of protein turnover is about 3 g/kg/d (i.e. 3 grams per kilogram of body weight per day). In terms of fat free mass (FFM) this is about 3.75 g/kg/d (Jeevanandam et al. 1985;Morais et al. 1997;Uauy et al. 1978;Winterer et al. 1976;Young et al. 1975). This is the equivalent of a fractional rate of WBPT of about 1.9% per d, assuming 200g proteins per kg FFM. Note that turnover data derived from studies, which use tracer for lengthy periods, can be expected to underestimate turnover, as there will be recycling of the label. At least two studies (Abumrad et al. 1985;Schwenk et al. 1985b) have shown that recycling of a leucine tracer can become significant during prolonged infusion studies. Naturally the precise moment when tracer recycling becomes an issue is dependent on the details of the study and on the subject, but a reasonable estimate is in the region of less than 6 hours. Studies where tracer administration exceeds 12 hours must consider the possibility of recycling. Most studies that measure essential amino acid kinetics tend to last only a few hours (typically 2 – 6 hours). This does not completely solve the problem, as there are considerable variations in turnover rates during any 24-hour period. For instance, breakdown of endogenous proteins is fastest when no food is being absorbed in the gut; and protein synthesis is slowest at these times. Table 2.4 shows postabsorptive data for various amino acids in healthy subjects.

The rate of appearance (R_a) of the essential amino acids into plasma is proportional to the concentration of that amino acid in body proteins (Bier 1989;Block and Weiss 1956;Welle 1999c). This relationship is consistent with the theory, the cornerstone of most protein turnover studies, that the rate of appearance of amino acid (i.e. amino acid R_a) into plasma is a marker of proteolysis in the postabsorptive state. The above data represent whole body data; an *estimate* of the relative contribution to synthesis from organs and other tissues in man is shown in Figure 2.14. The estimates are based on postabsorptive synthesis in a 75 kg man with 60 kg fat free mass (Welle 1999c). The author warns that 'this figure should be considered as an educated guess rather than a precise summary'.
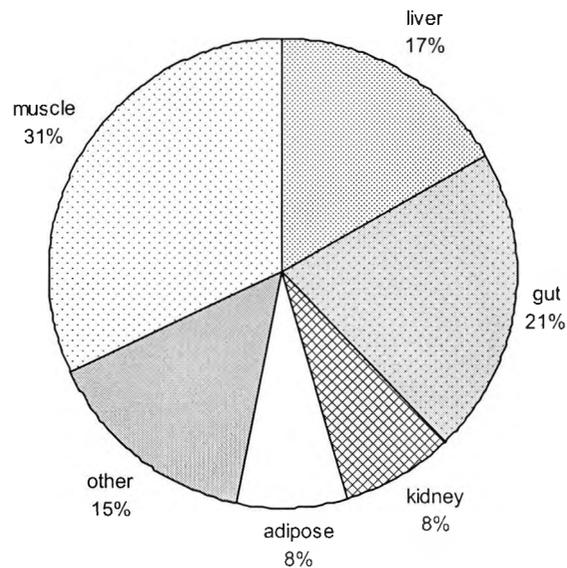
Figure 2.14: Estimated contribution of various tissues to total protein synthesis in a healthy adult

2.4 Modelling techniques and methods

The utilisation of mathematical modelling techniques in the study of metabolic and endocrine systems allows convenient and useful descriptions of metabolic processes to be formulated. Such mathematical models will, by definition, only represent an approximation of the system being modelled, and the validity of the model must be assessed in the context in which the model was developed, and on the purpose for which the model was intended.

Carson et al (1983) define a mathematical model of a system as '*a set of mathematical relationships between quantitative measures of system behaviour and properties*'. They emphasise that relationships between quantities in a model should correspond to the behaviour of 'real-world' variables to some extent, which is considered to be adequate. That is to say the model should be valid for the purposes for which the model was designed and conceptualised, and some effort should be made to define under which circumstances the model is considered to be valid - the model's domain of validity.

The design and detail of a mathematical model are determined principally by the purpose(s) for which the model is required. In general, the use of a model may be classified within the classical framework of descriptive, predictive and explanatory (Finkelstein and Carson 1979). The *descriptive* use of a mathematical model is the representation of quantitative relationships in the form of equations. Equations are concise and exact, for example, in a given system suppose a variable x was directly related to another one, say y, such that a change in x would lead to a

proportional change in y, this could be simple stated as: $y \propto x$ or even more succinctly as $y = \pmb{k} x$ (where $\pmb{k}$ is some constant). Additionally if the system being described consisted of several equations with several interacting relationships these equations may be manipulated and re-arranged to allow some analysis of the system and offer insights that may not be obvious from a wordy description. The *predictive* use of models would include cases where the model is used to make some inference on how the system might behave under certain stimuli. In metabolic modelling, a mathematical model may be used to predict the response to a drug or hormone. Mathematical models have an inherent *explanatory* nature. This is because such models require explicit definitions of the various interactions between elements in the system. The mathematical model itself is often the reason for further investigation. For example, if a model adequately describes the system under certain conditions, but predictions made by the model are not reflected by experimental data, further investigation may reveal a hidden interaction or the discovery of a new substance within the metabolic pathways. From observations on accessible variables, mathematical models allow the determination, identification and quantification of inaccessible system quantities.

2.4.1 The compartment system

A compartment system is a system, which is made up of a finite number of sub-systems or pools, which are called compartments. Atkins (1969) defines a compartment as '*a quantity of a substance which has uniform and distinguishable kinetics of transformation or transport.*' Therefore, a compartment may have no physical reality, but rather it represents a conceptual distinction of a substance, based not necessarily on its physiological location or purpose, but rather on how the substance is transported or metabolised within the body.

The transfer of a substance from one compartment to another may be represented by either the transport of the substance from one physical location to another (for example, the transfer of leucine from plasma to intracellular space) or may represent some chemical transformation of the substance within the same physiological boundaries (the conversion of leucine into KIC which occurs in intracellular space). Schoenheimer and Rittenberg (1935) first recognised the distinction between transport and chemical transformation.

Compartment models are used to model metabolic processes that do not involve active hormonal control (Carson et al. 1983), i.e., they are used to describe the kinetics of systems, which are metabolised by way of chemical reaction, storage and transport only. These models represent the flux of material from one compartment to another. This flux is assumed to depend, either linearly

or nonlinearly, on the mass or concentration of material in the source compartment only. Compartment models use circles to represent the various pools in the system and arrows to represent the flow of material between pools, a simple two compartment system is shown in Figure 2.15, and the main features are labelled.
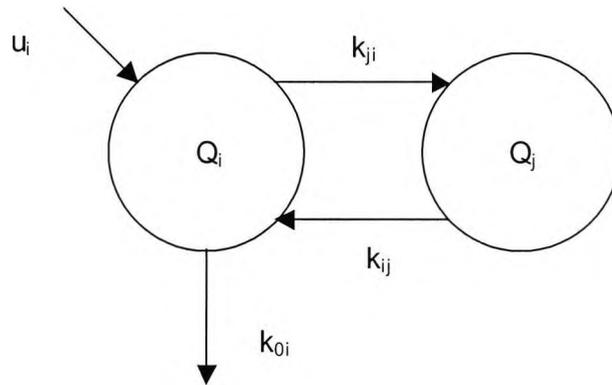
Figure 2.15: Compartment model definitions

The fractional transfer coefficient k_{ji} represents the fraction of substance that moves from compartment i to compartment j in unit time; $Q_i \geq 0$, represents the mass of substance in compartment i; and u_i represents the dosage of tracer. The flux F_{ji} may be defined as the product of the mass of a compartment and its fractional transfer coefficient:

$$F_{ji} = k_{ji} \cdot Q_i$$

In addition the model may be described by the following differential equations, (using dot notation):

$$\dot{Q}_i = u_i + k_{ij}Q_j - k_{ji}Q_i - k_{0i}Q_i$$

$$\dot{Q}_j = k_{ji}Q_i - k_{ij}Q_j$$

Atkins (1969) notes that the direct chemical analysis of a system will only yield information concerning the static condition of the system. In such analyses, data are confined to measurements of concentrations of material within a certain pool, or perhaps the amount of substance that is excreted by a system as a whole. This type of data is insufficient for analysing the kinetics of a

38

system, thus in order to investigate the dynamics of a system, one must label the substance; in compartmental analysis these labels are called tracers. However, compartmental analysis is used specifically to gain information on the behaviour of endogenous substance or tracee. The relationship between the tracer and the tracee is the tracer to tracee ratio (TTR), we use the symbol z to denote the tracer to tracee ratio. TTR may be formally defined as:

$$z = \frac{q_i}{Q_i}$$

where q_i is the mass of tracer in compartment i and Q_i is the mass of tracee in compartment i. Note that z is not defined as the ratio of the mass of labelled substance divided by the mass of unlabelled substance. We will deal extensively with this in later sections; nevertheless we note it now for completeness. It is timely to review the types of tracers used and the methods used in tracer studies.

2.4.2   Tracer methods

There are two types of tracers, radioactive isotope and stable isotope. Radioactive isotope tracers have been used for many years to study the kinetics of metabolites in humans. However, because radioactive isotopes release ionising radiation, which is potentially hazardous - especially for women in their reproductive years and children – their use has diminished and stable isotopes tracers are increasingly used in clinical investigation. Unlike radioactive isotopes, stable isotope tracers do not decay, and this has been the major factor for their popularity, as ethical considerations have become more significant. Stable labelled isotopes can be used safely, even in repetitive studies, to investigate metabolism in neonates, children, young adults and even during pregnancy. The input of these tracers into the system is commonly bolus, constant infusion or a combination of both (a primed infusion). Regardless of what tracer is used, one is only interested in the kinetics of the tracer – in order to make some inferences about the tracee. However, there are differences in converting measured or transient data into the crucial variable the tracer to tracee ratio.

2.4.3   Tracer models

A tracer when initially added to a system is not in equilibrium, by sampling some defined accessible pool over time, quantitative changes in the tracer concentration/mass can be mathematically analysed and described as a function of time. These changes reflect the rates of

transfer and transformation of the tracer. The results of *tracer dilution* may then be used to estimate the rate at which a *tracee* is lost from the same accessible pool. By making certain assumptions parameters derived from such a model will represent true rates of tracee synthesis and breakdown into some accessible sampled pool. The pool is assumed to be uniform and well mixed, such that a sample taken from any part of the pool is representative of the pool as a whole.

Consider the simplified single amino acid pool model in Figure 2.16. In this model under fasting conditions essential amino acids, i.e. those that cannot be synthesised *de novo*, enter the mixed free pool only from the degradation of body proteins. The simplified model in Figure 2.16 assumes that all of the free amino acids coming from protein breakdown are instantaneously mixed with the amino acids in the plasma. Thus there are only two pools or locations of amino acids in the body: in protein or in the free amino acid pool. Since the rate of infusion of the tracer (itself an essential amino acid) is known, and the dilution of the tracer (the tracer to tracee ratio) is measured, the rate of appearance of unlabelled amino acid (i.e. protein breakdown) may be calculated.
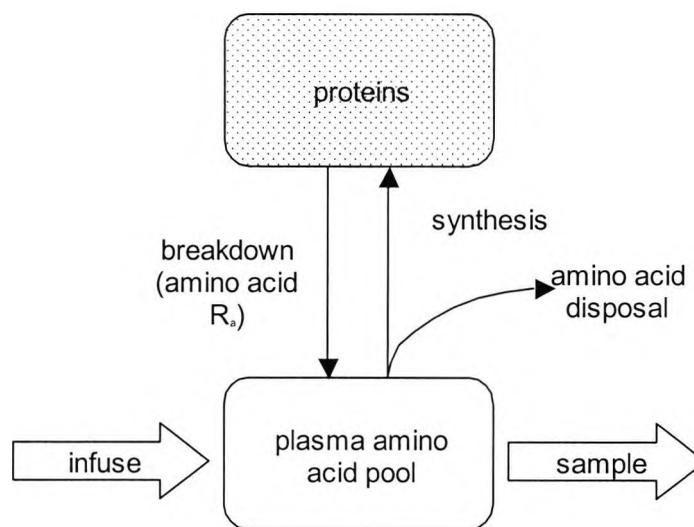
Figure 2.16: Simplified model of the use of an amino acid tracer to calculate whole body protein turnover according to a simplified model which contains a single pool of free amino acids, where both intracellular and extracellular free amino acids to mix freely.

2.4.4 Definition of tracer to tracee ratio

Much of the following is derived from the work of Cobelli and colleagues (Cobelli et al. 1987;Cobelli et al. 1992). The tracer to tracee ratio *z(t)* may be defined as the ratio of tracer mass

$q(t)$ to tracee mass, Q. Since the volume V is the same for both tracer and tracee, V can be expressed solely in terms of either tracer variables or tracee variables:

$$V = \frac{q(t)}{c(t)} = \frac{Q}{C} \qquad [2.1]$$

and $z(t)$ can be written in terms of either mass or concentration:

$$z(t) = \frac{q(t)}{Q} = \frac{c(t)}{C} \qquad [2.2]$$

Using this definition, we shall write expressions for $z(t)$ for both radioactive and stable isotope tracers.

2.4.4.1 Determining tracee to tracer ratio for a radioactive isotope

The occurrence of radioactive isotope tracer is measured by the energy it emits; but tracee data is usually measured in terms of mass or concentration. In order to calculate $z(t)$, it is necessary to express the amount of tracer in a sample as a mass or concentration. When quantifying radioactive isotope tracer in a given sample, what is in fact measured is the energy being released; and this energy release is proportional to the mass of tracer present. This is usually expressed as disintegrations per minute (*dpm* or the *curie* which equals 3.7×10^{10} disintegrations per second). However, one does not usually measure radioactivity in terms of dpm. For instance usually a beta or gamma counter is used to measure radioactivity in the sample in terms of counts per minute (*cpm*). The cpm data are a function of the counter and the isotope being analysed, and include background activity from electronic noise, detection of cosmic rays and natural radioactivity. For each counter and isotope, there are prescribed methods to convert cpm into dpm. Furthermore the measured variable is in terms of concentration, but the actual quantification of this is in terms of radioactivity. For each radioactive isotope of an element, there is a proportional relationship between the mass of the isotope and the dpm emitted by that mass:

$$q_{dpm}(t) = vq(t) \qquad [2.3]$$

where v is the proportionality constant. In order to calculate $z(t)$ it is necessary to express the measured radioactivity in terms of concentration. If $c(t)$ denotes the measurement or tracer concentration and V denotes the volume of distribution, we may express $c(t)$ in terms of dpm per unit volume, and obtain:

$$c(t) = \frac{vq(t)}{V} \qquad\qquad [2.4]$$

A measure of radioactivity that is frequently used in biomedical studies is the radioactivity per unit mass. This is defined as the quotient of disintegrations per minute to total mass and is known as the **specific activity**, denoted *sa*. It is defined:

$$sa(t) = \frac{vq(t)}{Q + q(t)} \qquad\qquad [2.5]$$

where Q is the mass of the tracee. The units of *specific activity* are **dpm/mass**. Since the mass of the tracer $q(t) \ll Q$ we may write:

$$sa(t) \approx \frac{vq(t)}{Q} = \frac{c(t)}{C} = z(t) \qquad\qquad [2.6]$$

2.4.4.2 Determining tracee to tracer ratio for a stable isotope

The situation with stable isotope tracers is different from radioactive isotope tracers because:

- The stable isotope tracer introduced into the system has non-negligible mass, i.e. we cannot make the assumption that $Q \cong q(t) + Q$.

- There is always some natural abundance of the labelled species in the tracee.

- There is some unlabelled substance in the tracer.

The fact that the tracer may have non-negligible mass is necessary in order to have enough tracer mass in a sample to be quantified. The assumption that the endogenous steady state is not perturbed by the stable isotope tracer needs to explicitly taken into account. Usually the tracer perturbation is confined to a few percent, and hence this assumption is likely to be satisfied.

The quantification of the amount of stable isotope of an element in a sample relies on the ability of the mass spectrometer to distinguish among isotopic species based on differences in their atomic mass number. The output is given in terms of peaks associated with each isotope along a mass scale; the peaks are proportional to the abundance of the isotopic combinations in a molecule having a given mass number. In order to derive from the peak intensities the measurements in terms of relative composition in the sample of labelled and unlabelled species certain calculations must be made between peak intensities and masses.

The outcome of these calculations may be to express the *isotopic ratio r(t)*, this is defined as the ratio of mass of species (subscript s) to the mass of the most abundant species (subscript a).

$$r(t) = \frac{Q^s + q^s(t)}{Q^a + q^a(t)} \qquad [4.7]$$

Another common expression is the *isotopic abundance a(t)*, which is a ratio of the mass of the labelled species to the total mass, so

$$a(t) = \frac{M^s + m^s(t)}{M^a + m^a(t) + M^s + m^s(t)} = \frac{r(t)}{1 + r(t)} \qquad [4.8]$$

However neither of these expressions explicitly gives the expression for *z(t)*,

$$z(t) = \frac{m(t)}{M} = \left[\frac{r(t) - r_N}{r_I - t(t)}\right]\left(\frac{1 + r_I}{1 + r_N}\right) = \frac{a(t) - a_N}{a_I - a(t)} \qquad [4.9]$$

where subscripts I and N refer to infusate and naturally occurring isotopes respectively. Cobelli (1987) provides a detailed account of the relationships between *z(t)* and *r(t)*, and between *z(t)* and *a(t)*.

A new method to determine *z* that explicitly accounts for the abundance of label that exists naturally has been developed and provides details of several correction factors which are necessary (Rosenblatt et al. 1992). This technique has been previously applied by the author for a [^{13}C]-KIC tracer (Carroll et al. 1997), and has been used here (Chapter 5) to determine tracer to tracee ratios for [^{15}N,^{13}C]-leucine and [^{13}C]-leucine following the infusion of a [^{15}N,^{13}C]-leucine tracer, details may be found in the Appendix IV. Table 2.5 shows the natural abundances of some elements commonly used in protein turnover studies.

Table 2.5: Isotopes commonly used in biological research, natural abundance shown in parentheses.

Common stable (abundance %)		Rare stable (abundance %)		Radioactive	
^{1}H	(99.985)	^{2}H	(0.015)	^{3}H	
^{12}C	(98.89)	^{13}C	(1.11)	^{14}C	
^{14}N	(99.63)	^{15}N	(0.37)	^{13}N	*
^{16}O	(99.76)	^{18}O	(0.20)	^{11}O	*

* No long lived radioisotopes of these elements

43

2.4.5   Stable isotope vs. radioactive isotope tracers

Traditionally radioactive tracers were used extensively in kinetic modelling, however, the use of stable isotopes (in metabolic investigation) is now far more widespread. The fact that stable isotope tracers may be used without endangering patients has seen their popularity rise as ethical concerns come to the foreground. And although stable isotopes are ethically tolerable alternatives to radioactive tracer, certainly an extremely important consideration in studies in children, etc., there are other important features that make stable isotopes preferred. These advantages, as noted by Bier (1997) include:

1. There are no practical radioactive isotopes for certain elements. Nitrogen is a prime and important example, especially when considering protein turnover studies.

2. Stable isotopes are 'environmentally safe'; there are no issues concerned with the handling and disposal of stable labelled isotopes.

3. When using radioactive tracers, there is an acceptable level of tracer that should not be exceeded because of safety concerns. There are cases when the amount of tracer needed to achieve proper measurement exceeds the allowed dosage. This is not an issue with stable labelled tracers *per se*.

4. Some radioactive isotopes, notably [^{3}H] and [^{14}C], are subject to greater *in vivo* tracer discrimination that their stable labelled counterparts, [^{2}H] and [^{13}C].

5. When using stable isotopes, both substrate content and tracer enrichment may be determined simultaneously.

6. The confidence of assays measuring stable isotopes is higher that those used for radioactive isotopes.

7. The location of the label in a stable labelled tracer can be determined relatively easily.

8. The use of stable isotope tracers allows the simultaneous and repeated use of multiple tracers in the same subject. The investigator may use a subject as his/her own experimental control. This allows paired comparisons to be used in statistical analysis and also means that fewer subjects are needed.

So while the benefits of using stable isotopic tracers are unmistakable, it is useful to note that there are several practical and conceptual differences between the two as well, these include:

1. The calculation of specific activity is fundamentally different from the calculation of the stable label equivalent – the tracer to tracee ratio.

2. Unlike radioactive isotopes, stable isotopes of all elements occur naturally, and the background abundance of the label must be incorporated into calculations in order to reflect accurately processes being analysed.

3. For radioactive isotopes, the mass of tracer present in a sample is determined by measuring energy emission; from this measured data, the concentration of tracee present can be calculated and this is used to calculate z. This is fundamentally different from the calculations involving stable isotope tracers, in this case a mass spectrometer is used to determine the abundance of different species - based on differences in atomic masses - in the mixture, various ratios may be expressed and used to calculate z.

4. For any given situation, it is necessary to infuse a considerably larger mass of stable isotope compared to the mass of radioactive tracer. This is because (as described above) stable isotope tracer calculations require a non-negligible mass, because a mass is measured. Since a non-negligible mass of substance is infused when using stable isotope tracers, one must take great care that the system being studied is not disturbed or affected by the tracer. For radioactive tracers, the equipment used is capable of detecting the energy emissions of considerably smaller masses. A mass perturbation is normally not an issue when using radioactive tracers.

2.5   Summary

The preceding sections provide an introduction to proteins, amino acids, protein metabolism, several of the methods used to measure protein turnover in man, and some supplementary techniques commonly used in the tracer modelling.

On surveying the literature, two main themes are apparent. Firstly, estimating protein turnover is an intrinsically difficult problem (the 'problems' are described in section 2.1.7), and this explains in part why many of the methods described above appear to be overly simplistic. Secondly, there is no definitive model for measuring WBPT even though the phenomenon has been known about for many decades. This is also, to some degree, because of the complexity of the protein system. However, it important to note that even though robust and conceptually accurate models are available (e.g., the seven compartment model developed by Cobelli *et al*), researchers continue to use models which are less robust and less accurate (e.g., the reciprocal pool model). A quick

survey of the citation indices reveals that the paper describing the use of the reciprocal pool model (Schwenk et al. 1985a) has been cited 293 times compared to only 28 for the paper describing the seven-compartment model describing leucine kinetics in man (Cobelli et al. 1991) (source: http://www.mimas.ac.uk, January 2002). This suggests that even though researchers are well aware of the limitations of the reciprocal pool model, it is still deemed the *de facto* model for estimating protein turnover via leucine kinetics. The principal reason for this must be the comparative difficulty of using a compartmental model.

In Chapter Three we compare the influence of the model (i.e., the primary and reciprocal pool models), along with the effect of various demographic/physiological variables on WBPT data. In Chapters Four and Five we propose a new model to describe leucine kinetics which makes less assumptions than the reciprocal pool model, but which is simpler (and less comprehensive) than the seven-compartment model proposed by Cobelli et al.

3 ASSSESSING THE INFLUENCE OF THE MODEL USED TO MEASURE PROTEIN TURNOVER, AGE, WEIGHT, BODY MASS INDEX AND LEUCINE CONCENTRATION ON WHOLE BODY PROTEIN TURNOVER ESTIMATES IN HEALTHY ADULTS

3.1 Introduction and Aims

The concept of whole-body protein turnover (WBPT) refers to the sum of all the rates of protein synthesis and breakdown occurring in the body at any given time. A high rate of WBPT is thought to occur to prevent the accumulation of abnormal and potentially harmful proteins and peptides, to help regulate the concentration of different proteins, to produce intermediates for the synthesis of other compounds, and to supply energy. The influence of physiological variables on protein metabolism is therefore important for a variety of reasons.

In the last decade relatively few studies have examined the effect of various demographic variables (age, gender etc.) on protein-turnover. For instance, leucine oxidation rate has been shown to be lower in women compared to men (Volpi et al. 1998). In addition, there is evidence to show that WBPT per kg body weight is faster in infants and children than in adults (Van Goudoever et al. 1995;Young et al. 1975). Prepubertal children have been reported to have postabsorptive leucine Ra about 65% higher than adults (Arslanian and Kalhan 1996), and there is evidence to show that leucine Ra is less in pubertal adolescents than in prepubertal children (Arslanian and Kalhan 1996;Beckett et al. 1997). Furthermore there is some indication that older adults have a lower protein turnover per kg body weight than young adults, although this difference decreases or disappears when considering fat free mass (Boirie et al. 1997;Millward et al. 1997;Morais et al. 1997;Welle et al. 1993). The slower protein turnover per kg of body weight in older subjects is thought to represent the fact that older people tend to have more body fat and less active cell mass.

The present study was undertaken to explore and quantify the effect of physiological and demographic variables (age, weight, body mass index, plasma leucine concentration and gender) on WBPT using the multiple linear regression technique. In addition we compared the influence of these variables on both primary and reciprocal pool model WBPT estimates.

47

3.2   Methods

3.2.1   Data collection

We collected whole body protein turnover (WBPT) data calculated on 29 normal subjects, from published (Bowes et al. 1997;Brillon et al. 1995;Matthews et al. 1990;Matthews et al. 1993;Russell-Jones et al. 1994;Umpleby et al. 1986;Umpleby et al. 1995) and unpublished sources. For each subject we recorded estimates for leucine Ra, non-oxidative leucine disposal (*Nold*), leucine oxidation rate (*Ox*) and metabolic clearance rate (*MCR*) using both the primary (denoted with subscript p) and reciprocal pool (subscript r) models. *MCR* was calculated as the ratio of leucine *Ra* to plasma leucine concentration (L/kg/min). In addition to WBPT data, the following covariates were recorded: age (years), gender, body mass index (kg/m^2), weight (kg) and plasma leucine concentration (mmol/L).   The details of experimental protocols between studies vary because the dataset contains pooled data from several different studies. However, all subjects were studied under fasting conditions and blood samples were collected following either a [^{14}C]-leucine (25 μCi) bolus injection or a continuous infusion of [^{13}C]-leucine. Leucine was infused for between 3 and 7.5 hours, while infusion rates were between 0.6 and 1mg/kg/h of tracer.

The dataset contained data from 29 subjects. There were 24 male and 5 female subjects, with mean age 28.1 years (range: 23.0 – 43.0) and mean BMI 22.6 kg/m^2 (range: 17.4 – 28.2). Table 3.1 shows mean, standard deviation and minimum and maximum values for all variables.

3.2.2   Data analysis

Graphical and statistical techniques were used to analyse the data. Selected bivariate scatterplots for Nold$_P$ vs. BMI (Figure 3.1); MCR$_r$ vs. Concentration (Figure 3.2) and MCR$_p$ vs. Concentration (Figure 3.3) are shown below; the other scatterplots can be found in Appendix I. The data were tested for normality using P-P Plots (shown in Appendix I) and Shapiro-Wilk tests; in addition a correlation analysis was performed between the variables, results of this are shown in Table 3.3. Finally a stepwise linear regression analysis was performed.

SPSS 10.0 (SPSS Inc., Chicago) was used in the analysis of sampling distributions, bivariate scatterplots, correlation coefficients, and the linear regression analysis.

Table 3.1: Data summary (N = 29, 24 Male 5 Female)

	Mean ± SD	Minimum – maximum
Age (years)	28.1 ± 5.1	23.0 – 43.0
BMI (kg/m^2)	22.6 ± 2.3	17.4 – 28.2
Weight (kg)	69.2 ± 8.6	55.0 – 88.0
Leucine concentration (μmol/L)	125.5 ± 21.9	76.4 –161.1
Ra$_p$ (μmol/kg/min) **Ra$_r$**	1.37 ± 0.18 1.98 ± 0.31	(1.12 – 1.76) (1.60 – 2.74)
Nold$_p$ (μmol/kg/min) **Nold$_r$**	1.12 ± 0.22 1.73 ± 0.30	(0.78 – 1.49) (1.32 – 2.43)
Leucine oxidation (μmol/kg/min)	0.26 ± 0.11	(0.05 – 0.42)
MCR$_p$ (L/kg/min) **MCR$_r$**	11.23 ± 2.30 16.40 ± 4.02	(7.1 – 16.3) (10.0 – 24.1)

Table 3.2: List of covariates, dependant variables and derived variables

	Variable
Independent variables (covariates)	Age (years) Centred age (age – 18) BMI (kg/m^2) Centred BMI (BMI – 22.6) Weight (kg) Centred weight (weight – 69.2) Leucine concentration (μmol/L) Centred Concentration (Concentration – 125.5)
Dependent variables (primary pool model)	Ra$_p$ Nold$_p$ Ox$_p$ MCR$_p$
Dependent variables (reciprocal pool model)	Ra$_r$ Nold$_r$ Ox$_r$ MCR$_r$
Derived variables	Ra$_r$ ÷ Ra$_p$ Nold$_r$ ÷ Nold$_p$ Ra$_r$ -Ra$_p$ Nold$_r$ - Nold$_p$

A forward stepwise variable selection method was used in the regression model. Variables were entered into (or removed from) the model depending on whether the entry (or removal) of the variable into the regression model caused a significant ($p < 0.05$) change to the F value. Each dependent variable was tested using both primary and reciprocal estimates of *Ra*, *Nold*, *Ox* and *MCR* while using the covariates (age, concentration, BMI, weight) as independent variables; Table 3.2 shows a full list of covariates and dependent variables. In addition to calculating WBPT using

the reciprocal pool (Schwenk et al. 1985a) and the primary pool (Matthews et al. 1982) models, the difference/ratio variables $Ra_r - Ra_p$; $Nold_r - Nold_p$; $Ra_r \div Ra_p$; $Nold_r \div Nold_p$ were also calculated. A linear regression analysis was performed to determine if the differences between the primary and reciprocal pool models could be explained by the covariates. Natural logs of all the variables were also recorded.

3.3   Results

There were significant correlations between $Nold_p$ and BMI; and very significant correlations between MCR_p and leucine concentration, and MCR_r and leucine concentration. Results of the (Pearson) correlation between the independent and dependant variables are shown in Table 3.3 below; the significant correlations are flagged. The results of the linear regression analysis are shown in Table 3.4 and Table 3.5 below. The data show that BMI is correlated with non-oxidative leucine disposal when using the primary pool model, but not when using reciprocal pool model estimates. In addition the analysis revealed that leucine concentration is a significant contributor to MCR irrespective of the calculation method.

Table 3.3: Correlation matrix

	Age	BMI	Weight	Leucine concentration
Ra_p	-0.15	-0.31	0.08	0.09
$Nold_p$	-0.13	-0.37 $(p < 0.05)$	0.04	0.11
Ox_p	0.11	0.05	-0.05	-0.06
MCR_p	0.01	-0.26	-0.08	-0.81 $(p < 0.01)$
Ra_r	-0.12	0.02	0.03	-0.08
$Nold_r$	-0.13	-0.07	0.01	-0.06
Ox_r	0.01	0.22	0.05	-0.06
MCR_r	0.02	-0.05	-0.11	-0.81 $(p < 0.01)$
$Ra_r \div Ra_p$	-0.00	0.27	-0.03	-0.21
$Nold_r \div Nold_p$	-0.00	0.30	-0.01	-0.20
$Ra_r - Ra_p$	-0.04	0.21	-0.02	-0.15
$Nold_r - Nold_p$	-0.04	0.21	-0.02	-0.15
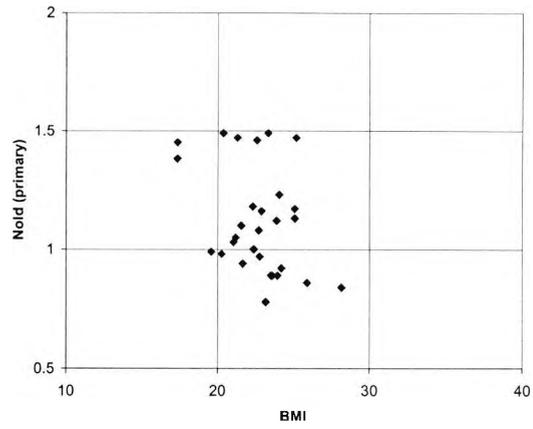
Figure 3.1 Scatterplot Nold$_p$ vs. BMI
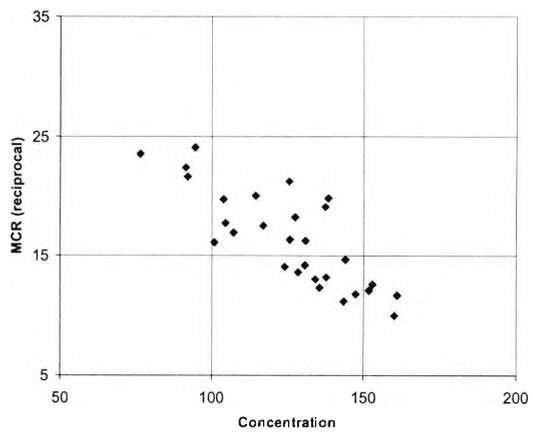
Figure 3.2: Scatterplot MCR$_r$ vs. plasma leucine concentration
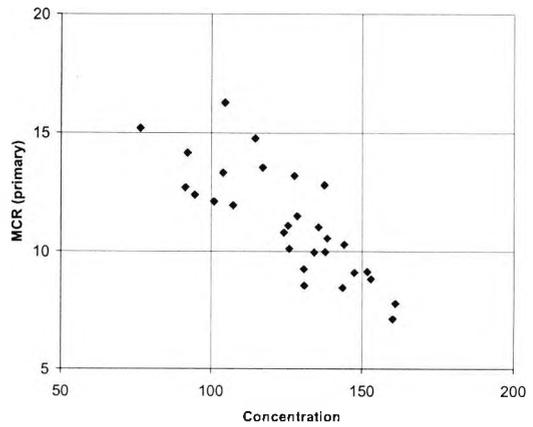
Figure 3.3: Scatterplot MCR$_p$ vs plasma leucine concentration

51

Table 3.4: Summary results from linear regression analysis

		Age	Weight	BMI	Leucine concentration
Primary pool model	**Leucine Ra**	(ns)	(ns)	(ns)	(ns)
	Non oxidative leucine disposal	(ns)	(ns)	$p < 0.05$	(ns)
	Leucine oxidation	(ns)	(ns)	(ns)	(ns)
	Metabolic clearance rate	(ns)	(ns)	(ns)	$p < 0.05$
Reciprocal pool model	**Leucine Ra**	(ns)	(ns)	(ns)	(ns)
	Non oxidative leucine disposal	(ns)	(ns)	(ns)	(ns)
	Leucine oxidation	(ns)	(ns)	(ns)	(ns)
	Metabolic clearance rate	(ns)	(ns)	(ns)	$p < 0.05$

Table 3.5: Regression coefficients.

Model	Variable	Model description	Percentage of explained variability.	
I	$Nold_p$	$1.915 - (0.035 \times BMI)$	17 %	$p < 0.05$
II	$MCR[Ra_p]$	$22.044 - (0.086 \times \text{Leucine concentration})$	66 %	$p < 0.001$
	$MCR[Nold_p]$	$30.436 - (0.129 \times \text{Leucine concentration})$	60%	$p < 0.001$
	$MCR[Ox_p]$	$4.822 - (0.022 \times \text{Leucine concentration})$	16%	$p < 0.05$
III	$MCR[Ra_r]$	$35.056 - (0.149 \times \text{Leucine concentration})$	66 %	$p < 0.001$
	$MCR[Nold_r]$	$17.376 - (0.066 \times \text{Leucine concentration})$	40%	$p < 0.001$
	$MCR[Ox_r]$	$3.911 - (0.017 \times \text{Leucine concentration})$	19%	$p < 0.05$

MCR[Ra] = Ra / Leucine concentration, MCR[Nold] = Nold / Leucine concentration, MCR[Ox] = Ox/Leucine concentration

Table 3.6: Summary for Primary and Reciprocal WBPT estimates

	Mean ± SD
$Ra_p{}^\dagger$	1.37 ± 0.18
$Ra_r{}^\dagger$	1.98 ± 0.31
$Nold_p{}^\ddagger$	1.12 ± 0.22
$Nold_r{}^\ddagger$	1.73 ± 0.30
MCR_p	11.23 ± 2.30
MCR_r	16.35 ± 4.02

[†] $Ra_p < Ra_r$, $P < 0.001$, paired t-test
[‡] $Nold_p < Nold_r$, $P < 0.001$, paired t-test

52

The effect of the covariates on the differences between the estimates provided by the reciprocal and primary pool models was also investigated. As expected the primary pool model estimates of leucine *Ra* and *Nold* are significantly smaller than the reciprocal pool model counterparts ($p <$ 0.001), results shown in Table 3.6.

Furthermore, a linear regression analysis was performed on several derived difference variables namely Ra_r - Ra_p; $Nold_r$ - $Nold_p$; Ra_r ÷ Ra_p; $Nold_r$ ÷ $Nold_p$ to determine whether the difference between the primary pool model and reciprocal pool model could be attributed to the age, leucine concentration, BMI or weight. The results (see Table 3.7) suggest that age, leucine concentration, BMI or weight do not contribute to the difference in WBPT estimates between the primary and reciprocal pool model estimates.

Table 3.7: Summary of difference tests between primary and reciprocal pool model

		Age	Weight	BMI	Leucine concentration
DIFFERENCE TEST Reciprocal – Primary	Ra_r - Ra_p	ns	ns	ns	ns
	$Nold_r$ - $Nold_p$	ns	ns	ns	ns
RATIO TEST Reciprocal ÷ Primary	Ra_r ÷ Ra_p	ns	ns	ns	ns
	$Nold_r$ ÷ $Nold_p$	ns	ns	ns	ns

3.4 Discussion

This above analysis reveals several features about WBPT data obtained using the primary and reciprocal pool models. Firstly, the data show that estimates of WBPT obtained using the primary pool model are lower than estimates obtained using the reciprocal pool model. If one uses reciprocal pool model estimate as the true value of WBPT, these data show that the primary pool model underestimates leucine turnover by around 30%. These results emphasise that there are fundamental problems with the assumptions that the primary pool model makes. The shortcomings of the primary pool model are well documented and have been examined in the previous chapter (Section 2.2.4.4).

Secondly, the data show that the difference between WBPT estimates obtained using the primary and reciprocal pool models cannot be attributed to the independent variables (age, body mass index, weight or plasma leucine concentration), see Table 3.7. It has been shown theoretically that WBPT estimates obtained by the primary and reciprocal pool model will differ (Cobelli and

Saccomani 1991); these data confirm that the differences observed are not due to variations in the independent variables: age, BMI, weight or plasma leucine concentration. These data demonstrate that it is primarily the *method* used to determine WBPT that is of importance, more so than matching subjects for age and gender.

In addition, the study also reveals a negative relationship between primary pool model estimates of Nold ($Nold_p$) and body mass index. This may reflect the fact that as BMI increases, the percentage of lean tissue per kg decreases; since Nold occurs in lean tissue and Nold is expressed per kg of body a negative relationship between Nold and BMI is thus not surprising (as it suggests Nold will be increase as lean tissue per kg increases). Although it is difficult to find other studies where the relationship between weight and WBPT have been explicitly analysed, there is evidence that protein turnover in obese adults is faster than in normal-weight adults (Caballero and Wurtman 1991;Welle et al. 1992); in contrast, Solini (1997) has found that rates of protein metabolism (adjusted for fat free mass) in obese women are similar to normal subjects. It should be noted that these data represent healthy subjects (BMI range 17.4 - 28.2), and although statistically significant, the influence of BMI was small.

These data suggest that neither age nor gender influence WBPT over the range of values analysed here. It is worth noting that the sample population (N = 29) was not evenly matched for gender (24 male, 5 female), so the effects of gender, if any, are difficult to ascertain. And with respect to the effect of age, others (Millward et al. 1997;Morais et al. 1997;Welle et al. 1993) have shown that older adults have a slower protein turnover per kg of body weight than young adults. Again, the range of ages of the subjects included here (range 23 - 43 years) is perhaps too small for the effect of age to be significant.

The analysis revealed that leucine clearance is inversely related to leucine concentration, a finding in agreement with the literature (Tessari et al. 1992). The relationship suggests that WBPT is saturable, and the transfer of amino acids across the plasma membrane requires a population of specific transporter molecules (Biolo et al. 1995;Christensen 1990). The transport mechanism is not thought to be the rate-limiting step of leucine metabolism, as leucine incorporation into protein and leucine appearance from protein breakdown are much slower than leucine transport across the cell membrane (Hovorka et al. 1999). While this study cannot reveal the level at which transporter saturation occurs (since the data is from normal subjects under fasting conditions), our regression model (see data in Table 3.5) indicates that concentration only accounts for about 19% of leucine oxidation clearance, but over 50% of both Nold and Ra clearance. Through a process of elimination, this suggests that it is leucine oxidation that is the rate-limiting step in normal human leucine metabolism, a finding that is in agreement with Matthews (1981).

In most protein turnover studies, the number of subjects (i.e. samples) is often less than 12. In this study, the sample size was 29. In general, the larger the sample size N, the smaller the sampling error tends to be (i.e., the approximation to the population under observation improves with larger samples). The sample here (N=29) cannot be considered to be large (usually, samples where N > 30 are considered to be 'large'), nevertheless the relative largeness of the sample suggests that sampling errors have been minimised.

In conclusion, the analysis was undertaken to determine the influence of certain demographic information of WBPT. These results demonstrate that the primary pool model underestimates WBPT. Furthermore, over the range of values in this study, the influence of demographic variables is small. It is clear from these data that the most important factor in determining WBPT is the model used. In the Chapter Four a new model is introduces, the model describes the kinetics of a $[^{15}N,^{13}C]$-leucine tracer and may be used to estimate whole body protein turnover in man.

4 A SIMULATION STUDY EXPLORING THE USE OF A [^{15}N-^{13}C]-LEUCINE TRACER TO ESTIMATE WHOLE BODY PROTEIN TURNOVER

The widespread use of the primary and reciprocal models over the last decade has seen the carbon labelled tracers ([^{13}C]-leucine, [^{13}C]-KIC) dominate the study of leucine kinetics. They are not, however, the only tracers available in the investigation of leucine metabolism. For instance, others (Cheng et al. 1985;Cheng et al. 1987;Matthews et al. 1981) have successfully used [^{15}N, ^{13}C]-leucine in clinical investigation, and more recently Tessari (1995) has explored skeletal-muscle leucine kinetics using [^{15}N]-leucine in conjunction with a [^{13}C]-leucine tracer. In this chapter a new model to estimate WBPT using a [^{15}N, ^{13}C]-leucine tracer is described and subsequently validated in a simulated experiment.

4.1 Aims

The aims of this study are a) to outline a conceptual model for leucine kinetics b) to validate the conceptual model using simulated experiments and c) to determine whether a [^{15}N, ^{13}C]-leucine tracer could be used to estimate parameters for a fast turning over protein pool.

4.2 Methods

In order to perform the simulated experiment several design variables need to be determined. These include:

- The model structure, including potential dosage and sampling sites

- The dosage of labelled tracer

- The sampling schedule

- A method for generating data.

4.2.1 Model structure

Leucine is an essential amino acid and is thus not synthesised *de novo*; within intracellular space, leucine may be incorporated into protein (protein synthesis) or it may be oxidised. Leucine is in constant flux with its keto-acid, KIC through a reversible transamination process (Taylor and Jenkins 1966). During transamination, the amino group (NH$_2$) is lost to the nitrogen pool. The

resulting KIC has two fates, it may be re-aminated to form leucine, or it may undergo an irreversible decarboxylation to CO_2. Leucine enters the system from protein breakdown. Here only fast-turning-over proteins are considered, as the breakdown and synthesis of slow-turning-over protein over the experimental period are assumed negligible in comparison with that of fast-turning-over proteins. A conceptual model describing leucine kinetics during fasting conditions, including two pools for leucine (extra- and intra- cellular), two pools for KIC (extra- and intra-cellular) and a single pool for fast-turning-over proteins is shown in Figure 4.1.
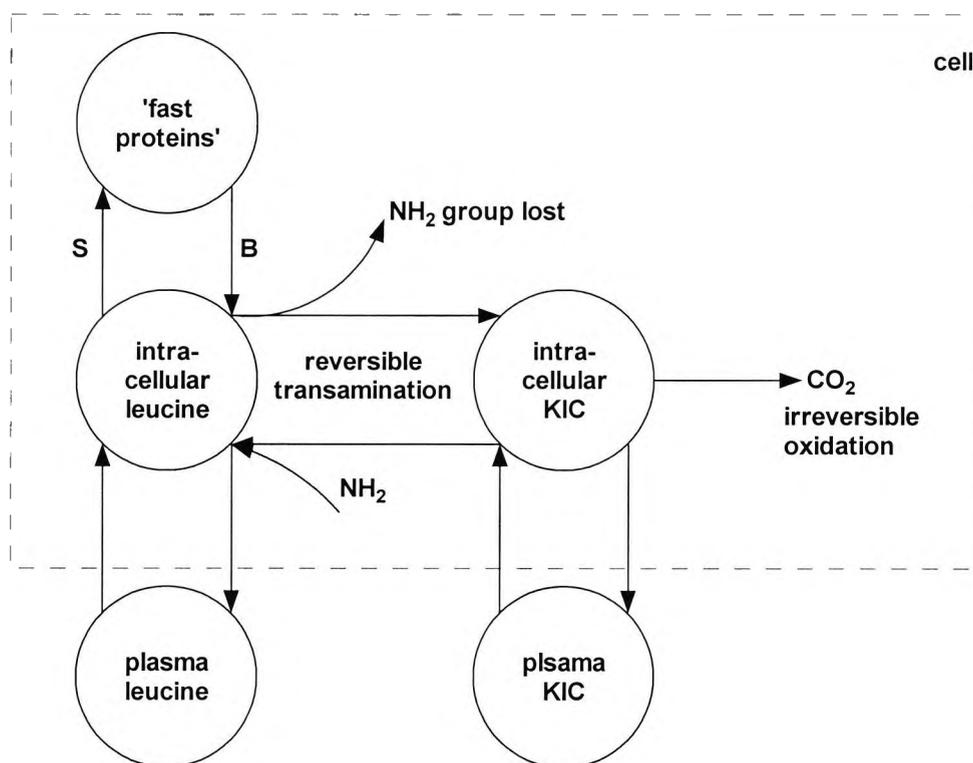

Figure 4.1: Schematic of the leucine system

Transamination is reversible for [^{13}C]-leucine and [^{13}C]-KIC tracers, for a [^{15}N]-leucine tracer transamination is irreversible, but undesirable negligible recycling of the [^{15}NH$_2$] group is possible. For the doubly-labelled [^{15}N,^{13}C]-leucine tracer, transamination is irreversible and tracer recycling is negligible and improbable. During deamination of [^{15}N, ^{13}C]-leucine, the ^{15}N label is lost to the nitrogen pool resulting in the production of [^{13}C]-KIC, for [^{15}N, ^{13}C]-leucine recycling to occur, a (deaminated) ^{15}NH$_2$ group must recombine with [^{13}C]-KIC to (re)form [^{15}N,^{13}C]-leucine; since the amount of tracer infused in small compared to whole body pool sizes, recycling of [^{15}N,^{13}C]-leucine highly unlikely. Transamination, which is reversible for a [^{13}C]-leucine/KIC tracer, is thus an irreversible step for [^{15}N, ^{13}C]-leucine tracer (Figure 4.2).
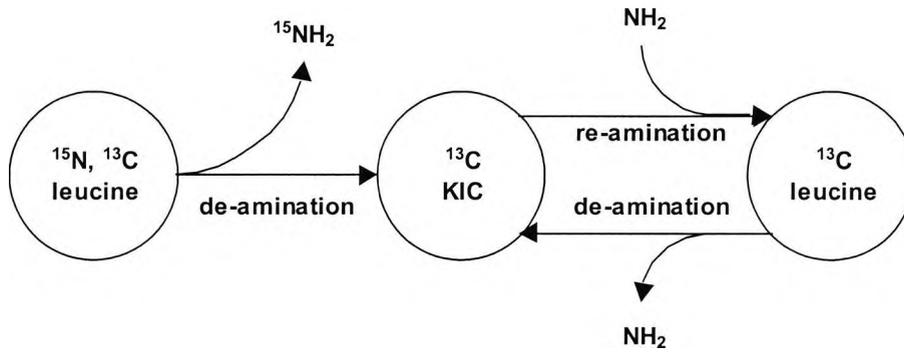
Figure 4.2: The kinetics of a $[^{15}N,^{13}C]$-leucine tracer. During deamination of $[^{15}N,^{13}C]$-leucine, the $^{15}NH_2$ label is lost to the nitrogen pool and $[^{13}C]$-KIC is formed. The reamination of $[^{13}C]$-KIC results in the formation of $[^{13}C]$-leucine. The chance of a $[^{15}N]$labelled atom recombining with $[^{13}C]$-KIC is negligible because of the small size of the ^{15}N pool.
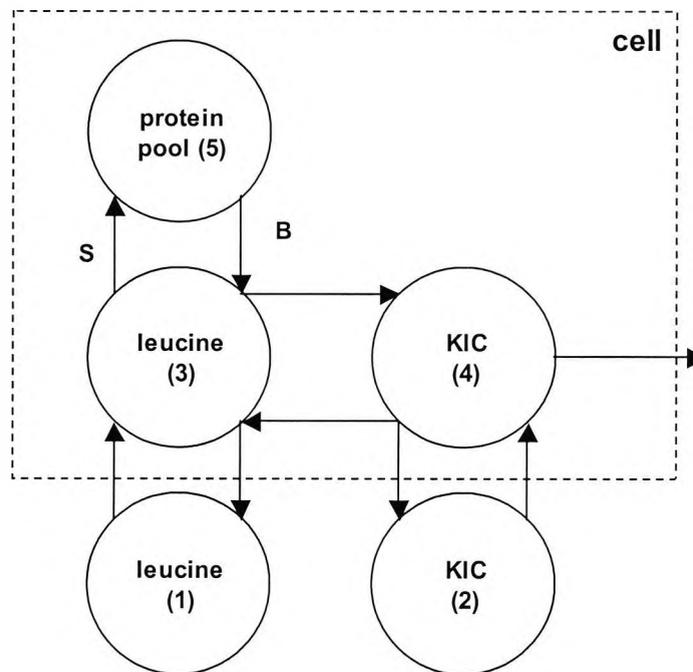
Figure 4.3: Proposed compartment structure of leucine kinetics, protein breakdown (B) and synthesis (S) are shown.

Since the metabolism of $[^{15}N, ^{13}C]$-leucine results in at least three different, measurable leucine species: $[^{15}N, ^{13}C]$-leucine, $[^{13}C]$-leucine, and $[^{13}C]$-KIC. A $[^{15}N, ^{13}C]$-leucine tracer thus allows more than one modelling option to be considered. Two modelling options have been considered (Proposed Model 1 and Proposed Model 2). These models emerge directly from the description of leucine kinetics shown in Figure 4.2 and Figure 4.3. Proposed Model 1 (PM1, Section 4.2.2.2

below) includes only the kinetics of the $[^{15}N, {}^{13}C]$-leucine tracer, and Proposed Model 2 (PM2, Section 4.2.2.3 below) includes all three measurable species $[^{15}N, {}^{13}C]$-leucine, $[^{13}C]$-leucine and $[^{13}C]$-KIC. Both models allow the estimation of fractional transfer rates for protein synthesis and proteolysis. The proposed models are analysed in detail in Section 4.2.2 below.

4.2.2   Model development

Three new models were developed and then tested using synthetic data (generated from three reference models). The Cobelli (1991) model was used to construct the reference models used for generating synthetic data since it is considered to be the most comprehensive compartment model of leucine kinetics available. The reference models are hybrids of the Cobelli (1991) model and are referred to as *implied Cobelli models* (ICMs). The Cobelli (1991) model lends itself to this sort of experimentation quite naturally, and the assumptions made by our ICMs are no different from the assumptions made in the Cobelli (1991) model. To simulate the data, the SAAM II program was used to construct each implied Cobelli model and data was generated, using the parameters reported by Cobelli (1991), the dosage suggested in Section 4.2.3 and the sampling schedule described in Section 4.2.4.

For each proposed model (PM) there is an accompanying ICM. Thus, three ICMs were constructed, these are: ICM0 (analogous to the Cobelli (1991) model, with similar inputs and outputs); ICM1 (infusion of $[^{15}N, {}^{13}C]$-leucine in the plasma, measuring only $[^{15}N, {}^{13}C]$-leucine) and ICM2 (same input as ICM1, however this time measuring all available tracer species: $[^{15}N, {}^{13}C]$-leucine, $[^{13}C]$-leucine, and $[^{13}C]$-KIC) – these details are summarised in Table 4.1. The term '*case*' has been used to describe the combination of a proposed model together with its accompanying reference model (ICM). There are three cases Case 0, 1 and 2 (details of these cases are shown in Table 4.1).

Table 4.1: Case definitions: the proposed models and their corresponding reference models

	Implied Cobelli Model (ICM)	Proposed Model (PM)	Inputs	Measurements required	Described and analysed in
Case 0	ICM0	PM0	$[^{13}C]$-KIC $[^{2}H]$-leucine	$[^{13}C]$-KIC $[^{2}H]$-leucine $[^{13}C]$-leucine $[^{2}H]$ KIC	Section 4.2.2.1 below
Case 1	ICM1	PM1	$[^{15}N, {}^{13}C]$-leucine	$[^{15}N, {}^{13}C]$-leucine	Section 4.2.2.2 below
Case 2	ICM2	PM2	$[^{15}N, {}^{13}C]$-leucine	$[^{15}N, {}^{13}C]$-leucine $[^{13}C]$-leucine $[^{13}C]$-KIC	Section 4.2.2.3 below

4.2.2.1   Case 0: PM0 and ICM0

The aim of this scenario was to determine if the model structure proposed (i.e., Figure 4.3) is compatible (similar) with the Cobelli (1991) model. A compatible structure would indicate that this model could be used to simulate $[^{15}N,^{13}C]$-leucine kinetics.

4.2.2.1.1   Implied Cobelli Model 0

ICM0 is analogous to the Cobelli (1991) model, with similar inputs and outputs. The model is shown in Figure 4.4.

^{13}C pathways ^2H pathways
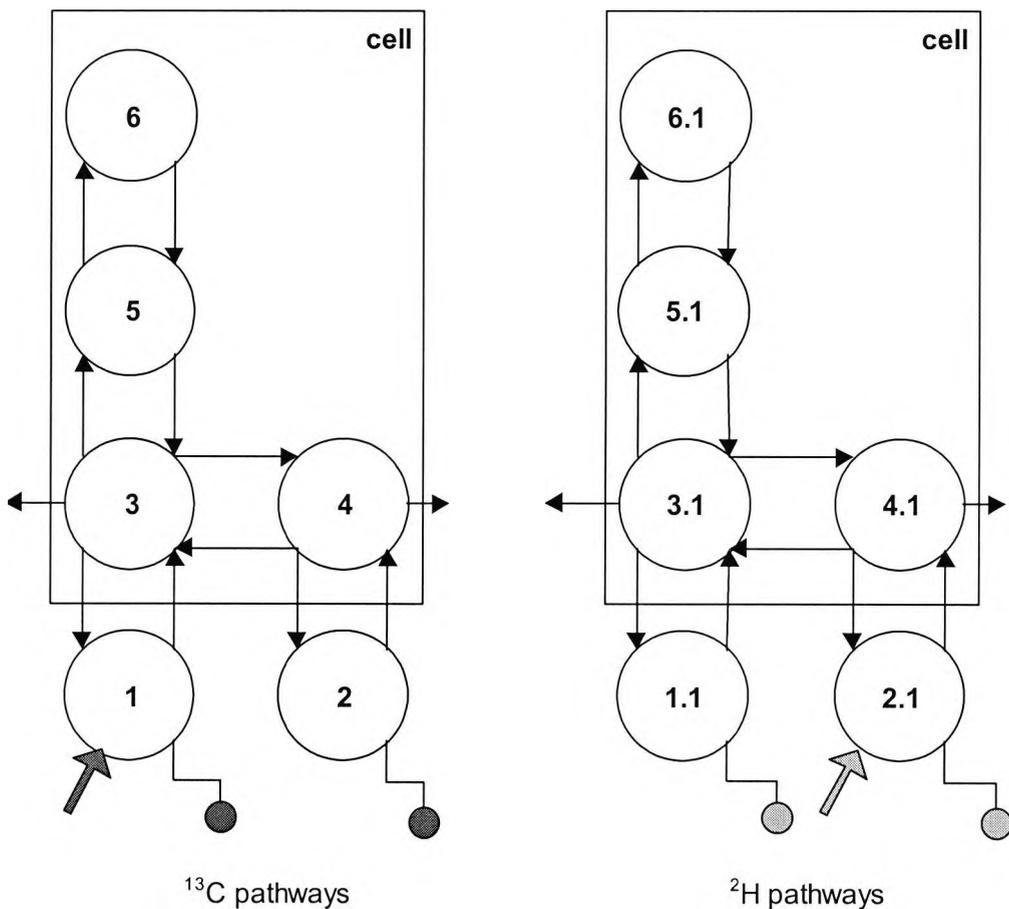
Figure 4.4: The implied Cobelli model (ICM0) used to simulate data for PM0. The diagram shows the infusion $[^{13}C]$-leucine (into compartment 1) and $[^2H]$-KIC (into compartment 2.1); all four species are measured ($[^2H]$-leucine and $[^2H]$-KIC, $[^{13}C]$-leucine and $[^{13}C]$-KIC). All compartments represent tracer locations. Compartments 1,2,3,4, 5 and 6 represent pathways for ^{13}C tracers: plasma leucine (compartment 1), plasma KIC (2), intracellular leucine (3,5), intracellular KIC (4) and a protein linked leucine pool (6). The compartments represented by 1.1, 2.1, 3.1, 4.1, 5.1 and 6.1 represent pathways for ^2H tracers, and the descriptions of these compartments are as for the carbon-based tracer.

4.2.2.1.2 Proposed Model 0

The proposed model 0 (PM0) recreates the Cobelli experiment, using similar input and outputs, but using a different model structure to describe the data. As with the Cobelli experiment, two tracers [^{13}C]-leucine and [^{2}H]-KIC were infused into the plasma, and four data sets collected: [^{13}C]-leucine, [^{2}H]-leucine, [^{13}C]-KIC and [^{2}H]-KIC. In order to monitor both tracers, it was necessary to run simultaneous experiments, one for labelled carbon and the other for labelled hydrogen pathways (Figure 4.5).
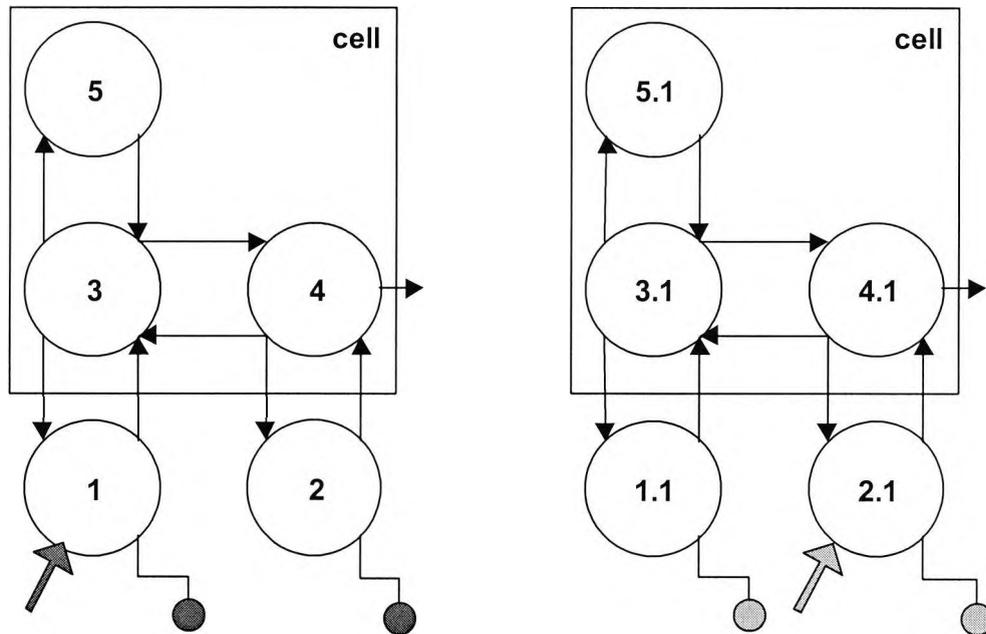

Figure 4.5: PM0 tracer model showing the infusion of both [^{13}C]-KIC (into compartment 1) and [^{2}H]-leucine (into compartment 2.1). All compartments represent tracer locations. All four species are measured: [^{2}H]-leucine, [^{2}H]-KIC, [^{13}C]-leucine and [^{13}C]-KIC. Compartments 1,2,3,4 and 5 represent pathways for ^{13}C tracers: plasma leucine (1), plasma KIC (2), intracellular leucine (3), intracellular KIC (4) and a fast turning over protein pool (5). The compartments 1.1, 1.2, 1.3, 1.4 and 1.5 represent pathways for the ^{2}H tracer, and the descriptions of these compartments are as for the ^{13}C tracer.

PM0 may be described by the following differential equations:

$$\dot{q}_1 = k_{13}q_3 - k_{31}q_1 + u_{CL}$$

$$\dot{q}_2 = +k_{42}.q_2 - k_{24}.q_4$$

$$\dot{q}_3 = k_{35}q_5 - k_{53}q_3 - k_{13}q_3 + k_{31}q_1 - k_{43}q_3 + k_{34}q_4$$

$$\dot{q}_4 = +k_{43}.q_3 + k_{42}q_2 - k_{24}q_4 + k_{43}q_3 - k_{34}q_4 - k_{04}.q_4$$

$$\dot{q}_5 = k_{53}q_3 - k_{35}q_5$$

$$\dot{q}_{1.1} = k_{13}q_{3.1} - k_{31}q_{1.1} + u_{HK}$$

$$\dot{q}_{2.1} = +k_{42}.q_{2.1} - k_{24}.q_{4.1}$$

$$\dot{q}_{3.1} = k_{35}q_{5.1} - k_{53}q_{3.1} - k_{13}q_{3.1} + k_{31}q_{1.1} - k_{43}q_{3.1} + k_{34}q_{4.1}$$

$$\dot{q}_{4.1} = +k_{43}.q_{3.1} + k_{42}q_{2.1} - k_{24}q_{4.1} + k_{43}q_{3.1} - k_{34}q_{4.1} - k_{04}.q_{4.1}$$

$$\dot{q}_{5.1} = k_{53}q_{3.1} - k_{35}q_{5.1}$$

$$z_{CL} = \frac{q_1}{Q_1} \qquad z_{CK} = \frac{q_2}{Q_2} \qquad z_{HL} = \frac{q_{1.1}}{Q_1} \qquad z_{HK} = \frac{q_{2.1}}{Q_2}$$

where the subscript: $_{CL}$ indicates C-labelled leucine, $_{CK}$ indicates C-labelled KIC, $_{HL}$ indicates H-labelled leucine and $_{HK}$ indicates H-labelled KIC. Since the tracee is the same for both [^{13}C] and [^{2}H]-leucine thus:

$$Q_1 = Q_{1.1} \; ; \; Q_2 = Q_{2.1} \; ; \; Q_3 = Q_{3.1} \; ; \; Q_4 = Q_{4.1} \; ; \; Q_5 = Q_{5.1}$$

where q_i is tracer mass of compartment i, $i = 1,2...5$, with the condition that q_i at $t = 0$ is 0; q_i ($i = 1,2 ... 5$) is the mass of [^{13}C] labelled material introduced by the exogenous infusion of [^{13}C]-leucine and q_i ($i = 1.1, 1.2 ... 1.5$) is the mass [^{2}H] labelled material introduced by the exogenous infusion of [^{2}H] KIC; and; $k_{i,j}$ is the transfer rate parameter from compartment j to i; and u_C and u_H represent the infusion of [^{13}C]-KIC (into compartment 1) and [^{2}H]-leucine (into compartment 2.1) respectively. Q_1 is the mass of cold (endogenous) leucine in compartment 1, and Q_2 is the mass of cold KIC in compartment 2.

4.2.2.2 Case 1: PM1 and ICM1

This case tests the use of the $[^{15}N,^{13}C]$-leucine tracer. The metabolism of $[^{15}N,^{13}C]$-leucine results in at least three different, measurable leucine species: $[^{15}N,^{13}C]$-leucine, $[^{13}C]$-leucine, and $[^{13}C]$-KIC. In Case 1, however, only $[^{15}N,^{13}C]$-leucine pathways are included.

4.2.2.2.1 Reference model ICM1

ICM1 is shown in Figure 4.6. The model retains the structure of the original model described by Cobelli (Figure 2.12), however completely excludes the KIC system.
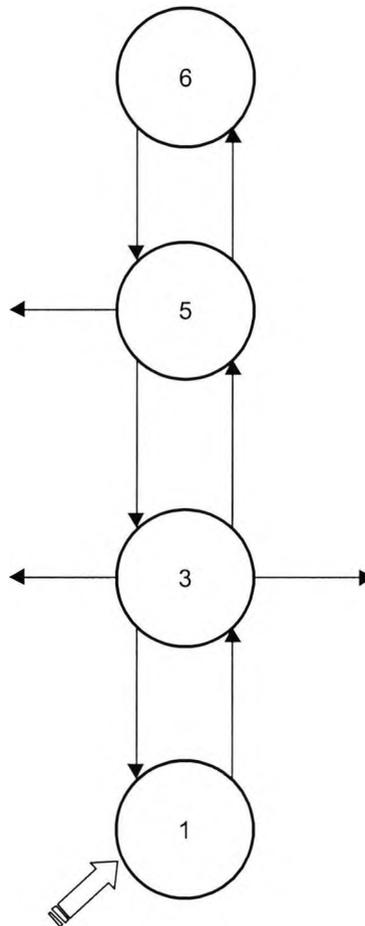

Figure 4.6: Implied Cobelli Model 1 (ICM1) used to simulate synthetic data, based on the Cobelli (1991) model, but describing pathways of $[^{15}N, ^{13}C]$-leucine tracer only. According to Cobelli (1991) compartment 1 is an extracellular leucine pool; compartments 3 and 5 are intracellular leucine pools; and compartment 6 is a protein linked leucine pool. The parameter k_{03} represents the reversible transamination of leucine to KIC, for the $[^{15}N, ^{13}C]$-leucine tracer, the step is irreversible.

4.2.2.2.2 Proposed model PM1

Case 1 considers $[^{15}N,^{13}C]$-leucine kinetics only, thus PM1 is a three compartment catenary model with $[^{15}N,^{13}C]$-leucine input and sampling occurring in the plasma leucine compartment. The model allows the estimation of the rate of incorporation of leucine into a fast turning over protein pool, k_{53}, leucine release from a fast turning over protein pool, k_{35}, and the deamination of leucine, k_{03}.
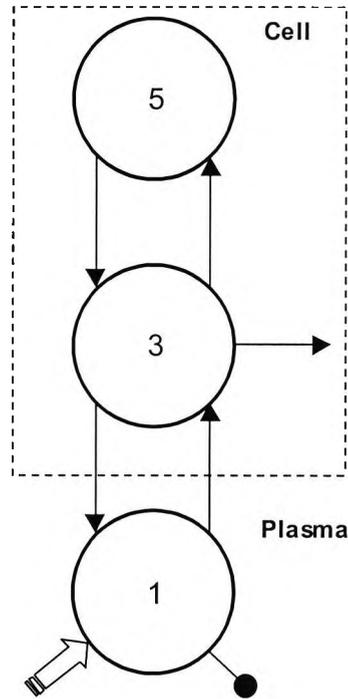

Figure 4.7: The tracer model for $[^{15}N,^{13}C]$-leucine. The model describes the kinetic events during an intravenous infusion of $[^{15}N,^{13}C]$-leucine (arrow entering *compartment 1*) and assumes measurements in extracellular compartment (●). Infused $[^{15}N,^{13}C]$-leucine tracer enters the plasma leucine pool (*compartment 1*), it may then enter intracellular space (*compartment 3*) where it may be either irreversibly de-aminated (*k_{03}*) or incorporated into a fast-turning over protein pool (*compartment 5*). Protein breakdown is represented by the flux of material from *compartment 5* into *compartment 3* (*k_{35}*).

The three-compartment model (Figure 4.7) which represents $[^{15}N,^{13}C]$-leucine tracer kinetics, is described by a set of differential equations:

$$\dot{q}_1 = k_{13}q_3 - k_{31}q_1 + u_N$$

$$\dot{q}_3 = k_{35}q_5 - k_{53}q_3 - k_{13}q_3 + k_{31}q_1 - k_{03}q_3$$

$$\dot{q}_5 = k_{53}q_3 - k_{35}q_5$$

$$z_N = \frac{q_1}{Q_1}$$

where q_i is mass of $[^{15}N,^{13}C]$-leucine tracer in *compartment i*, $i = 1$, 3 and 5, with the condition that $q_i\ (0) = 0$; $k_{i,j}$ is the fractional transfer rate constant from *compartment j* to *compartment i*; u_N is the infusion rate of $[^{15}N,^{13}C]$-leucine, Q_1 is the mass of leucine in *compartment 1* originating from endogenous supplies and z_N is the TTR of $[^{15}N,^{13}C]$-leucine. The mass Q_1 is assumed to be constant during the experiment.

There are six unknown parameters for the model, transfer rate constants k_{ij} and the mass Q_1. A catenary compartmental system with one leak is theoretically uniquely identifiable if the single-input/single output is performed in an extremal compartment (Carson et al. 1983), guaranteeing theoretical identifiability of our model.

4.2.2.3   Case 2: PM2 and ICM2

In Case 1, the KIC system was excluded, Case 2 includes the KIC sub-system. Instead of measuring only $[^{15}N,^{13}C]$-leucine, PM2 requires the collection of $[^{15}N,^{13}C]$-leucine, $[^{13}C]$-leucine and $[^{13}C]$-KIC. The rationale for this has been discussed, but to re-iterate $[^{15}N,^{13}C]$-leucine undergoes an irreversible deamination. Thus the metabolic pathways of a $[^{15}N,^{13}C]$-leucine tracer exclude the pathways involving KIC (see Figure 4.2). However, leucine deamination produces $[^{13}C]$-KIC, which in turn may be reaminated to $[^{13}C]$-leucine. Thus in PM2, the $[^{15}N,^{13}C]$-leucine tracer allows a full description of leucine kinetics. The model allows the measurement of several leucine kinetic events, including the incorporation of leucine into a fast turning over protein pool, k_{53}, leucine release from a fast turning over protein pool, k_{35}, and the irreversible oxidation of KIC, k_{04}.

4.2.2.3.1   Reference model ICM2

ICM2 (shown in Figure 4.8) is an expanded version of ICM1 and includes the KIC sub-system.
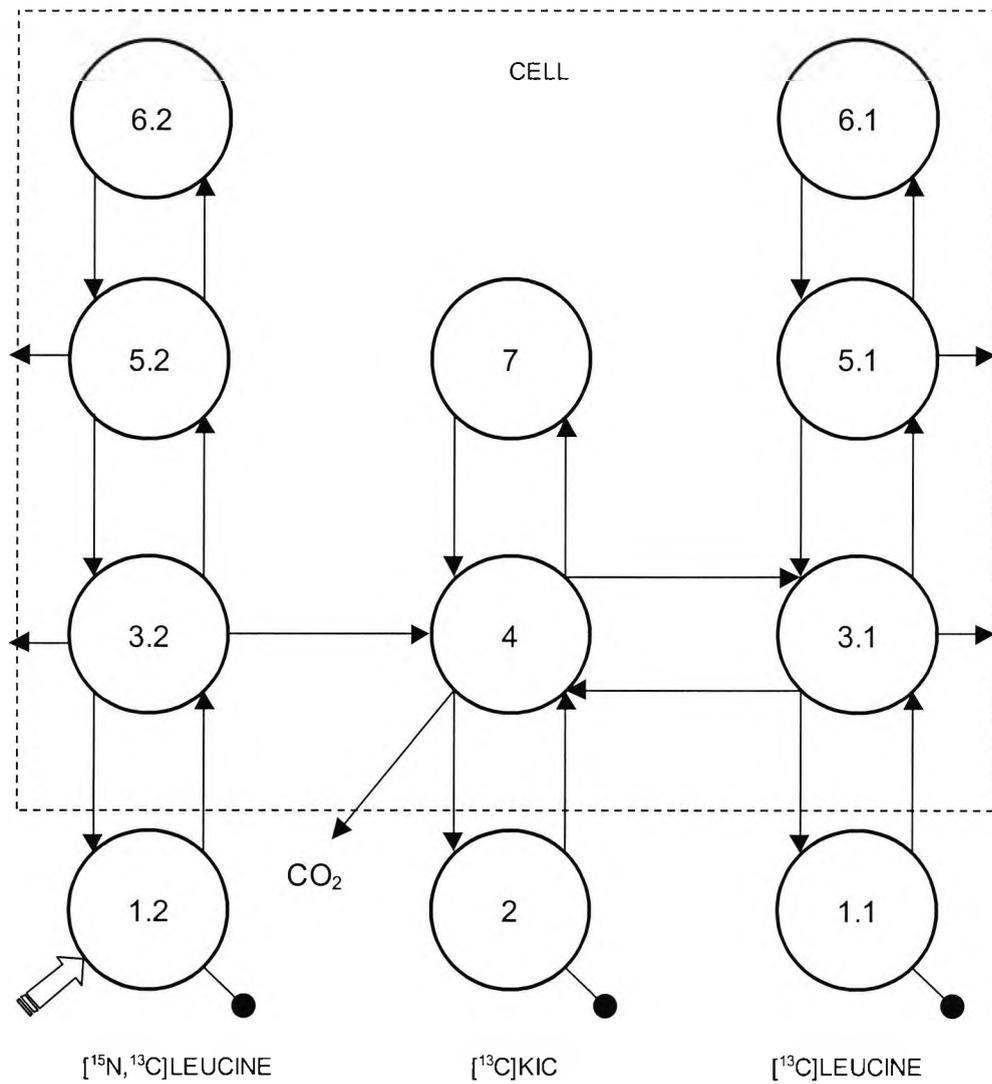
Figure 4.8: ICM2, $[^{15}N,^{13}C]$-leucine infusion into compartment 1.1, with sampling in compartments 1.1 ($[^{15}N,^{13}C]$-leucine), 2 ($[^{13}C]$-KIC) and 1.1 ($[^{13}C]$-leucine). Parameter k_{04} represents irreversible oxidation of KIC and k_{43} represents $[^{15}N,^{13}C]$ leucine deamination to $[^{13}C]$-KIC.

4.2.2.3.2   Proposed model PM2

PM2 (shown in Figure 4.9) is expanded versions of PM1and includes the KIC sub-system. The model is based on the infusion of $[^{15}N,^{13}C]$-leucine into the plasma and measuring $[^{15}N,^{13}C]$-leucine, $[^{13}C]$-KIC and $[^{13}C]$-leucine.
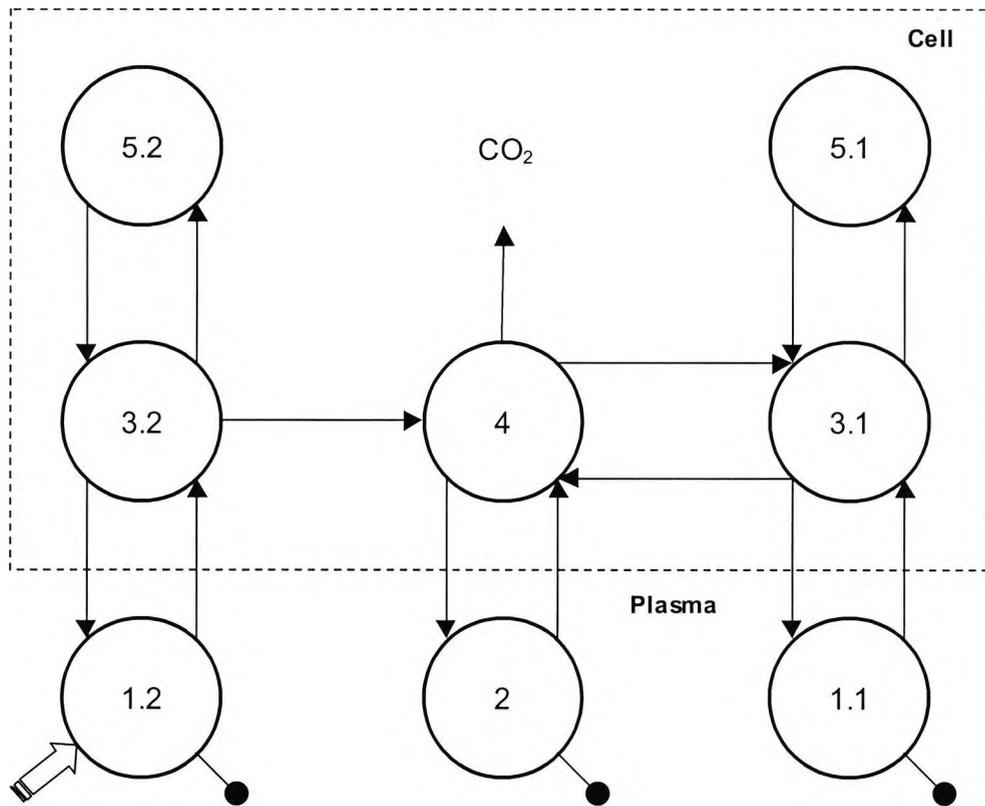
Figure 4.9: PM2 tracer model showing the infusion of $[^{15}N,^{13}C]$-leucine (into compartment 1.2). All three resulting species are measured: $[^{15}N,^{13}C]$-leucine, $[^{13}C]$-KIC and $[^{13}C]$-leucine. Compartments 1.2, 3.2 and 5.2 represent pools of $[^{15}N,^{13}C]$ leucine; compartments 2 and 4 represent pools of $[^{13}C]$-KIC. Compartments 1.1, 3.1 and 5.1 represent pools of $[^{13}C]$-leucine and these are assumed to behave identically to their counterparts compartments 1.2, 3.2 and 5.2.

PM2 may be described by the following equations:

$$\dot{q}_{1.2} = +k_{13}.q_{3.2} - k_{31}.q_{1.2} + u_L$$

$$\dot{q}_{1.1} = +k_{13}.q_{3.1} - k_{31}.q_{1.1}$$

$$\dot{q}_2 = +k_{42}.q_2 - k_{24}.q_4$$

$$\dot{q}_{3.2} = +k_{35}.q_{5.2} - k_{53}.q_{3.2} - k_{13}q_{3.2} + k_{31}.q_1 - k_{43}.q_3$$

$$\dot{q}_{3.1} = +k_{35}q_{5.1} - k_{53}q_{3.1} - k_{13}q_{3.1} + k_{31}q_{1.1} - k_{43}q_{3.1} + k_{34}q_4$$

$$\dot{q}_4 = +k_{43}.q_{3.2} + k_{42}q_2 - k_{24}q_4 + k_{43}q_{3.1} - k_{34}q_4 - k_{04}.q_4$$

$$\dot{q}_{5.2} = k_{53}q_{3.2} - k_{35}q_{5.2}$$

$$z_N = \frac{q_{1.2}}{Q_1} \qquad z_K = \frac{q_2}{Q_2} \qquad z_L = \frac{q_{1.1}}{Q_1}$$

where subscript N denotes [^{15}N,^{13}C]-leucine tracer, subscript K denotes [^{13}C]-KIC tracer and subscript L denotes [^{13}C]-leucine, q_i is tracer mass of *compartment i*, $i = 1,2,3...$ with the condition that $q_i(0)=0$; q_i is the mass of [^{15}N,^{13}C]-leucine introduced by the exogenous infusion of material; k_{ij} is the transfer rate parameter from *compartment j* to i; and u_L is the tracer infusion of [^{15}N,^{13}C]-leucine. Q_1 is the mass of cold leucine in *compartment 1*.

4.2.3 Dosage

The aim was to determine what dosage would attain a tracer to tracee ratio between 4% and 6% over 360 minutes. The Cobelli (1991) model was reproduced and reported parameter estimates (Cobelli et al. 1991) were used to simulate the effect of different doses of tracer. A dosage of 0.064 µmol kg^{-1} min^{-1} of tracer (over 360 minutes) was sufficient to achieve a TTR enrichment of between 4% and 6% (Gowrie et al. 1999).

Simulated TTR profiles following the infusion of [^{13}C]-leucine (Figure 4.10), [^{2}H]-KIC (Figure 4.11) and [^{15}N,^{13}C]-leucine (Figure 4.12) are shown below.
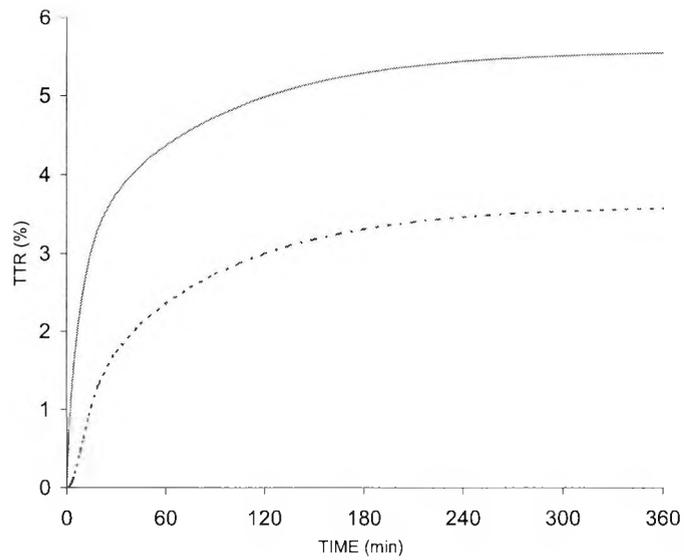
Figure 4.10: Simulated data profiles for PM0 (generated using the reference model ICM0) during constant infusion of 0.064 umol/kg/min [^{13}C]-leucine over 360 minutes, solid line represents [^{13}C]-leucine and dotted line represents [^{13}C]-KIC.
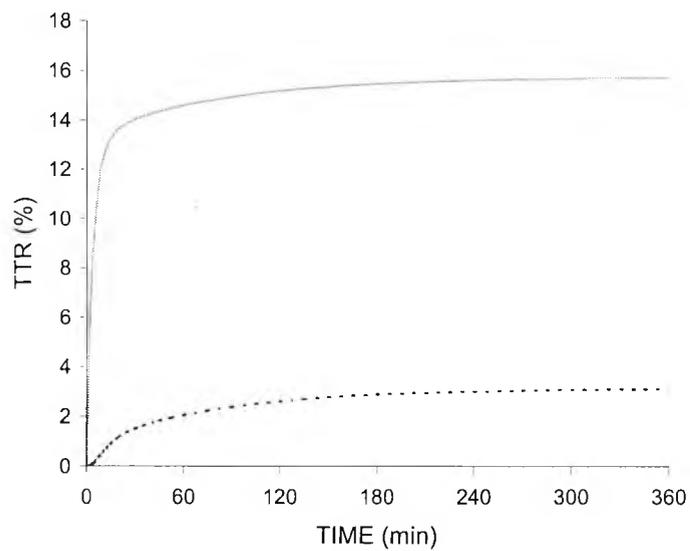

Figure 4.11: Simulated data profiles for PM0 (generated using the reference model ICM0) during constant infusion of 0.064 umol/kg/min [^{2}H] KIC over a 360 minutes, solid line represents [^{2}H] KIC and dotted line represents [^{2}H]-leucine.
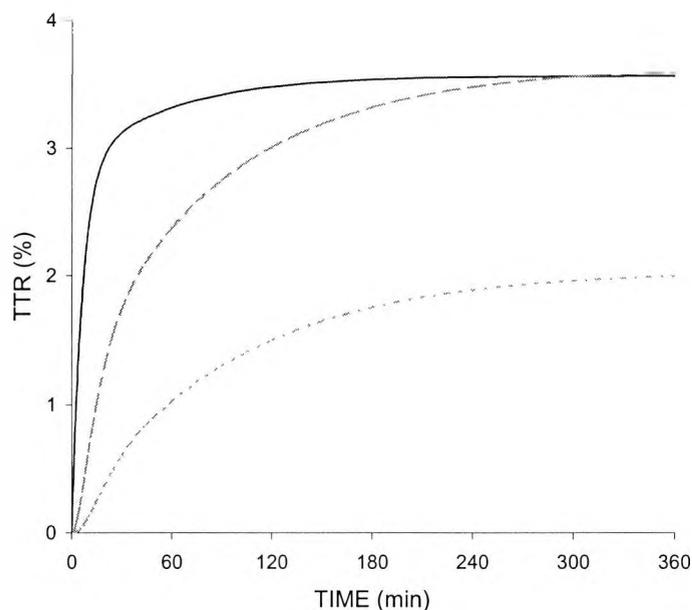
Figure 4.12: Simulated data profiles for PM1 and PM2 (generated using the reference model ICM1 and ICM2) during constant infusion of 0.064 μmol/kg/min [^{15}N, ^{13}C]-leucine over 360 minutes, solid line represents [^{15}N, ^{13}C]-leucine, dashed line (---) represents [^{13}C]-KIC and dotted line (....) represents [^{13}C]-leucine. Note that the dosage profile for [^{15}N, ^{13}C]-leucine is the same for both PM1 and PM2.

4.2.4   Sampling schedule

The ideal sampling schedule should aim to minimise the number of samples needed from a patient without significantly reducing the accuracy with which the parameters of clinical interest can be resolved. It should therefore represent a compromise between collecting as few data as possible, while at the same time ensuring that sufficient data are collected to allow model parameters to be estimated accurately.

In this exercise the sampling schedules used were similar to those used in the Cobelli paper (Cobelli et al. 1991). Samples were taken at t = 0 and at 1, 2, 3, 4, 5, 8, 10, 12.5, 15, 20, 30, 45, 60, 75, 90, 105, 120, 135, 150, 165, 180, 195, 210, 225, 240, 255, 270, 285, 300, 315, 330, 345, 360 min relative to the time of the start of the tracer infusion.

4.2.5   Measurement error

Measurement error was added to our synthetic error-free measurements in order to investigate its influence on parameter estimation. For each proposed model several additional data sets were

created by adding measurement error (details below) and so called 'virtual' subjects created. Two methods of adding measurement error were considered.

Firstly, data for three subjects was simulated where measurement error was drawn from a normal distribution with zero mean and a constant coefficient of variation (CV). Data was simulated using CVs of 5%, 7.5% and 10%.

Three additional data sets were simulated (data sets 4, 5 and 6) where CV was defined as

$$CV(z) = 5.01e^{-0.2844z} \qquad\qquad [4.1]$$

where z is the error-free measurement. The formula for $CV(z)$ (%) was derived by the non-linear regression analysis of 20 duplicate TTR measurements of $[^{13}C]$-leucine from the range 0.5% - 12% (data not shown). For small values of TTR (< 0.5%) the CV predicted by our error model was deemed to be unrealistic and an SD of 0.02% was used instead. For each Case there were six data sets, three with constant CV error added (data sets 1, 2 and 3) and an additional three with error as defined in equation 4.1 (data sets 4,5 and 6).

4.2.6 Parameter estimation

Parameter estimation was carried out using the SAAM II program (SAAM Institute, Seattle WA, USA) employing a non-linear weighted regression analysis. The weights were defined as reciprocals of the variance of the measurement error. The measurement error model described by equation 4.1 was employed to calculate the variance. SAAM II also calculated the precision or parameter estimates from the inverse of the Fisher information matrix (Carson et al. 1983). The precision was expressed as the fractional standard deviation.

4.3 Results

It was possible to estimate fractional rate constants (k_{ij}) and the mass of the plasma leucine pool (Q_1) in all cases described above. The results for each case are shown below (Case 0 in Section 4.3.1; Case 1 in Section 4.3.2; Case 2 in Section 4.3.3). Steady state pool sizes and fluxes of endogenous leucine (tracee) were calculated for each model (PM0, PM1 and PM2) using the tracer-derived parameters. In addition, the masses Q_3 (intracellular leucine pool), Q_5 (fast turning-over protein pool) and the flux from protein breakdown B ($k_{35} . Q_5$) were calculated under steady

state conditions. The results of parameter estimation are shown in Table 4.2 (Case 0), Table 4.3 (Case 1) and Table 4.4 (Case 2).

4.3.1   Case 0

Case 0 was performed to determine if the proposed model structure (Figure 4.3) is compatible with the Cobelli (1991) model structure. For Case 0 parameter estimates were generally good, and results of estimates are shown in Table 4.2. An example fit is shown in Figure 4.13 and Figure 4.14. Curves for all six subjects and a plot of the mean weighted residuals are shown in Appendix II.1. There is no regular pattern in the plot of the weighted residuals; this indicates that the model provided unbiased fit with an acceptable goodness-of-fit (weighted residuals distributed randomly within the ±SD region of the measurement error). These results are sufficiently encouraging to suggest that our proposed model structure is compatible with the Cobelli structure, and that the Cobelli (1991) model may be used to simulate data for the purposes of this study.

Table 4.2: Estimated tracer model parameters (k_{ij}), masses (Q_i) for Proposed Model 0 (PM0)

	Data set						Mean (SD)
	1	2	3	4	5	6	
	CV = 5%	CV = 7.5%	CV = 10%	CV model	CV model	CV model	
k_{13}	0.19 (9)	0.18 (12)	0.20 (10)	0.33 (24)	0.21 (10)	0.32 (28)	0.24 (0.07)
k_{31}	0.26 (5)	0.26 (3)	0.33 (12)	0.25 (4)	0.38 (8)	0.25 (4)	0.29 (0.05)
k_{24}	0.31 (45)	0.24 (56)	0.47 (36)	0.21 (52)	0.40 (40)	0.18 (54)	0.30 (0.11)
k_{42}	0.29 (2)	0.30 (2)	0.29 (3)	0.27 (0)	0.29 (1)	0.29 (0)	0.29 (0.01)
k_{43}	1.17 (25)	1.17 (19)	0.47 (28)	1.11 (26)	0.39 (15)	1.09 (29)	0.90 (0.36)
k_{34}	9.45 (44)	7.68 (57)	6.69 (41)	3.85 (53)	4.74 (42)	3.29 (54)	5.95 (2.40)
k_{04}	1.04 (44)	0.80 (56)	1.55 (36)	0.69 (52)	1.32 (40)	0.62 (54)	1.00 (0.37)
k_{35}	0.03 (6)	0.03 (4)	0.03 (8)	0.02 (4)	0.03 (8)	0.03 (4)	0.03 (0.00)
k_{53}	0.14 (15)	0.13 (16)	0.09 (18)	0.19 (26)	0.10 (16)	0.21 (31)	0.14 (0.05)
Q_1	11.91 (2)	11.67 (2)	11.33 (4)	13.35 (3)	10.16 (5)	12.89 (3)	11.88 (1.14)
Q_2	1.81 (2)	1.76 (2)	1.82 (3)	1.95 (0)	1.84 (1)	1.81 (0)	1.83 (0.06)
Q_3	15.88	16.74	18.61	10.15	18.56	10.15	15.02 (3.92)
Q_5	72.52	72.86	64.54	90.66	68.38	73.18	73.69 (8.97)
B	2.16	2.14	1.76	1.94	1.83	2.17	2.00 (0.18)

Values are in min^{-1} (k_{ij}), μmol/kg (Q_i) and μmol/kg/min (B). Precision of estimated parameter is reported in parenthesis and expressed as a fractional standard deviation. The *masses Q_3* and *Q_5* were calculated from the solution of the model assuming steady state conditions. The *flux B* represents leucine release from proteins (protein breakdown) and under steady state conditions is equal to the incorporation of leucine into protein (protein synthesis, S).

4.3.2 Case 1

PM1 requires a constant infusion of $[^{15}N, ^{13}C]$-leucine with sampling of $[^{15}N, ^{13}C]$-leucine only. It was possible to estimate parameters with good precision, and results of parameter estimation estimates are shown in Table 4.3. An example fit is shown in Figure 4.15. The plot of the weighted residuals (Figure 4.16) indicates that the model provided unbiased fit with an acceptable goodness-of-fit (weighted residuals distributed randomly within the $\pm$SD region of the measurement error). Curves, fits and weighted residuals for all subjects are shown in the Appendix II.2.

Table 4.3: Estimated tracer model parameters (k_{ij}), masses (Q_i) for Proposed Model 1 (PM1)

	Data set						
	1	**2**	**3**	**4**	**5**	**6**	**Mean (SD)**
	CV = 5%	**CV = 7.5%**	**CV = 10%**	**CV model**	**CV model**	**CV model**	
k_{03}	0.17 (16)	0.12 (22)	0.11 (21)	0.10 (28)	0.18 (18)	0.10 (19)	0.13 (0.03)
k_{13}	0.27 (49)	0.23 (87)	0.12 (40)	0.11 (57)	0.38 (68)	0.12 (40)	0.20 (0.11)
k_{31}	0.57 (30)	0.71 (73)	0.41 (18)	0.38 (21)	0.72 (51)	0.42 (17)	0.53 (0.16)
k_{35}	0.02 (11)	0.01 (73)	0.01 (40)	0.01 (28)	0.02 (18)	0.01 (21)	0.02 (0.01)
k_{53}	0.06 (15)	0.03 (22)	0.05 (32)	0.04 (24)	0.06 (20)	0.04 (21)	0.05 (0.01)
Q_1	11.61 (9)	9.92 (28)	12.41 (7)	13.14 (6)	10.80 (15)	12.50 (5)	11.73 (1.12)
Q_3	24.15	42.86	31.40	45.74	20.49	44.02	34.78 (10.9)
Q_5	65.11	143.90	117.76	156.28	72.32	105.65	110.17 (36.8)
B	1.50	2.01	0.94	1.88	1.23	1.58	1.524 (0.40)

Values are in min^{-1} (k_{ij}), $\mu mol/kg$ (Q_i) and $\mu mol/kg/min$ (B). Precision of estimated parameter is reported in parenthesis and expressed as a fractional standard deviation. The *masses Q_3* and *Q_5* were calculated from the solution of the model assuming steady state conditions. The *flux B* represents leucine release from proteins (protein breakdown) and under steady state conditions is equal to the incorporation of leucine into protein (protein synthesis).

4.3.3 Case 2

Case 2 is identical to Case 1 except that in addition [^{13}C]-leucine and [^{13}C]-KIC are measured. It was possible to estimate parameters but with poor precision, and CV's were found to be in excess of 100%; results of parameter estimation estimates are shown in Table 4.4. An example fit is shown in Figure 4.17. Curves for all six subjects and plots of the weighted residuals are shown in the Appendix II.3. The plot of the weighted residuals indicates that the model provided unbiased fit with an acceptable goodness-of-fit (weighted residuals distributed randomly within the ±SD region of the measurement error).

Table 4.4: Estimated tracer model parameters (k_{ij}), masses (Q_i) for Proposed Model 2 (PM2)

	Data set						Mean (SD)
	1	**2**	**3**	**4**	**5**	**6**	
	CV = 5%	**CV = 7.5%**	**CV = 10%**	**CV model**	**CV model**	**CV model**	
k_{13}	1.74 (73)	1.45 (106)	3.07 (140)	2.51 (134)	0.98 (14)	1.04 (16)	1.80 (0.84)
k_{31}	0.25 (1)	0.24 (2)	0.25 (5)	0.26 (6)	0.25 (2)	0.24 (6)	0.25 (0.01)
k_{24}	4.48 (114)	5.02 (192)	2.24 (120)	1.76 (145)	8.75 (44)	12.49 (61)	5.79 (4.12)
k_{42}	0.82 (14)	0.91 (31)	1.08 (24)	1.13 (26)	0.80 (6)	0.76 (5)	0.92 (0.15)
k_{43}	2.00 (72)	1.75 (103)	3.29 (141)	2.83 (134)	1.11 (16)	1.24 (23)	2.04 (0.87)
k_{34}	0.81 (114)	0.83 (201)	0.35 (101)	0.29 (109)	1.67 (46)	2.32 (56)	1.05 (0.80)
k_{04}	0.66 (114)	0.66 (200)	0.30 (102)	0.24 (109)	1.35 (52)	1.82 (70)	0.84 (0.62)
k_{35}	0.03 (1)	0.03 (3)	0.03 (5)	0.03 (5)	0.03 (3)	0.03 (4)	0.03 (0.00)
k_{53}	0.97 (73)	0.83 (104)	1.68 (143)	1.36 (136)	0.57 (17)	0.60 (25)	1.00 (0.44)
Q_1	15.47 (1)	15.30 (1)	15.43 (2)	14.99 (2)	15.26 (1)	15.36 (1)	15.30 (0.17)
Q_2	16.40 (14)	16.68 (21)	14.01 (42)	13.13 (61)	15.90 (4)	17.40 (4)	15.59 (1.66)
Q_3	2.22	2.53	1.26	1.55	3.89	3.54	2.50 (1.05)
Q_5	71.87	70.06	70.36	70.39	73.96	70.89	71.26 (1.47)
B	2.16	2.10	2.11	2.11	2.22	2.13	2.14 (0.04)

Values are in min^{-1} (k_{ij}), µmol/kg (Q_i) and µmol/kg/min (B). Precision of estimated parameter is reported in parenthesis and expressed as a fractional standard deviation. The *masses Q_3 and Q_5* were calculated from the solution of the model assuming steady state conditions. The *flux B* represents leucine release from proteins (protein breakdown) and under steady state conditions is equal to the incorporation of leucine into protein (protein synthesis).
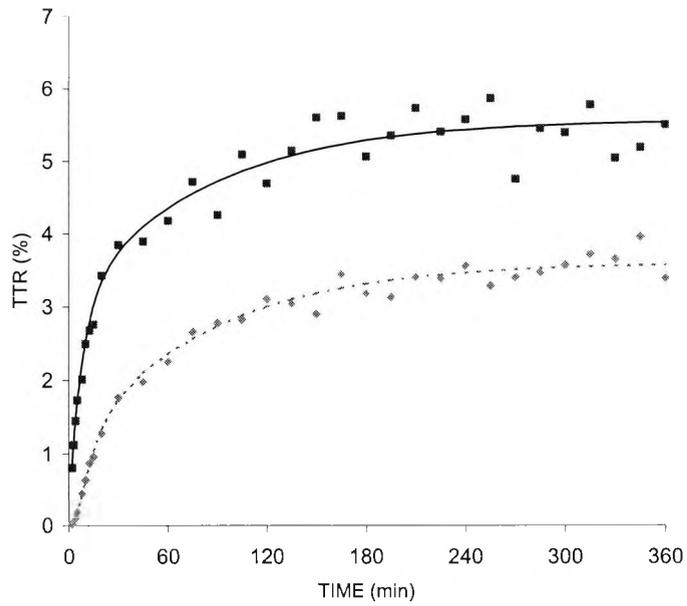
Figure 4.13: Tracer data curves for synthetic data (ICM0/PM0 with CV=5%). The chart shows simulated data for $[^{13}C]$-leucine (■) and $[^{13}C]$-KIC (◆) during a constant infusion of $[^{13}C]$-leucine over 360 minutes. The curves represent the fit using model PM0.
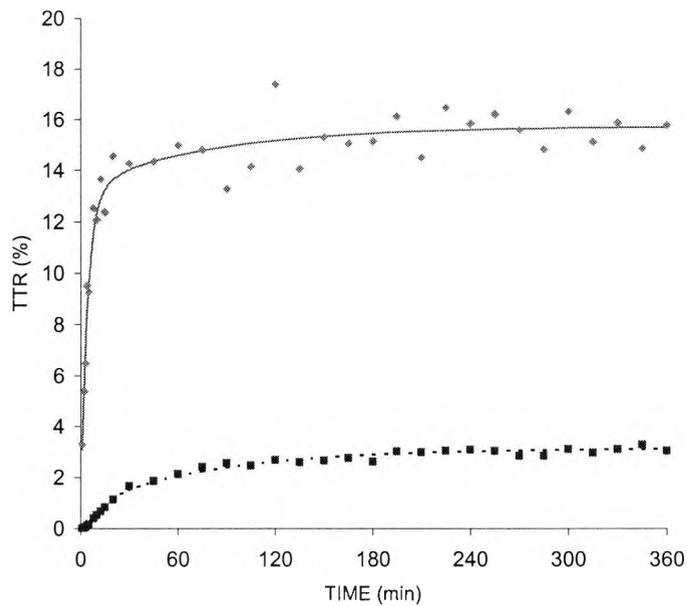

Figure 4.14: Tracer data curves for synthetic data (ICM0/PM0 with CV=5%). The chart shows simulated data for $[^{2}H]$-leucine (■) and $[^{2}H]$KIC (◆) during a constant infusion of $[^{2}H]$KIC over 360 minutes. The curves represent the fit using model PM0.
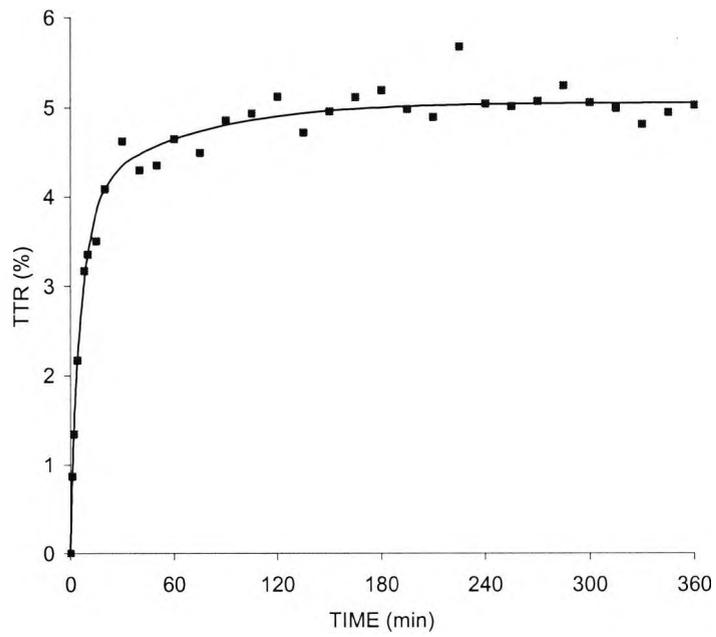
Figure 4.15: Tracer data curve for synthetic data (PM1/ICM1 with CV = 5%). The chart shows simulated data for $[^{15}N,^{13}C]$-leucine (■) during a constant infusion of $[^{15}N,^{13}C]$-leucine over 360 minutes. The curve represents the fit using model PM0.
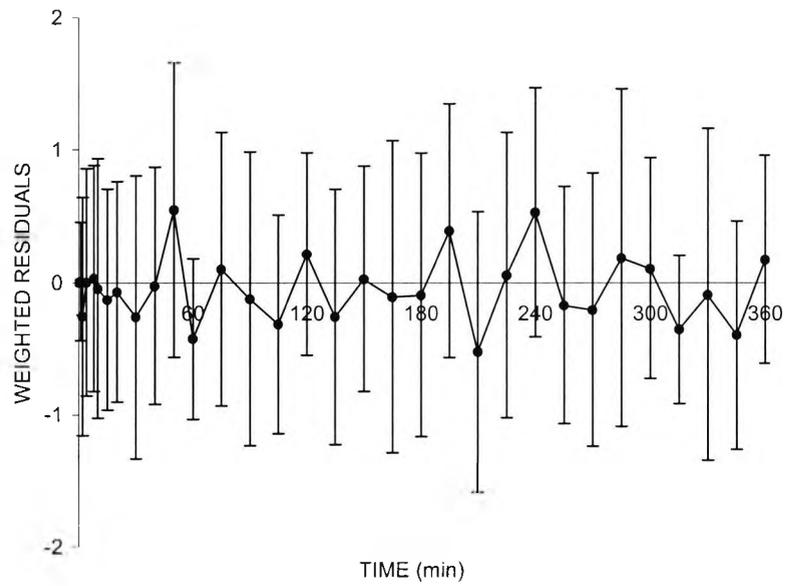
Figure 4.16: Mean ± standard deviation of weighted residuals (n=6) for Proposed Model 1
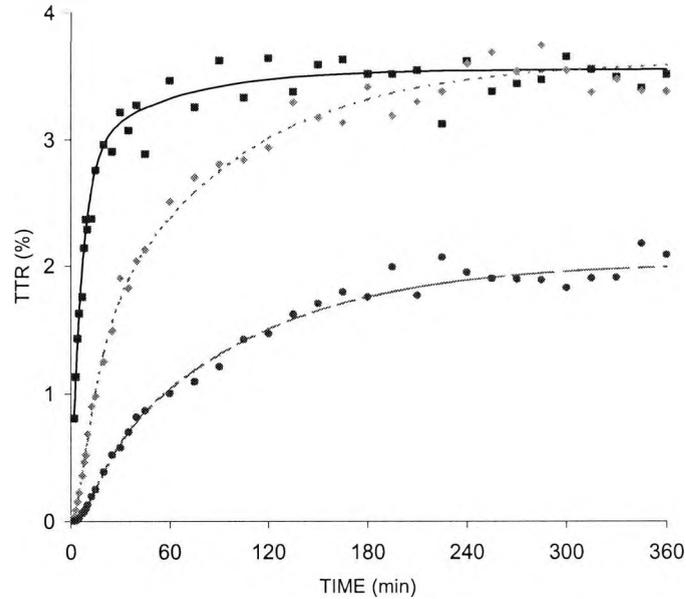
Figure 4.17: Tracer data curve for synthetic data PM2, CV = 5%. The chart shows simulated data for $[^{15}N,^{13}C]$-leucine (■), $[^{13}C]$-KIC (◆) and $[^{13}C]$-leucine (●) during a constant infusion of $[^{15}N,^{13}C]$-leucine over 360 minutes. The curves represent the fit using model PM1.

4.4   Discussion

Modelling leucine kinetics with commonly used tracers – $[^{13}C]$-leucine, $[^{14}C]$-leucine, etc. – is difficult due to the need to model the KIC sub-system. KIC metabolism is non-trivial and consists of irreversible oxidation and reversible transamination in intracellular space. In this study, the use of $[^{15}N,^{13}C]$-leucine tracer is proposed as its use can simplify the modelling of leucine metabolism. This is because $[^{15}N,^{13}C]$-leucine tracer is irreversibly transaminated and so there is no recycling of $[^{15}N,^{13}C]$-leucine tracer through the KIC sub-system. In modelling terms its kinetics are therefore simpler than the kinetics of the more commonly used leucine tracers. Using the $[^{15}N,^{13}C]$-leucine tracer in the manner suggested here, potentially allows the estimation of fractional rates of fast-turning over protein breakdown and synthesis without involving the KIC sub-system.

In this chapter a minimal configuration to describe leucine kinetics was introduced (Figure 4.3) and tested using simulated data (Case 0). We found our model to be compatible with the reference model and proceeded to use the new configuration to explore some compartmental models based on a $[^{15}N,^{13}C]$-leucine tracer. The reference model (Cobelli 1991) is based upon what is, to our

knowledge, the most comprehensive model of leucine kinetics to date. It includes intra- and extra-cellular pools for both leucine and KIC, the reversible transamination of leucine and KIC, the irreversible oxidation of KIC, and parameters for protein synthesis and breakdown. We used the reference model to simulate the kinetics of $[^{15}N,^{13}C]$-leucine tracer, and estimated parameters (see Table 4.2) for PM0 using this simulated data with measurement error added.

The Cobelli (1991) model is more complicated and more detailed than the model proposed here. It includes two intracellular leucine compartments (the proposed model has only one); in addition it includes three compartments to describe KIC kinetics, and includes irreversible oxidation of KIC. The model proposed here (PM1) models leucine kinetics without including the KIC sub-system. This has significant implications. The ultimate goal of amino-acid turnover studies is to enable the estimation of protein breakdown and synthesis; the KIC sub-system is only studied because using current methods, its quantification is necessary in order to estimate protein turnover.

The rest of this discussion our attention will be focussed on PM1. Firstly, PM1 is both theoretically and practically identifiable - we were able to estimate fractional rates for fast turning-over protein with low, but acceptable precision (Gowrie et al. 1999). Secondly, the experimental protocol of the new model is simpler than that the Cobelli (1991) model; involving the infusion of one tracer, and the measurement of one tracer species (the Cobelli (1991) model involves two tracers and the measurement of four tracer species). Furthermore, in modelling terms, the new model is simpler, not because of any new assumptions made but because the kinetics of $[^{15}N, ^{13}C]$-leucine allows us to by-pass the complex KIC sub-system. Bier (1989) questions the domain of validity of the model proposed by Umpleby et al (1986) because the KIC system is overlooked, while Cobelli (1991) use three compartments to describe the KIC sub-system and assume that both transamination and oxidation occur from the same KIC pool. This may well be correct, but it is also conceivable that oxidation and transamination occur in different intracellular KIC pools. Finally, this is but one of the modelling options available. The use of the $[^{15}N,^{13}C]$-leucine tracer also enables the development of a more complicated model. A combined model describing $[^{15}N, ^{13}C]$-leucine, $[^{13}C]$-leucine, and $[^{13}C]$-KIC kinetics is attainable by also measuring $[^{13}C]$-leucine and $[^{13}C]$-KIC enrichments; such a model would allow the domain of validity of this model to be explored, while at the same time matching the Cobelli (1991) model for complexity. However, it is felt that exploring other modelling options such as these is best left until clinical data are available.

Through simulated experiments, we tested the effect of simulated measurement error on parameter estimation. Of utmost concern was to determine whether the model we designed was likely to allow practical identification of certain parameters (the fractional rates of a fast turning over

protein pool). This practice of testing new models, methods and ideas using simulated data is not necessarily novel. However, considering the need for ethical approval and the cost of clinical studies in the field of physiological modelling, it is a step that is too often overlooked. Certainly, in this case the simulation study has justified a clinical evaluation of the $[^{15}N,^{13}C]$-leucine tracer to estimate protein turnover.

4.5 Conclusion

Unlike traditional leucine tracers – $[^{13}C]$-leucine, $[^{14}C]$-leucine, etc., – $[^{15}N,^{13}C]$-leucine tracer is irreversibly transaminated and its kinetics are simpler due to the absence of recycling through the KIC sub-system. Using simulated data we have demonstrated that a three-compartment model of whole body $[^{15}N,^{13}C]$-leucine kinetics allows the fractional turnover rates of a fast-turning-over protein pool to be represented and estimated (Gowrie et al. 1999). These results are sufficient to merit a study using the $[^{15}N,^{13}C]$-leucine as a tracer. In the next chapter we explore $[^{15}N,^{13}C]$-leucine in a clinical setting.

5   A NEW MODEL TO ESTIMATE WHOLE BODY PROTEIN TURNOVER IN MAN USING [^{15}N,^{13}C]-LEUCINE

5.1   Introduction and Aims

Leucine is an essential amino acid and by studying isotopic tracer data of this amino acid, researchers are able to estimate whole body protein turnover. The leucine system has been extensively studied using a variety of isotopically labelled tracers including ^{13}C, ^{14}C, ^{2}H, etc. In practise, however the reciprocal pool model has become the *de facto* standard, because it is simple to use, and because the only other similar method, the primary pool model, is known to under-estimate protein turnover. In the previous chapter we described a new model describing leucine kinetics and demonstrated (by way of simulation) how a [^{15}N,^{13}C]-leucine tracer could be used to estimate protein turnover. This chapter presents the details of the use of the [^{15}N,^{13}C]-leucine tracer in a clinical environment.

The objective of this experiment is to estimate fractional turnover rates of a fast turning over protein pool using the previously described 3-compartment model (PM1 from Chapter 4) and a [^{15}N,^{13}C]-leucine tracer in a clinical setting. The proposed model only measures leucine pathways and omits both the KIC sub-system and leucine oxidation pathways; it is therefore necessary to demonstrate the validity of the proposed model experimentally and theoretically.

5.2   Model development

The model structure and the leucine system have already been defined in Chapter 4. A diagram of leucine metabolism is shown in Figure 4.1. The pertinent processes are the de-amination of leucine (Dx), the re-amination of KIC (Rx), the oxidative disposal of leucine (Ox), the non-oxidative disposal of leucine (S), and the release of leucine from protein breakdown (B). Our compartmental model is based upon the simplest configuration of the leucine system. There are several modelling configurations available, but we will focus on:

1. the [^{15}N,^{13}C]-leucine tracer system

2. the complete tracer system including the tracer species: [^{15}N,^{13}C]-leucine, [^{13}C]-leucine and [^{13}C]-KIC,

3. the tracee system

5.2.1 The [^{15}N,^{13}C]-leucine tracer model

The tracer model has been described before in Chapter Four (Section 4.2.2.2), but is included here again for convenience. The three-compartment model (Figure 5.1) which represents [^{15}N,^{13}C]-leucine tracer kinetics, is described by a set of differential equations:

$$\dot{q}_1 = k_{13}q_3 - k_{31}q_1 + u_N \qquad [5.1]$$

$$\dot{q}_3 = k_{35}q_5 - k_{53}q_3 - k_{13}q_3 + k_{31}q_1 - k_{03}q_3 \qquad [5.2]$$

$$\dot{q}_5 = k_{53}q_3 - k_{35}q_5 \qquad [5.3]$$

$$z_N = \frac{q_1}{Q_1} \qquad [5.4]$$

where q_i is tracer mass of [^{15}N,^{13}C]-leucine in *compartment i*, $i = 1$, 3 and 5, with the condition that q_i (0) = 0; $k_{i,j}$ is the fractional transfer rate constant from *compartment j* to *compartment i*; u_N is the infusion rate of [^{15}N,^{13}C]-leucine, Q_1 is the mass of leucine in *compartment 1* originating from endogenous supplies and z_N is the tracer to tracee ratio (TTR) of [^{15}N,^{13}C]-leucine. The mass Q_1 is assumed to be constant during the experiment.

There are six unknown parameters for the model, transfer rate constants k_{ij} and the mass Q_1. A catenary compartmental system with one leak is theoretically uniquely identifiable if the single-input/single output is performed in an extremal compartment (Carson et al. 1983), guaranteeing theoretical identifiability of our model.
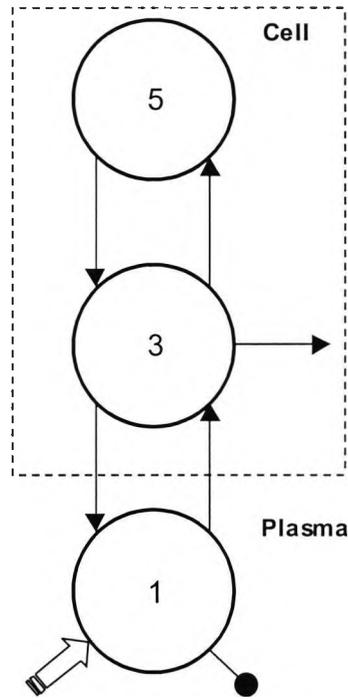
Figure 5.1: The tracer model for $[^{15}N,^{13}C]$-leucine. The model describes the kinetic events during an intravenous infusion of $[^{15}N,^{13}C]$-leucine (arrow entering compartment *1*) and assumes measurements in the extracellular compartment (•). Infused $[^{15}N,^{13}C]$-leucine tracer enters the plasma leucine pool (arrow entering *compartment 1*), it may then enter intracellular space (compartment *3*) where it may be either irreversibly de-aminated (k_{03}) or incorporated into a fast-turning over protein pool (compartment *5*). Protein synthesis is represented by the flux of material from compartment *3* into compartment *5* *(i.e., S = $k_{53}Q_3$)*.

5.2.2 The complete tracer model

Following the infusion of $[^{15}N,^{13}C]$-leucine tracer, three labelled tracer species exist i.e., $[^{15}N,^{13}C]$-leucine, $[^{13}C]$-leucine and $[^{13}C]$-KIC. The complete tracer model (shown in Figure 5.2) describes all three tracers and it is this model that is referred to in the calculations in Sections 5.3.7 and 5.4.3. The complete tracer model may be described by the following differential equations:

$$\dot{q}_{1.2} = k_{13}q_{3.2} - k_{31}q_{1.2} + u_N \qquad [5.5]$$

$$\dot{q}_{3.2} = k_{35}q_{5.2} - k_{53}q_{3.2} - k_{13}q_{3.2} + k_{31}q_{1.2} - k_{03}q_{3.2} \qquad [5.6]$$

$$\dot{q}_2 = k_{24}q_4 - k_{42}q_2 \qquad [5.7]$$

$$q_{3.2} = k_{35}q_{5.2} - k_{53}q_{3.2} - k_{13}q_{3.2} + k_{31}q_{1.2} - k_{43}q_{3.2} \tag{5.8}$$

$$q_4 = k_{43}q_{3.1} + k_{42}q_2 - k_{24}q_4 + k_{43}q_{3.2} - k_{34}q_4 - k_{04}q_4 \tag{5.9}$$

$$q_{5.2} = k_{53}q_{3.2} - k_{35}q_{5.2} \tag{5.10}$$

$$q_{5.1} = k_{53}q_{3.1} - k_{35}q_{5.1} \tag{5.11}$$

$$q_{1.1} = k_{13}q_{3.1} - k_{31}q_{1.1} \tag{5.12}$$

$$q_{3.1} = k_{31}q_{1.1} - k_{13}q_{3.1} + k_{35}q_{5.1} - k_{53}q_{3.1} + k_{34}q_4 - k_{43}q_{3.1} \tag{5.13}$$

$$z_N = \frac{q_{1.2}}{Q_1} \tag{5.14}$$

$$z_K = \frac{q_2}{Q_2} \tag{5.15}$$

$$z_C = \frac{q_{1.1}}{Q_1} \tag{5.16}$$

where q_i is tracer mass of compartment i, $i = 1,2,3…5$, with the condition that $q_i(0)=0$. In addition $q_{i.2}$ is the mass of $[^{15}N,^{13}C]$labelled species and $q_{i.1}$ represents $[^{13}C]$species; $k_{i.j}$ is the transfer rate parameter from compartment j to i; and u_N is the tracer infusion of $[^{15}N,^{13}C]$-leucine. Q_1 is the mass of cold leucine in compartment 1. Subscript z_N, z_C and z_K denote TTR's for $[^{15}N,^{13}C]$-leucine, $[^{13}C]$-leucine tracer and $[^{13}C]$-KIC respectively.
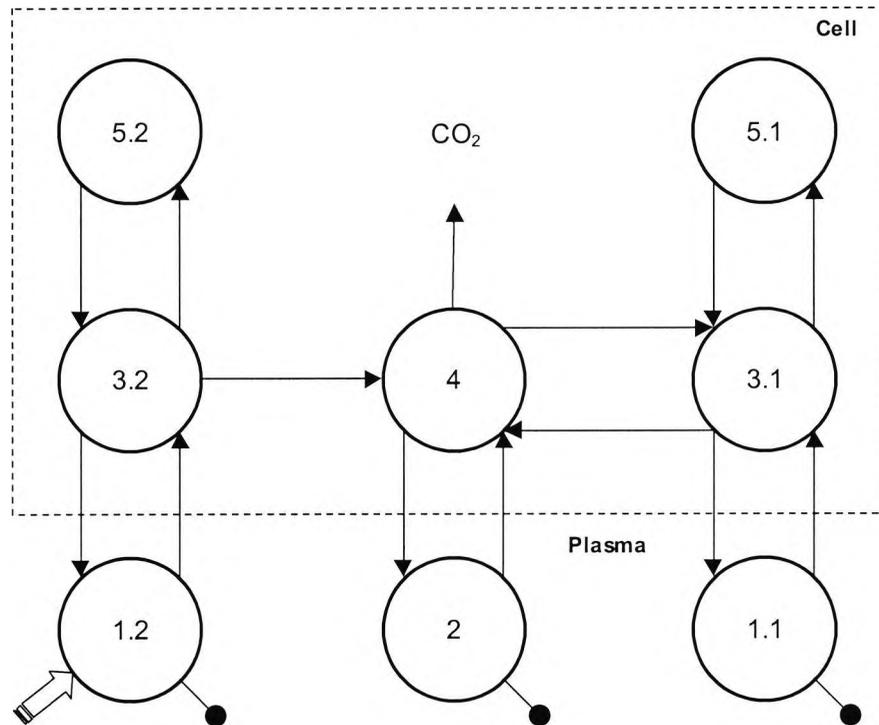
Figure 5.2: The complete tracer model showing the infusion of $[^{15}N,^{13}C]$-leucine into compartment 1. All three resulting species are measured: $[^{15}N,^{13}C]$-leucine, $[^{13}C]$-KIC and $[^{13}C]$-leucine. Compartments '1.2', '3.2' and '5.2' represent pools of $[^{15}N,^{13}C]$-leucine; compartments 2 and 4 represent pools of $[^{13}C]$-KIC; and compartments '1.1', '3.1' and '5.1' represent pools of $[^{13}C]$-leucine. The compartments '1.1', '3.1' and '5.1' represent pathways and compartments for the deaminated $[^{15}N,^{13}C]$ tracer, i.e., a $[^{13}C]$ label. The compartments '1.1', '3.1' and '5.1' are assumed to behave identically to their counterparts compartment '1.2', '3.2' and '5.2'.

5.2.3 Tracee model

There are several differences and naturally similarities between the tracee model (Figure 5.3) and the $[^{15}N,^{13}C]$-leucine tracer model (Figure 5.1). The differences stem from the fact that although the tracee and $[^{13}C]$-leucine are reversibly transaminated, $[^{15}N,^{13}C]$-leucine is not. The tracee model thus includes leucine deamination (Dx_m), and reamination (Rx_m). Note however that the fractional rate constant k_{43} in the tracee model is equivalent to k_{03} in the $[^{15}N,^{13}C]$-leucine tracer tracer model. The tracee model also includes pools for plasma and intracellular KIC, these are represented by compartments 2 and 4 respectively. The flux U represents the release of leucine from a slow turning over protein pool, the kinetics of this pool are too slow to be accounted for during this short experiment. It should be noted also that the flux U is not present in the four pool model implied by the primary and reciporcal pool models (Figure 2.9).
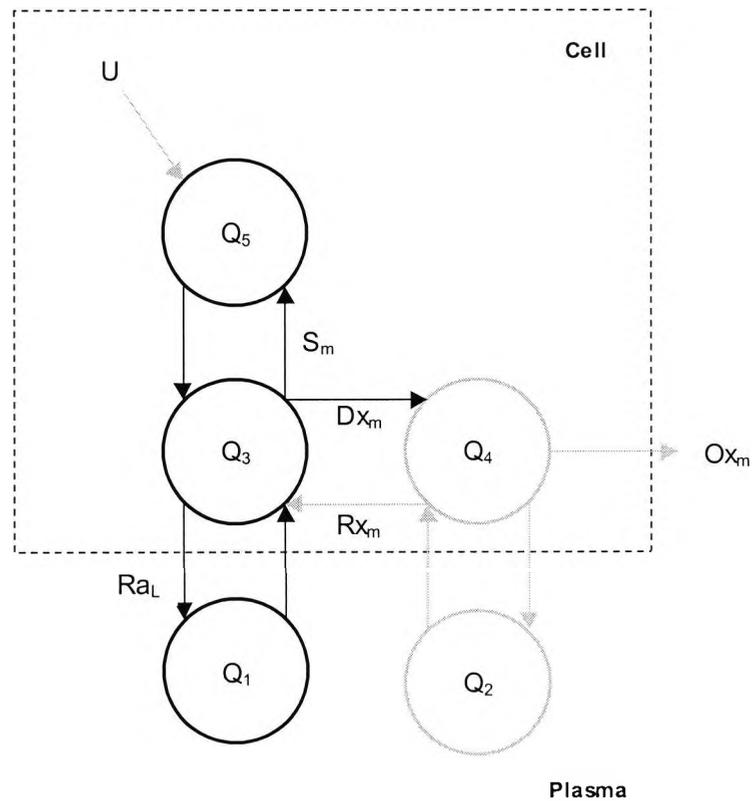
Figure 5.3: The tracee (endogenous leucine) model. Leucine is in constant flux with its keto-acid, KIC, through a reversible transamination reaction, Dx_m represents leucine de-amination and Rx_m represents leucine re-amination. During de-amination, the amino (NH_2) group is lost to the nitrogen pool; the resulting KIC has two fates, it may be re-aminated to leucine (Rx_m), or it may undergo an irreversible decarboxylation to CO_2 (Ox_m). U represents the appearance of material from protein breakdown, and S_m represents protein synthesis. The lighter coloured section of the model (including compartments 2 and 4) represent the differences between the $[^{15}N,^{13}C]$-leucine tracer model and the tracee model.

5.3   Methods

5.3.1   Subjects

We studied six healthy males who ranged in age from 26 to 43 years (mean $30.7 \pm$ SD 6.7 yr.) with body weight ranging from 55.9 to 87.6 kg (mean $68.0 \pm$ SD 10.9 kg) and height ranging from 160.5 to 187 cm (mean $174.4 \pm$ SD 10.3 cm). Details are shown in Table 5.1. Their informed consent was obtained after explaining the protocol to them. The Ethics Committee at St. Thomas's Hospital, London approved the research, (Ethics committee form and patient consent form in Appendix III).

Table 5.1: Subject details

	Subject						Mean	SD
	1	**2**	**3**	**4**	**5**	**6**	**Mean**	**SD**
Age (years)	43	27	26	27	27	34	30.7	6.7
Height (cm)	170	187	168	178	161	184	174.6	10.0
Weight (kg)	69	88	63	55	65	69	68.0	11.0

5.3.2 Materials

Sterile solutions of L-[1-^{15}N,1-^{13}C]-leucine (99 %; Mass Trace MA, USA) and L-[^{3}D]KIC (98%) (Cambridge Isotope Ltd, UK) were prepared in 0.9% saline with an aseptic technique by the Pharmacy Department, Guy's and St. Thomas' Hospital (London, UK)

5.3.3 Study design

At 8:00 am after an overnight fast, a cannula was inserted into an arm and three baseline plasma samples were taken at t = -15, -10 and -5 minutes before the administration of the tracer. A constant infusion of [^{15}N,^{13}C]-leucine (1 mg/kg/h) was started at 0 minutes and stopped at 240 minutes, blood samples were taken t = 0 and 1, 2, 4, 6, 8, 10, 12, 15, 20, 25, 30, 40 ,50 60, 75, 90, 120, 150, 180, 210, 240 minutes relative to the time of the start of the tracer infusion. Measurements were taken for another 60 minutes after the infusion ended at t = 241 and 242, 244, 246, 248, 250, 252, 255, 260, 265, 270, 280, 290 and 300 minutes. Baseline and expired breath samples were also collected at 30-minute intervals throughout the experiment.

5.3.4 Assays

Plasma [^{15}N,^{13}C]-leucine and [^{13}C]-leucine were measured as the t-butyldimethylsilyl derivative under selected ion monitoring by GCMS (GC: Hewlett-Packard 5890 series II, Woking, UK) (MS: Hewlett-Packard 5971A MSD Woking, UK) monitoring the ions at 302, 303 (for [^{13}C]-leucine) and 304 (for [^{15}N,^{13}C]-leucine) representing the [m-57] natural abundance, the [(m-57)+1] and the [(m-57)+2] enriched fragments respectively. Leucine concentration was measured with an internal standard of norleucine.

Plasma α-ketoisocaproic acid (KIC) enrichment and concentration was measured (using [^{3}D]-KIC as the internal standard) as the quinoxalinol-trimethylsilyl derivative under selected ion monitoring by GCMS (GC: Hewlett-Packard 5890 series II, Woking, UK) (MS: Hewlett-Packard 5971A MSD Woking, UK) monitoring the ions at 259, 260 (for [^{13}C]-KIC) and 262 (for [^{3}D]-

KIC) representing the [*m*-42] natural abundance, the [(*m*-42)+1] and the [(*m*-42)+3] enriched fragments respectively.

[^{13}C] enrichment of breath CO_2 was measured on a VG SIRA series II isotope ratio mass spectrometer (VG Isotech, Cheshire, UK).

The plasma amino acid profile was measured using an Alpha Plus II automated amino acid analyser (Pharmacia, Cambridge, UK). Plasma samples were deproteinized prior to analysis using 10% SSA containing norleucine as an internal standard.

5.3.5   Tracer to tracer ratios

Tracer to tracee ratios of [^{15}N,^{13}C]-leucine (z_N), [^{13}C]-leucine (z_C) and [^{13}C]-KIC (z_K) were calculated from raw peak isotope ratios of individual samples and corrected for spectra overlap (Rosenblatt et al. 1992). The calculations for these may be viewed in Appendix IV.

5.3.6   Leucine oxidation rate

Leucine oxidation rates are calculated from expired breath samples. Resting energy expenditure (REE), respiratory quotient (RQ), O_2 consumption and CO_2 production rate were estimated using a computerised open-loop gas analyser system (Medical Graphics, St, Paul, MN, US). Leucine oxidation rate was calculated as

$$Ox_p = \frac{(APE_{CO_2} \times CO_2 Ra)}{c \times z_L}$$

$$Ox_r = \frac{(APE_{CO_2} \times CO_2 Ra)}{c \times z_K}$$

where $CO_2 Ra$ is the production rate of CO_2 corrected for body weight (μmol/min/kg), APE_{CO_2} is the enrichment of expired CO_2, c represents a factor to account for the incomplete recovery of label in CO_2 and was assumed to be 0.80 (James et al. 1976). The subscripts p and r indicate calculations for the primary and reciprocal pool models respectively.

5.3.7 Steady state calculations

The rate of appearance or leucine into the plasma or Ra, is a measure of protein breakdown, B. Using a $[^{15}N,^{13}C]$-leucine tracer it is possible to calculate protein breakdown in the steady state using the primary pool model (B_p), the reciprocal pool model (B_r) and the proposed 3-compartment model (B_m). In practice, there are several methods for calculating leucine turnover from the primary and reciprocal pool models, i.e., either a leucine tracer, a KIC tracer or both leucine and KIC tracers may be used, however this is discussed elsewhere.

5.3.7.1 Primary pool model calculations using a $[^{15}N, ^{13}C]$-leucine tracer

When using the primary pool model with a $[^{13}C]$-leucine tracer the rate of appearance of leucine (Ra_L) is used as a measure of protein breakdown (B_p)

$$Ra_L = \frac{u_L}{z_L} \qquad [5.17]$$

where z_L represents tracer to tracee ratio, and u_L is the dosage of tracer administered. Ra_L is a measure of leucine appearance in the plasma, and is thus an index of protein breakdown. So, for the primary pool model, protein breakdown (B_p) is characterised by the following equation:

$$B_p = Ra_L \qquad [5.18]$$

the subscript p indicates primary pool model.

For carbon labelled leucine tracers the primary pool model (specifically equation 5.17) underestimates leucine release from protein breakdown because Ra_L measures the appearance of leucine in the plasma and this is not strictly the same as the release of leucine from protein breakdown. That is, according to Figure 5.3, Ra_L measures the flow of material from compartment 3 to 1, and not from compartment 5 to 3.

For nitrogen leucine labelled tracers, the situation is worse because tracer enrichment of intracellular leucine is decreased by de-amination as well as by protein breakdown. The rate of appearance of $[^{15}N,^{13}C]$-leucine in the plasma $(Ra_N$ in equation 5.19) is therefore not equivalent to traditional primary pool model estimates of protein breakdown (B_p).

$$Ra_N = \frac{u_N}{z_N} \neq B_p \qquad\qquad [5.19]$$

the subscript N indicates [^{15}N,^{13}C]-leucine tracer. Ra_N represents the rate of appearance of [^{15}N,^{13}C]-leucine in plasma, but does not represent the flux of endogenous leucine, because transamination is irreversible for the [^{15}N,^{13}C]-leucine, but is reversible for [^{13}C]-leucine and tracee. To get an estimate equivalent to the primary pool model estimate we must account for the contribution to enrichment caused by both [^{15}N,^{13}C]-leucine and reaminated [^{13}C]-leucine:

$$z_T = \frac{q_N + q_C}{Q_1} = \frac{q_N}{Q_1} + \frac{q_C}{Q_1} = z_N + z_C \qquad\qquad [5.20]$$

where q_N and q_C represent the mass of [^{15}N,^{13}C]-leucine and [^{13}C]-leucine in compartment 1 respectively. Q_1 is the mass of unlabelled leucine in compartment 1 and z_T represents the total enrichment for both species. z_N and z_C are tracer to tracee ratios of [^{15}N,^{13}C]-leucine and [^{13}C]-leucine respectively. Thus, to estimate B_p (when using a [^{15}N,^{13}C]-leucine tracer) the following calculation has to be used:

$$Ra_T = \frac{u_N}{z_T} = \frac{u_N}{z_N + z_C} = B_p \qquad\qquad [5.21]$$

5.3.7.2   Reciprocal pool model for [^{15}N,^{13}C]-leucine tracer

For reciprocal pool calculations the doubly labelled [^{15}N,^{13}C]-leucine tracer behaves exactly like a [^{13}C]-leucine tracer and requires no modifications, protein breakdown (B_r) was calculated as:

$$Ra_K = \frac{u_N}{z_K} = B_r \qquad\qquad [5.22]$$

where subscript N denotes [^{15}N,^{13}C]-leucine tracer, subscript K indicates KIC, and subscript r indicates reciprocal pool model.

5.3.7.3   Compartmental model steady state calculations

We can calculate the mass of Q_3 under steady state conditions, because by definition the flow of material into any compartment is equal to the flow out. During steady state conditions, for compartment 1 (Figure 5.3) we can write:

$$\dot{Q}_1 = k_{31}Q_1 + k_{13}Q_3 = 0 \tag{5.23}$$

$$Q_3 = \frac{k_{31}}{k_{13}}Q_1 \tag{5.24}$$

$$\dot{Q}_3 = k_{35}Q_5 - k_{53}Q_3 + k_{34}Q_4 - k_{43}Q_3 = 0 \tag{5.25}$$

although we do not have estimates for Q_4, k_{43} or k_{34}, we know that the fluxes $k_{43}Q_3$ and $k_{34}Q_4$ represent deamination (Dx_m) and reamination (Rx_m) respectively, so

$$Dx_m = k_{43}Q_3 \tag{5.26}$$

$$Rx_m = k_{34}Q_4 \tag{5.27}$$

and

$$Ox = Dx_m - Rx_m = k_{43}Q_3 - k_{34}Q_4 \tag{5.28}$$

rearranging equation 5.25 and substituting equations 5.26 and 5.27, we have:

$$Q_5 = \frac{k_{53}Q_3 + Ox}{k_{35}} \tag{5.29}$$

We can obtain estimates for Q_1, k_{13}, k_{13}, k_{35}, k_{53} and k_{03} using numerical methods. Using our tracee model (Figure 5.2) and assuming steady state conditions, we can write expressions for B_m

$$B_m + Rx = S_m + Dx$$

$$B_m = S_m + (Dx - Rx)$$

$$S_m = Q_3 . k_{53} \tag{5.30}$$

$$B_m = S_m + Ox_m = Q_3 . k_{53} + Ox_m \tag{5.31}$$

90

where Q_3 is the mass of the intracellular leucine pool (in μmol), B_m and S_m represent protein breakdown and synthesis respectively estimated obtained using the proposed model (Figure 5.3). Leucine oxidation is derived from expired $^{13}CO_2$ measurements, and these calculations are described in Section 5.3.6.

5.3.8   Parameter estimation

The model was quantified for each subject by using non-linear least-squares parameter estimation. This was done using the SAAM II program (Washington USA). Model fit and parameter estimates are shown with their precision in Table 5.2. Model fit was good, and acceptable levels of precision were obtained.

5.3.9   Statistics

SPSS (version 10, SPSS Inc. Chicago, IL, USA) was used to perform all statistical analyses. These include a pairwise correlation matrix of B_p, B_r and B_m, and a two-factor ANOVA testing for differences between the estimates provided by the primary pool model, the reciprocal pool model and the compartmental model.

5.4   Results

Parameter estimates for the proposed (compartment) model, and WBPT estimates for the primary and reciprocal pool model are shown below.

5.4.1   Compartmental model estimates results

It was possible to estimate fractional rate constants (k_{ij}) and the mass of the plasma leucine pool (Q_1) in all subjects. The results of the parameter estimation are shown in Table 5.2, plots of tracer data curves, model fit and weighted residuals are shown for each subject (Figure 5.4 to Figure 5.9). These indicate that the fit was, in general, good and unbiased. The mean value for S_m was 2.41 ± SD 0.49 μmol/kg/min. We derived estimates of leucine oxidation from expired CO_2; and from this calculated B. Mean estimates for B_m and Ox were 2.65 ± SD 0.55 μmol/kg/min and 0.25 ± SD 0.08 μmol/kg/min respectively.
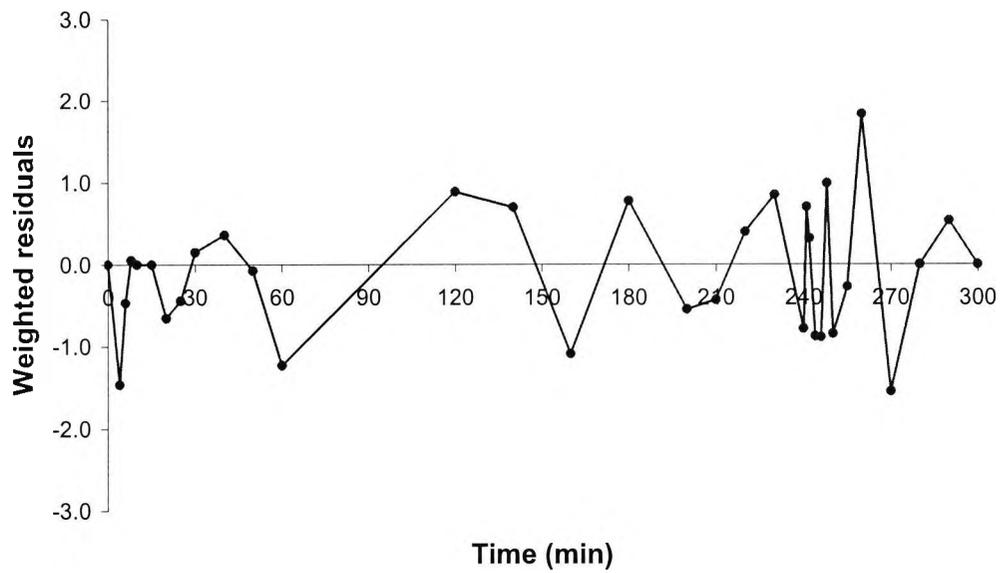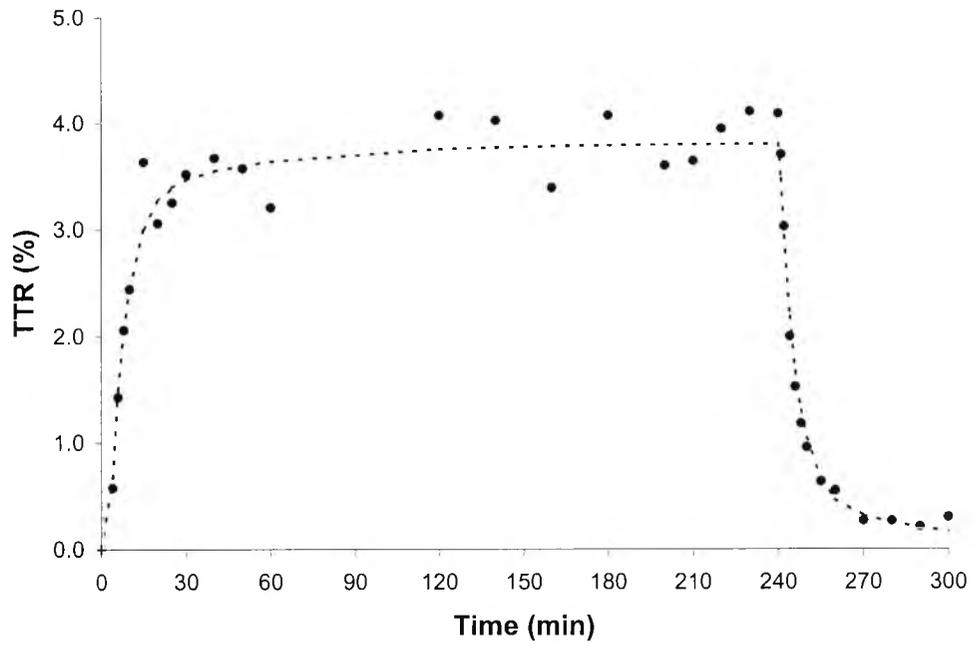
Figure 5.4 Data fit (top) and weighted residuals (bottom) for subject 1
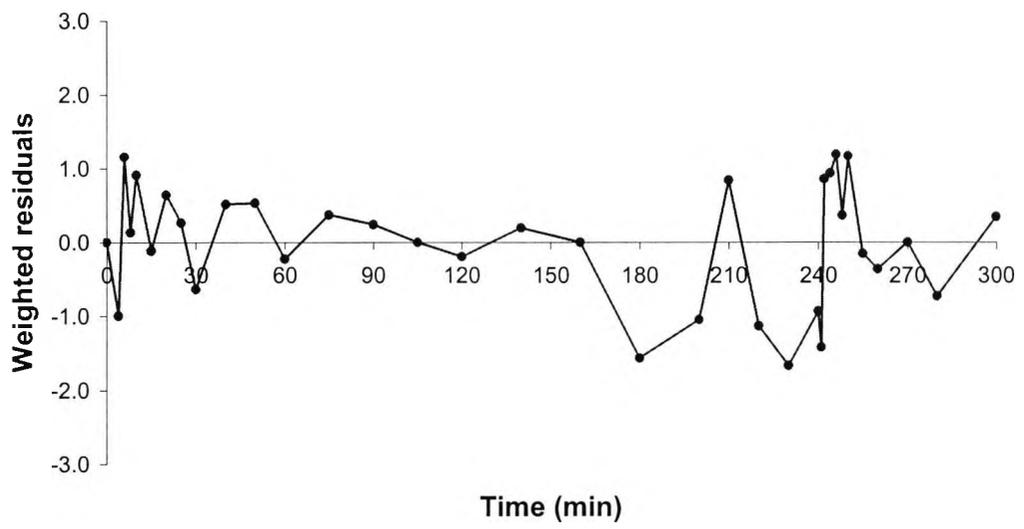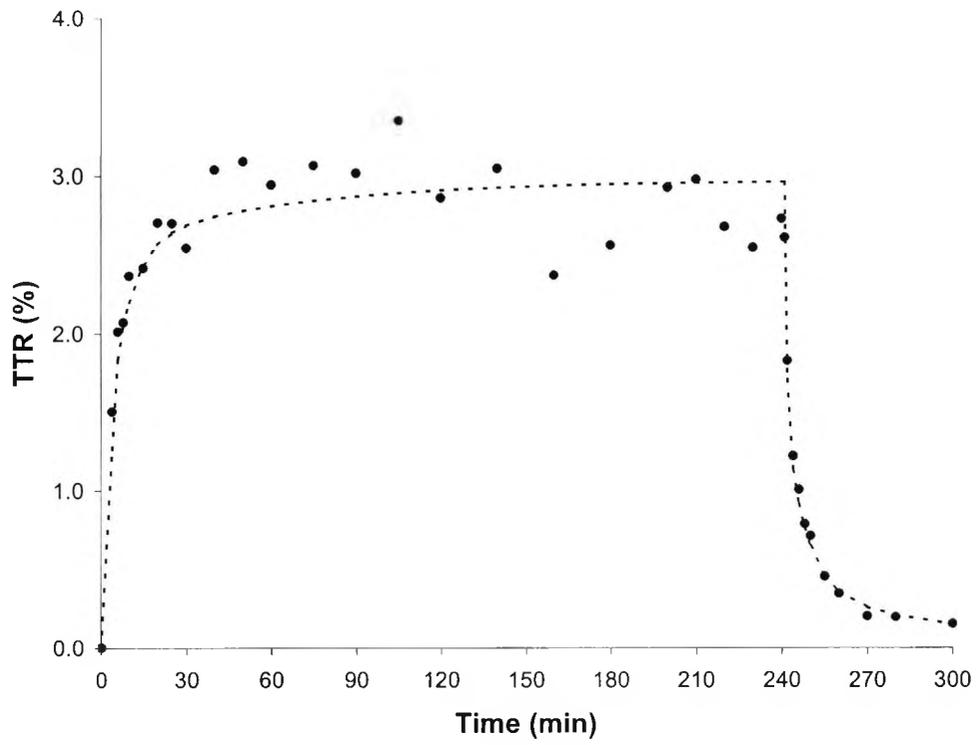
Figure 5.5: Data fit (top) and weighted residuals (bottom) for subject 2
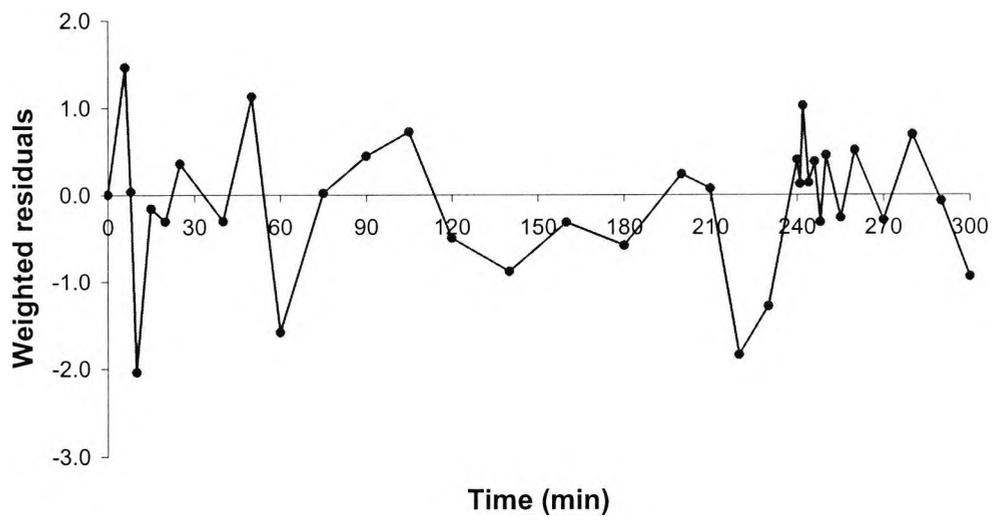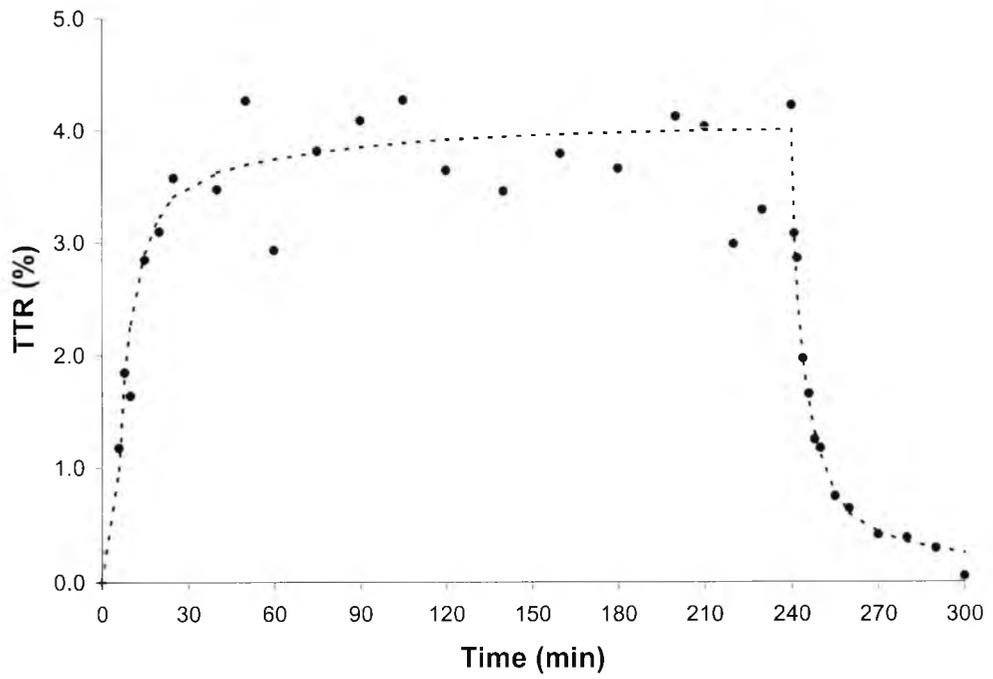
Figure 5.6: Data fit (top) and weighted residuals (bottom) for subject 3
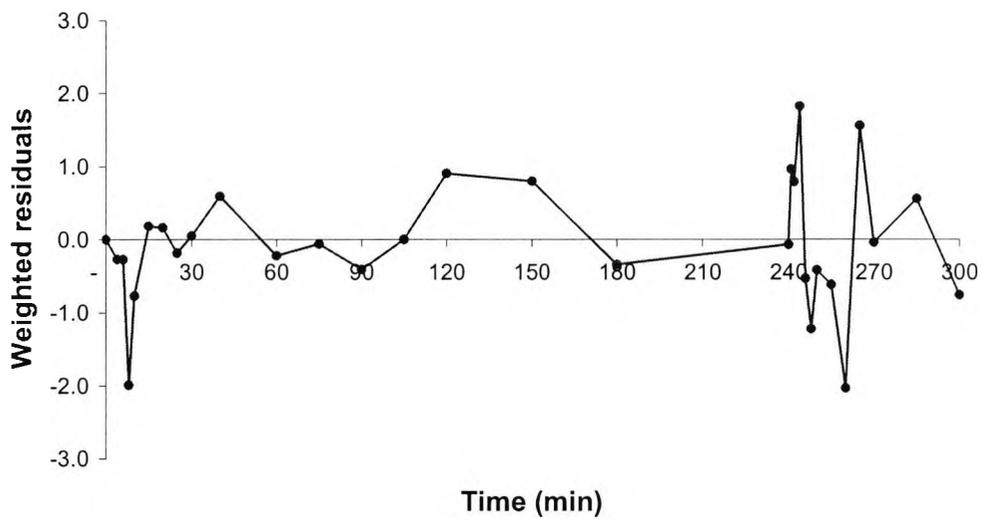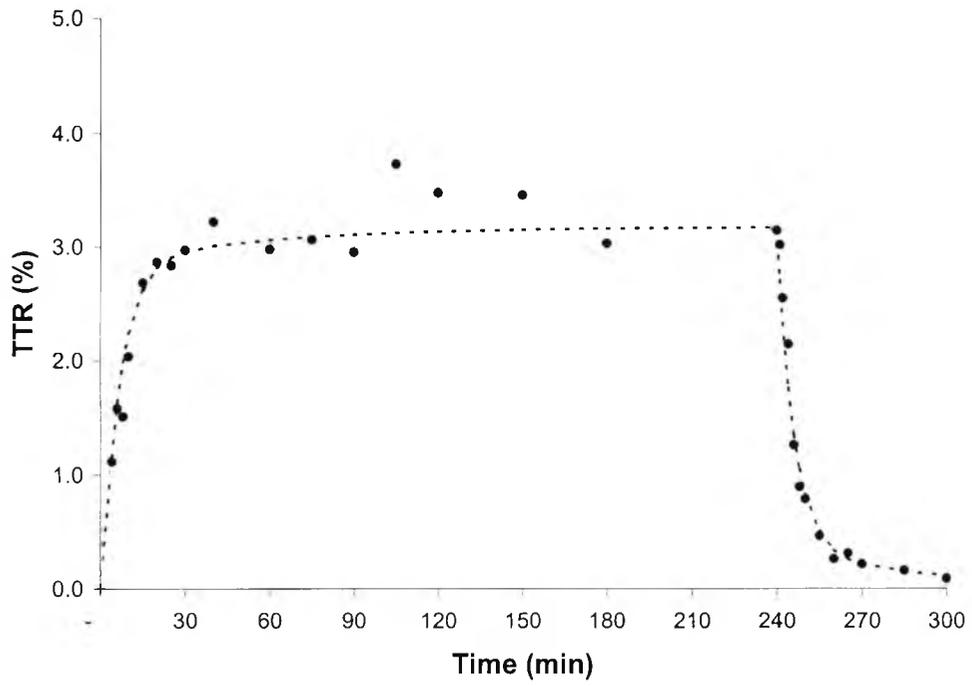
Figure 5.7: Data fit (top) and weighted residuals (bottom) for subject 4
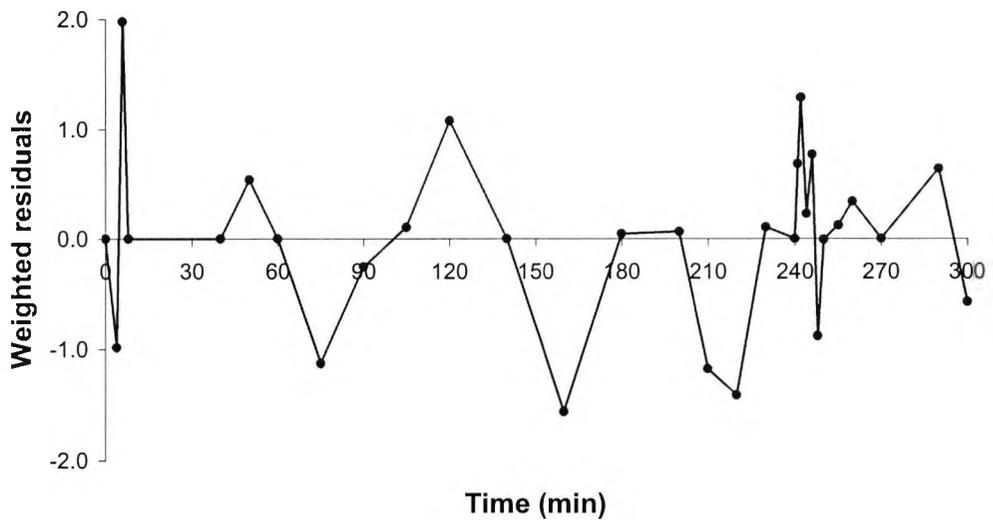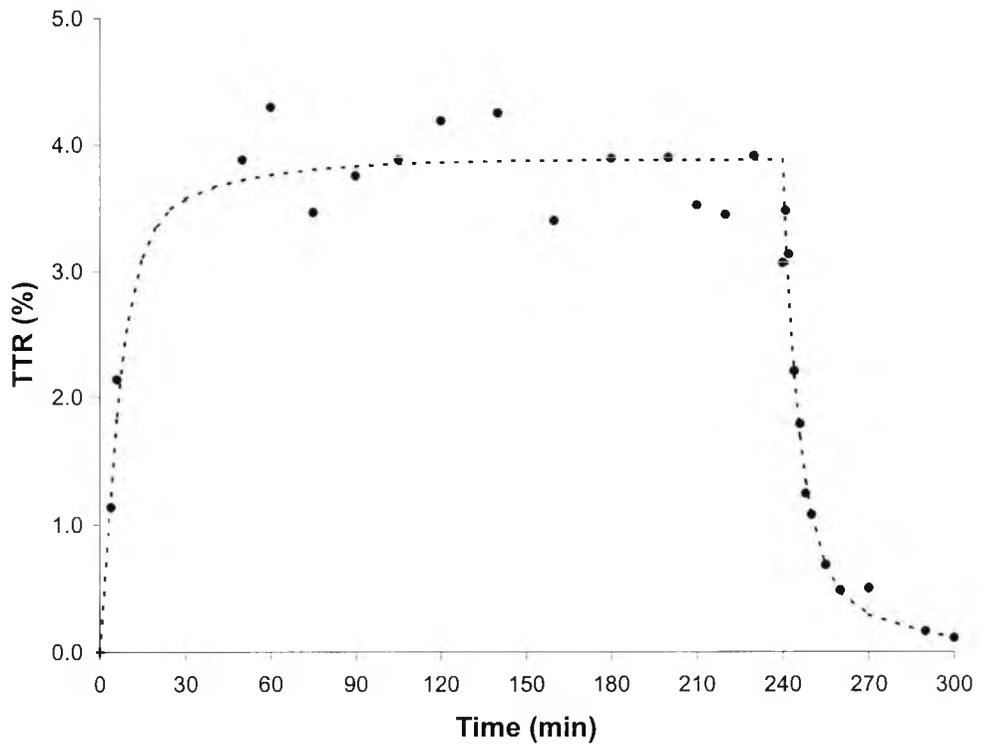
Figure 5.8: Data fit (top) and weighted residuals (bottom) for subject 5
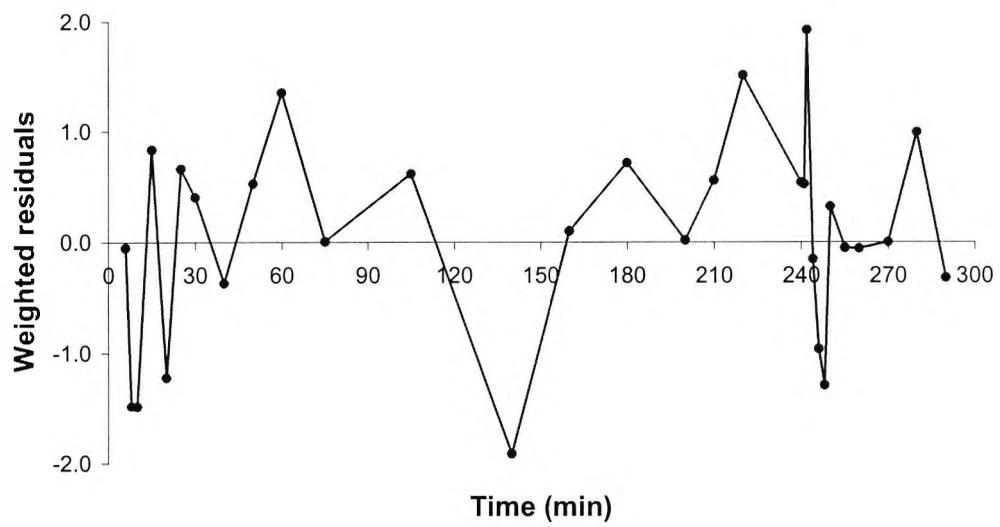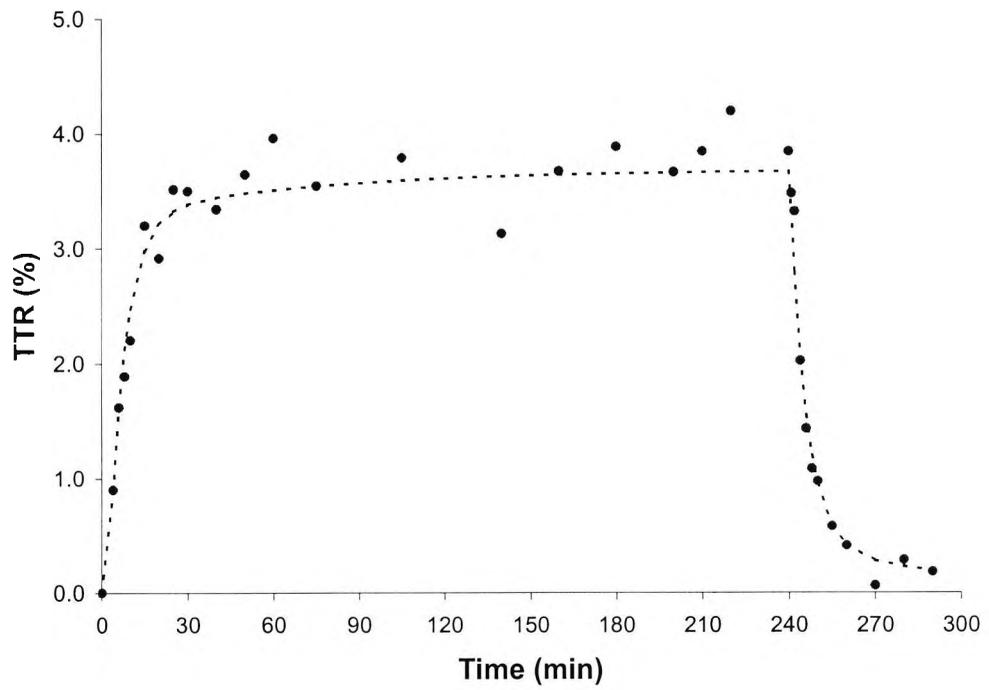
Figure 5.9: Data fit (top) and weighted residuals (bottom) for subject 6

Table 5.2: Parameter estimates for proposed 3-compartment model

	Subject							
	1	2	3	4	5	6	Mean	SD
Q_1	16.99 (7)	4.48 (10)	9.98 (12)	23.27 (8)	15.32 (7)	20.48 (9)	15.09	6.90
k_{03}	0.32 (19)	0.11 (12)	0.14 (16)	0.38 (22)	0.26 (19)	0.28 (27)	0.25	0.10
k_{13}	0.28 (34)	0.09 (23)	0.17 (32)	0.26 (33)	0.27 (34)	0.21 (22)	0.21	0.07
k_{31}	0.35 (19)	1.34 (13)	0.78 (20)	0.28 (19)	0.43 (19)	0.35 (29)	0.59	0.41
k_{35}	0.03 (27)	0.02 (20)	0.02 (30)	0.03 (18)	0.06 (20)	0.02 (45)	0.03	0.01
k_{53}	0.09 (27)	0.03 (18)	0.04 (25)	0.11 (32)	0.13 (24)	0.07 (34)	0.08	0.04
Derived parameters								
Q_3	21.57 (39)	67.80 (29)	44.98 (40)	25.35 (39)	24.01 (40)	34.56 (37)	36.38	17.65
Q_5	87.75 (55)	117.21 (39)	92.16 (56)	92.89 (54)	58.67 (50)	136.95 (67)	97.03	26.82
S_m	2.03	2.36	1.74	2.88	3.03	2.42	2.41	0.49

Values are in min^{-1} (k_{ij}), µmol/kg (Q_i) and µmol/kg/min (S_m). Precision of estimated parameter is reported in parenthesis and expressed as a fractional standard deviation. The S_m, Q_3 and Q_5 are derived from steady state solutions (see Section 5.3.7.3.)

Table 5.3: *B*, *Ox* and *S* calculated using the proposed model and primary and reciprocal pool approaches

Subject	1	2	3	4	5	6	Mean	SD
Protein Breakdown (B)								
$B_p = (u_N / (z_C + z_N))$	1.35	1.68	1.34	1.76	1.46	1.69	1.55	0.19
$B_r = (u_N / z_C)$	1.92	2.32	1.73	2.62	2.74	2.29	2.27	0.38
$B_m = (S_m + Ox_r)$	2.26	2.57	1.90	3.25	3.31	2.61	2.65	0.55
Leucine oxidation (Ox)								
Ox_p	0.27	0.25	0.20	0.47	0.28	0.25	0.29	0.09
Ox_r	0.23	0.21	0.16	0.38	0.33	0.20	0.25	0.08
Non-oxidative leucine disposal (S)								
$S_p = (B_p - Ox_p)$	1.08	1.43	1.14	1.29	1.18	1.43	1.26	0.15
$S_r = (B_r - Ox_r)$	1.69	2.11	1.57	2.23	2.41	2.09	2.02	0.32
$S_m = k_{53}.Q_3$	2.03	2.36	1.74	2.88	3.03	2.42	2.41	0.49

All values in µmol/kg/min. The subscript *P* denotes primary pool model calculation, *R* indicates reciprocal pool model calculation and *M* indicates proposed model calculation. In addition $B = S + Ox$.

5.4.2 Steady state estimates

We calculated steady state pool sizes and endogenous leucine (tracee) fluxes for each subject using the tracer-derived parameters. In particular, we calculated estimates for the masses Q_3 (intracellular leucine pool), Q_5 (fast turning-over protein pool) and the flux of leucine incorporation into proteins ($S_m = k_{35}$. Q_5). In addition to estimating B and S for the compartmental

model (B_m, S_m) we also calculated estimates using the primary (B_p, S_p) and reciprocal pool (B_r, S_r) models, details of these are shown in Table 5.3.

We found a high and very significant correlation ($p < 0.001$, shown in Table 5.4) between the reciprocal pool model estimate of protein breakdown (B_r) and the estimate provided by the model (B_m). This is consistent with our expectations and as shown in Section 5.4.3 we expect that our model will consistently provide a higher estimate of B than the reciprocal pool model.

Table 5.4: Pearson Correlation Matrix

	B_p	B_r	B_m
B_p	-	(0.10)	(0.12)
B_r	0.62	-	(0.0002)
B_m	0.56	0.98 **	-

The values marked ** are significant at the $p < 0.001$ level.

Table 5.5: Summary of protein turnover estimates using the primary pool model, the reciprocal pool model and the compartmental model

	Compartmental model (B_m)	Mean difference from compartmental model	
		Primary pool model ($B_m - B_p$)	Reciprocal pool model ($B_m - B_r$)
Protein breakdown (B)	2.65 ± 0.22	$1.10 \pm 0.14^{\ddagger}$	$0.38 \pm 0.14^{\dagger}$
Protein synthesis (S)	2.41 ± 0.20	$1.15 \pm 0.14^{\ddagger}$	$0.39 \pm 0.14^{\dagger}$

Data are means $\pm$ SE for 6 subjects. All values in μmol/kg/min. Two-factor ANOVA was used to test the differences between the various model estimates. $^{\ddagger} p < 0.001$ difference between estimates. $^{\dagger} p < 0.05$ difference between estimates.

In addition we performed a two-factor ANOVA (factors: subject, model used) on the estimates provided by the primary pool model, the reciprocal pool model and the compartmental model. The estimate of protein breakdown obtained by the primary pool model B_p ($1.55 \pm$ SD 0.19 μmol/kg/min) is significantly lower ($p < 0.001$) than that obtained by the reciprocal pool model B_r ($2.27 \pm$ SD 0.38 μmol/kg/min) and also lower than that obtained by the compartmental model B_m ($2.65 \pm$ SD 0.55 μmol/kg/min). Similarly the estimate for protein synthesis obtained by using the primary pool model S_p ($1.26 \pm$ SD 0.15 μmol/kg/min) is significantly lower ($p < 0.001$) than that obtained by the reciprocal pool model S_r ($2.02 \pm$ SD 0.32 μmol/kg/min) and also lower than the estimate obtained by the compartmental S_m ($2.41 \pm$ SD 0.49 μmol/kg/min). More importantly we also found that reciprocal pool model estimates for both B and S were significantly lower ($p < 0.05$) than estimates obtained using the compartmental model. Some of these results are summarised in Table 5.5 and shown graphically in Figure 5.10.
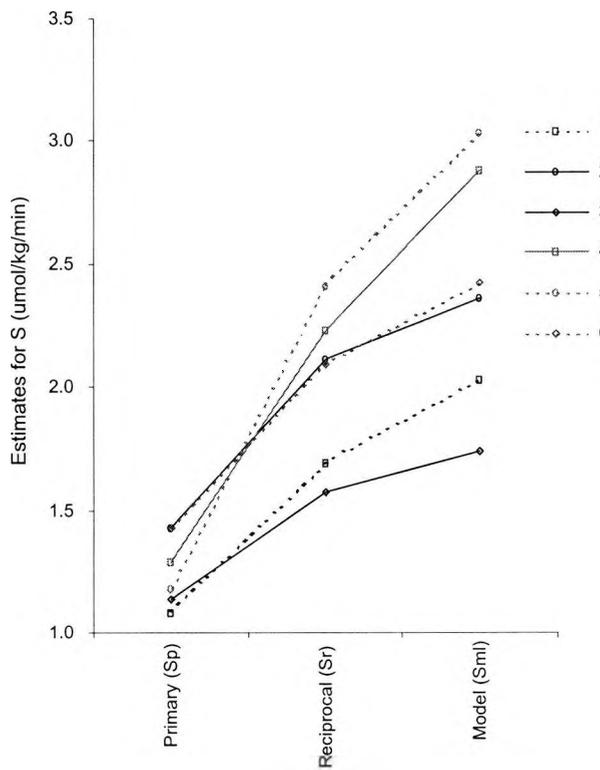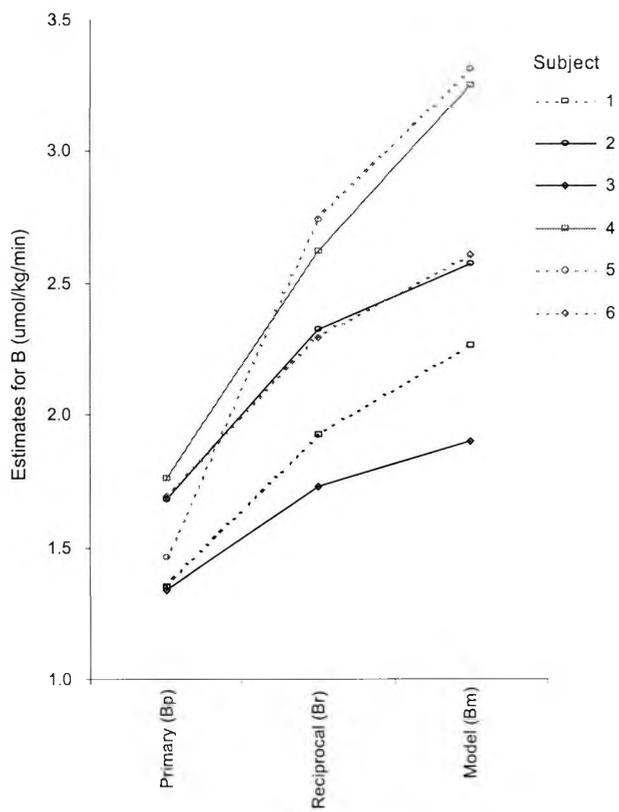
Figure 5.10: Comparison of estimates for primary pool model (*p*), reciprocal pool model (*r*) and the proposed compartmental model (*m*) for protein breakdown (left) and synthesis (right).

100

5.4.3   Theoretical comparison of the reciprocal pool and compartmental models

To derive the formulae, which describe the differences between the reciprocal pool model and the compartmental model, we must be able to compare them in terms of parameters k_{ij} and masses Q_i. Using the tracer and tracee models shown in Figure 5.2 and Figure 5.3 respectively, the reciprocal pool model estimate for protein breakdown (B_r) is given by:

$$B_r = \frac{u_N}{z_K} = \frac{u_N}{\dfrac{q_4}{Q_4}}$$

[5.32]

where u represents the infusion of leucine tracer, q_i represents the mass of tracer in compartment i and Q_i represents the mass of cold substance in compartment i. The tracer to tracee ratio is represented by z; the tracer to tracee ratio for compartment i is defined as q_i / Q_i. The subscript K indicates KIC measurements, and the N indicates $[^{15}N,^{13}C]$-leucine measurements. The reciprocal pool model assumes steady state conditions.

In the steady state, let us consider compartment 4 of the tracer model. The masses $q_{3.2}$ and $q_{3.1}$ represent $[^{15}N,^{13}C]$ and $[^{13}C]$ labelled substances respectively.

$$\dot{q}_4 = k_{43}q_{3.1} + k_{43}q_{3.2} - k_{04}q_4 - k_{34}q_4 = 0$$

so

$$q_4 = \frac{k_{43}(q_{3.1} + q_{3.2})}{(k_{04} + k_{34})}$$

And similarly for the tracee model we have:

$$Q_4 = \frac{k_{43}Q_3}{(k_{04} + k_{34})}$$

We can rewrite equation [5.32] substituting for q_4 and Q_4, giving:

$$B_r = \frac{u_N}{\dfrac{q_4}{Q_4}} = \frac{Q_3.u_N}{(q_{3.1} + q_{3.2})}$$

[5.33]

Now considering the $[^{15}N, ^{13}C]$ tracer model under steady state conditions we have:

$$u_N = q_{3.2} k_{43}$$

and so

$$q_{3.2} = \frac{u_N}{k_{43}} \qquad [5.34]$$

Similarly considering compartment 4 for the $[^{13}C]$ tracer model we can write:

$$\dot{q}_4 = k_{43} q_{3.2} - k_{04} q_4 = 0$$

and so

$$q_4 = \frac{k_{43} q_{3.2}}{k_{04}} \qquad [5.35]$$

We can also express q_4 in terms of $q_{3.1}$ by considering the fluxes for compartment $q_{3.1}$ thus:

$$k_{34} q_4 = k_{43} q_{3.1}$$

so

$$q_4 = \frac{k_{43} q_{3.1}}{k_{34}} \qquad [5.36]$$

Equating [5.35] and [5.36]

$$q_4 = \frac{k_{43} q_{3.1}}{k_{34}} = \frac{k_{43} q_{3.2}}{k_{04}}$$

gives

$$q_{3.1} = \frac{k_{34}}{k_{04}} q_{3.2}$$

[5.37]

Now substituting for $q_{3.2}$ [5.35] and $q_{3.1}$ [5.37] into [5.2] we have

$$B_r = \frac{k_{43}k_{04}}{k_{34} + k_{04}} Q_3$$

[5.38]

The estimate for protein synthesis for the proposed model is

$$S_m = k_{53}Q_3$$

[5.39]

and for leucine oxidation

$$Ox = k_{04}Q_4$$

Since B may be expressed as the sum of S and Ox, we can write an expression for B in terms of k_{ij} and Q_i, thus:

$$B_m = S_m + Ox = k_{53}Q_3 + k_{04}Q_4 = k_{53}Q_3 + \frac{k_{04}k_{43}}{k_{34} + k_{04}} Q_3$$

[5.40]

$$B_r = \frac{k_{43}k_{04}}{k_{34} + k_{04}} Q_3$$

[5.41]

We can see that the estimate for B provided by the model (B_m) is greater than the estimate provided by the reciprocal pool model (B_r) or

$$k_{53}Q_3 + \frac{k_{04}k_{43}}{k_{34} + k_{04}} Q_3 > \frac{k_{04}k_{43}}{k_{34} + k_{04}} Q_3 \Rightarrow B_m > B_r$$

[5.42]

Our calculations show [equation 5.42] that B_m, the estimate provided by our model, is larger than the estimate provided by the reciprocal model, B_r, and this expectation is confirmed by our results (data shown in Table 5.3).

5.5   Discussion

In this study we have used a three-compartment model and a $[^{15}N,^{13}C]$-leucine tracer to quantify leucine turnover. The model contains an extracellular-plasma leucine, compartment *1*; an intracellular leucine, compartment *3*; and a pool for 'fast-turning-over' proteins, compartment *5* (Gowrie et al. 1999). Conceptually the 3-compartment model is no more complex than the reciprocal pool model. The model requires a single input and output and allows the estimation of the fractional rates for the release of leucine from protein breakdown (k_{35}) and the incorporation of leucine into protein (k_{53}). The experiment proposed here also allows the estimation of B and S using both the primary and reciprocal pool models. Furthermore, because of the rich kinetic picture (there are three labelled species $[^{13}C]$-leucine and $[^{13}C]$-KIC and $[^{15}N,^{13}C]$-leucine), the potential for future investigation using different configurations is good. The model proposed is experimentally simple, versatile and flexible; it makes no assumptions about the KIC sub-system; and introduces no new assumptions about the leucine-KIC system.

5.5.1   Modelling and physiological interpretation

Although it is difficult to assign compartments to specific physiological entities, Table 5.6 shows the size of our compartments Q_1, Q_3 and Q_5 compared with known physiological entities. The size of the plasma pool and interstitial fluid 'compartments' in a 70 kg healthy adult male are 0.04 L/kg and 0.11 L/kg respectively. Our estimate of Q_1 (0.11 L/kg) is larger than we would expect for a plasma-only pool; thus, according to our data (and confirming our assumption), compartment 1 includes both plasma and interstitial fluid components. Our estimate for Q_1 (mean 15.1 ± 6.9 μmol/kg) is similar to the estimate (12.1 ± 3.5 μmol/kg) obtained using a different compartmental model (Cobelli et al. 1991). According to our model, compartment 3 represents an 'intracellular leucine pool'; our estimate of Q_3 (0.27 μmol/kg) is slightly smaller than the theoretical expectation (0.39 μmol/kg in a 70 kg healthy adult male). Our underestimation of intracellular space may be due in part to the short duration of the study (since these estimates assume steady state) and additionally the actual volume of distribution for leucine may well be less that the estimate for the whole-body. Nevertheless our estimates for Q_1 and Q_3 are reasonable; and furthermore, our estimates for breakdown and synthesis are in agreement with theoretical expectations; these observations demonstrate that the model is capable of quantifying several components of the physiological system involved in protein turnover. We examine the physiological significance of compartment 5 in the following section.

Table 5.6: Comparison of Q_1, Q_3 and Q_5 with real body compartments

Compartments	Weight (µmol/kg)	Body weight (%)	Volume (L)	Volume normalised for body weight (L/kg)
Physiological entities				
Extracellular fluid		24%	17	0.24
Plasma		4%	3	0.04
Interstitial fluid		11%	8	0.11
Other minor compartments		8%	6	0.09
Intracellular fluid		36%	27	0.39
Model derived parameters				
Compartment Q_1	15.1 ± 6.9		8	0.11
Compartment Q_3	36.4 ± 17.7		19	0.27
Compartment Q_5	97.0 ± 26.8		40	0.59

The table above shows theoretical values for volume of distribution for several major body compartments and estimates for our model-derived parameters. The data for 'physiological entities' is for a 70-kg healthy adult male, and this data may be found in many physiology textbooks. For the model-derived parameters, volumes are calculated as Q_i ÷ Concentration. Concentrations in compartments Q_1, Q_3 and Q_5 were assumed to be the same as plasma, for Q_3 and Q_5 the estimates for V are thus an overestimate.

5.5.2   Comparison with alternative models

There are several methods for estimating whole-body protein turnover; these include the 7-compartmental Cobelli (1991) model, the primary pool model and the *de facto* model, the reciprocal pool model. The Cobelli (1991) model is more elaborate, describes three 'free' pools of leucine and a 'protein-linked leucine' pool. This multi-compartment leucine configuration may be physiologically correct as others have shown (in-vitro) the existence of distinct and separate leucine pools involved in protein synthesis (Clark and Zak 1981;Everett et al. 1981;Kelley et al. 1984;Martin et al. 1977). Nevertheless, the size of 'our' protein-linked pool (Q_5) is similar to the size of the protein-linked leucine pool that Cobelli describes. The reported size of the protein linked pool in the Cobelli (1991) model was 5% of whole body protein, assuming whole body protein content is 14% of body weight and 8% of protein is leucine. The individual estimates are in fact 1.5, 1.5, 2.7, 2.7, 3.2 and 8.0%. The individual values calculated for our subjects were 1.1, 1.7, 1.8, 1.8, 2.3 and 2.7% (again assuming whole body protein content is 14% of body weight and 8% of protein is leucine). Apart from the value of 8%, our values are very similar to those reported by Cobelli. In our model, fast turning over proteins (Q_5) accounts for about 2% of whole body proteins. This compartment is assumed to contain very fast turning over proteins, as only these are accessible to our model during the 300 minutes of the experiment.

Before we make any comparisons between the proposed model and the primary and reciprocal pool models, it is worth emphasising that they measure different, although related variables (i.e.

theoretically $B_m \neq B_r \neq B_p$). The primary and reciprocal pool models allow the calculation of protein turnover fluxes (mol/min or g/min). For example, leucine Ra (mol/min or g/min) is an estimate of the mass of leucine that is released from proteins per minunte. This is conceptually different from the variables that are derived from a compartmental model. In a compartmental model the parameters are masses Q_i (mass of a compartment i) and fractional rate constants k_{ij} (the fraction of substance that 'moves' from compartment j to compartment i); the flux from compartment i to j is defined as the product of Q_i and k_{ji}. This observation leads directly to the two main advantages the proposed model has over the primary and reciprocal pool models. Firstly, isotopic dilution methods (such as the primary and reciprocal pool models) rely on the tracer-system reaching the steady state. This is not a problem *per se*, but it does mean that a) these methods are very sensitive the actual value of the steady state that is used and b) reaching the steady state is a necessary condition of using these models. Neither of these is true for compartmental models. Secondly, the primary and reciprocal pool models measure the appearance of either leucine or KIC into the plasma, but conceptually and physiologically this is not protein breakdown, but rather a measure of protein breakdown. The proposed model allows the estimation of the fractional turnover rates of Q_5 (which we assume to be a fast turning over protein pool). The model parameters k_{35} and k_{53} represent the rate at which leucine derived from proteins enters the intracellular leucine pool (k_{35}) and conversely the rate at which intracellular leucine is incorporated into proteins (k_{53}). In addition, the $[^{15}N,^{13}C]$-leucine tracer model makes very few assumptions about the KIC sub-system.

In practical terms the experiment proposed here is no more difficult to perform than the experiments traditionally used in the primary or reciprocal pool model. However, compartmental modelling does require more samples to be measured, and in terms of calculations, compartmental model parameter estimation is considerably more difficult than the calculations used for steady state models. Nevertheless, we have shown theoretically that the proposed compartmental model will provide a larger estimate than the reciprocal pool model. A comparison of the various estimates reveals that the primary and reciprocal pool model estimates are significantly less than the compartmental model estimate by about 40% and 15% respectively (Table 5.3 and Table 5.5). This discrepancy has been explained theoretically (Section 5.4.3).

5.6   Conclusions

We have developed a 3-compartment model for leucine kinetics in normal humans. The model is a priori uniquely identifiable. Using an infusion of $[^{15}N,^{13}C]$-leucine tracer and measuring $[^{15}N,^{13}C]$-leucine in plasma, we were able to quantify a 3 compartment model using both simulated and experimental data with good precision. The model is conceptually no more complex than the

reciprocal pool model, and it allows the estimation of the intracellular rate of appearance of leucine derived from protein breakdown; the incorporation of leucine into proteins and the rate of leucine transamination. Furthermore, the model provides estimates of the sizes of various compartments including a plasma/interstitial fluid compartment, an intracellular fluid compartment and a fast turning over protein pool. The model proposed here offers estimates close to other similar and more comprehensive models, furthermore, the proposed model is on firm theoretical ground, and in practice may prove easier to use.

6   FINAL DISCUSSION

The primary aim of this work was to develop a new method to estimate whole body protein turnover in man, this was to be accomplished by achieving a set of secondary objectives. These objectives were: to assess the current methods, to propose a new model and to validate the proposed model (these are a concise version of the objectives which appear in Section 1.2). In Chapters Two and Three the current methods used to estimate WBPT were reviewed and analysed, a new method was proposed in Chapter Four and then validated in Chapter Five. The following discussion provides a concise summary of the work presented here.

There are several methods available for those wishing to estimate protein turnover in man; many of these methods are described in Chapter Two. In general, estimating protein turnover involves administration of an amino acid tracer - although this is not the case with balance techniques like the nitrogen balance method. On examining the techniques currently available, it was apparent that none of the models can be considered to be definitive or comprehensive, even though several different methods are available, employing a variety of different amino acid tracers. This is primarily because modelling the entire protein system is difficult since there are 20 amino acids in man and 20 different amino acid subsystems. This is the major obstacle to those wishing to estimate WBPT.

In the particular case of leucine system modelling, two steady state models, the reciprocal pool model (Schwenk et al. 1985a) and the primary pool model (Matthews et al. 1982;Wolfe et al. 1982) have achieved great popularity, and these have been used to measure leucine turnover in man in a variety of circumstances. However, both these models have been shown to be over-simplified and in error, the errors are both structural and conceptual (Cobelli and Saccomani 1991). Despite these known limitations, and although more comprehensive modelling alternatives are available, these steady state models remain in use largely because they are simple to use and conceptualise.

In Chapter Three, the analysis of demographic and whole body turnover data showed that compared to the reciprocal pool model, the primary pool model will underestimate leucine Ra by about 30%; furthermore, these data show that of the variables age, gender, BMI, weight and leucine concentration and model used (to estimate WBPT), the single most important factor in determining WBPT is the model used. It was against this background that the new model to estimate WBPT was proposed; as it is clear that a more robust, yet simple, alternative is needed.

The proposed model was introduced in Chapter Four. The model employs the infusion of a $[^{15}N,^{13}C]$-leucine tracer over 4 hours (Gowrie et al. 1999). The model takes advantage of the unusual metabolism of labelled $[^{15}N,^{13}C]$-leucine tracer. For this tracer, leucine transamination is irreversible, and a three-compartment model describes the kinetics of the tracer. The model is theoretically and practically identifiable and the model was quantified using both simulated data (Chapter 4) and experimental data (Chapter 5). Thus the proposed model allows the estimation of the fractional rates of protein breakdown and synthesis. It was also possible to estimate the size of a plasma/interstitial fluid compartment. The estimates for WBPT parameters were in good agreement with the literature and in line with expectations; furthermore, it was possible to explain the observed differences between the proposed model and the primary pool model and reciprocal pool model theoretically.

A comparison of the features of the $[^{15}N,^{13}C]$-leucine, the seven compartment model developed by Cobelli *et al* (1991) and the primary/reciprocal pool models is shown in Table 6.1. The suggested three-compartment model has several advantages and improvements over its steady state rivals (see Section 5.5). Firstly the $[^{15}N,^{13}C]$-leucine model explicitly allows the estimation of the fractional turnover rates of a 'fast turning-over' protein pool – this is in contrast to both the primary and reciprocal pool models which measure the appearance of leucine or KIC in the plasma. Secondly, the model makes no new assumptions about KIC metabolism. In addition, the model allows the estimation of the sizes of various physiological pools. So, although parameter estimation of the $[^{15}N,^{13}C]$-leucine model does require greater mathematical proficiency and a larger number of samples than steady state calculations, the advantages outweigh these minor difficulties.

The proposed model is simpler to use than the more comprehensive model proposed by Cobelli et al (1991). The Cobelli model remains the most comprehensive model available, it includes, for instance, the KIC sub-system and a parameter to estimate leucine oxidation, it also requires the administration of two tracers and the measurement of four tracer curves. In contrast, the proposed model requires the infusion and measurement of a single tracer: $[^{15}N,^{13}C]$-leucine. Therefore, in practice, the $[^{15}N,^{13}C]$-leucine model may prove easier to use, and furthermore, parameter estimation for the three-compartment model may be simpler than for the seven-compartment model. The comparative simplicity of the $[^{15}N,^{13}C]$-leucine model is a definite advantage.

The $[^{15}N,^{13}C]$-leucine model allows the omission of the KIC system. Initially this may be viewed as a flaw of the proposed method, but it can be viewed in a more positive light. In its defence, two points should be made. Firstly, KIC modelling is only necessary as means an end, the end being the estimation of protein turnover; investigators are not necessarily interested in KIC *per se.*

Secondly since the KIC system is omitted in its entirety, it is not necessary to make *any* assumptions about KIC metabolism. In either case, the $[^{15}N,^{13}C]$-leucine tracer does allow other model configurations to be considered including the KIC system; and we describe one such model in Chapter 4 (i.e. PM2). However, we consider this model to be unnecessarily complex, and it works in opposition to the elegance and simplicity of the proposed three-compartment structure.

Table 6.1: Comparison of features of primary pool model, reciprocal pool model, the seven compartment model (Cobelli et al. 1991) and the proposed $[^{15}N,^{13}C]$-leucine three compartment model (Gowrie et al. 1999).

	Primary (Matthews et al. 1982;Wolfe et al. 1982) and reciprocal (Schwenk et al. 1985a) pool models	Seven compartment model (Cobelli et al. 1991)	$[^{15}N,^{13}C]$-leucine three compartment model (Gowrie et al. 1999)
Tracers	$[^{13}C]$-leucine or $[^{13}C]$-KIC	$[^{13}C]$-leucine $[^2H]$-KIC	$[^{15}N,^{13}C]$-leucine
Samples required	$[^{13}C]$-leucine or $[^{13}C]$-KIC $^{13}CO_2$	$[^{13}C]$-leucine $[^{13}C]$-KIC $[^2H]$-leucine $[^2H]$-KIC	$[^{15}N,^{13}C]$-leucine $^{13}CO_2$
Number of samples required	≈ 4	> 20	> 20
Includes KIC subsystem	Yes	Yes	No
Explicitly measures B and S	No	Yes	Yes
Can estimate pool sizes	No	Yes	Yes
Number of compartments	N/A (four pools implied)	seven	three
Steady state required	Yes	No	No

A research question based on the hypothesis stated in Section 1.2 can be posed: Is it possible to develop a new method to estimate whole-body protein in man? Since several methods already exist (as evidenced in Section 2.1), it is reasonable to assume that other methods are possible. There are however implied constraints on the development of a new model, i.e., for any new model to be of value, it must improve on current models/methods. The research question becomes: Is it possible to develop a 'better' model to estimate whole body protein turnover. Bier's (1989) comprehensive review outlines the way forward for the study of whole body protein turnover in man, and outlines the criteria for 'better' models. He notes that more comprehensive models of protein metabolism 'are sorely needed' especially when considering the critical

Secondly since the KIC system is omitted in its entirety, it is not necessary to make *any* assumptions about KIC metabolism. In either case, the $[^{15}N,^{13}C]$-leucine tracer does allow other model configurations to be considered including the KIC system; and we describe one such model in Chapter 4 (i.e. PM2). However, we consider this model to be unnecessarily complex, and it works in opposition to the elegance and simplicity of the proposed three-compartment structure.

Table 6.1: Comparison of features of primary pool model, reciprocal pool model, the seven compartment model (Cobelli et al. 1991) and the proposed $[^{15}N,^{13}C]$-leucine three compartment model (Gowrie et al. 1999).

	Primary (Matthews et al. 1982;Wolfe et al. 1982) and reciprocal (Schwenk et al. 1985a) pool models	Seven compartment model (Cobelli et al. 1991)	$[^{15}N,^{13}C]$-leucine three compartment model (Gowrie et al. 1999)
Tracers	$[^{13}C]$-leucine or $[^{13}C]$-KIC	$[^{13}C]$-leucine $[^{2}H]$-KIC	$[^{15}N,^{13}C]$-leucine
Samples required	$[^{13}C]$-leucine or $[^{13}C]$-KIC $^{13}CO_2$	$[^{13}C]$-leucine $[^{13}C]$-KIC $[^{2}H]$-leucine $[^{2}H]$-KIC	$[^{15}N,^{13}C]$-leucine $^{13}CO_2$
Number of samples required	≈ 4	> 20	> 20
Includes KIC subsystem	Yes	Yes	No
Explicitly measures B and S	No	Yes	Yes
Can estimate pool sizes	No	Yes	Yes
Number of compartments	N/A (four pools implied)	seven	three
Steady state required	Yes	No	No

A research question based on the hypothesis stated in Section 1.2 can be posed: Is it possible to develop a new method to estimate whole-body protein in man? Since several methods already exist (as evidenced in Section 2.1), it is reasonable to assume that other methods are possible. There are however implied constraints on the development of a new model, i.e., for any new model to be of value, it must improve on current models/methods. The research question becomes: Is it possible to develop a 'better' model to estimate whole body protein turnover. Bier's (1989) comprehensive review outlines the way forward for the study of whole body protein turnover in man, and outlines the criteria for 'better' models. He notes that more comprehensive models of protein metabolism 'are sorely needed' especially when considering the critical

pathophysiological importance of protein metabolism. These models should describe system dynamics and the models should allow the identification of physiologically plausible interactions between amino acids and proteins. Furthermore, he notes that the models must be tested to define their validity and robustness and the models must be practically useful. The model proposed here meets all these criteria. It is robust and on solid theoretical ground, and allows the estimation of the fractional breakdown and synthesis rates of a fast turning-over protein pool, furthermore, the model allows the estimation of the sizes of physiologically meaningful pools.

The $[^{15}N,^{13}C]$-leucine model has only been used in a study involving healthy adult males. Further experimentation using different demographics and diseased conditions should be performed in order to assess the validity of the model under these conditions. In addition, it would be interesting to perform an experiment including the infusion of a $[^2H]$-KIC tracer, so that the proposed model could be directly compared with the model described by Cobelli et al. (1991).

This work provides novel contributions in three areas. Firstly, the model is in itself a novel contribution to the domain of medical research. Secondly, the use of simulation in model development as performed in Chapter Four is innovative and in this case provided the justification for clinical investigation. Finally, Appendix IV provides equations that correct for spectra overlap (using a method described by Rosenblatt et al. 1992) and allow the calculation of $[^{15}N,^{13}C]$-leucine, $[^{13}C]$-leucine and $[^{13}C]$-KIC tracer-to-tracer ratios from raw peak isotope data.

In conclusion, the $[^{15}N,^{13}C]$-leucine model described here is a useful and important addition to the tools available to those wishing to estimate whole body protein turnover in humans. Compared to the reciprocal pool model, the suggested model is simpler in concept, and in theory it is more correct, making fewer assumptions than the reciprocal pool model. This combination of simplicity and theoretical soundness should encourage its use.

REFERENCES

Abumrad, N. N., Abumrad, N. A., Sandler, M. P., and Lacy, W. W. (1985) The metabolic effects and fate of branched chain amino acids across skeletal muscle. Proceedings of the 5th International Symposium on Ammonia Metabolism, 216-228. Basel

Adibi SA (1976) Metabolism of Branched-Chain Amino Acids in Altered Nutrition. Metabol. 25:1287-301

Arslanian SA, Kalhan SC (1996) Protein turnover during puberty in normal children. Am. J. Physiol. 270:E79-E84

Atkins GL (1969) Multicompartment Models for Biological Systems. Metheun & Co. Ltd, London

Ballmer PE, McNurlan MA, Hulter HN, Anderson SE, Garlick PJ, Krapf R (1995) Chronic metabolic acidosis decreases albumin synthesis and induces negative nitrogen balance in humans. J. Clin. Invest. 95:39-45

Barrett EJ, Revkin JH, Young LH, Zaret BL, Jacob R, Gelfand RA (1987) An isotopic method for measurement of muscle protein synthesis and degradation in vivo. Biochem. J. 245:223-8

Beckett PR, Jahoor F, Copeland KC (1997) The efficiency of dietary protein utilization is increased during puberty. J. Clin. Endocrinol. Metab. 82:2445-9

Bergstrom J, Furst P, Noree LO, Vinnars E (1974) Intracellular free amino acid concentration in human muscle tissue. J. Appl. Physiol. 36:693-7

Bier DM (1989) Intrinsically difficult problems: The kinetics of body proteins and amino acids in man. Diabetes Metab. Rev. 5:111-32

Bier DM (1997) Stable isotopes in biosciences, their measurement and models for amino acid metabolism. Eur. J. Pediatr. 156:S2-S8

Biolo G, Fleming RD, Maggi SP, Wolfe RR (1995) Transmembrane transport and intracellular kinetics of amino-acids in human skeletal-muscle. Am. J. Physiol. 268:E75-E84

Birkhahn RH, Long CL, Fitkin D, Jeevanandam M, Blakemore WS (1981) Whole-body protein metabolism due to trauma in man as estimated by L-[^{15}N]alanine. Am. J. Physiol. 241:E64-E71

Block RJ, Weiss KW (1956) Amino Acid Handbook: Methods and Results of Protein Analysis. Chas C Thomas, Springfield, US

Boirie Y, Gachon P, Beaufrere B (1997) Splanchnic and whole-body leucine kinetics in young and elderly men. Am. J. Clin. Nutr. 65:489-95

Bowes SB, Umpleby M, Cummings MH, Jackson NC, Carroll PV, Lowy C, Sonksen PH, Russell-Jones DL (1997) The effect of recombinant human growth hormone on glucose and leucine metabolism in Cushing's syndrome. J. Clin. Endocrinol. Metab. 82:243-6

Brillon DJ, Zheng B, Campbell RG, Matthews DE (1995) Effect of cortisol on energy-expenditure and amino-acid-metabolism in humans. Am. J. Physiol. 31:E501-E513

Caballero B, Wurtman RJ (1991) Differential-effects of insulin resistance on leucine and glucose kinetics in obesity. Metabol. 40:51-8

Calloway DH, Odell AC, Margen S (1971) Sweat and miscellaneous nitrogen losses in human balance studies. J. Nutr. 101:775-86

Carroll P, Christ E, Gowrie I, Jackson N, Hovorka R, Albany E, Bowes S, Umpleby M, Sonksen P, Russell-Jones DL (1997) Daily rhIGF-I augments the anabolic effect of insulin in adults with IDDM. Diabetes 46:945

Carson ER, Cobelli C, Finkelstein L (1983) The Mathematical Modelling of Metabolic and Endocrine Systems. John Wiley & Sons Ltd, New York

Cheng KN, Dworzak F, Ford GC, Rennie MJ, Halliday D (1985) Direct determination of leucine metabolism and protein breakdown in humans using 1-[1-^{13}C,^{15}N]-leucine and the forearm model. Eur. J. Clin. Invest. 15:349-54

Cheng KN, Pacy PJ, Dworzak F, Ford GC, Halliday D (1987) Influence of fasting on leucine and muscle protein metabolism across the human forearm determined using L-[1-13C,15N]leucine as the tracer. Clin. Sci. 73:241-6

Christensen HN (1990) Role of amino acid transport and countertransport in nutrition and metabolism. Physiol. Rev. 70:43-77

Clark WA, Zak R (1981) Assessment of fractional rates of protein synthesis in cardiac muscle cultures after equilibrium labelling. J. Biol. Chem.4863-70

Clarke JT, Bier DM (1982) The conversion of phenylalanine to tyrosine in man. Direct measurement by continuous intravenous tracer infusions of L-[ring-2H5]phenylalanine and L-[1-13C] tyrosine in the postabsorptive state. Metabol. 31:999-1005

Cobelli C, Saccomani MP (1991) Domain of validity of classical-models of leucine metabolism assessed by compartmental modeling. Math. Biosci. 107:3-20

Cobelli C, Saccomani MP, Tessari P, Biolo G, Luzi L, Matthews DE (1991) Compartmental model of leucine kinetics in humans. Am. J. Physiol. 261:E539-E550

Cobelli C, Toffolo G, Bier DM, Nosadini R (1987) Models to interpret kinetic data in stable isotope tracer studies. Am. J. Physiol. 253:E551-E564

Cobelli C, Toffolo G, Foster DM (1992) Tracer to Tracee ratio for analysis of stable isotope tracer data: link with radioactive kinetic formalism. Am. J. Physiol. 262:E968-E975

Coppack SW, Persson M, Miles JM (1996) Phenylalanine kinetics in human adipose tissue. J. Clin. Invest. 98:692-7

Cortiella J, Matthews DE, Hoerr RA, Bier DM, Young VR (1988) Leucine kinetics at graded intakes in young men: quantitative fate of dietary leucine. Am. J. Clin. Nutr. 48:998-1009

Costa G, Ullrich L, Kantor F, Holland JF (1968) Production of elemental nitrogen by certain mammals including man. Nature 218:546-51

Cowgill RW, Freeberg B (1957) The metabolism of methylhistidine compounds in animals. Arch. Biochem. Biophys. 71:466-72

Darmaun D, Matthews DE, Bier DM (1986) Glutamine and glutamate kinetics in humans. Am. J. Physiol. 251:E117-E126

Everett A, Prior WJ, Zak R (1981) Equilibrium of leucine between plasma compartment and leucyl-t- RNA in the heart and turnover of cardiac myosin heavy chain. Biochem. J.365-8

Fern EB, Garlick PJ, Mcnurlan MA, Waterlow JC (1981) The excretion of isotope in urea and ammonia for estimating protein turnover in man with [15N]glycine. Clin. Sci. 61:217-28

Fern EB, Garlick PJ, Waterlow JC (1985) Apparent compartmentation of body nitrogen in one human subject: its consequences in measuring the rate of whole-body protein synthesis with 15N. Clin. Sci. 68:271-82

Finkelstein L, Carson ER (1979) Mathematical Modelling of Dynamic Biological Systems. Research Studies Press Letchworth: [Distributed by] International Scholarly Book Services (Europe)

Forbes GB (1987) Human Body Composition. Springer-Verlag, New York

Fryburg DA, Barrett EJ, Louard RJ, Gelfand RA (1990) Effect of starvation on human muscle protein metabolism and its response to insulin. Am. J. Physiol. 259:E477-E482

Garlick PJ (1969) Turnover rate of muscle protein measured by constant intravenous infusion of 14C-glycine. Nature 223:61-2

Garlick PJ, Wernerman J, Mcnurlan MA, ESSEN P, Lobley GE, Milne E, Calder GA, Vinnars E (1989) Measurement of the rate of protein synthesis in muscle of postabsorptive young men by injection of a 'flooding dose' of [1-13C]leucine. Clin. Sci. 77:329-36

Garlick PJ, Mcnurlan MA, Essen P, Wernerman J (1994) Measurement of tissue protein-synthesis rates in-vivo - a critical analysis of contrasting methods. Am. J. Physiol. 266:E287-E297

Gelfand RA, Barrett EJ (1987) Effect of physiologic hyperinsulinemia on skeletal muscle protein synthesis and breakdown in man. J. Clin. Invest. 80:1-6

Golden MH, Jackson AA (1981) Assumptions and errors in the use of ^{15}N-excretion data to estimate whole body protein turnover. In: Waterlow JC, Stephen JML (eds) Applied Science Publishers, London, pp 323-61

Gowrie IJ, Roudsari AV, Umpleby AM, Hovorka R (1999) Estimating protein turnover with a [N-15,C-13]leucine tracer: a study using simulated data. J. Theor. Biol. 198:165-72

Hegsted DM (1963) Variation in requirements of nutrients amino acids. Fed. Proc. 22:1424-9

Hegsted DM (1976) Balance Studies. J. Nutr.307-11

Hoerr RA, Yong-Ming D, Wagner DA, Burke JF, Young VR (1989) Recovery of ^{13}C in breath fron NaH^{13}CO$_2$ infused by gut and vein: effect of feeding. Am. J. Physiol. 257:E426-E438

Hovorka R, Carroll PV, Gowrie IJ, Jackson NC, Russell-Jones DL, Umpleby AM (1999) A surrogate measure of whole body leucine transport across the cell membrane. Am. J. Physiol. 276:E573-E579

Irving CS, Thomas MR, Malphus EW, Marks L, Wong WW, Boutton TW, Klein PD (1986) Lysine and protein metabolism in young women. Subdivision based on the novel use of multiple stable isotopic labels. J. Clin. Invest. 77:1321-31

Jackson AA, Golden MH (1980) [15N]Glycine metabolism in normal man: the metabolic alpha-amino-nitrogen pool. Clin. Sci. 58:517-22

James WPT, Garlick PJ, Sender PM, Waterlow JC (1976) Studies of Amino Acids and Protein Metabolism in normal man with 1-[U-14C] tyrosine. Clin. Sci. Mol. Med.525-32

Jeevanandam M, Brennan MF, Horowitz GD, Rose D, Mihranian MH, Daly J, Lowry SF (1985) Tracer priming in human protein turnover studies with [^{15}N]glycine. Biochem. Med. 34:214-25

Jeevanandam M, Long CL, Kinney JM (1979) Kinetics of intravenously administered ^{15}N-L-alanine in the evaluation of protein turnover. Am. J. Clin. Nutr. 32:975-80

Kelley J, Stirewalt WS, Chrin L (1984) Protein synthesis in rat lung. Measurements in vivo based on leucyl- tRNA and rapidly turning-over procollagen I. Biochem. J. 222:77-83

Kopple JD (1987) Uses and limitations of the balance technique. J. Parenter. Enteral. Nutr. 11:79S-85S

Kurzer MS, Calloway DH (1981) Nitrate and nitrogen balances in men. Am. J. Clin. Nutr. 34:1305-13

Loftfield RB, Harris A (1956) Participation of free amino acids in protein synthesis. J. Biol. Chem. 219:151-9

Long CL, Haverberg LN, Young VR, Kinney JM, Munro HN, Geiger JW (1975) Metabolism of 3-methylhistidine in man. Metabol. 24:929-35

Lundholm K, Bennegard K, Zachrisson H, Lundgren F, Eden E, Moller-Loswick AC (1987) Transport kinetics of amino acids across the resting human leg. J. Clin. Invest. 80:763-71

Macdonald IA (1999) Arterio-venous differences to study macronutrient metabolism: introduction and overview. Proc. Nutr. Soc. 58:871-5

Martin AF, Rabinowitz M, Blough R, Prior G, Zak R (1977) Measurements of half-life of rat cardiac myosin heavy chain with leucyl- tRNA used as precursor pool. J. Biol. Chem. 252:3422-9

Matthews DE, Cobelli C (1991) Leucine metabolism in man: Lessons from modelling. J. Parenter. Enteral. Nutr. 15:86S-9S

Matthews DE, Pesola G, Campbell RG (1990) Effect of epinephrine on amino acid and energy metabolism in humans. Am. J. Physiol. 258:E948-E956

Matthews DE, Bier DM, Rennie MJ, Edwards RHT, Millward DJ, Clugston GA (1981) Regulation of leucine metabolism in man: A stable isotope study. Science 214:1129-31

Matthews DE, Marano MA, Campbell RG (1993) Splanchnic bed utilization of leucine and phenylalanine in humans. Am. J. Physiol. 264:E

Matthews DE, Schwarz HP, Yang RD, Motil KJ, Young VR, Bier DM (1982) Relationship of plasma leucine and α-ketoisocaproate During L-[1- ^{13}C]leucine infusion in man: A method for measuring human intracellular leucine tracer enrichment. Metabol. 31:1105-12

Meguid MM, Matthews DE, Bier DM, Meredith CN, Young VR (1986) Valine kinetics at graded valine intakes in young men. Am. J. Clin. Nutr. 43:781-6

Millward DJ, Fereday A, Gibson N, Pacy PJ (1997) Aging, protein requirements, and protein turnover. Am. J. Clin. Nutr. 66:774-86

Morais JA, Gougeon R, Pencharz PB, Jones PJ, Ross R, Marliss EB (1997) Whole-body protein turnover in the healthy elderly. Am. J. Clin. Nutr. 66:880-9

Munro HN, Fleck A (1969) Analysis of tissues and body fluids for nitrogenous constituents. Academic Press, New York, pp 423-525

Nissim I, Yudkoff M, Segal S (1983) A model for determination of total body protein synthesis based upon compartmental analysis of the plasma [15N] glycine decay curve. Metabol. 32:646-53

O'Keefe SJD, Sender PM, James WPT (1974) 'Catabolic' loss of body nitrogen in response to surgery. Lancet ii:1035-43

Olesen K, Heilskov NCS, Schonheyder F (1954) The excretion of ^{15}N in urine after administration of ^{15}N-glycine. Biochim. Biophys. Acta 15:95-107

Pacy PJ, Thompson GN, Halliday D (1991) Measurement of whole-body protein-turnover in insulin-dependent (Type-1) diabetic-patients during insulin withdrawal and infusion - comparison of [C-13]Leucine and [H-2(5)]Phenylalanine methodologies. Clin. Sci. 80:345-52

Picou D, Taylor-Roberts T (1969) The measurement of total protein synthesis and catabolism and nitrogen turnover in infants in different nutritional states and receiving different amounts of dietary protein. Clin Sci. 36:283-96

Picou D, Taylor-Roberts T, Waterlow JC (1969) The measurement of total protein synthesis and nitrogen flux in man by constant infusion of 15N-glycine. J. Physiol. 200:52P-3P

Rathmacher JA (2000) Measurement and Significance of Protein Turnover. In: Farm Animal Metabolism and Nutrition, CABI Publishing, Wallingford, UK, pp 25-47

Rennie MJ, Bennegard K, Eden E, Emery PW, Lundholm K (1984) Urinary excretion and efflux from the leg of 3-methylhistidine before and after major surgical operation. Metabol. 33:250-6

Rennie MJ, Millward DJ (1983) 3-Methylhistidine excretion and the urinary 3-methylhistidine/creatinine ratio are poor indicators of skeletal muscle protein breakdown. Clin. Sci. 65:217-25

Rennie MJ, Smith K, Watt PW (1994) Measurement of human tissue protein synthesis: an optimal approach. Am. J. Physiol. 266:E298-E307

Robert JJ, Bier DM, Zhao XH, Matthews DE, Young VR (1982) Glucose and insulin effects on the novo amino acid synthesis in young men: studies with stable isotope labeled alanine, glycine, leucine, and lysine. Metabol. 31:1210-8

Rosenblatt J, Chinkes D, Wolfe M, Wolfe RR (1992) Stable isotope tracer analysis by GC-MS, including quantification of isotopomer effects. Am. J. Physiol. 263:E584-E596

Russell-Jones DL, Umpleby AM, Hennessy TR, Bowes SB, Shojaee-Moradie F, Hopkins KD, Jackson NC, Kelly JM, Jones RH, Sonksen PH (1994) Use of a leucine clamp to demonstrate that IGF-I actively stimulates protein-synthesis in normal humans. Am. J. Physiol. 30:E591-E598

San Pietro A, Rittenberg D (1953a) A study of the rate of protein synthesis in humans. I. Measurement of the urea pool and urea space. J. Biol. Chem. 201:445-55

San Pietro A, Rittenberg D (1953b) A study of the rate of protein synthesis in humans. II. Measurement of the metabolic pool and the rate of protein synthesis. J. Biol. Chem. 201:457-73

Schoenheimer R (1942) The Dynamic State of Body Constituents. Harvard University Press, Cambridge, Mass.

Schoenheimer R, Ratner S, Rittenberg D (1939) Studies in protein metabolism. J. Biol. Chem. 130:703-32

Schoenheimer R, Rittenberg D (1935) Deuterium as an indicator in the study of intermediary metabolism. J. Biol. Chem. 111:163-9

Schoenheimer R, Rittenberg D (1938) The application of isotopes to the study of intermediary metabolism. Science 87:221-6

Schwenk WF, Beaufrere B, Haymond MW (1985a) Use of reciprocal pool specific activities to model leucine metabolism in humans. Am. J. Physiol. 249:E646-E650

Schwenk WF, Tsalikian E, Beaufrere B, Haymond MW (1985b) Recycling of an amino acid label with prolonged isotope infusion: implications for kinetic studies. Am. J. Physiol. 248:E482-E487

Short KR, Meek SE, Moller N, Ekberg K, Nair KS (1999) Whole body protein kinetics using Phe and Tyr tracers: an evaluation of the accuracy of approximated flux values. Am. J. Physiol. 276:E1194-E1200

Sjolin J, Stjernstrom H, Henneberg S, Andersson E, Martensson J, Friman G, Larsson J (1989) Splanchnic and peripheral release of 3-methylhistidine in relation to its urinary excretion in human infection. Metabol. 38:23-9

Smith K, Rennie MJ (1996) The measurement of tissue protein turnover. Baillieres Clin. Endocrinol. Metab 10:469-95

Solini A, Bonora E, Bonadonna R, Castellino P, DeFronzo RA (1997) Protein metabolism in human obesity: Relationship with glucose and lipid metabolism and with visceral adipose tissue. J. Clin. Endocrinol. Metab. 82:2552-8

Sprinson DB, Rittenberg D (1949) The rate of interaction of the amino acids of the diet with the tissue of the proteins. J. Biol. Chem. 180:715-26

Staten MA, Matthews DE, Bier DM (1986) Leucine metabolism in type II diabetes mellitus. Diabetes 35:1249-53

Tallen H, Stein WH, Moore S (1954) 3-Methylhistidine, a new amino acid from human urine. J. Biol. Chem. 206:825-34

Taruvinga M, Jackson AA, Golden MH (1979) Comparison of 15N-labelled glycine, aspartate, valine and leucine for measurement of whole-body protein turnover. Clin. Sci. 57:281-3

Taylor RT, Jenkins WT (1966) Leucine aminotransferase. II. Purification and characterization. J. Biol. Chem. 241:4396-405

Tessari P, Biolo G, Inchiostro S, Saggin L, Piccoli A, Tiengo A (1992) Relationship between plasma leucine concentration and clearance in normal and type 1 diabetic subjects. Acta Diabetol. 29:6-10

Tessari P, Garibotto G, Inchiostro S, Robaudo C, Saffioti S, Vettore M, Zanetti M, Russo R, Deferrari G (1996a) Kidney, splanchnic, and leg protein-turnover in humans - insight from leucine and phenylalanine kinetics. J. Clin. Invest. 98:1481-92

Tessari P, Inchiostro S, Zanetti M, Barazzoni R (1995) A model of skeletal-muscle leucine kinetics measured across the human forearm. Am. J. Physiol. 32:E127-E136

Tessari P, Zanetti M, Barazzoni R, Vettore M, Michielan F (1996b) Mechanisms of postprandial protein accretion in human skeletal-muscle - insight from leucine and phenylalanine forearm kinetics. J. Clin. Invest. 98:1361-72

Thompson GN, Pacy PJ, Merritt H, Ford GC, Read MA, Cheng KN, Halliday D (1989) Rapid measurement of whole body and forearm protein turnover using a [2H5]phenylalanine model. Am. J. Physiol. 256:E631-E639

Toffolo G, Foster DM, Cobelli C (1993) Estimation of protein fractional synthetic rate from tracer data. Am. J. Physiol. 264:E128-E135

Tschudy DP, Bacchus H, Weissman S, Watkin DM, Eubanks M, White J (1959) Studies of the effect of dietary protein and calorific levels on the kinetics of nitrogen metabolism using N^{15} L-aspartic acid. J. Clin. Invest. 38:892-901

Uauy R, Winterer JC, Bilmazes C, Haverberg LN, Scrimshaw NS, Munro HN, Young VR (1978) The changing pattern of whole body protein metabolism in aging humans. J. Gerontol. 33:663-71

Umpleby AM, Boroujerdi MA, Brown PM, Carson ER, Sonksen PH (1986) The effect of metabolic control on leucine metabolism in type-1 (insulin-dependent) diabetic-patients. Diabetologia 29:131-41

Umpleby AM, Scobie IN, Boroujerdi MA, Sonksen PH (1995) The effect of starvation on leucine, alanine and glucose- metabolism in obese subjects. Eur. J. Clin. Invest. 25:619-26

Van Goudoever JB, Sulkers EJ, Halliday D, Degenhart HJ, Carnielli VP, Wattimena JD, Sauer PJ (1995) Whole-body protein turnover in preterm appropriate for gestational age and small for gestational age infants: Comparison of [15N]glycine and [1- 13C]leucine administered simultaneously. Pediatr. Res. 37:381-8

van HG, Gonzalez-Alonso J, Sacchetti M, Saltin B (1999) Skeletal muscle substrate metabolism during exercise: methodological considerations. Proc. Nutr. Soc. 58:899-912

Volpi E, Lucidi P, Bolli GB, Santeusanio F, Defeo P (1998) Gender differences in basal protein kinetics in young adults. J. Clin. Endocrinol. Metab. 83:4363-7

Wagenmakers AM (1999) Tracers to investigate protein and amino acid metabolism in human subjects. Proc. Nutr. Soc. 58:987-1000

Waterlow JC (1967) Lysine turnover in man measured by intravenous infusion of L-[U- ^{14}C] lysine. Clin. Sci. 33:507-15

Waterlow JC (1980) Protein turnover in the whole animal. Invest. Cell Pathol. 3:107-19

Waterlow JC (1981) ^{15}N end-product methods for the study of whole body protein turnover. Proc. Nutr. Soc. 40:317-20

Waterlow JC (1995) Whole-body protein-turnover in humans - past, present, and future. Annu. Rev. Nutr. 15:57-92

Waterlow JC (1999) The mysteries of nitrogen balance. Nutr. Res. Rev. 12:25-54

Waterlow JC, Garlick PJ, Millward DJ (1978a) Protein Turnover in Mammalian Tissues and in the Whole Body. North-Holland, Amsterdam

Waterlow JC, Golden MH, Garlick PJ (1978b) Protein turnover in man measured with ^{15}N: comparison of end products and dose regimes. Am. J. Physiol. 235:E165-E174

Waterlow JC, Stephen JM (1966) Adaptation of the rat to a low-protein diet: the effect of a reduced protein intake on the pattern of incorporation of L-[14C] lysine. Br. J. Nutr. 20:461-84

Waterlow JC, Stephen JM (1968) The effect of low protein diets on the turn-over rates of serums, liver and muscle proteins in the rat, measured by continuous infusion of L-[14C]lysine. Clin Sci. 35:287-305

Welle S (1999a) Basic Mechanisms of Protein Turnover. In: Human Protein Metabolism, Welle S (ed), Springer-Verlag, New York, pp 11-28

Welle S (1999b) Methods for Studying Protein Metabolism in Humans. In: Human Protein Metabolism, Welle S (ed), Springer-Verlag, New York, pp 29-70

Welle S (1999c) Normative Data from Infancy to Old Age. In: Human Protein Metabolism, Welle S (ed), Springer-Verlag, New York, pp 72-90

Welle S, Barnard RR, Statt M, Amatruda JM (1992) Increased protein-turnover in obese women. Metabol. 41:1028-34

Welle S, Nair KS (1990) Relationship of resting metabolic rate to body composition and protein turnover. Am. J. Physiol. 258:E990-E998

Welle S, Thornton C, Jozefowicz R, Statt M (1993) Myofibrillar protein synthesis in young and old men. Am. J. Physiol. 264:E693-E698

Winterer JC, Steffee WP, Davy W, Perera A, Uauy R, Scrimshaw NS, Young VR (1976) Whole body protein turnover in aging man. Exp. Gerontol. 11:79-87

Wolfe RR, Goodenough RD, Wolfe MH, Royle GT, Nadel ER (1982) Isotopic analysis of leucine and urea metabolism in exercising humans. J. Appl. Physiol. 52:458-66

Wu H, Bishop CS (1959) Pattern of N^{15}-excretion in man following administration of N^{15}-labeled glycine. J. Appl. Physiol. 14:1-5

Wu H, Sendroy JJr (2001) Pattern of N^{15}-excretion in man following administration of N^{15}-labeled phenylalanine. J. Appl. Physiol. 14:6-10

Wu H, Sendroy JJr, Bishop CS (1959) Interpretation of urinary N^{15}-excretion data following administration of N^{15}-labeled amino acid. J. Appl. Physiol. 14:11-21

Yang RD, Matthews DE, Bier DM, Lo C, Young VR (1984) Alanine kinetics in humans: influence of different isotopic tracers. Am. J. Physiol. 247:E634-E638

Yang RD, Matthews DE, Bier DM, Wen ZM, Young VR (1986) Response of alanine metabolism in humans to manipulation of dietary protein and energy intakes. Am. J. Physiol. 250:E39-E46

Young LH, McNulty PH, Morgan C, Deckelbaum LI, Zaret BL, Barrett EJ (1991) Myocardial protein turnover in patients with coronary artery disease. Effect of branched chain amino acid infusion. J. Clin. Invest. 87:554-60

Young VR (1986) Nutritional balance studies: Indicators of human requirements or of adaptive mechanisms? J. Nutr. 4:700-3

Young VR (1987) 1987 McCollum award lecture - kinetics of human amino-acid metabolism - nutritional implications and some lessons. Am. J. Clin. Nutr. 46:709-25

Young VR, Munro HN (1978) Ntau-methylhistidine (3-methylhistidine) and muscle protein turnover: an overview. Fed. Proc. 37:2291-300

Young VR, Scrimshaw N.S., Steffee W.P., Pencharz P.B., Winterer J.C. (1975) Total human body protein synthesis in relation to protein requirements at various ages. Nature 253:192-4

APPENDICIES

APPENDICES

APPENDIX I   NORMAL Q-Q PLOTS AND SCATTERPLOTS
FOR CHAPTER THREE

I.1 Normal Q-Q plots

Normal Q-Q Plot of Age

Normal Q-Q Plot of BMI

Normal Q-Q Plot of Weight

Normal Q-Q Plot of Leucine concentration
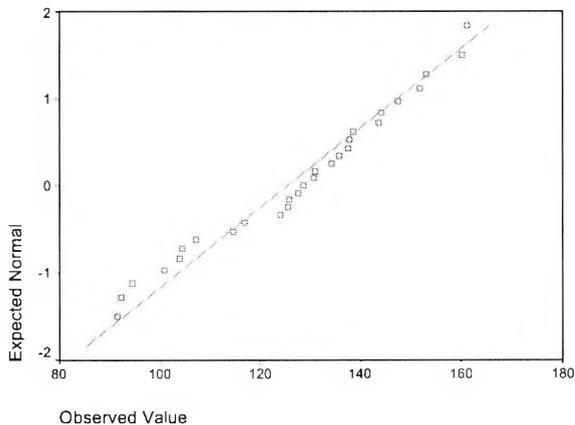
Normal Q-Q Plot of (Reciprocal / Primary) Ra
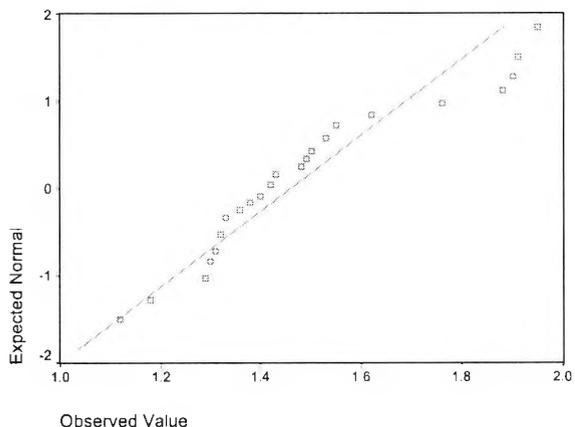
Normal Q-Q Plot of (Reciprocal / Primary) Nold

129
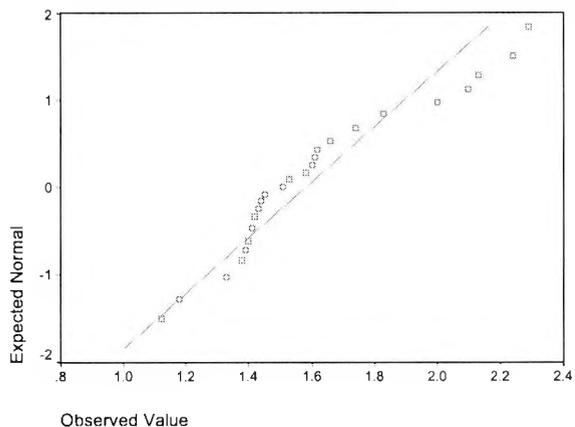
Normal Q-Q Plot of (Reciprocal / Primary) MCF
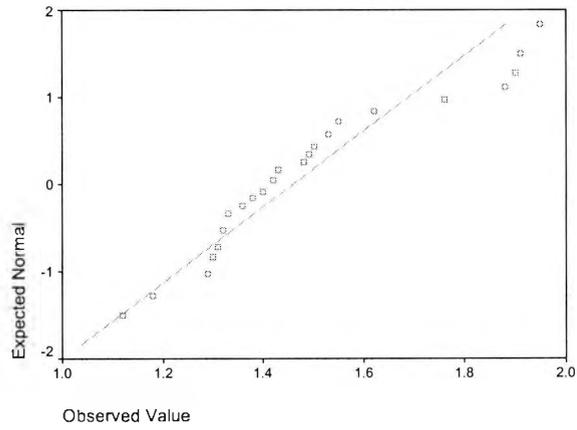
Normal Q-Q Plot of (Reciprocal - Primary) Ra
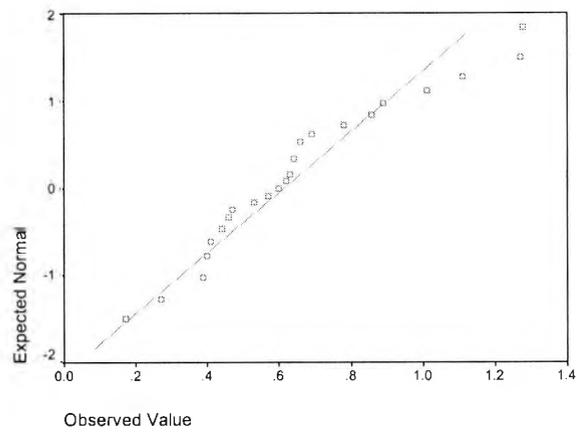
Normal Q-Q Plot of (Reciprocal - Primary) Nolc

130

Normal Q-Q Plot of (Reciprocal - Primary) MCF

Observed Value
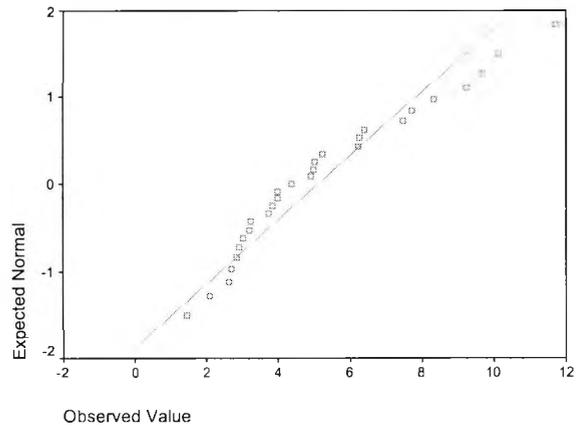
Normal Q-Q Plot of nlog centered Age

Observed Value

Normal Q-Q Plot of nlog (R/P) Ra

Observed Value

131
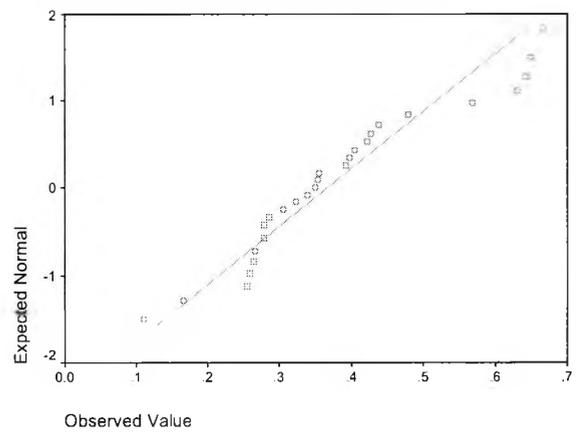
Normal Q-Q Plot of nlog (R/P) Nold

Normal Q-Q Plot of nlog (R/P) MCR

Normal Q-Q Plot of nlog (R/P) Ra

Normal Q-Q Plot of nlog (R - P) Nold

Observed Value

Normal Q-Q Plot of nlog (R - P) MCR

Observed Value
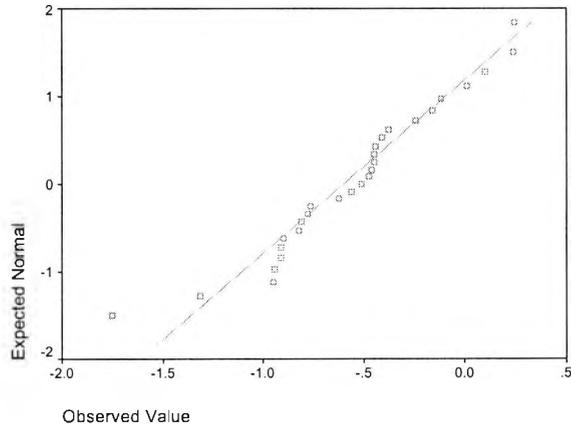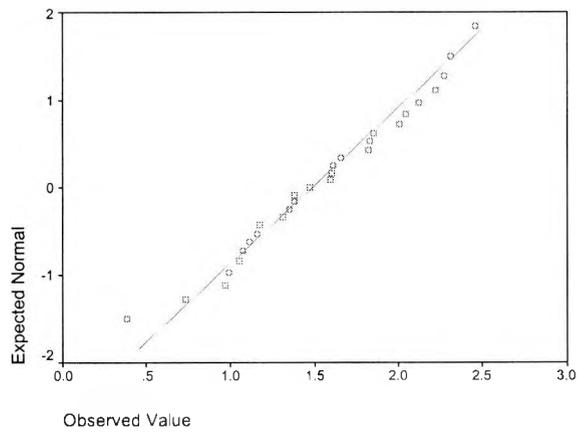
Normal Q-Q Plot of Ra (Primary)

Observed Value
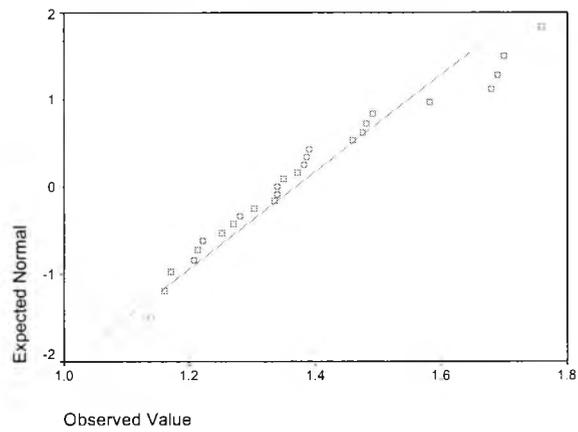
Normal Q-Q Plot of Nold (Primary)
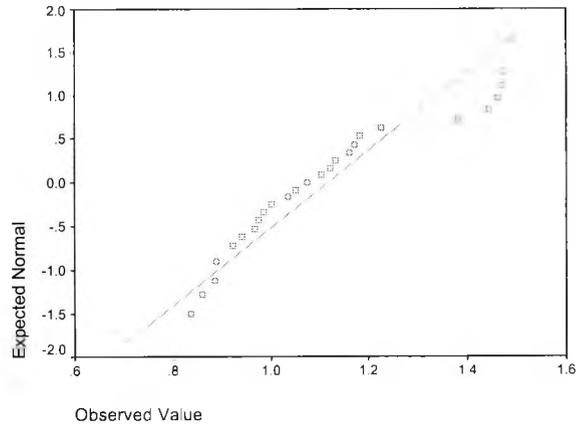
Normal Q-Q Plot of Ox (Primary)
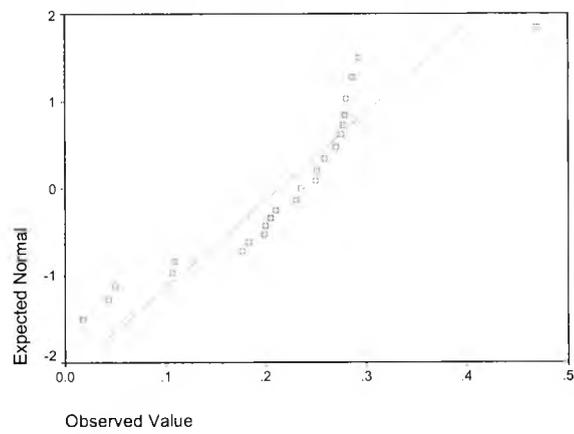
Normal Q-Q Plot of MCR (Primary)
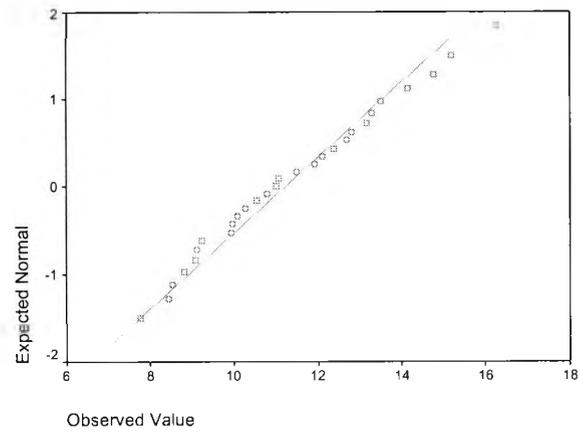
Normal Q-Q Plot of Ra (Reciprocal)
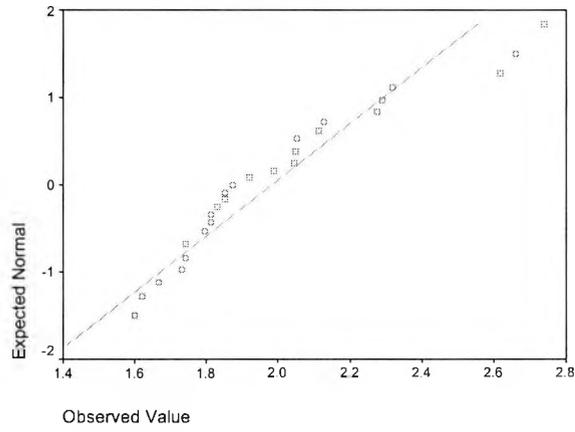
Normal Q-Q Plot of Nold (Reciprocal)
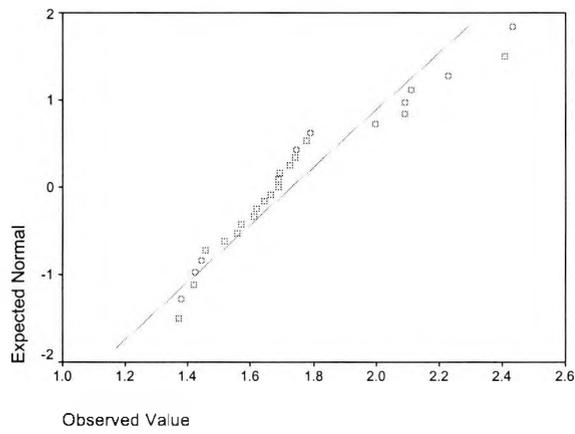
Normal Q-Q Plot of Ox (Reciprocal)
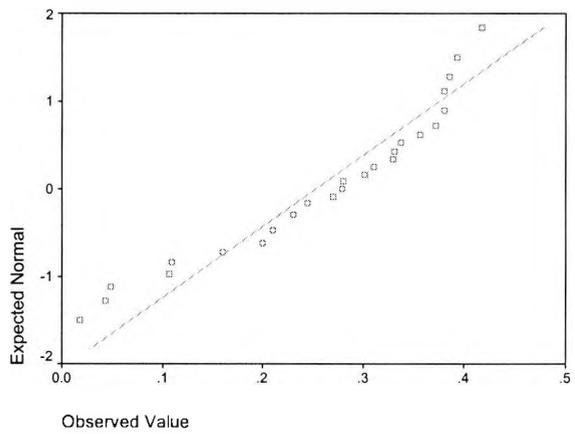
Normal Q-Q Plot of MCR (Reciprocal)
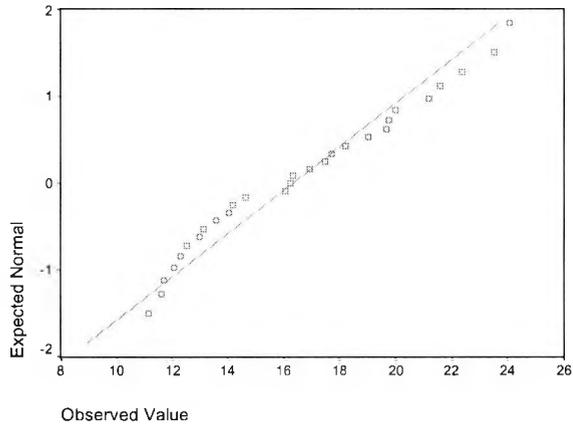
Normal Q-Q Plot of nlog Ra (Primary)
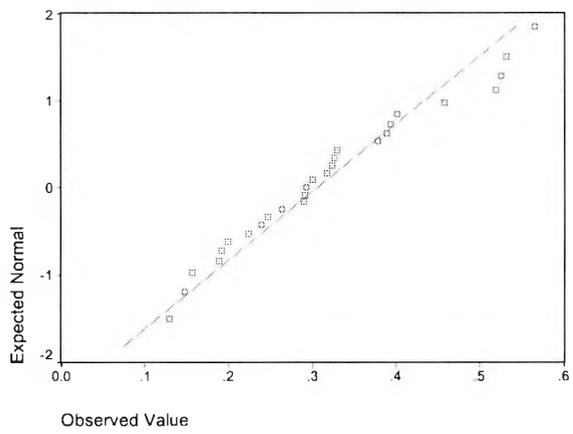
Normal Q-Q Plot of nlog Nold (Primary)
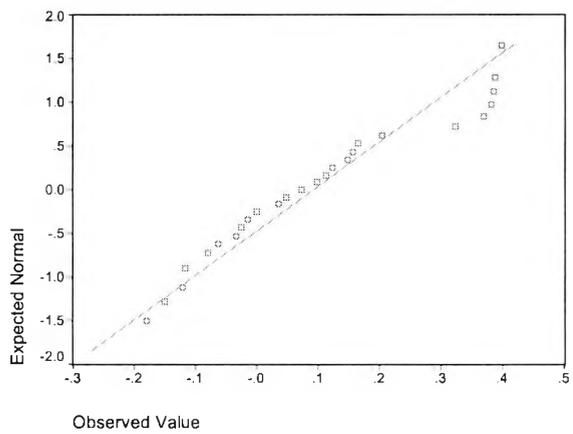
Normal Q-Q Plot of nlog MCR (Primary)
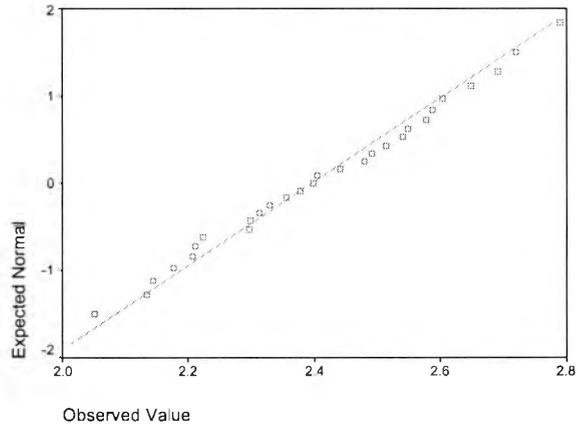
Normal Q-Q Plot of nlog Ra (Reciprocal)
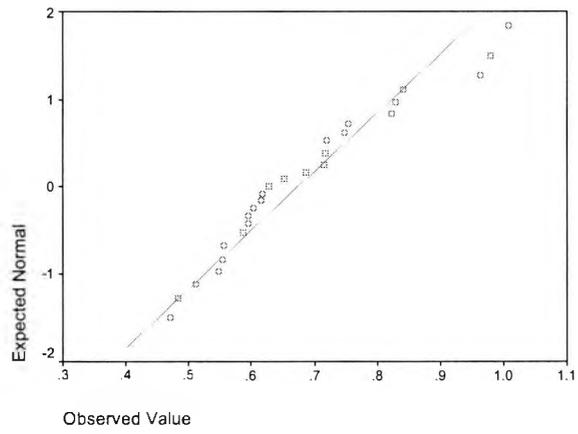
Normal Q-Q Plot of nlog Nold (Reciprocal)
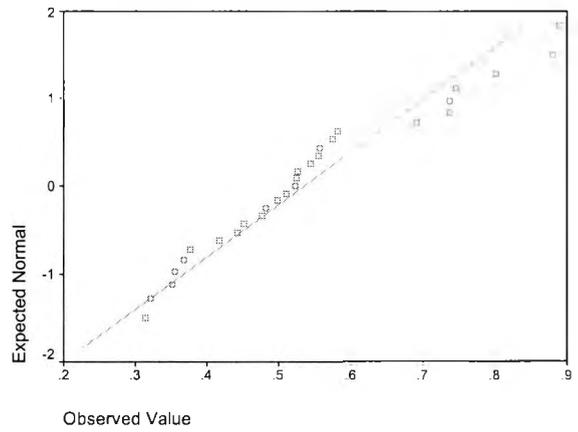
Normal Q-Q Plot of nlog MCR (Reciprocal)

I.2 Scatterplots

Ra (Primary)

Nold (Primary)

Ox (Primary)

139

MCR (Primary)

Ra (Reciprocal)

Nold (Reciprocal)

140

Ox (Reciprocal)

MCR (Reciprocal)

Ra (Primary)

Nold (Primary)

Ox (Primary)

MCR (Primary)

Ra (Reciprocal)

Nold (Reciprocal)

Ox (Reciprocal)

143

144

Leucine concentration

MCR (Reciprocal)

Leucine concentration

Ox (Reciprocal)

Leucine concentration

Nold (Reciprocal)

146
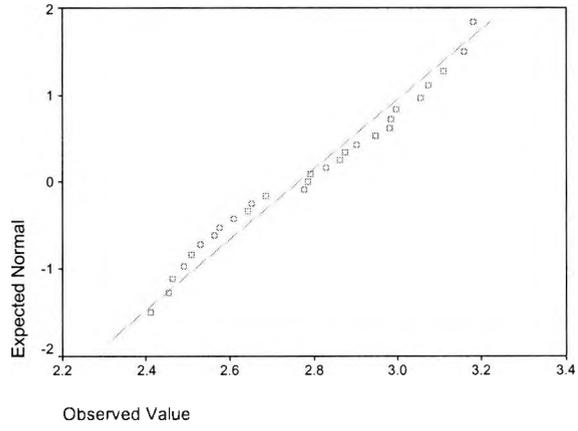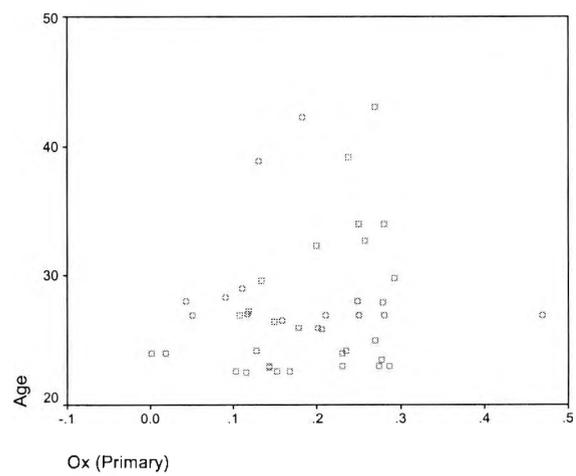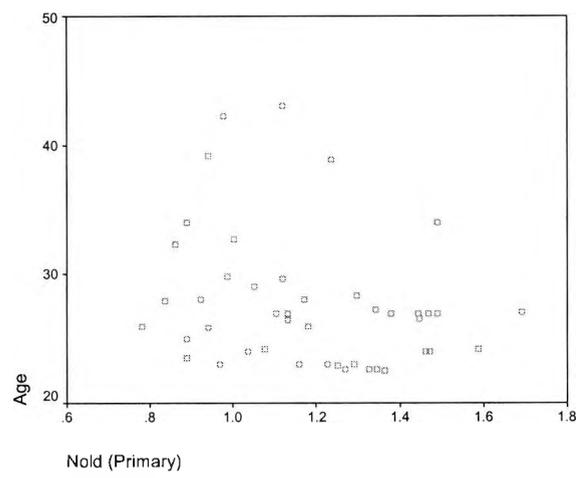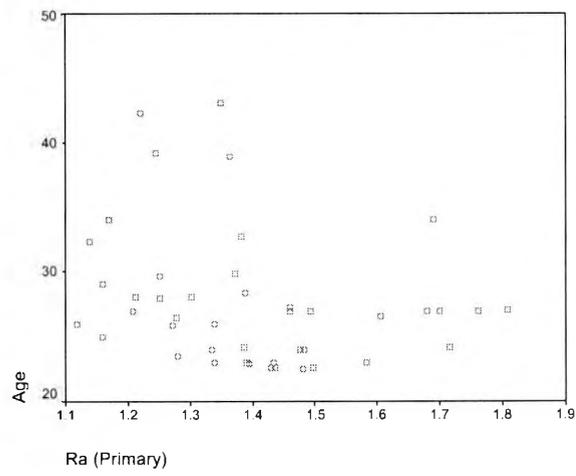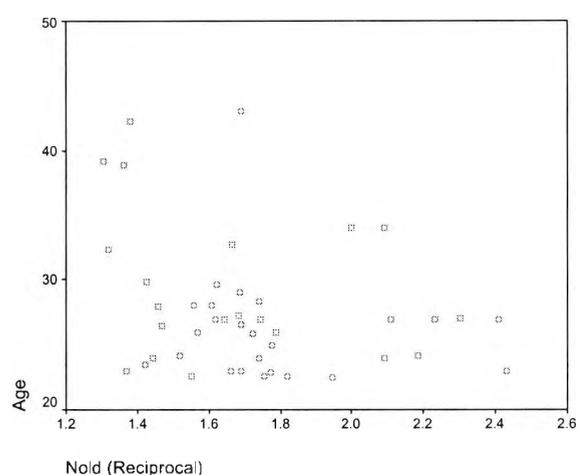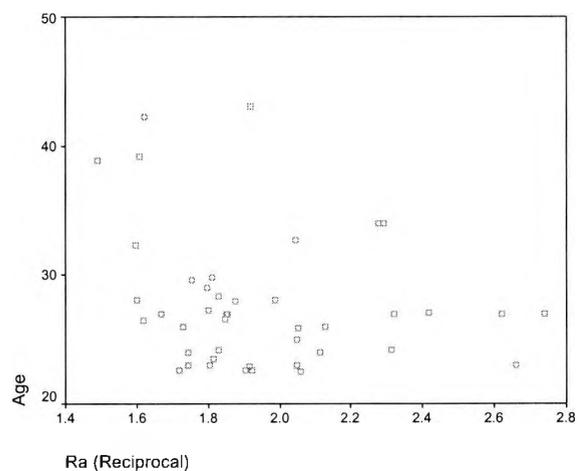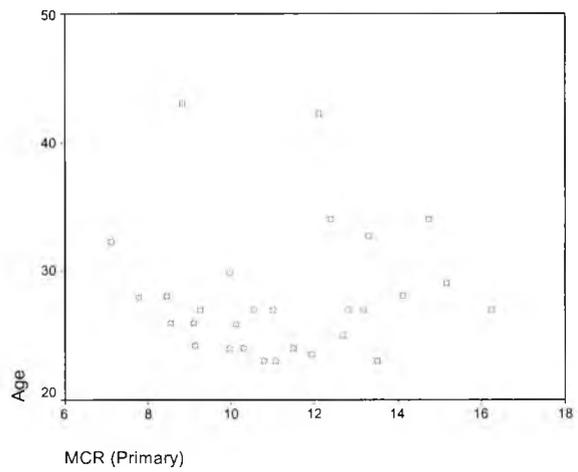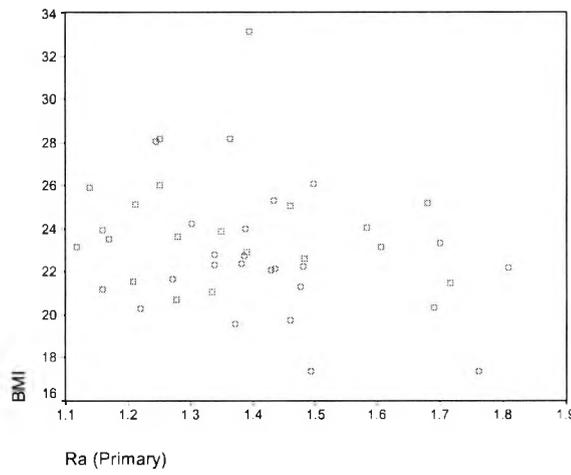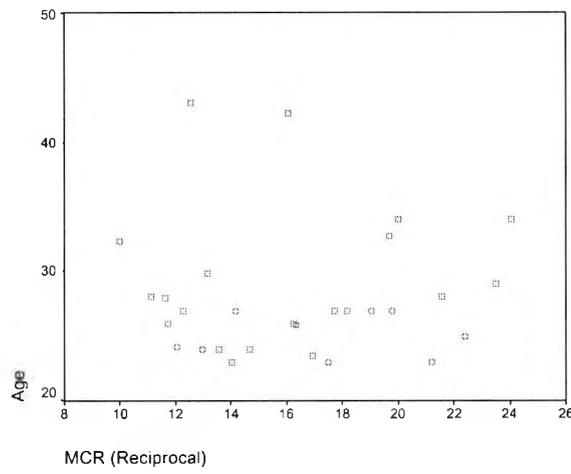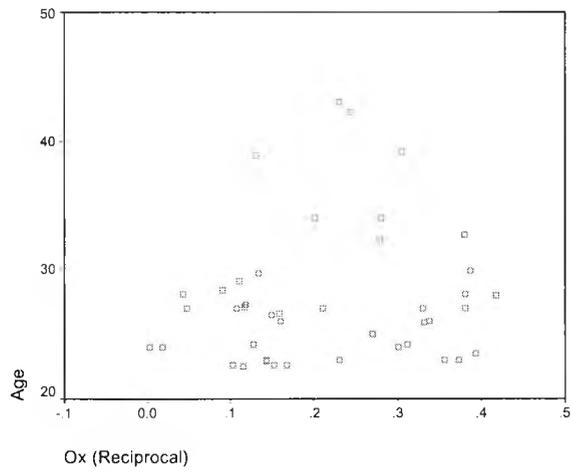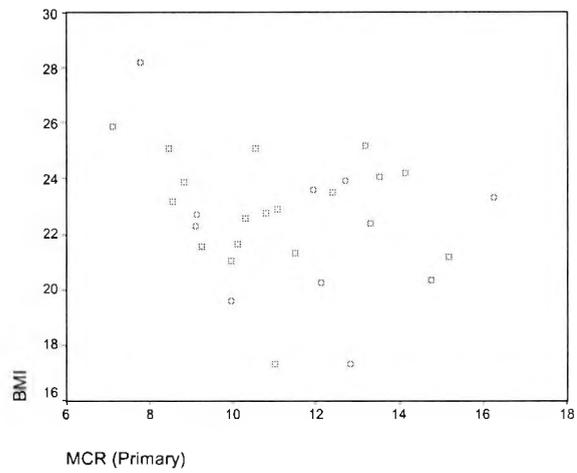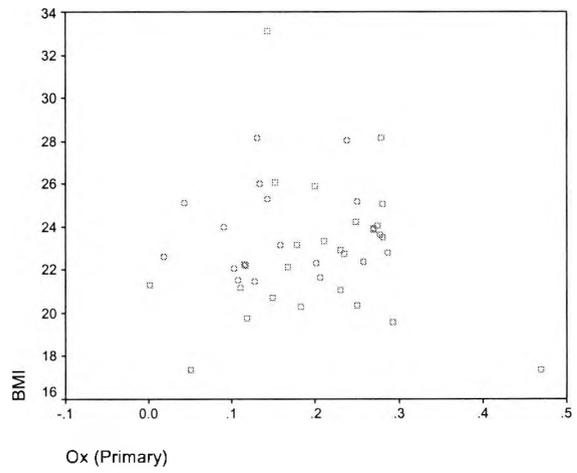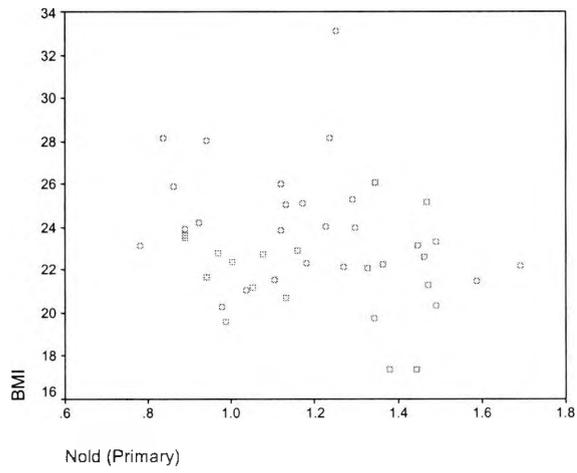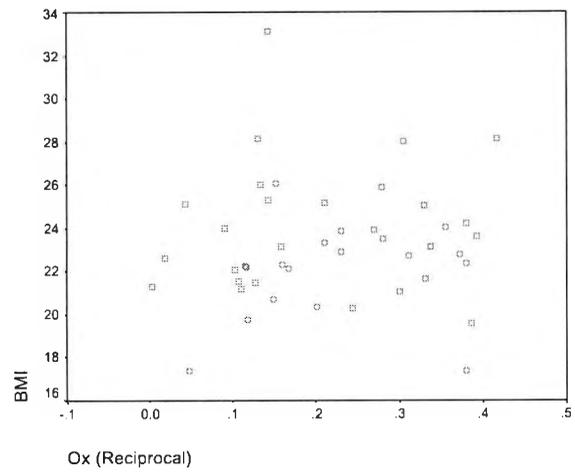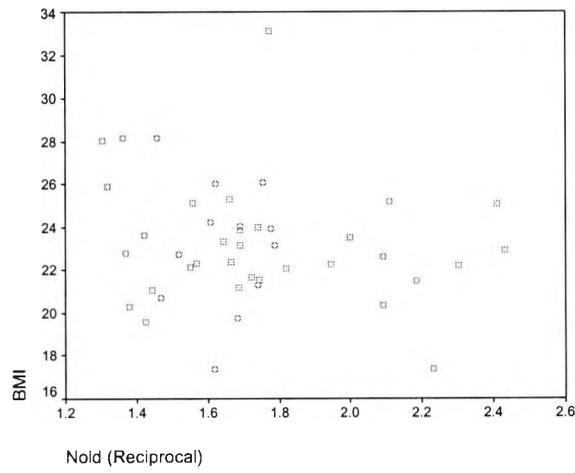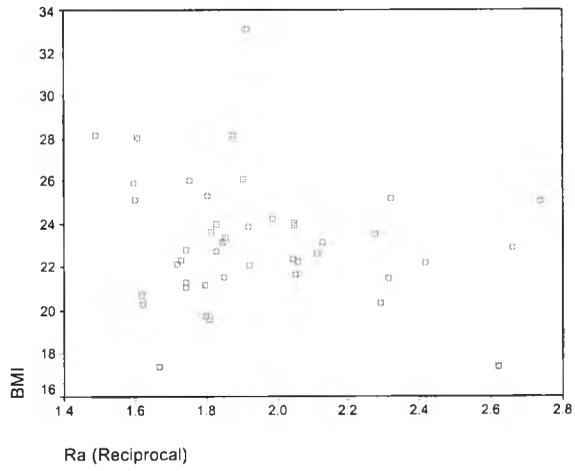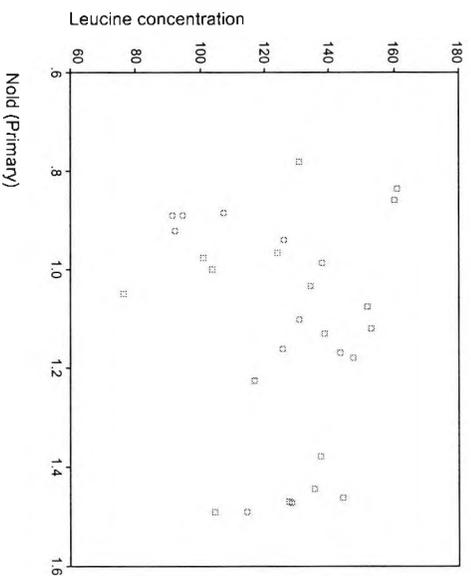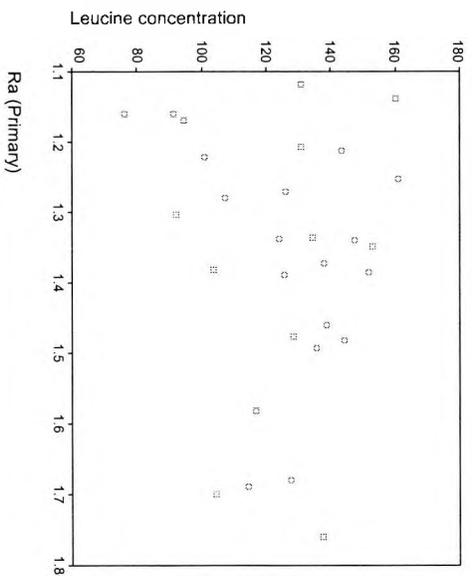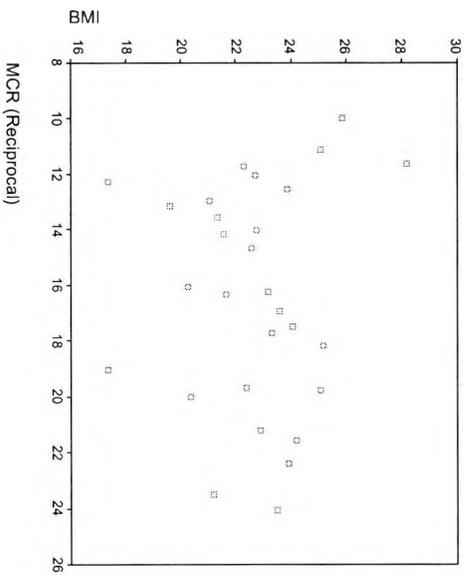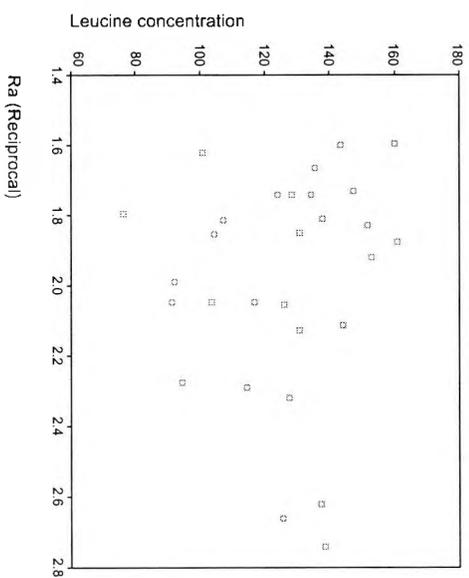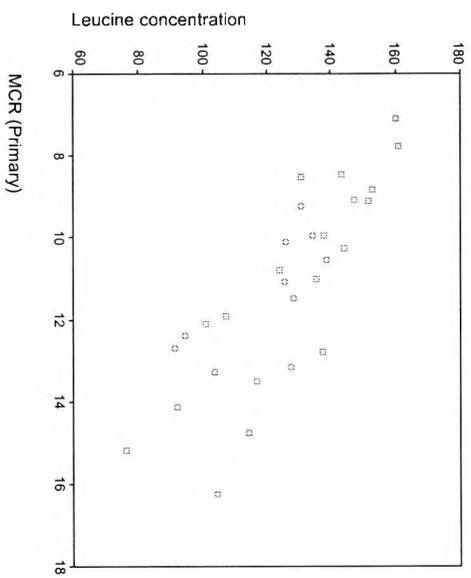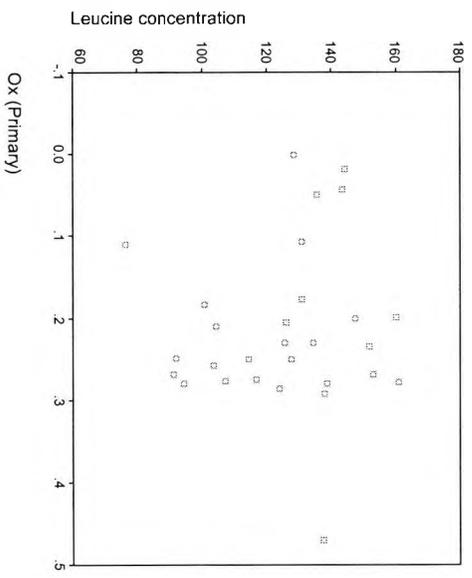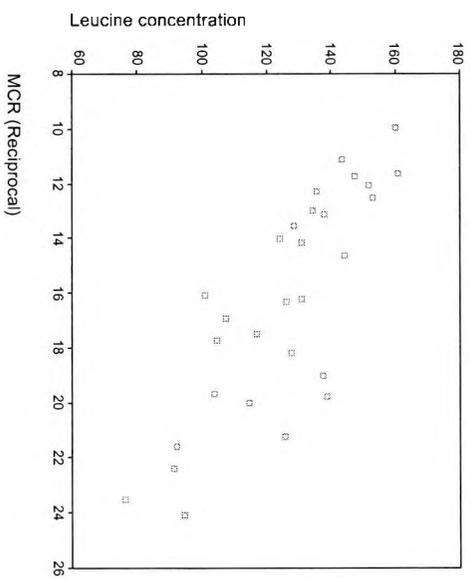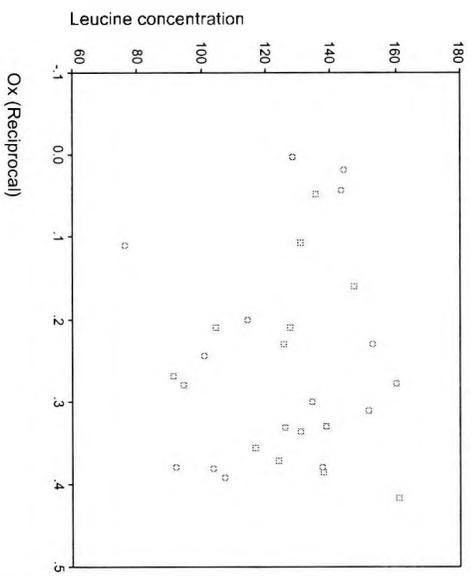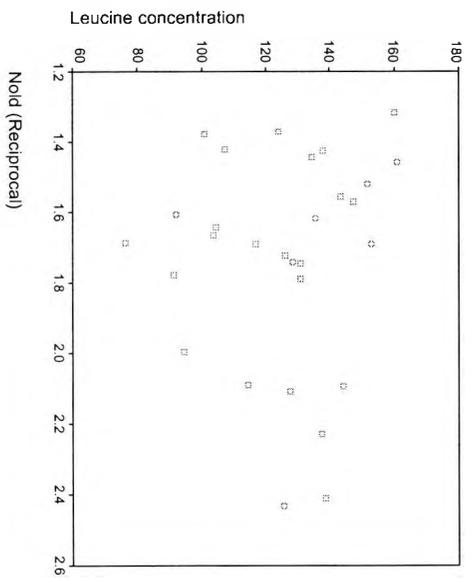
APPENDIX II   TRACER DATA CURVES, FITS AND RESIDUALS FOR CHAPTER THREE

List of Figures for Appendix II

II.1 Tracer data curves and residuals for PM0

Figure II.1: Tracer data curves for synthetic data for Subject 1 (ICM0/PM0 with CV=5%). The charts shows simulated data for [^{13}C]leucine (■), [^{13}C]KIC (◆), [^{2}H]leucine (×) and [^{2}H]KIC (●), during a constant infusion of [^{13}C]leucine and [^{2}H]KIC over 360 minutes. The curves represent the fit using model PM0. TTR (%) on *y-axis* and time (min) on *x-axis*.
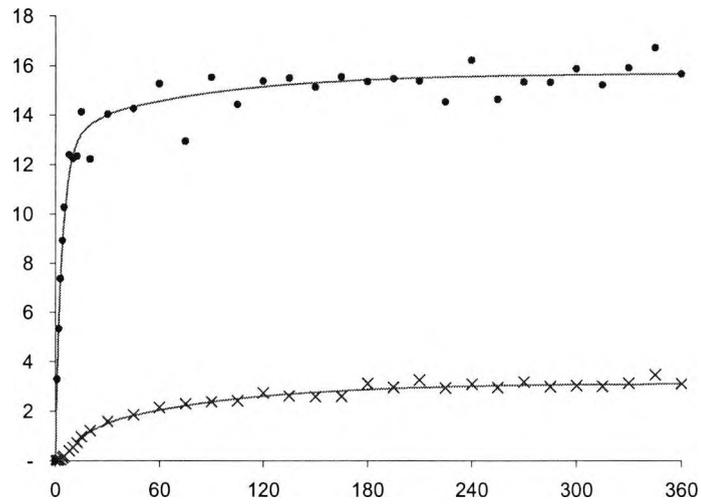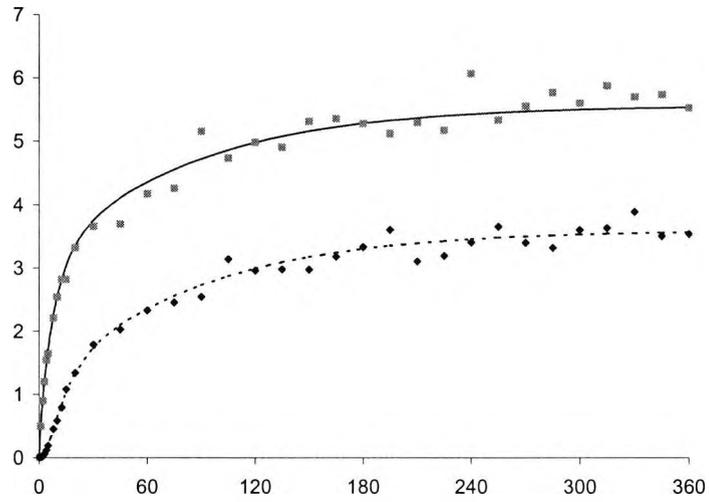
Figure II.2: Tracer data curves for synthetic data for Subject 2 (ICM0/PM0 with CV=7.5%). The charts shows simulated data for [^{13}C]leucine (■), [^{13}C]KIC (◆), [^{2}H]leucine (×) and [^{2}H]KIC (●), during a constant infusion of [^{13}C]leucine and [^{2}H]KIC over 360 minutes. The curves represent the fit using model PM0. TTR (%) on *y-axis* and time (min) on *x-axis*.
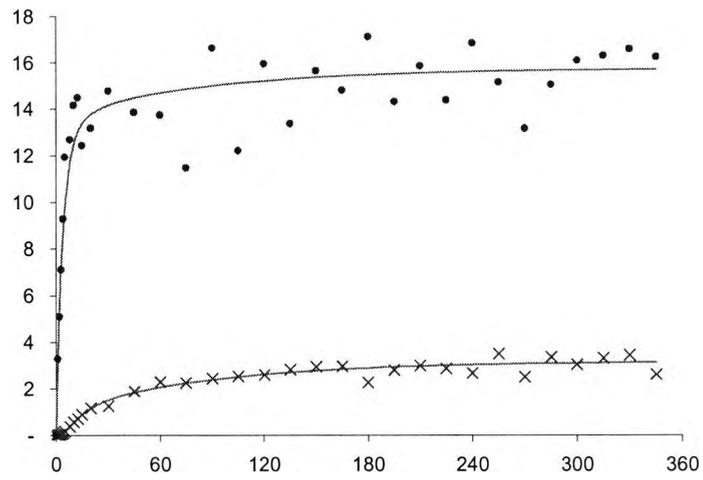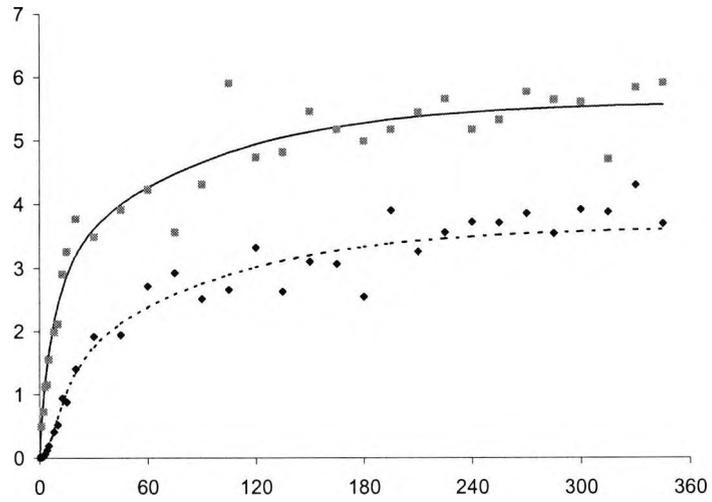
Figure II.3: Tracer data curves for synthetic data for Subject 3 (ICM0/PM0 with CV=10%). The charts shows simulated data for [^{13}C]leucine (■), [^{13}C]KIC (◆), [^{2}H]leucine (×) and [^{2}H]KIC (●), during a constant infusion of [^{13}C]leucine and [^{2}H]KIC over 360 minutes. The curves represent the fit using model PM0. TTR (%) on *y-axis* and time (min) on *x-axis*.
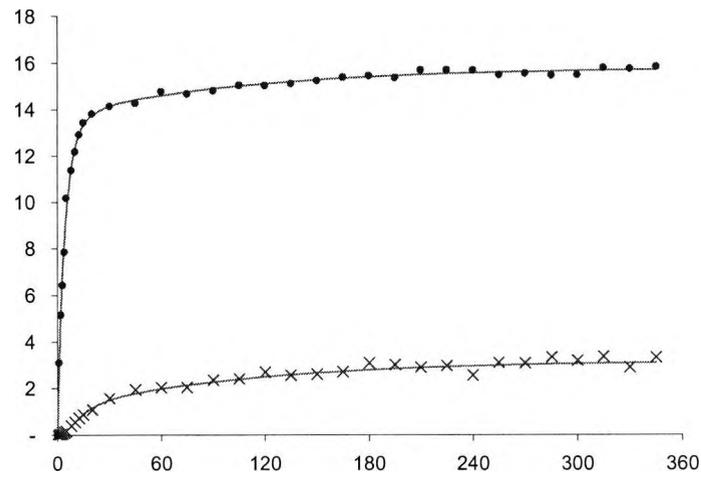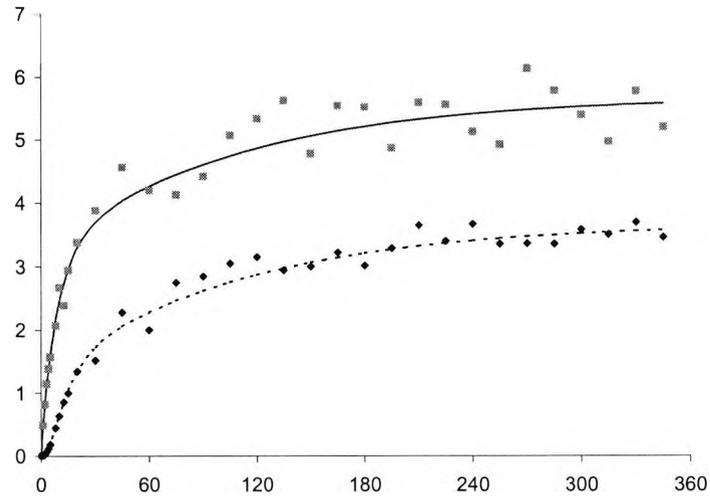
Figure II.4: Tracer data curves for synthetic data for Subject 4 (ICM0/PM0 and generated using the CV error model). The charts shows simulated data for [^{13}C]leucine (■), [^{13}C]KIC (◆), [^{2}H]leucine (×) and [^{2}H]KIC (●), during a constant infusion of [^{13}C]leucine and [^{2}H]KIC over 360 minutes. The curves represent the fit using model PM0. TTR (%) on *y-axis* and time (min) on *x-axis*.
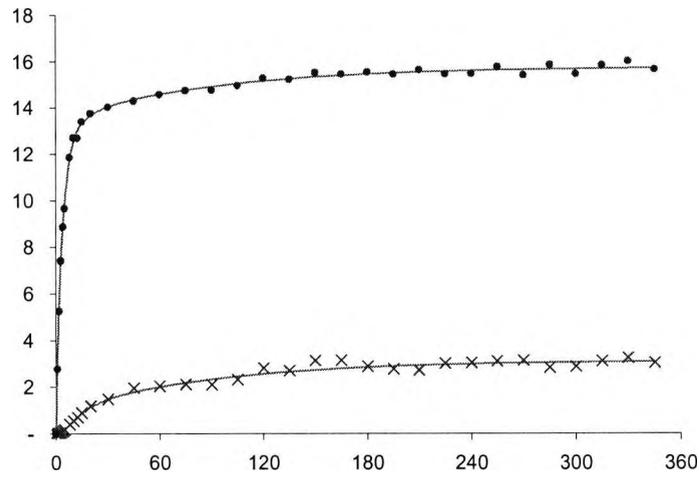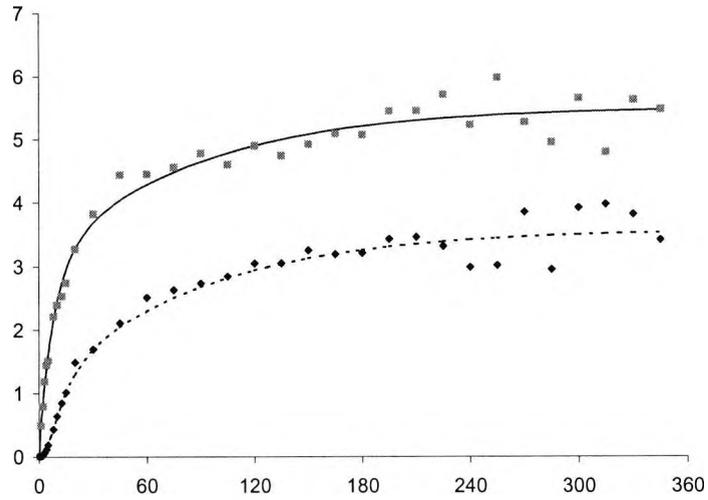
Figure II.5: Tracer data curves for synthetic data for Subject 5 (ICM0/PM0 and generated using the CV error model). The charts shows simulated data for [^{13}C]leucine (■), [^{13}C]KIC (◆), [^{2}H]leucine (×) and [^{2}H]KIC (●), during a constant infusion of [^{13}C]leucine and [^{2}H]KIC over 360 minutes. The curves represent the fit using model PM0. TTR (%) on *y-axis* and time (min) on *x-axis*.
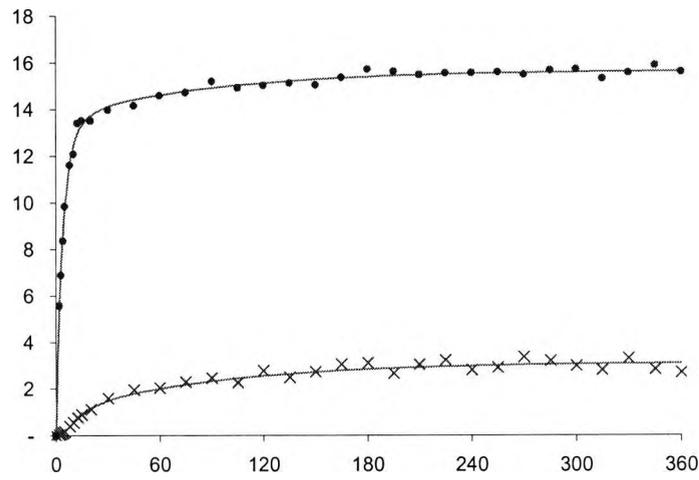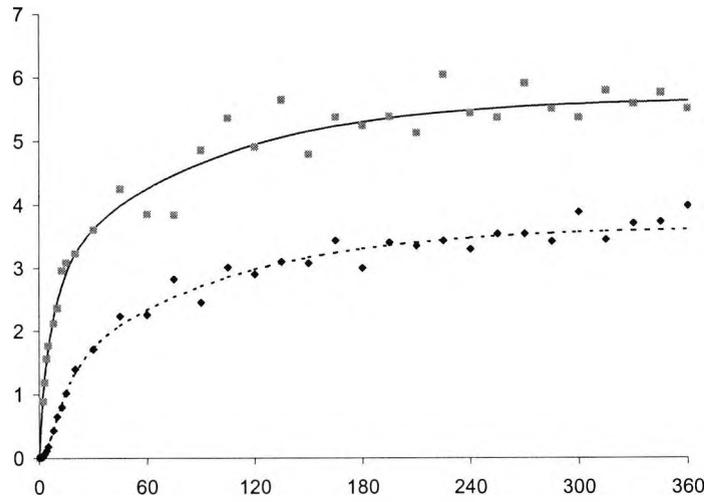
Figure II.6: Tracer data curves for synthetic data for Subject 6 (ICM0/PM0 and generated using the CV error model). The charts shows simulated data for $[^{13}C]$leucine (■), $[^{13}C]$KIC (◆), $[^2H]$leucine (×) and $[^2H]$KIC (●), during a constant infusion of $[^{13}C]$leucine and $[^2H]$KIC over 360 minutes. The curves represent the fit using model PM0. TTR (%) on *y-axis* and time (min) on *x-axis*.
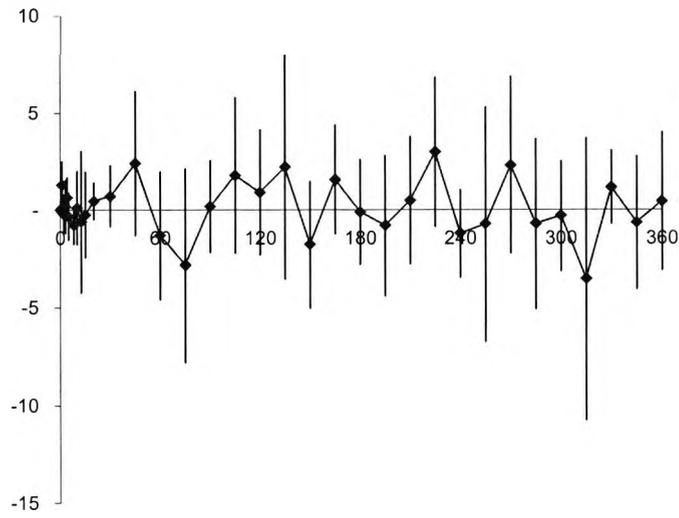
Figure II.7: Mean ± standard deviation of weighted residuals (n=6) for [¹³C]-leucine data according to Proposed Model 0.
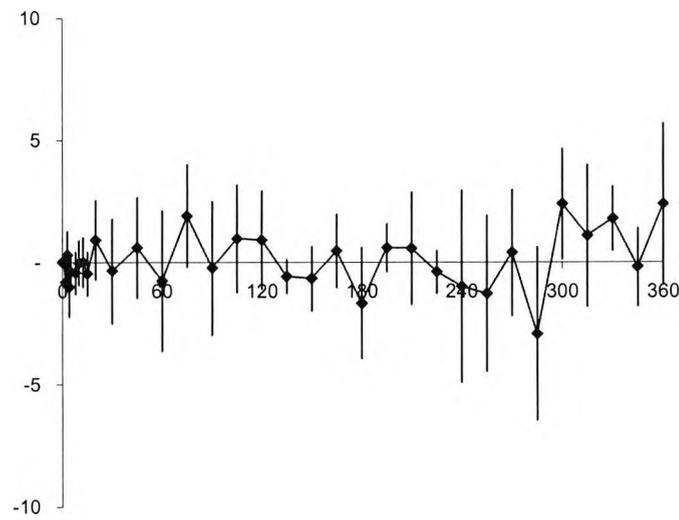
Figure II.8: Mean ± standard deviation of weighted residuals (n=6) for [¹³C]-KIC data according to Proposed Model 0.

155
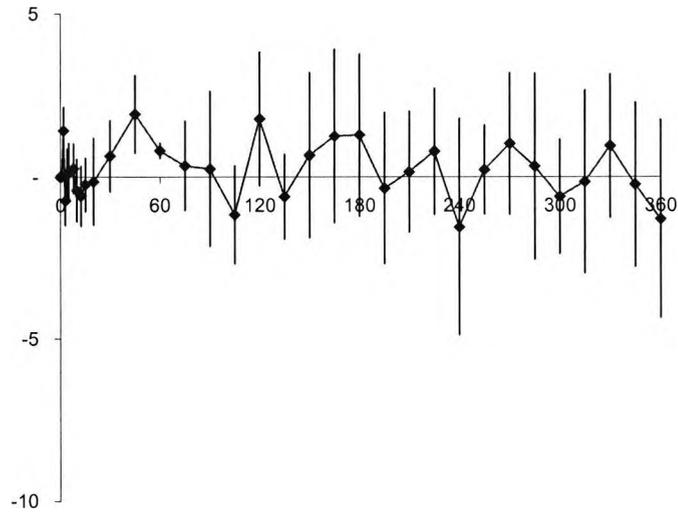
Figure II.9: Mean ± standard deviation of weighted residuals (n=6) for [^{2}H]-leucine data according to Proposed Model 0.
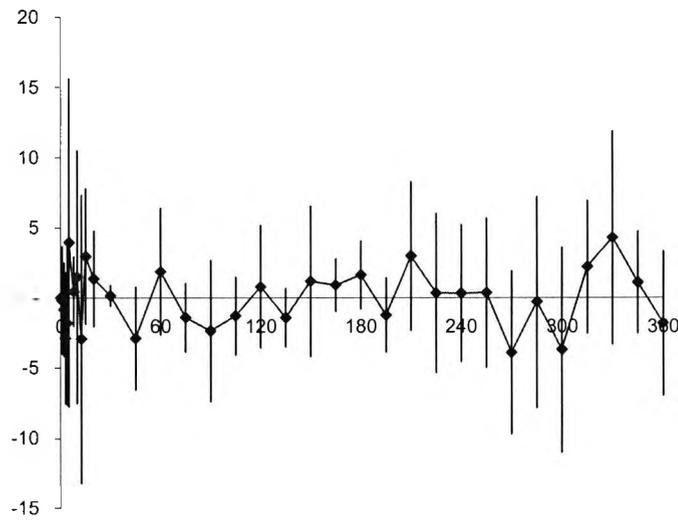
Figure II.10: Mean ± standard deviation of weighted residuals (n=6) for [^{2}H]-KIC data according to Proposed Model 0.

156

II.2 Tracer data curves and residuals for PM1
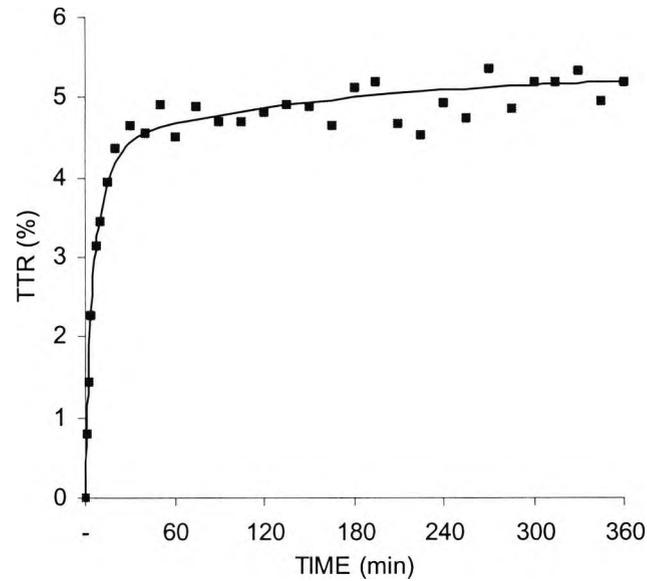
Figure II.11: Tracer data curves for synthetic data for Subject 4 (ICM1/PM1 and CV = 5%). The charts shows simulated data for $[^{15}N,^{13}C]$leucine (■) during a constant infusion of $[^{15}N,^{13}C]$leucine over 360 minutes. The curves represent the fit using model PM1
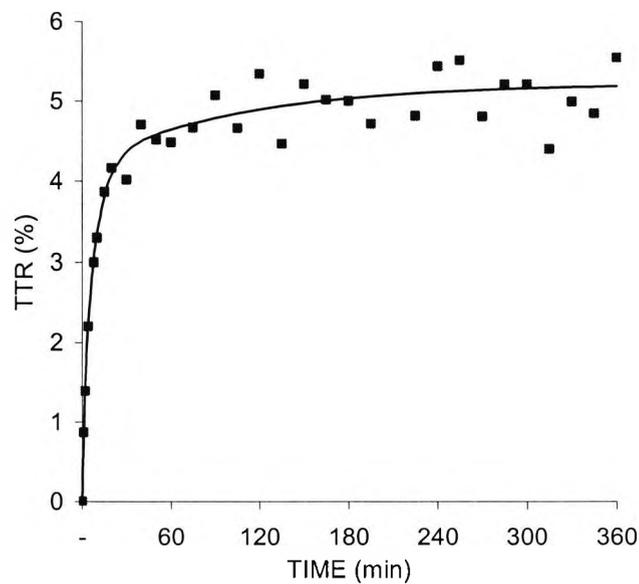

Figure II.12: Tracer data curves for synthetic data for Subject 5 (ICM1/PM1 and CV = 7.5%). The charts shows simulated data for $[^{15}N,^{13}C]$leucine (■) during a constant infusion of $[^{15}N,^{13}C]$leucine over 360 minutes. The curves represent the fit using model PM1
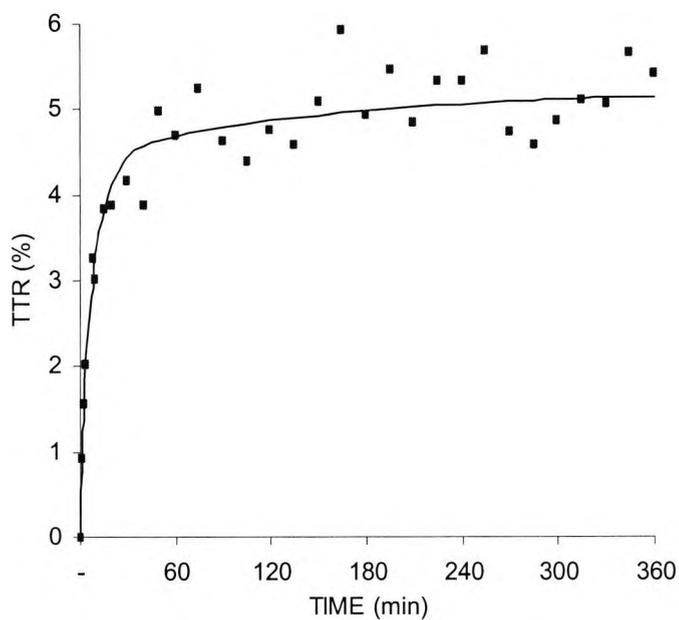
Figure II.13: Tracer data curves for synthetic data for Subject 4 (ICM1/PM1 and CV = 10%). The charts shows simulated data for [^{15}N,^{13}C]leucine (■) during a constant infusion of [^{15}N,^{13}C]leucine over 360 minutes. The curves represent the fit using model PM1
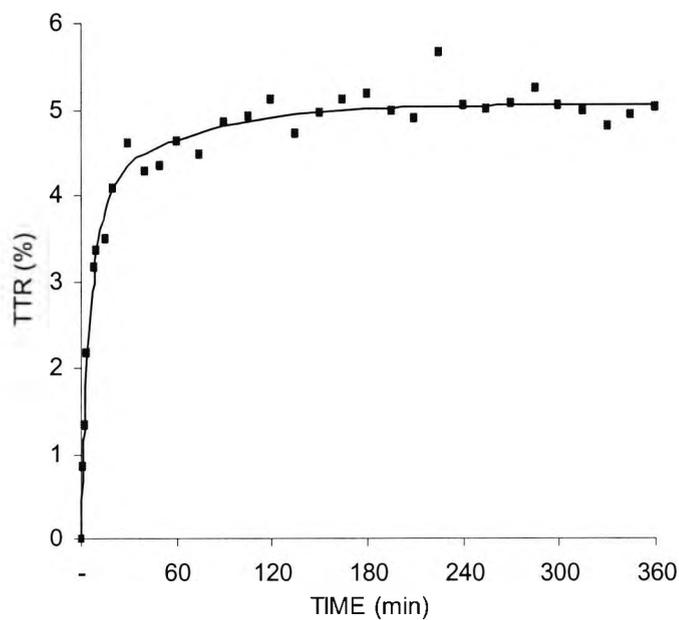
Figure II.14: Tracer data curves for synthetic data for Subject 1 (ICM1/PM1 and generated using the CV error model). The charts shows simulated data for [^{15}N,^{13}C]leucine (■) during a constant infusion of [^{15}N,^{13}C]leucine over 360 minutes. The curves represent the fit using model PM1.
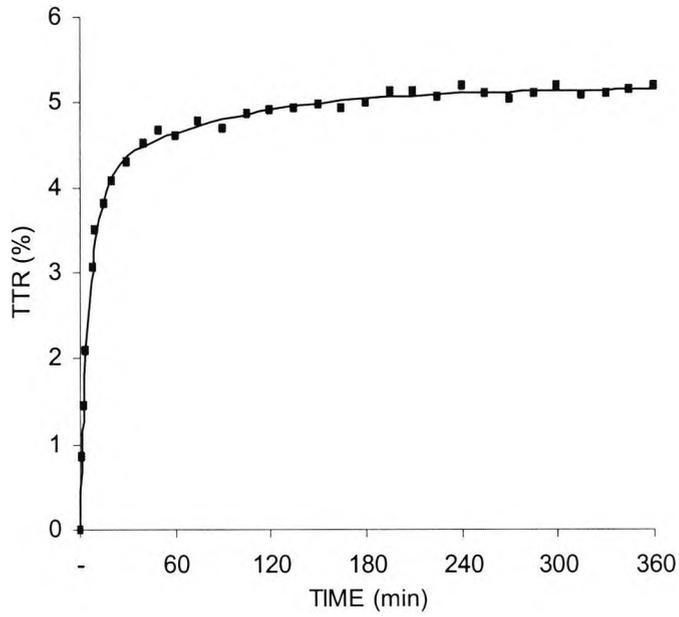
Figure II.15: Tracer data curves for synthetic data for Subject 2 (ICM1/PM1 and generated using the CV error model). The charts shows simulated data for [^{15}N,^{13}C]leucine (■) during a constant infusion of [^{15}N,^{13}C]leucine over 360 minutes. The curves represent the fit using model PM1.
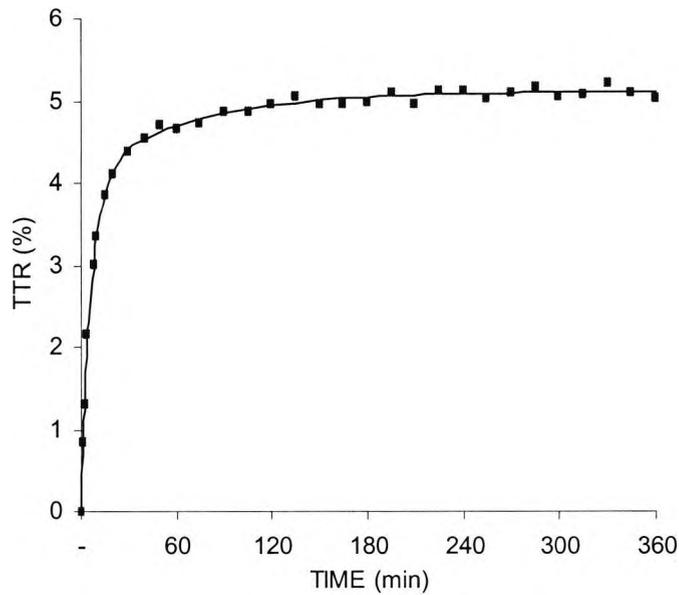

Figure II.16: Tracer data curves for synthetic data for Subject 3 (ICM1/PM1 and generated using the CV error model). The charts shows simulated data for [^{15}N,^{13}C]leucine (■) during a constant infusion of [^{15}N,^{13}C]leucine over 360 minutes. The curves represent the fit using model PM1.
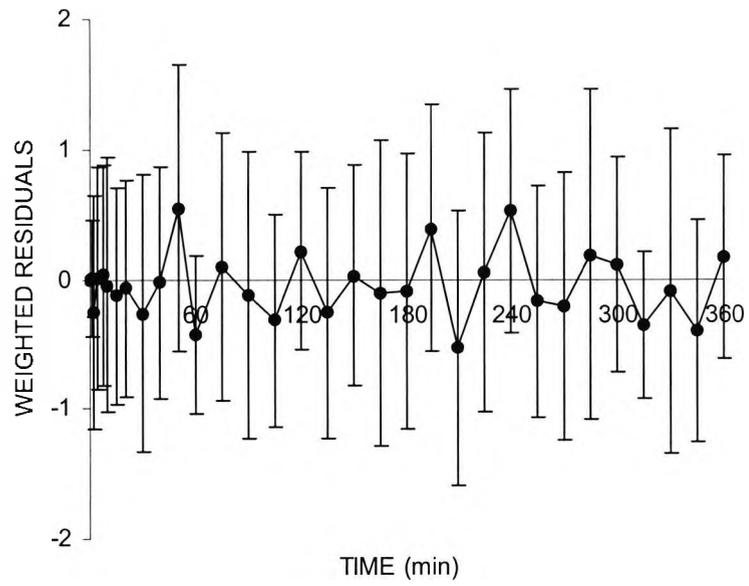
Figure II.17: Mean ± standard deviation of weighted residuals (n=6) for [^{15}N,^{13}C]leucine data according to Proposed Model 1.

II.3   Tracer data curves and residuals for PM2
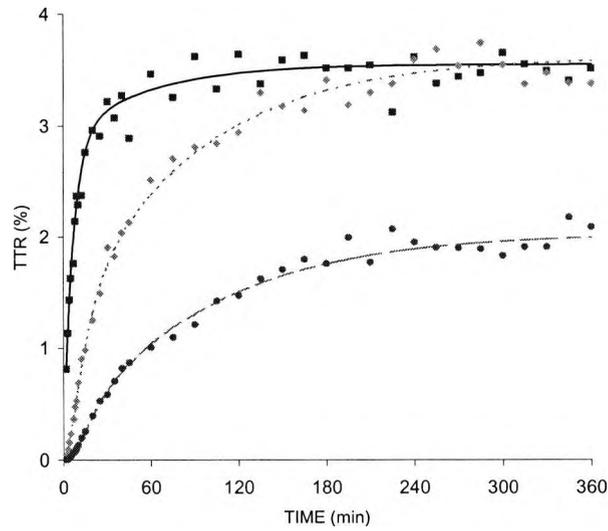
Figure II.18: Tracer data curve of synthetic data for PM1 Subject 1 (ICM1, CV = 5%). The chart shows simulated data for $[^{15}N,^{13}C]$leucine (■), $[^{13}C]$KIC (◆) and $[^{13}C]$leucine (●) during a constant infusion of $[^{15}N,^{13}C]$leucine over 360 minutes. The curves represent the fit using model PM1.
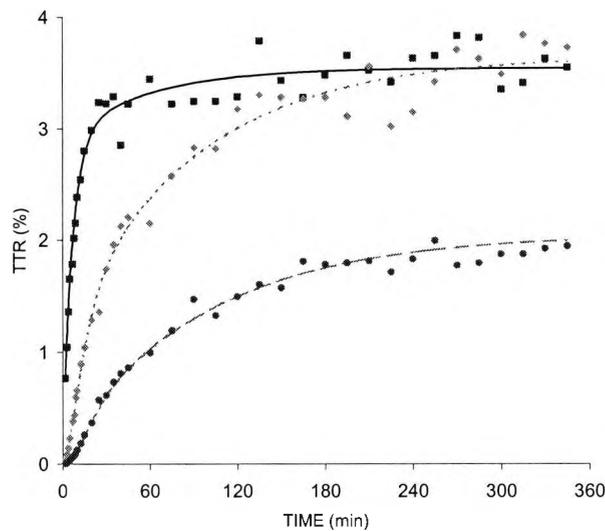
Figure II.19: Tracer data curve of synthetic data for PM1 Subject 2 (ICM1, CV = 7.5%). The chart shows simulated data for $[^{15}N,^{13}C]$leucine (■), $[^{13}C]$KIC (◆) and $[^{13}C]$leucine (●) during a constant infusion of $[^{15}N,^{13}C]$leucine over 360 minutes. The curves represent the fit using model PM1.

161
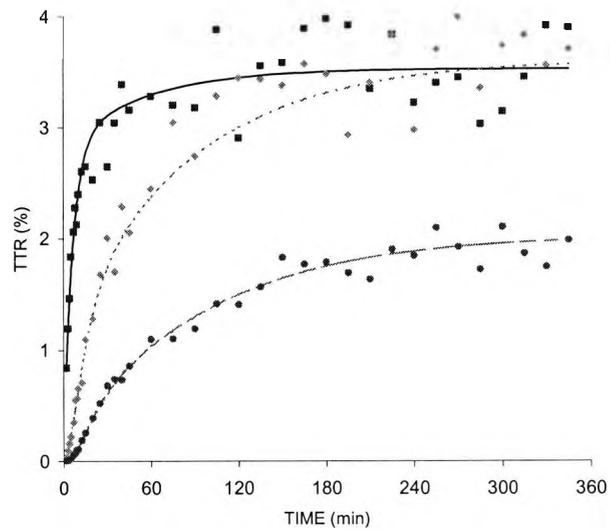
Figure II.20: Tracer data curve of synthetic data for PM1 Subject 3 (ICM1, CV = 10%). The chart shows simulated data for [^{15}N,^{13}C]leucine (■), [^{13}C]KIC (◆) and [^{13}C]leucine (●) during a constant infusion of [^{15}N,^{13}C]leucine over 360 minutes. The curves represent the fit using model PM1.
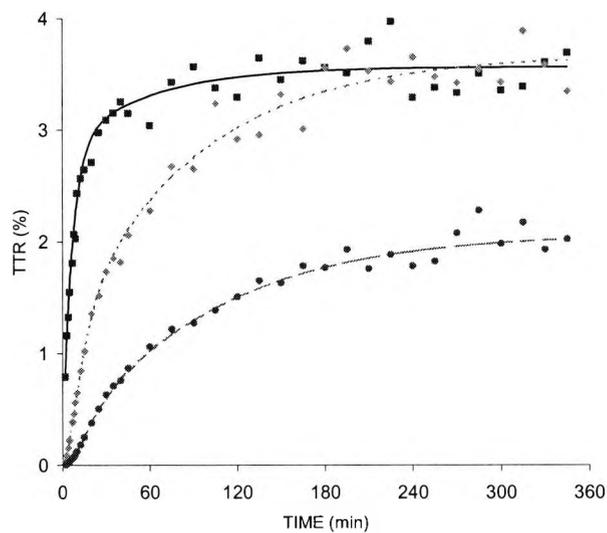
Figure II.21: Tracer data curve of synthetic data for PM1 Subject 4 (ICM1, CV based on error model). The chart shows simulated data for [^{15}N,^{13}C]leucine (■), [^{13}C]KIC (◆) and [^{13}C]leucine (●) during a constant infusion of [^{15}N,^{13}C]leucine over 360 minutes. The curves represent the fit using model PM1.
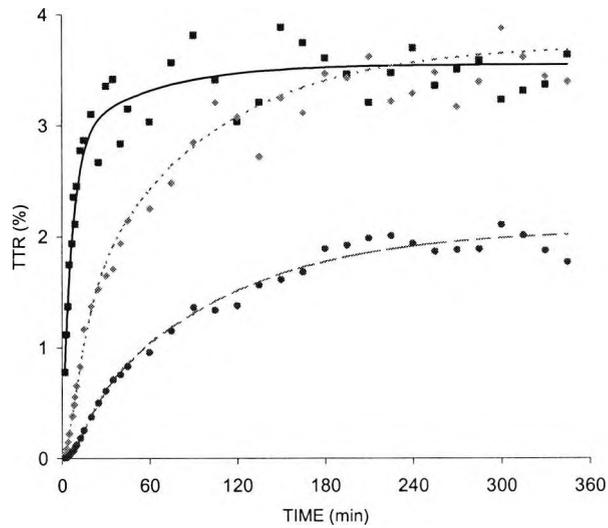
Figure II.22: Tracer data curve of synthetic data for PM1 Subject 5 (ICM1, CV based on error model). The chart shows simulated data for $[^{15}N,^{13}C]$leucine (■), $[^{13}C]$KIC (◆) and $[^{13}C]$leucine (●) during a constant infusion of $[^{15}N,^{13}C]$leucine over 360 minutes. The curves represent the fit using model PM1.
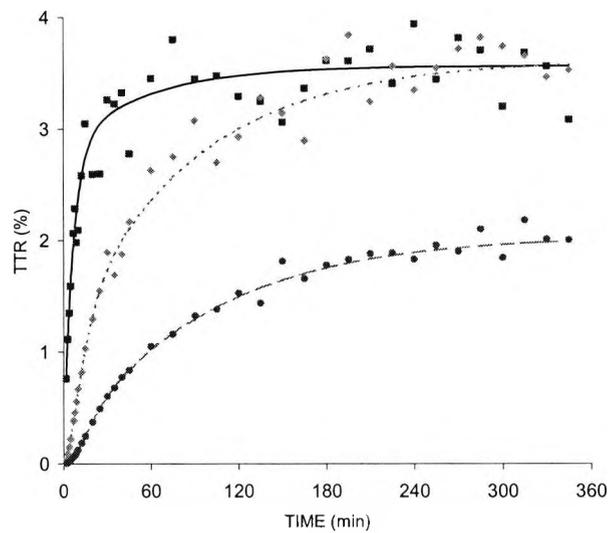
Figure II.23: Tracer data curve of synthetic data for PM1 Subject 6 (ICM1, CV based on error model). The chart shows simulated data for $[^{15}N,^{13}C]$leucine (■), $[^{13}C]$KIC (◆) and $[^{13}C]$leucine (●) during a constant infusion of $[^{15}N,^{13}C]$leucine over 360 minutes. The curves represent the fit using model PM1.
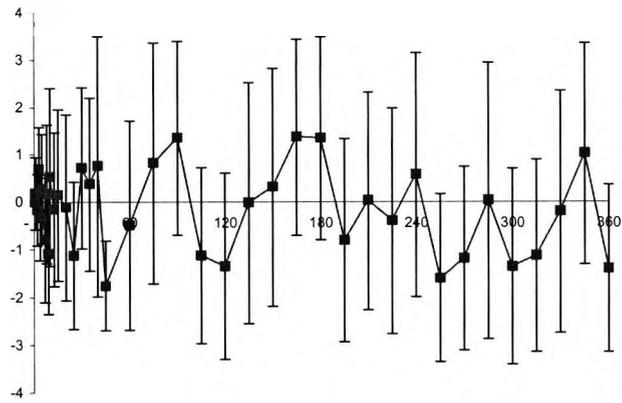
Figure II.24: Mean ± standard deviation of weighted residuals (n=6) for [^{15}N,^{13}C]leucine data according to PM2.
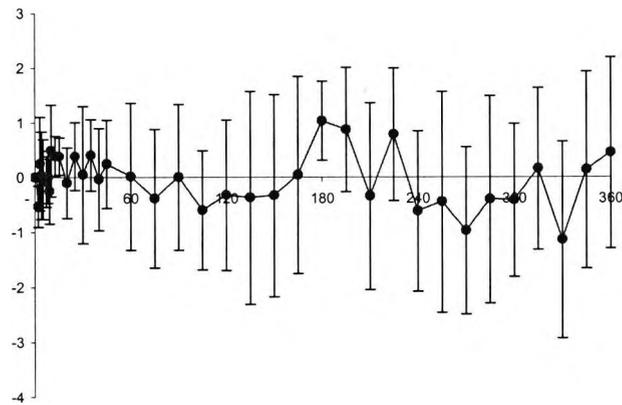
Figure II.25: Mean ± standard deviation of weighted residuals (n=6) for [^{13}C]-KIC data according to PM2.
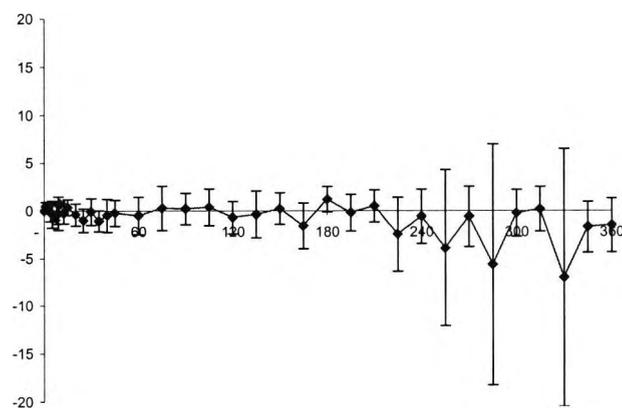
Figure II.26: Mean ± standard deviation of weighted residuals (n=6) for [^{13}C]-leucine data according to PM2.

164

APPENDIX III   ETHICS COMMITTEE FORM AND PATIENT CONSENT FORM

Lambeth, Southwark & Lewisham Health Commission
Guy's & St Thomas' Hospital Trust, St Thomas' Hospital

ETHICS COMMITTEE

1) TITLE OF PROJECT	2) STARTING DATE
The use of [^{15}N,^{13}C]leucine to study protein metabolism in healthy subjects.	June 1998

3) INVESTIGATORS

Name	Position	Dept	Phone Ext	Membership of MDU, MPS or other body
Prof. P. Sonksen		Medicine	2265	Yes
Dr. M. Umpleby		Medicine	2265	N/A
Dr. P. Carroll		Medicine	2265	Yes

4) WILL OTHER STAFF BE INVOLVED IN THE RESEARCH PROJECT?

Nursing Staff
(give particulars of involvement)

No

Social Workers
Laboratory Staff
And other Staff

No
Sample analyses
No

5) PLACES WHERE RESEARCH WILL BE DONE

Diabetic Day Centre (St Thomas' Hospital)

Are the patients to be admitted?   No

If so, is their admission part of a routine clinical admission?   N/A

If so, will this research involve an extended stay in hospital?

If so, how long will this extension of their stay be?   N/A

N/A

6) BACKGROUND OF STUDY

Knowledge about the rates of whole body protein synthesis and breakdown is important for understanding how different physiological and patho-physiological factors influence protein balance and body composition. The use of stable isotopes (non-radioactive isotopes) in the study of protein turnover is well established and a new compartmental model has been developed using ^{15}N-^{13}C leucine tracer.

Modelling leucine kinetics with commonly used tracers - [^{13}C]leucine, [^{14}C]leucine, etc. - is difficult due to the need to model the α-ketoisocaproate (KIC) sub-system. KIC metabolism is non-trivial and consists of irreversible oxidation and reversible transamination in intracellular space.

In this study we propose the use of [^{15}N,^{13}C]leucine tracer as its use can simplify the modelling of leucine metabolism. (This is because the [^{15}N,^{13}C]leucine tracer is irreversibly transaminated and so there is no recycling of [^{15}N,^{13}C]leucine tracer through the KIC sub-system). Furthermore, the use of [^{15}N,^{13}C]leucine as we suggest may also remove the need to measure expired CO_2.

Current methods of determining leucine turnover rely heavily on the modelling of KIC and CO_2, and much time and effort has gone into describing their metabolism. It is important to remember however, that the reason for these studies has always been to determine the kinetics of the amino-acid - and not to study KIC or CO_2 *per se*.

In modelling terms the kinetics of [^{15}N,^{13}C]leucine are simpler than those of traditional leucine tracers. Using simulated data we have demonstrated that a three-compartment model of [^{15}N,^{13}C]leucine allows the fractional turnover rates of a fast-turning-over protein pool to be represented and estimated.

The objective of this study is to perform experiments on normal subjects to validate findings made with simulated data.

7) AIMS OF STUDY

The aims of this experiment are:
- To further our understanding of protein metabolism.
- To develop and validate a new model for estimating fractional rates of protein synthesis and breakdown using a [^{15}N,^{13}C]leucine tracer.
- To provide an alternative method/model for determining protein turnover without relying on the KIC and/or CO_2 subsystems.

8) DESIGN OF STUDY

We plan to study healthy volunteers. Each subject be studied only once. Each study will be performed with the subject in the fasted state, with studies beginning at 9 am.

Study:
The volunteers will be weighed and a cannula will be inserted into a vein in each forearm using local anaesthetic. Baseline blood samples will be taken for measurement of leucine and KIC enrichment. A continuous intravenous infusion of ^{15}N-^{13}C leucine (0.07 µmol/kg/min) will be administered for a total of four hours through one of the cannulae. During the period of the infusion, blood and breath samples will be taken from the free cannula at 1,2,4, 6, 8, 10, 15, 20, 25, 30, 40, 50, 60, 75, 90, 110, 130, 150, 180, 210, and 240 minutes. Each sample will contain approximately 5 millilitres of blood. Breath samples will be also be taken (at the times stated above) using the Metabolic Measurement Cart (MMC) which has an open-loop system with a mouthpiece and nose clip.

9) <u>SUBJECTS</u>

Please state: 0

    a)   Number of patients to be studied   8

    b)   The number of healthy volunteers   >20 – <60

    c)   Age range   Staff, friends & family.

    d)   Method of recruitment   Pregnancy,

    e)   Exclusions   Diabetes mellitus,
    Use of medications likely to interfere with protein metabolism,

    f)   Details of any payments or other inducements to be made to the subjects

            i)   Expenses   NONE

            ii)   Rewards   NONE

    g)   Are medical students to be involved? (The Head of the appropriate Institute must be notified of those involved).

NO

10) DETAILS OF PROCEDURES

A. Drugs

Name	Formulation	Dose/Frequency of Administration	Route	Legal Status (CTC, CTZ, Product Licence)

NONE

What adverse effects are expected of these drugs?

N/A

Are there any possible serious risks or dangers associated with their use?
(Append details if space is insufficient)

N/A

B. Isotopes

Details of any isotopes to be used including dose, frequency and route

$^{15}N-^{13}C$ leucine 0.07 μmol/kg/min for 4 hours administered IV

- Has advice of the Radiation Protection Officer been sought?   Stable Isotope
- Has the applicant a DHSS Licence for this purpose?   N/A
- Specify a routine investigation of equivalent radiation exposure

C. Other additional investigations, substances or agents required for the research

D. Questionnaires

(Please enclose 16 copies of any questionnaire to be used)

Are the questionnaires to be filled in by the subject or administered by someone else?

If so, by whom, and by what method (e.g. postal)

What published evidence is there of validation of questionnaire design?

11) PHARMACEUTICAL COMPANY INNVOLVEMENT

Does the project involve participation or sponsorship by a pharmaceutical company

NO

If so, has the company signified its acceptance of the guidelines provided by the Committee for such projects?

N/A

If so, what kind of financial support will be provided by the pharmaceutical company (if any)?

N/A

12) WHAT ASPECT OF THE PROCEDURES DESCRIBED ARE NOT PART OF ROUTINE CARE?

Isotope studies are a research tool and not part of routine care

13) THE HEALTH AND COMFORT OF SUBJECTS

Will there be any risk of damage to health of the subjects, or of any pain, discomfort, distress or inconvenience?   No
If so, please give an assessment of the seriousness of any possible damage to health, and of any pain, discomfort, etc., and of the degree of risk.

No serious risk or discomfort is identifiable

14) <u>CONSENT</u>

    a) <u>Explanation</u>

       Will the subjects be given an oral, a written , or no explanation of the research? Written

       (If written explanation is to be given, 16 copies must be submitted with this application).

       If no explanation is to be given, please justify.

    b) <u>Consent Form</u> (Available from Acute Unit Administration)

       Is the standard research consent from to be used?
       If not, justify this departure and submit 16 copies of the substitute form which is to be used.

15) <u>INFORMATION TO THE G.P.</u>

    Will the General Practitioner be informed?   No
    If so, how?
    If not, justify:

    The subjects are healthy controls and the methods proposed are known to be safe.

16) <u>COSTS</u>

    Have any arrangements been made to defray the costs of the research to the District?

                                              N/A

17) <u>WHAT ARE THE ETHICAL PROBLEMS WHICH APPEAR TO THE APPLICANTS FROM THIS APPLICATION</u>

    There are no identifiable ethical difficulties, the tools being used here are established and safe techniques.

SIGNATURE OF INVESTIGATORS   **DATE**

                                            DATE

SIGNATURE OF HEAD OF DEPARTMENT

Lambeth, Southwark & Lewisham Health Commission
Guy's & St Thomas' Hospital Trust, St Thomas' Hospital

Consent Form For Participation In Research Projects & Clinical Trials

Title of Project: The use of $[^{15}N,^{13}C]$leucine tracer to study protein metabolism in healthy subjects.

Principal Investigator: Prof. Sonksen

Other Investigator/s: Dr. P. Carroll
　　　　　　　　　　Dr. M. Umpleby

Enrolling Patients:

Ethics Committee Code No:

Outline explanation:

We are inviting you to participate in a clinical experiment exploring how quickly protein is metabolised in the human body. To do this we use labelled amino acids – the building blocks of protein. By taking blood samples we are able to track the movement of labelled amino acids and calculate protein metabolism in the body. These labelled amino acids are not radioactive.

We will ask you to attend the Diabetic Day Centre on one occasion. It is important that you come fasting on the day of the experiment. For the experiment it is required that you do not have anything to eat after 12:00 midnight the day before the experiment, although you may continue to drink black tea, coffee (without sugar) or water.

When you arrive we will weigh you accurately and once comfortable we will place small cannulae in a vein in each forearm (using local anaesthetic). A cannula is a small tube which is inserted into the body to allow fluid to enter or escape. Through one of the cannulae, we will infuse the labelled amino acid, and through the other we will take blood samples. There will be about 30-35 blood samples taken, each sample will be about 5 ml (5 ml = 1 teaspoon), the total amount of blood taken will be less than a cupful. We also need to measure breath samples, for this purpose you will be asked to breathe into a small bag, this procedure will be similar to blowing up a very small balloon.

The experiment will last for a period of up to six hours, after which you will be given a meal. All records of this study will remain confidential. You may withdraw from the study at any time and this will not affect any future care or treatment.

I (name)　　_____

of (address)　_____

　　　　　　_____

hereby consent to take part in the above investigation, the nature and purpose of which have been explained to me. Any questions I wished to ask have been answered to my satisfaction. I understand that I may withdraw from the investigation at any stage without necessarily giving a reason for doing so and that this will in no way affect the care I receive as a patient

SIGNED (Volunteer)　_____　Date _____

(Doctor)　_____　Date _____

(witness, where appropriate)　_____　Date _____

APPENDIX IV   TRACER TO TRACEE RATIO CALCULATIONS

IV.1 Calculating [^{15}N,^{13}C]-leucine and [^{13}C]-leucine tracer to tracee ratios

Tracer-to-tracee ratio (TTR) was calculated from the isotope (area) ratio, employing the method given by Rosenblatt et al (43).

Let:

r_N denote the raw measurement isotope ratio $M+2/M+0$ in the mixture of tracer and tracee.

r_C denote the raw measurement isotope ratio $M+1/M+0$ in the mixture of tracer and tracee.

T_I is the proportion of molecules of rounded molecular weight (RMW) $M+i$ in the mixture.

L_i is proportion of molecules of RMW $M+i$ in the endogenous leucine, n is the total number of molecules in the mixture.

N_i is the proportion of molecules of RMW $M+i$ in the [^{15}N,^{13}C]-leucine tracer;

C_i is the proportion of molecules of RMW $M+i$ in the [^{13}C]-leucine tracer species.

n_N is the number of molecules in the mixture originating from [^{15}N,^{13}C]-leucine.

n_C is the number of molecules in the mixture originating from [^{13}C]-leucine.

n_L is the number of molecules in the mixture originating from endogenous leucine.

n is the total number of molecules in the mixture.

r_{NB} is the measured peak ratio $M+2/M+0$ in the baseline, i.e. the ratio of the most abundant isotopomer in [^{15}N,^{13}C]-leucine to the most abundant isotopomer in the endogenous leucine in the basal sample.

r_{CB} is the measured peak ratio $M+1/M+0$ in basal sample i.e. the ratio of the most abundant isotopomer [^{13}C]-leucine to the most abundant isotopomer in the endogenous leucine in the basal sample.

z_N is the tracer to tracee ratio for $[^{15}\text{N},^{13}\text{C}]$-leucine, i.e., the ratio of the mass of $[^{15}\text{N},^{13}\text{C}]$-leucine to the mass endogenous leucine

z_C is the tracer to tracee ratio for $[^{13}\text{C}]$-leucine, i.e., the ratio of the mass of $[^{13}\text{C}]$-leucine to the mass endogenous leucine

From the definitions above we may write an expression for the measured peak ratio (r_N) found in the sample. We can write an expression for r_N which accounts for M+2 isotopmers coming from either $[^{15}\text{N},^{13}\text{C}]$-leucine ($N_2$), $[^{13}\text{C}]$-leucine (C_2), or endogenous leucine (L_2).

$$r_N = \frac{T_2}{T_0} = \frac{T_2.n}{T_0.n} = \frac{n_N N_2 + n_C C_2 + n_L L_2}{n_N N_0 + n_C C_0 + n_L L_0}$$

Dividing through by $n_L.L_0$ gives

$$r_N = \frac{\dfrac{L_2}{L_0} + \dfrac{n_N}{n_L}\dfrac{N_2}{L_0} + \dfrac{n_C}{n_L}\dfrac{C_2}{L_0}}{1 + \dfrac{n_N}{n_L}\dfrac{N_0}{L_0} + \dfrac{n_C}{n_L}\dfrac{C_0}{L_0}}$$

And by definition we may write expressions for z_N, z_C, r_{NB} and r_{CB}

$$z_N = \frac{n_N}{n_L}$$

$$z_C = \frac{n_C}{n_L}$$

$$r_{NB} = \frac{L_2}{L_0}$$

$$r_{CB} = \frac{L_1}{L_0}$$

Substituting for z_N, z_C, r_{NB} and r_{CB}

$$r_N = \frac{r_{NB} + z_N \dfrac{N_2}{L_0} + z_C \dfrac{C_2}{L_0}}{1 + z_N \dfrac{N_0}{L_0} + z_C \dfrac{C_0}{L_0}} \qquad \text{[A1]}$$

Using similar derivations to those for Equation 1, an expression for the raw measurement (isotope ratio) r_C can be written as:

$$r_C = \frac{r_{CB} + z_C \dfrac{C_1}{L_0} + z_N \dfrac{N_1}{L_0}}{1 + z_C \dfrac{C_0}{L_0} + z_N \dfrac{N_0}{L_0}} \qquad \text{[A2]}$$

Solving Equations A1 and A2 for z_N and z_C, we obtain that

$$z_C = \frac{(r_{NB} - r_N)(r_C \dfrac{N_0}{L_0} - \dfrac{N_1}{L_0}) + (r_{CB} - r_C)(\dfrac{N_2}{L_0} - r_D \dfrac{N_0}{L_0})}{(r_D \dfrac{C_0}{L_0} - \dfrac{C_2}{L_0})(r_C \dfrac{N_0}{L_0} - \dfrac{N_1}{L_0}) - (\dfrac{C_1}{L_0} - r_C \dfrac{C_0}{L_0})(\dfrac{N_2}{L_0} - r_N \dfrac{N_0}{L_0})} \qquad \text{[A3]}$$

and

$$z_N = \frac{(r_{CB} - r_C)(r_D \dfrac{C_0}{L_0} - \dfrac{C_2}{L_0}) + (r_{NB} - r_N)(\dfrac{C_1}{L_0} - r_C \dfrac{C_0}{L_0})}{(r_C \dfrac{D_0}{L_0} - \dfrac{D_1}{L_0})(r_D \dfrac{C_0}{L_0} - \dfrac{C_2}{L_0}) - (\dfrac{N_2}{L_0} - r_D \dfrac{N_0}{L_0})(\dfrac{C_1}{L_0} - r_C \dfrac{C_0}{L_0})} \qquad \text{[A4]}$$

Values N_i, C_i, and L_i, were calculated from the natural abundance of atoms in the monitored fragment C_{14},H_{32},Si_2,N,O_2 (M=300) employing knowledge of the atomic purity of the infusates, [^{15}N,^{13}C] leucine infusate and the internal APE=99%. The values used were (in %) $L_0 = 77.8764$, $C_0 = 0.7309$, $C_1 = 72.5398$, $C_2 = 18.2587$, $N_0 = 0.0073$, $N_1 = 1.4543$, $N_2 = 72.2576$; these were used to calculate z_N and z^C from the measured isotope ratios r_N, r_C, r_{NB} and r_{CB}.

IV.2   Calculating [^{13}C]-KIC tracer to tracee ratios

We can employ very similar reasoning for determining the TTR for [13C]-KIC from mass spectrometry peak ratio data.

Let:

r_K denote the raw measurement isotope ratio $M+1/M+0$ in the mixture of tracer and tracee.

r_D denote the raw measurement isotope ratio $M+3/M+0$ in the mixture of tracer and tracee.

S_i is the proportion of molecules of rounded molecular weight (RMW) $M+i$ in the mixture.

A_i is proportion of molecules of RMW $M+i$ in the endogenous KIC.

K_i is the proportion of molecules of RMW $M+i$ in the [^{13}C]-KIC tracer.

D_i is the proportion of molecules of RMW $M+i$ in the [^{3}D]-KIC tracer species.

n is the total number of molecules in the mixture.

n_K is the number of molecules in the mixture originating from [^{13}C]-KIC.

n_D is the number of molecules in the mixture originating from [^{3}D]-KIC.

n_A is the number of molecules in the mixture originating from endogenous leucine;

r_{KB} is the measured peak ratio $M+1/M+0$ in the baseline, i.e. the ratio of the most abundant isotopomer in [^{13}C]-KIC to the most abundant isotopomer in the endogenous KIC in the basal sample.

r_{DB} is the measured peak ratio $M+3/M+0$ in basal sample i.e. the ratio of the most abundant isotopomer [^{3}D]-KIC to the most abundant isotopomer in the endogenous KIC in the basal sample.

z_K is the tracer to tracee ratio for [^{13}C]-KIC, i.e., the ratio of the mass of [^{13}C]-KIC tracer to the mass endogenous KIC.

z_D is the tracer to tracee ratio for [^{13}C]-leucine, i.e., the ratio of the mass of [^{3}D]-KIC to the mass endogenous KIC

Following the reasoning as for the $[^{15}N,^{13}C]$leucine tracer we may write expressions for z_K and z_C:

$$z_C = \frac{(r_{DB} - r_D)(r_K \frac{D_0}{A_0} - \frac{D_1}{A_0}) + (r_{KB} - r_K)(\frac{D_3}{A_0} - r_D \frac{D_0}{A_0})}{(r_D \frac{K_0}{A_0} - \frac{K_3}{A_0})(r_K \frac{D_0}{A_0} - \frac{D_1}{A_0}) - (\frac{K_1}{A_0} - r_K \frac{K_0}{A_0})(\frac{D_3}{A_0} - r_D \frac{D_0}{A_0})}$$

and

$$z_D = \frac{(r_{KB} - r_K)(r_D \frac{K_0}{A_0} - \frac{K_3}{A_0}) + (r_{DB} - r_D)(\frac{K_1}{A_0} - r_K \frac{K_0}{A_0})}{(r_D \frac{K_0}{A_0} - \frac{K_3}{A_0})(r_K \frac{D_0}{A_0} - \frac{D_1}{A_0}) - (\frac{K_1}{A_0} - r_K \frac{K_0}{A_0})(\frac{D_3}{A_0} - r_D \frac{D_0}{A_0})}$$

Values D_i, K_i and A_i, were calculated from the natural abundance of atoms in the monitored fragment $C_{14}N_2OSiH_{19}$ (M=259) employing knowledge of the atomic purity of the infusates; $[^{15}N,^{13}C]$leucine infusate and the internal standard ^3D-KIC, were 99% and 98% respectively. The values used were (in %) A_0 = 77.8764, K_0 = 0.7875, K_1 = 78.1265, K_3 = 4.2901, D_0 = 0.0001, D_1 = 0.0232, D_3 = 76.0988; these were used to calculate z_D and z_K from the measured isotope ratios r_C, r_D, r_{CB} and r_{DB}.

APPENDIX V PUBLICATIONS

V.1   Gowrie, I.J., Roudsari, A.V., Umpleby, A.M. and Hovorka, R. (1999) Estimating protein turnover with a [N-15,C-13]leucine tracer: a study using simulated data. *Journal Of Theoretical Biology* 198, 165-172.

Estimating Protein Turnover with a [15N,13C]Leucine Tracer: a Study Using Simulated Data

Ian J. Gowrie*, Abdul V. Roudsari*, A. Margot Umpleby† and
Roman Hovorka*‡

Centre for Measurement and Information in Medicine, City University, Northampton Square, London EC1V 0HB, U.K. and †Department of Endocrinology, St Thomas' Hospital, London SE1 7EH, U.K.

We explore the use of [15N,13C]leucine tracer to estimate whole-body fractional rates of a fast-turning-over protein pool employing synthetic data. The kinetics of [15N,13C]leucine tracer are simplified compared with those of traditional leucine tracers and benefit from irreversible transamination to [13C]α-ketoisocaproaic acid (KIC) resulting in a simplified model structure. A three-compartment model of [15N,13C]leucine kinetics was proposed and evaluated using data generated by a Reference Model (based on a model by Cobelli *et al.*). The results suggest that fractional turnover rates of a fast-turning-over protein pool can be estimated with low but acceptable precision during a six-hour constant intravenous infusion of [15N,13C]leucine with frequent sampling of plasma tracer-to-tracee ratio (TTR) of [15N,13C]leucine. We conclude that [15N,13C]leucine may be useful for the measurement of protein kinetics and its full potential should be explored in clinical studies with compartmental data analysis.

© 1999 Academic Press

Introduction

Several practical requirements and ethical constraints hinder investigators wishing to introduce new methods to study the pathophysiology of metabolic disorders and metabolic systems in man. In particular such methods must provide unambiguous identification of both known and potentially new metabolites. In addition, these methods must not only be able to precisely quantify metabolite concentrations in various body fluids, but also have the ability to measure the movement of these materials along biochemical pathways within cells and between organs. Furthermore, investigational studies should be non-invasive or nearly so, and sampling should be kept to a minimum as sample volumes are generally limited (Bier, 1997). The only certain way to test a new method (against the criteria outlined above) is through clinical evaluation. However, clinical evaluation requires ethical considerations and is costly, utilising expensive materials and man-hours. On the contrary, computer simulation studies do not require ethical approval or expensive materials. In this paper we have used simulation techniques to aid in validating our new method, in effect justifying the use of this method in a clinical setting.

Quantifying rates of whole-body protein synthesis and breakdown (i.e. protein turnover)

‡Author to whom correspondence should be addressed.
E-mail: r.hovorka@city.ac.uk

in man is fundamentally difficult, and several approaches have been developed to determine these rates (Bier, 1989; Bier & Matthews, 1982; Young, 1987). In essence, protein-turnover has been determined either from (a) the turnover of the entire free amino acid pool or (b) the kinetics of an essential amino acid. Assessing the turnover of the entire free amino acid pool is based upon the administration of a [^{15}N]labelled amino acid (almost always [^{15}N]glycine) and the measurement of the dilution of the tracer in the free amino acid pool by sampling an end-product of protein metabolism such as ammonia or urea. The advantages, problems and indeed limitations associated with the end-product method have been extensively discussed (Bier & Matthews, 1982; Young, 1987; Bier, 1989).

Waterlow (1967) originally proposed a compartmental model to describe the kinetics of an essential amino acid, initially using a lysine tracer. O'Keefe *et al.* (1974) was the first to use this model for a leucine tracer. In hindsight, the model seems over simplistic, for instance, it contains only a single pool for leucine and a single pool for protein. It has been established that there are at least two leucine pools (intra- and extra-cellular) and several hundred proteins each with their own metabolic pathways. To overcome some of the shortcomings of the Waterlow/O'Keefe model, two models were proposed in the 1980s and they have long dominated the study of leucine kinetics, the so-called primary and reciprocal models (Matthews *et al.*, 1982; Wolfe *et al.*, 1982; Schwenk *et al.*, 1985). Both models are based on infusing labelled tracer over a few hours and then analysing the resulting isotopic plateau. These two models represent the only tools available to assess *in vivo* leucine kinetics using tracer studies excluding the less frequently used arterio-venous balance technique (Tessari *et al.*, 1995) and the bolus injection method (Umpleby *et al.*, 1986).

Cobelli and co-workers (Saccomani *et al.*, 1989; Cobelli *et al.*, 1991; Matthews & Cobelli, 1991; Saccomani & Cobelli, 1993) have formulated an alternative model and have questioned the validity of the primary and reciprocal models (Cobelli & Saccomani, 1991). They propose a seven-compartment model which involves the infusion of two tracers, [^{13}C]leucine and [^{2}H]α-ke-toisocaproate (KIC). Using this model and frequent sampling it was possible to estimate fractional turnover rates for protein synthesis and breakdown with precision (Cobelli *et al.*, 1991).

The widespread use of the primary and reciprocal models over the last decade has seen carbon labelled tracers—[^{13}C]leucine, [^{13}C]KIC— dominate the study of leucine kinetics. They are not, however, the only tracers available in the investigation of leucine metabolism. Others (Matthews *et al.*, 1981; Cheng *et al.*, 1985; Thompson *et al.*, 1988) have successfully used [^{15}N,^{13}C]leucine in clinical investigation, and more recently Tessari *et al.* (1995) have explored skeletal–muscle leucine kinetics using [^{15}N]leucine in conjunction with a [^{13}C]leucine tracer.

In this paper we explore the use of [^{15}N,^{13}C]leucine tracer to quantify protein turnover, in particular to estimate not only leucine fluxes to and from the whole-body protein pool, but also to estimate the fractional turnover rates of protein metabolism. A model proposed by Cobelli *et al.* (1991) was employed to simulate experimental data and a new compartmental model was evaluated.

Model Development

CONCEPTUAL MODEL OF LEUCINE KINETICS

A conceptual model describing leucine kinetics during fasting conditions, including two pools for leucine (extra- and intra-cellular), two pools for KIC (extra- and intra-cellular) and a single pool for fast-turning-over proteins is shown in Fig. 1. Leucine is an essential amino acid and is thus not synthesised *de novo*; within intracellular space, leucine may be incorporated into protein (protein synthesis) or it may be oxidised. Leucine is in constant flux with its keto-acid, KIC through a reversible transamination process (Taylor & Jenkins, 1966). During transamination, the amino group (NH_2) is lost to the nitrogen pool. The resulting KIC has two fates, it may be re-aminated to form leucine, or it may undergo an irreversible decarboxylation to CO_2. Both leucine and KIC are transported across the cell membrane into the extracellular fluid by a
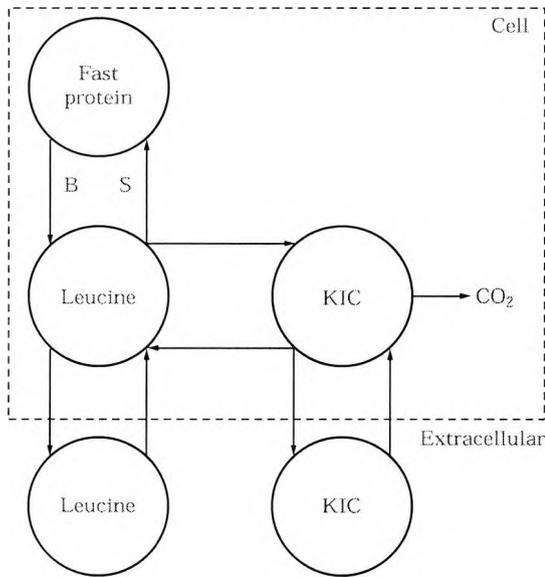
FIG. 1. Whole-body leucine kinetics under fasting conditions. Protein breakdown is denoted by B and synthesis by S.

facilitated transport system (Christensen, 1990). Leucine enters the system from protein breakdown. Here we consider only fast-turning-over proteins, as the breakdown and synthesis of slow-turning-over proteins over the experimental period are assumed negligible in comparison with that of fast-turning-over proteins (Fig. 1).

KINETICS OF [^{15}N,^{13}C]LEUCINE

The di-labelled [^{15}N,^{13}C]leucine tracer is valuable to the study of protein metabolism because it is not reversibly transaminated to KIC. During de-amination of [^{15}N,^{13}C]leucine, the ^{15}N label is lost to the nitrogen pool resulting in the production of [^{13}C]KIC. The chance of a ^{15}NH$_2$

group being attached to [^{13}C]KIC instead of a ^{14}NH$_2$ during re-amination is negligible given the very small size of [^{15}N]body-pool compared with [^{14}N]body-pool. Transamination, which is reversible for a [^{13}C]leucine tracer, is thus an irreversible step for [^{15}N,^{13}C]leucine tracer (Fig. 2). The metabolism of [^{15}N,^{13}C]leucine therefore results in at least three different, measurable leucine species: [^{15}N,^{13}C]leucine, [^{13}C]leucine, and [^{13}C]KIC.

The presence of three measurable tracer species allows several modelling options to be considered. We chose to model [^{15}N,^{13}C]leucine kinetics only, omitting the KIC sub-system in its entirety. The KIC sub-system may be omitted because the ^{15}N label is lost irreversibly during transamination to KIC. The model which describes [^{15}N,^{13}C]leucine is a catenary three-compartment model (Fig. 3).

Methods

DATA GENERATION

Synthetic data sets were employed to evaluate the proposed model structure. Data were simulated using an "implied" version of the model developed by Cobelli *et al.* (1991), which describes the pathways of a [^{15}N,^{13}C]leucine tracer. We called this model the *Reference Model* (Fig. 4).

This model was used to simulate an intravenous infusion of 0.072 μmol kg^{-1} min^{-1} of [^{15}N,^{13}C]leucine tracer over 360 minutes into the extracellular leucine compartment (Fig. 3, compartment 1) during fasting conditions,
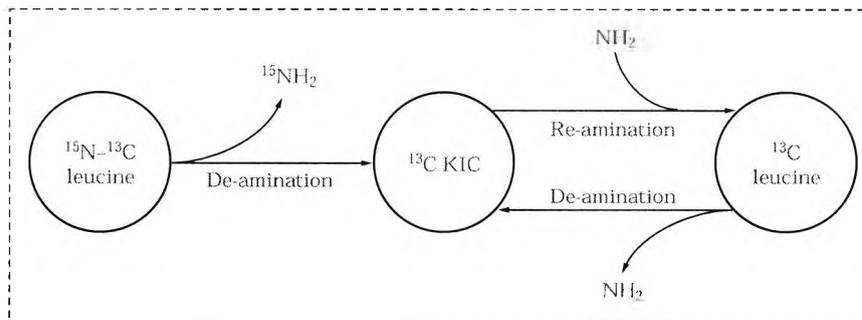
FIG. 2. During de-amination of [^{15}N^{13}C]leucine, the ^{15}NH$_2$ label is lost to the nitrogen pool and [^{13}C]KIC is formed. The re-amination of [^{13}C]KIC results in the formation of [^{13}C]leucine. The chance of a [^{15}N]labelled atom recombining with [^{13}C]KIC is negligible because of the small size of the ^{15}N pool.
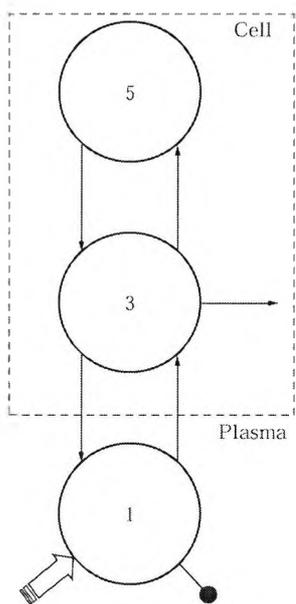
FIG. 3. The tracer model for [^{15}N,^{13}C]leucine. The model describes the kinetic events during an intravenous infusion of [^{15}N,^{13}C]leucine (arrow entering *compartment* 1) and assumes measurements in extracellular compartment (●). Infused [^{15}N,^{13}C]leucine tracer enters the plasma leucine pool (*compartment* 1), it may then enter intracellular space (*compartment* 3) where it may be either irreversibly de-aminated (k_{03}) or incorporated into a fast-turning over protein pool (*compartment* 5). Protein breakdown is represented by the flux of material from *compartment* 5 into *compartment* 3 (k_{35}).

employing the mean parameter values reported in Table 3 in Cobelli *et al*. (1991). The measurements were expressed as tracer-to-tracee ratios (TTR), i.e. the ratio of the amount of tracer (species originating from tracer infusion) vs. the amount of tracee (species originating from endogenous supplies) in extracellular pools. Simulated error-free TTR profiles are shown in Fig. 5. Error-free TTRs were recorded at $t = 0$, 1, 2, 3, 4, 5, 8, 10, 12.5, 15, 20, 30, 45, 60, 75, 90, 105, 120, 135, 150, 165, 180, 195, 210, 240, 270, 300, 330 and 360 min relative to the start of the tracer infusion.

MEASUREMENT ERROR

Measurement error was added to our synthetic error-free measurements in order to investigate its influence on parameter estimation. Measurement error was drawn from a normal distribution with zero mean and standard deviation $SD(z) = CV(z).z/100$; we assumed measurement

error to be additive. For data sets 1, 2 and 3 the coefficient of variation $CV(z)$ used was 5, 7.5 and 10%, respectively. Three additional data sets were simulated, namely data sets 4, 5, and 6, where CV was defined as

$$CV(z) = 5.01e^{-0.2844z} \qquad (1)$$

where z is the error-free measurement. The formula for $CV(z)$ (%) was derived by the nonlinear regression analysis of 20 duplicate TTR measurements of [^{13}C]leucine from the range 0.5–12% (data not shown). For small values of TTR ($<0.5\%$) the CV predicted by our error model was deemed to be unrealistic and an SD of 0.02% was used instead.
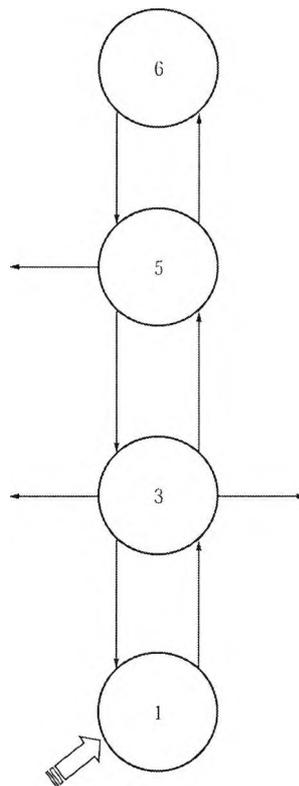
FIG. 4. Model used to simulate synthetic data, based on model developed by Cobelli *et al*. (1991), but describing pathways of [^{15}N,^{13}C]leucine tracer only. According to Cobelli *et al*. compartment 1 is an extracellular leucine pool; compartments 3 and 5 are intracellular leucine pools and compartment 6 is a protein linked leucine pool. For Cobelli, and more generally, the parameter k_{03} represents the reversible transamination of leucine to KIC, for the [^{15}N,^{13}C]leucine tracer, the step is irreversible. The idea is described in more detail in Fig. 2.
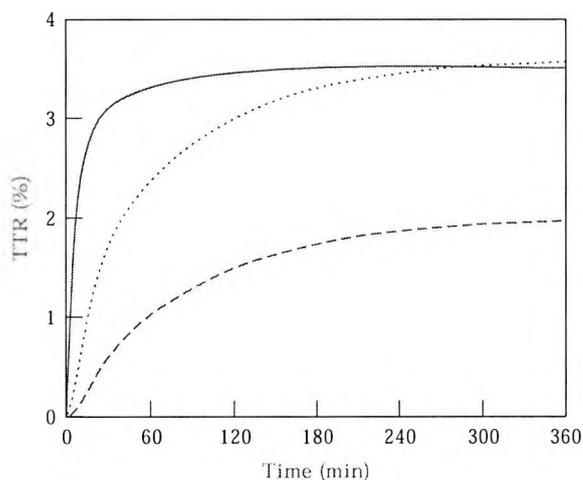
FIG. 5. Simulated error-free profiles using the Reference Model during the constant intravenous infusion of [^{15}N,^{13}C]leucine. (———) [^{15}N,^{13}C]leucine; (.....) [^{13}C]KIC; (– – –) [^{13}C]leucine.

TRACER MODEL

The three-compartment model (Fig. 3) which represents [^{15}N,^{13}C]leucine tracer kinetics, is described by a set of differential equations

$$q_1' = k_{13}.q_3 - k_{31}.q_1 + u_L$$
$$q_3' = k_{35}.q_5 - k_{53}.q_3 - k_{13}.q_3 + k_{31}.q_1 - k_{03}.q_3$$
$$q_5' = -k_{35}.q_5 + k_{53}.q_3$$
$$z_L = 100.q_1/Q_1$$

where q_i is tracer mass of [^{15}N,^{13}C]leucine in *compartment i*, $i = 1, 3$ and 5, with the condition that $q_i(0) = 0$; k_{ij} is the fractional transfer rate constant from *compartment j* to *compartment i*; u_L is the infusion rate of [^{15}N,^{13}C]leucine, Q_1 is the mass of leucine in *compartment* 1 originating from endogenous supplies and z is the TTR of [^{15}N,^{13}C]leucine. The mass Q_1 is assumed to be constant during the experiment.

There are six unknown parameters for the model, transfer rate constants k_{ij} and the mass Q_1. A catenary compartmental system with one leak is theoretically uniquely identifiable if the single-input/single-output is performed in an extremal compartment (Carson *et al.*, 1983), guaranteeing theoretical identifiability of our model.

PARAMETER ESTIMATION

Parameter estimation was carried out using the SAAM II program (SAAM Institute, Seattle, WA, U.S.A.) employing a nonlinear weighted regression analysis. The weights were defined as reciprocals of the variance of the measurement error. The measurement error model described by eqn (1) was employed to calculate the variance. SAAM II also calculated the precision or parameter estimates from the inverse of the Fisher information matrix (Carson *et al.*, 1983). The precision was expressed as the fractional standard deviation.

Results

It was possible to estimate fractional rate constants (k_{ij}) and the mass of the plasma leucine pool (Q_1) from synthetic measurements (with added measurement error) with acceptable precision (Table 1). Steady-state pool sizes and fluxes of endogenous leucine (tracee) can be calculated for each data set by using the tracer derived parameters. In particular, it is possible to calculate the masses Q_3 and Q_5 and the flux from protein breakdown B ($k_{35}.Q_5$); under these steady-state conditions $\mathbf{B} = \mathbf{S}$. Results of these calculations are shown also in Table 1.

Example fit is shown in Fig. 6. The plot of the weighted residuals indicates that the model provided unbiased fit with an acceptable goodness-of-fit [weighted residuals distributed randomly within the $\pm$SD region of the measurement error (see Fig. 7)].

Discussion

Modelling leucine kinetics with commonly used tracers—[^{13}C]leucine, [^{14}C]leucine, etc.—is difficult due to the need to model the KIC sub-system. KIC metabolism is non-trivial and consists of irreversible oxidation and reversible transamination in intracellular space. In this study we propose the use of [^{15}N,^{13}C]leucine tracer, as its use can simplify the modelling of leucine metabolism. This is because [^{15}N,^{13}C]leucine tracer is irreversibly trans-aminated and so there is no recycling of [^{15}N,^{13}C]leucine tracer through the KIC sub-system. In modelling terms its kinetics are therefore simpler than the kinetics of the more commonly used leucine tracers. Using the [^{15}N,^{13}C]leucine tracer in the manner we suggest, potentially

TABLE 1
Estimated tracer model parameters (k_{ij}), *masses* (Q_i)

| | Data set | | | | | | | |
	1 CV = 5%	2 CV = 7.5%	3 CV = 10%	4 CV model	5 CV model	6 CV model	Mean	Standard deviation
k_{03}	0.169 (16)	0.109 (21)	0.119 (22)	0.105 (28)	0.176 (18)	0.105 (19)	0.131	0.033
k_{13}	0.272 (49)	0.119 (40)	0.225 (87)	0.108 (57)	0.380 (68)	0.119 (40)	0.204	0.109
k_{31}	0.566 (30)	0.411 (18)	0.712 (73)	0.376 (21)	0.721 (51)	0.419 (17)	0.534	0.156
k_{35}	0.023 (11)	0.014 (40)	0.008 (73)	0.012 (28)	0.017 (18)	0.015 (21)	0.015	0.005
k_{53}	0.062 (15)	0.047 (32)	0.030 (22)	0.041 (24)	0.060 (20)	0.036 (21)	0.046	0.013
Q_1	11.60 (09)	12.411 (07)	9.924 (28)	13.138 (06)	10.80 (15)	12.502 (05)	11.730	1.199
Q_3	24.15	42.86	31.40	45.74	20.49	44.02	34.779	10.948
Q_5	65.11	143.90	117.76	156.28	72.32	105.65	110.171	36.892
B	1.50	2.01	0.94	1.88	1.23	1.58	1.524	0.398

Values are in $\min^{-1}$ (k_{ij}), μmol kg^{-1} (Q_i) and μmol kg^{-1} min^{-1} (B). Precision of estimated parameter is reported in parenthesis and expressed as a fractional standard deviation. The *masses* Q_3 and Q_5 were calculated from the solution of the model assuming steady-state conditions. The *flux B* represents leucine release from proteins (protein breakdown) and the incorporation of leucine into protein (protein synthesis).

allows the estimation of fractional rates of fast-turning-over protein breakdown and synthesis without involving the KIC sub-system.

In this study, we have explored only the kinetics of [^{15}N,^{13}C]leucine tracer using data simulated by a Reference Model (Fig. 4). The Reference Model is based upon what is, to our knowledge, the most comprehensive model of leucine kinetics to date. It includes intra- and extra-cellular pools for both leucine and KIC, the reversible transamination of leucine and KIC, the irreversible oxidation of KIC, and parameters for protein synthesis and breakdown. We used the Reference Model to simulate the kinetics of [^{15}N,^{13}C]leucine tracer, and estimated parameters for our model (Fig. 3) using this simulated data with measurement error added.

The Cobelli model is more complicated, and indeed more comprehensive than the model proposed here. It includes two intracellular leucine compartments (the proposed model has only one); in addition it includes three compartments to describe KIC kinetics, and includes irreversible oxidation. The proposed model attempts to model leucine kinetics without including the KIC sub-system.

The implications of this for the proposed model are significant, however, that is not to say
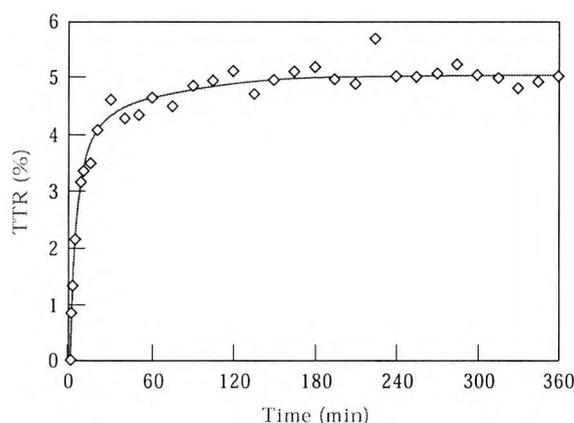
FIG. 6. Example fit to synthetic measurements (data set 1) of tracer-to-tracee ratio of [^{15}N,^{13}C]leucine.
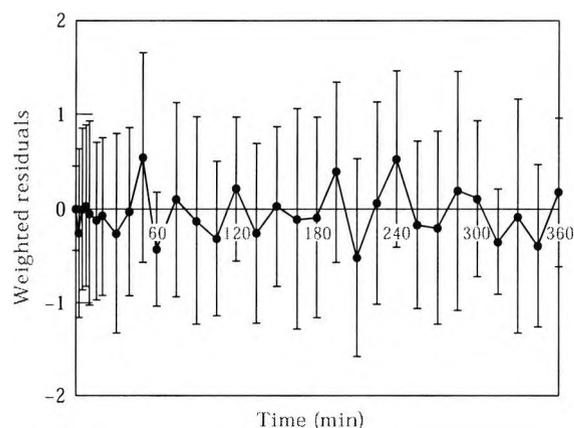

FIG. 7. Mean $\pm$ standard deviation of weighted residuals ($n = 6$).

that these are necessarily shortcomings. The ultimate goal of amino-acid turnover studies is, simply, to enable the estimation of protein breakdown and synthesis; the KIC sub-system is only studied because using current methods, its quantification is necessary in order to estimate protein turnover.

The Cobelli model is robust and comprehensive, but we feel the proposed can be useful in the study of leucine kinetics. Firstly, the proposed model is both theoretically and practically identifiable (we were able to estimate fractional rates for fast-turning-over protein with low, but acceptable precision). Secondly, the experimental protocol of the new model is simpler than that of the Cobelli model; involving the infusion of one tracer, and the measurement of one tracer species (the Cobelli model involves two tracers and the measurement of four tracer species). Furthermore, in modelling terms, the new model is simpler, not because of any new assumptions made but because the kinetics of [^{15}N,^{13}C]leucine allows us to by-pass the complex KIC sub-system. Bier (1989) questions the domain of validity of the model proposed by Umpleby et al. (1986) because the KIC system is overlooked; while Cobelli et al. (1991) use three compartments to describe the KIC sub-system and assume that both transamination and oxidation occur from the same KIC pool. This may well be correct, but it is also conceivable that oxidation and transamination occur in different intracellular KIC pools. Finally, this is but one of the modelling options available. The use of the [^{15}N,^{13}C]leucine tracer also enables the development of a more complicated model. A combined model describing [^{15}N,^{13}C]leucine, [^{13}C]leucine, and [^{13}C]KIC kinetics is attainable by also measuring [^{13}C]leucine and [^{13}C]KIC enrichments; such a model would allow the domain of validity of this model to be explored, while at the same time matching the Cobelli model for complexity. However, it is felt that exploring other modelling options such as these is best left until clinical data are available.

Through simulated experiments, we tested the affect of simulated measurement error on parameter estimation. Of utmost concern was to determine whether the model we designed was likely to allow practical identification of certain parameters (the fractional rates of a fast-turning-over protein pool). This practice of testing new models, methods and ideas using simulated data is not necessarily novel. However, considering the need for ethical approval and the cost of clinical studies in the field of physiological modelling, it is a step that is too often overlooked. Certainly, in this case the simulation study has justified a clinical evaluation of the [^{15}N,^{13}C]leucine tracer to estimate protein turnover.

Conclusion

Unlike traditional leucine tracers—[^{13}C]leucine, [^{14}C]leucine, etc.,—[^{15}N,^{13}C]leucine tracer is irreversibly transaminated and its kinetics are simpler due to the absence of recycling through the KIC sub-system. Using simulated data we have demonstrated that a three-compartment model of whole body [^{15}N,^{13}C]leucine kinetics allows the fractional turnover rates of a fast-turning-over protein pool to be represented and estimated.

The use of [^{15}N,^{13}C]leucine tracer with compartmental data analysis is thus a serious option in the study of leucine kinetics/protein turnover and should be explored in clinical studies.

REFERENCES

BIER, D. M. (1989). Intrinsically difficult problems: the kinetics of body proteins and amino acids in man. *Diabetes/Metabolism Rev.* **5,** 111–132.

BIER, D. M. (1997). Stable isotopes in biosciences, their measurement and models for amino acid metabolism. *Eur. J. Pediatr.* **156(Suppl.1),** S2–S8.

BIER, D. M. & MATTHEWS, D. E. (1982). Stable isotope tracer methods for *in vivo* investigations. *Fed. Proc.* **41,** 2679–2685.

CARSON, E. R., COBELLI, C. & FINKELSTEIN, L. (1983). *The Mathematical Modeling of Metabolic and Endocrine Systems.* New York: John Wiley & Sons.

CHENG, K. N., DWORZAK, F., FORD, G. C., RENNIE, M. J. & HALLIDAY, D. (1985). Direct determination of leucine metabolism and protein breakdown in humans using 1-[1-^{13}C,^{15}N]-leucine and the forearm model. *Eur. J. Clin. Invest.* **15,** 349–354.

CHRISTENSEN, H. N. (1990). Role of amino acid transport and countertransport in nutrition and metabolism. *Physiol. Rev.* **70,** 43–77.

COBELLI, C. & SACCOMANI, M. P. (1991). Domain of validity of classical-models of leucine metabolism assessed by compartmental modeling. *Math. Biosci.* **107,** 3–20.

COBELLI, C., SACCOMANI, M. P., TESSARI, P., BIOLO, G., LUZI, L. & MATTHEWS, D. E. (1991). Compartmental model of leucine kinetics in humans. *Am. J. Physiol.* **261,** E539–E550.

MATTHEWS, D. E. & COBELLI, C. (1991). Leucine metabolism in man: lessons from modelling. *J. Parenter. Enteral Nutr.* **15,** 86S–89S.

MATTHEWS, D. E., BIER, D. M., RENNIE, M. J., EDWARDS, R. H. T., MILLWARD, D. J. & CLUGSTON, G. A. (1981). Regulation of leucine metabolism in man: a stable isotope study. *Science* **214,** 1129–1131.

MATTHEWS, D. E., SCHWARZ, H. P., YANG, R. D., MOTIL, K. J., YOUNG, V. R. & BIER, D. M. (1982). Relationship of plasma leucine and α-ketoisocaproate during L-[1-^{13}C]leucine infusion in man: a method for measuring human intracellular leucine tracer enrichment. *Metabol.* **31,** 1105–1112.

O'KEEFE, S. J. D., SENDER, P. M. & JAMES, W. P. T. (1974). 'Catabolic' loss of body nitrogen in response to surgery. *Lancet* **ii,** 1035–1043.

SACCOMANI, M. P. & COBELLI, C. (1993). A minimal input–output configuration for *a priori* identifiability of a compartmental model of leucine metabolism. *IEEE Trans. Biomed. Eng* **40,** 797–803.

SACCOMANI, M. P., COBELLI, C., LUZI, L., MATTHEWS, D., BIOLO, G. & TESSARI, P. (1989). Leucine metabolism in man: insight from compartmental modeling. In: *Modelling and Control in Biomedical Systems* (Cobelli, C. & Mariani, L., eds) pp. 377–383. Oxford: Pergamon.

SCHWENK, W. F., BEAUFRERE, B. & HAYMOND, M. W. (1985). Use of reciprocal pool specific activities to model leucine metabolism in humans. *Am. J. Physiol.* **249,** E646–E650.

TAYLOR, R. T. & JENKINS, W. T. (1966). Leucine aminotransferase. II. Purification and characterization. *J. Biol. Chem.* **241,** 4396–4405.

TESSARI, P., INCHIOSTRO, S., ZANETTI, M. & BARAZZONI, R. (1995). A model of skeletal-muscle leucine kinetics measured across the human forearm. *Am. J. Physiol.* **269,** E127–E136.

THOMPSON, G. N., PACY, P. J., FORD, G. C., MERRITT, H. & HALLIDAY, D. (1988). Relationships between plasma isotope enrichments of leucine and alpha-ketoisocaproic acid during continuous infusion of labelled leucine. *Eur. J. Clin. Invest* **18,** 639–643.

UMPLEBY, A. M., BOROUJERDI, M. A., BROWN, P. M., CARSON, E. R. & SONKSEN, P. H. (1986). The effect of metabolic control on leucine metabolism in type-1 (insulin-dependent) diabetic-patients. *Diabetologia* **29,** 131–141.

WATERLOW, J. C. (1967). Lysine turnover in man measured by intravenous infusion of L-[U-^{14}C] lysine. *Clin. Sci.* **33,** 507–515.

WOLFE, R. R., GOODENOUGH, R. D., WOLFE, M. H., ROYLE, G. T. & NADEL, E. R. (1982). Isotopic analysis of leucine and urea metabolism in exercising humans. *J. Appl. Physiol.* **52,** 458–466.

YOUNG, V. R. (1987). McCollum award lecture—kinetics of human amino-acid metabolism—nutritional implications and some lessons. *Am. J. Clin. Nutr.* **46,** 709–725.

APPENDIX VI   BIBLIOGRAPHY

Carroll P, Christ E, Gowrie I, Jackson N, Hovorka R, Albany E, Bowes S, Umpleby M, Sonksen P, Russell-Jones DL (1997) Daily rhIGF-I augments the anabolic effect of insulin in adults with IDDM. Diabetes 46:945

Carroll PV, Christ ER, Umpleby AM, Gowrie I, Jackson N, Bowes SB, Hovorka R, Croos P, Sonksen PH, Russell-Jones DL (2000) IGF-I treatment in adults with type 1 diabetes - Effects on glucose and protein metabolism in the fasting state and during a hyperinsulinemic-euglycemic amino acid clamp. Diabetes 49:789-96

Gowrie IJ, Roudsari AV, Umpleby AM, Hovorka R (1999) Estimating protein turnover with a [N-15,C-13]leucine tracer: a study using simulated data. J. Theor. Biol. 198:165-72

Hovorka R, Carroll PV, Gowrie IJ, Jackson NC, Russell-Jones DL, Umpleby AM (1999) A surrogate measure of whole body leucine transport across the cell membrane. Am. J. Physiol. 276:E573-E579

Hovorka R, Shojaee-Moradie F, Carroll PV, Chassin LJ, Gowrie IJ, Jackson NC, Tudor RS, Umpleby AM, Jones RH (2002) Partitioning glucose distribution/transport, disposal, and endogenous production during IVGTT. Am. J. Physiol. 282:E992-E1007

Shojaee-Moradie F, Carroll PV, Chassin LJ, Gowrie IJ, Jackson NC, Jones RH, Tudor RS, Umpleby AM, Hovorka R (2001a) Partitioning glucose transport/distribution and disposal during euglycaemic clamp. Diabetologia 44:792

Shojaee-Moradie F, Carroll PV, Chassin LJ, Gowrie IJ, Jackson NC, Jones RH, Tudor RS, Umpleby MA, Hovorka R (2001b) Partitioning glucose transport/distribution, disposal. and endogenous production during IVGTT. Diabetes 50:A281-A282